Universidad de Oviedo

La Universidad de Asturias

Departamento de Biología Funcional

Programa de doctorado: Biología Funcional y Molecular

Desarrollo de *Streptomyces*: regulación y aplicaciones industriales

TESIS DOCTORAL

Beatriz Rioseras de Bustos

Oviedo, 2017

RESUMEN DEL CONTENIDO DE TESIS DOCTORAL

1.- Título de la Tesis	
Español/Otro Idioma: Desarrollo de *Streptomyces*: regulación y aplicaciones industriales	Inglés: *Streptomyces* development: regulation and industrial applications

2.- Autor	
Nombre: Beatriz Rioseras de Bustos	
Programa de Doctorado: Biología Funcional y Molecular	
Órgano responsable: Universidad de Oviedo	

RESUMEN (en español)

Las bacterias del género *Streptomyces* son bacterias con un ciclo de vida complejo que incluyen procesos de muerte celular programada (MCP), diferenciación morfológica y esporulación y son considerados modelos procarióticos de multicelularidad. Estas bacterias tienen gran importancia biotecnológica por su capacidad para producir gran cantidad de metabolitos secundarios con actividades biológicas variadas: antitumorales, inmunosupresoras, antibióticas, herbicidas, etc.

Durante la última década, nuestro grupo de investigación amplió el ciclo de desarrollo tradicional de *Streptomyces*. El objetivo de esta tesis fue caracterizar las rutas biomoleculares que regulan los procesos de diferenciación y MCP en *Streptomyces*, centrándose principalmente en las fases no contempladas en el ciclo de vida tradicional; así como analizar estos procesos de diferenciación en fermentaciones industriales a escala piloto.

Se llevó a cabo un análisis cuantitativo de los cambios en el proteoma y fosfoproteoma durante la diferenciación de *S. coelicolor*. Esto nos ha permitido, por un lado, hacer una revisión acerca de lo que se conoce hasta el momento sobre la biología de *Streptomyces,* y por otro, generar una base de datos de los cambios en el proteoma y fosfoproteoma durante el desarrollo, que puede contribuir a diseñar futuros experimentos con el objetivo de caracterizar potenciales reguladores y efectores de diferenciación. Además, se hicieron hallazgos sobre las fases tempranas del ciclo de desarrollo. En cuanto a la germinación, se descubrió una nueva fase en la que se ha visto que participan enzimas responsables de la remodelación del peptidoglicano como la carboxipeptidasa SCO4439. También se ha descubierto un nuevo tipo división celular que tiene lugar durante la fase vegetativa temprana en las hifas y se basa en la formación de tabiques de membrana (sin pared), un tipo de división celular inédita en bacterias. Por último, se analizaron los procesos de desarrollo, diferenciación y producción de antibióticos en fermentaciones industriales a escala piloto (biorreactor), lo que ha permitido definir nuevos parámetros que resultan importantes para la optimización y monitorización de la producción de metabolitos secundarios en fermentaciones de *Streptomyces*.

RESUMEN (en Inglés)

Bacteria of genus *Streptomyces* have a complex cycle of life that includes programmed cell death (PCD) processes, morphological differentiation and sporulation, and they are considered prokaryotic models of multicellularity. These bacteria have biotechnological importance because of their capacity for producing a large amount of secondary metabolites: antitumorals, inmunosupresors, antibiotics, herbicides, etc.

During the last decade, our research group extended the traditional development cycle of *Streptomyces*. The aim of this thesis was to characterize the biomolecular pathways that are regulating the differentiation and PCD processes of *Streptomyces*, focusing mainly on the not considered stages of the traditional cycle of life; as well as to analyze the differentiation processes in pilot scale industrial fermentations.

A quantitative analysis of the changes in proteome and phosphoproteome during *S. coelicolor* differentiation was carried out. This has allowed us, on the one hand, to make a review about what is known on the biology of *Streptomyces*, and on the other hand, to generate a database of the changes in proteome and phosphoproteome during development, which can contribute to design future experiments with the aim of characterizing potencial regulators and effectors of differentiation. In addition, findings about the early stages of the developmental cycle were made. Regarding germination, it was discovered a new stage in which was observed the participation of some enzymes involved in peptidoglucan remodeling like the SCO4439 carboxypeptidase. In addition, it was discovered a new mechanism of cell division that occurs during the early vegetative phase and it is based on membrane septa formation (without cellular wall); this is an unprecedented type of cell in bacteria. Finally, development, differentiation and antibiotic production processes in pilot scale industrial fermentations (bioreactors) were analyzed, which have allowed to define new parameters for the optimization and monitoring of the secondary metabolites production in *Streptomyces* fermentations.

SR. DIRECTOR DE DEPARTAMENTO DE BIOLOGÍA FUNCIONAL/
SR. PRESIDENTE DE LA COMISIÓN ACADÉMICA DEL PROGRAMA DE DOCTORADO EN BIOLOGÍA FUNCIONAL Y MOLECULAR

ÍNDICE

ÍNDICE DE FIGURAS

ÍNDICE DE TABLAS

ÍNDICE DE PUBLICACIONES

ABREVIATURAS

CDA: "*Calcium-Dependent Antibiotic*"
CPK: "*Cryptic Polyketide Synthase*"
CPP: "*Calcium phosphate precipitation"*
D-Ala: Alanina dextrógira
D-Lac: Lactato dextrógiro
D-iglu: ácido isoglutámico dextrógiro
HMM: "*High Molecular Mass"*
IMAC: *"Immobilized Metal Affinity Chromatography"*
iTRAQ: "*Isobaric Tag for Relative and Absolute Quantitation*"
L-Ala: Alanina levógira
LC-MS/MS: *"Liquid Chromatography tandem-Mass Spectrometry*
L,LA$_2$pm: Ácido L,L-diaminopimélico
LMM: "*Low Molecular Mass"*
MALDI-TOF: *"Matrix-Assisted Laser Desorption/Ionization Time of Flight"*
MCP: Muerte cellular programada
MI: Primer micelio
MII: Segundo micelio
MS: *"Mass Spectrometer"*
NAG: N-acetilglucosamina
NAM: N-acetilmurámico
NAM-Ac: N aceteilmurámico acetilado
PBPs: "*Penicillin Binding Proteins*"
ppGpp: Guanosín-3',5'-bispirofosfato
SALPs: "*SsgA-like proteins*"
SEDS: "*shape, elongation, división and sporulation"*
SILAC: *"Stable Isotope Labeling with Amino acids in Cell culture"*
SRM: *"Selected Reaction Monitoring"*
TiO$_2$: Dióxido de titanio
TMT: *"Tandem Mass Tag"*

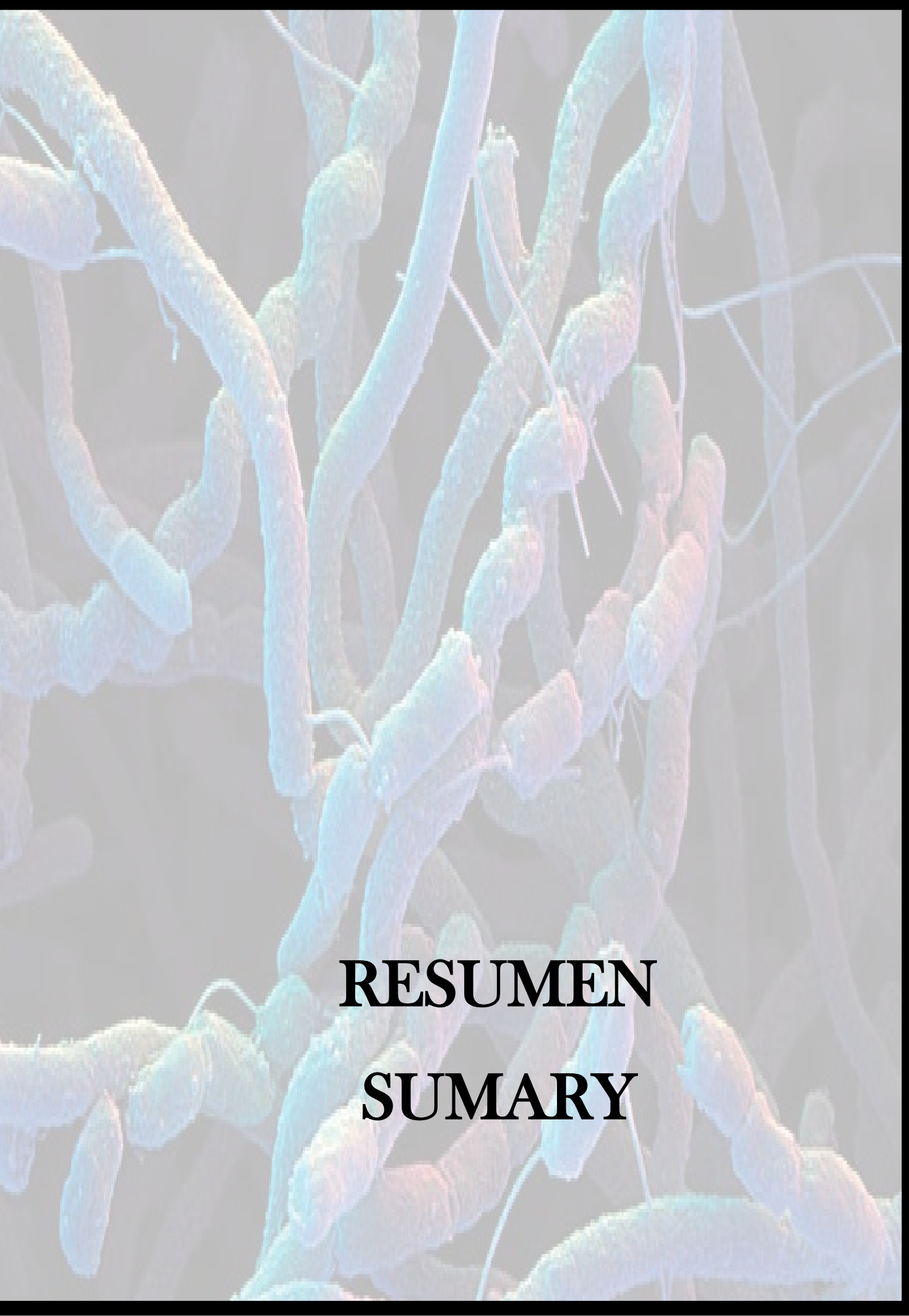

RESUMEN

SUMARY

Las bacterias del género *Streptomyces* son bacterias con un ciclo de vida complejo que incluyen procesos de muerte celular programada (MCP), diferenciación morfológica y esporulación y son considerados modelos procarióticos de multicelularidad. Estas bacterias tienen gran importancia biotecnológica por su capacidad para producir gran cantidad de metabolitos secundarios con actividades biológicas variadas: antitumorales, inmunosupresoras, antibióticas, herbicidas, etc.

Durante la última década, nuestro grupo de investigación amplió el ciclo de desarrollo tradicional de *Streptomyces*. El objetivo de esta tesis fue caracterizar las rutas biomoleculares que regulan los procesos de diferenciación y MCP en *Streptomyces*, centrándose principalmente en las fases no contempladas en el ciclo de vida tradicional; así como analizar estos procesos de diferenciación en fermentaciones industriales a escala piloto.

Se llevó a cabo un análisis cuantitativo de los cambios en el proteoma y fosfoproteoma durante la diferenciación de *S. coelicolor*. Esto nos ha permitido, por un lado, hacer una revisión acerca de lo que se conoce hasta el momento sobre la biología de *Streptomyces,* y por otro, generar una base de datos de los cambios en el proteoma y fosfoproteoma durante el desarrollo, que puede contribuir a diseñar futuros experimentos con el objetivo de caracterizar potenciales reguladores y efectores de diferenciación. Además, se hicieron hallazgos sobre las fases tempranas del ciclo de desarrollo. En cuanto a la germinación, se descubrió una nueva fase en la que se ha visto que participan enzimas responsables de la remodelación del peptidoglicano como la carboxipeptidasa SCO4439. También se ha descubierto un nuevo tipo división celular que tiene lugar durante la fase vegetativa

temprana en las hifas y se basa en la formación de tabiques de membrana (sin pared), un tipo de división celular inédita en bacterias. Por último, se analizaron los procesos de desarrollo, diferenciación y producción de antibióticos en fermentaciones industriales a escala piloto (biorreactor), lo que ha permitido definir nuevos parámetros que resultan importantes para la optimización y monitorización de la producción de metabolitos secundarios en fermentaciones de *Streptomyces*.

Bacteria of genus *Streptomyces* have a complex cycle of life that includes programmed cell death (PCD) processes, morphological differentiation and sporulation, and they are considered prokaryotic models of multicellularity. These bacteria have biotechnological importance because of their capacity for producing a large amount of secondary metabolites: antitumorals, inmunosupresors, antibiotics, herbicides, etc.

During the last decade, our research group extended the traditional development cycle of *Streptomyces*. The aim of this thesis was to characterize the biomolecular pathways that are regulating the differentiation and PCD processes of *Streptomyces*, focusing mainly on the not considered stages of the traditional cycle of life; as well as to analyze the differentiation processes in pilot scale industrial fermentations.

A quantitative analysis of the changes in proteome and phosphoproteome during *S. coelicolor* differentiation was carried out. This has allowed us, on the one hand, to make a review about what is known on the biology of *Streptomyces*, and on the other hand, to generate a database of the changes in proteome and phosphoproteome during development, which can contribute to design future experiments with the aim of characterizing potencial regulators and effectors of differentiation. In addition, findings about the early stages of the developmental cycle were made. Regarding germination, it was discovered a new stage in which was observed the participation of some enzymes involved in peptidoglucan remodeling like the SCO4439 carboxypeptidase. In addition, it was discovered a new mechanism of cell division that occurs during the early vegetative phase and it is based on membrane septa formation (without cellular wall); this is an

unprecedented type of cell in bacteria. Finally, development, differentiation and antibiotic production processes in pilot scale industrial fermentations (bioreactors) were analyzed, which have allowed to define new parameters for the optimization and monitoring of the secondary metabolites production in *Streptomyces* fermentations.

INTRODUCCIÓN

1. Importancia del género *Streptomyces*

1.1 Contexto histórico

A finales del siglo XIX y principios del XX, el estudio de la microbiología del suelo era un tema que suscitaba poco interés ya que los microbiólogos de la época tenían como principal objetivo identificar bacterias patógenas e intentar controlar las enfermedades que producían.

El primer *Streptomyces* se describió en 1875 cuando Ferdinand Cohn publicó un tratado resumiendo las observaciones de una gran cantidad de microorganismos donde incluía uno llamado *Streptothrix foersteri* (Cohn, 1875). *Streptothrix* significa "pelo retorcido".

En el año 1877 se descubrió el agente causal de una enfermedad del ganado llamada *jumpy jaw (*mandíbula abultada) la cual causaba proliferación y distensión del hueso produciendo abultamientos incurables en el rostro de los animales que les impedía comer con normalidad, acuñándose el nombre de Actinomyces para el agente causal de dicha enfermedad. Un botánico alemán, Carl Otto Harz, fue el primero en describir este microorganismo y lo definió como un hongo con filamentos finos que se disponen formando estructuras regulares en forma de rayos, dándole el nombre de *Actinomyces bovis* (*Actinomyces* significa hongo de rayos), (Hopwood, 2007). En esta época también se describieron otros microorganismos, que más tarde se incluyeron en el grupo de los actinomicetos, responsables de graves enfermedades como la lepra producida por *Mycobacterium leprae* o bacilo de Hansen, o la tuberculosis causada por *Mycobacterium tuberculosis* o bacilo de Koch (Hopwood, 2007).

En décadas posteriores, fueron descritos otros microrganismos del grupo de los actinomicetos entre los que se encontraban muchas bacterias

del suelo. En este contexto Selman Waksman comenzó su carrera investigadora estudiando las capacidades bioquímicas de este grupo de bacterias del suelo tan poco conocido hasta entonces. Los actinomicetos fueron reconocidos como Actinomycetales en 1916 por R.E. Buchanan (Buchanan, 1916) y en 1943 Selman Waksman y Arthur Henrici establecieron una primera subdivisión de este nuevo grupo (Waksman & Henrici, 1943).

1.2 *Streptomyces* y la producción de antibióticos

En 1943 Albert Schatz, un estudiante de doctorado del Cook College en la Universidad de Rutgers (New Jersey), descubrió la estreptomicina, un antibiótico producido por *Streptomyces griseus* que resultó ser efectivo en la cura de la tuberculosis. Originalmente, el descubrimiento fue acreditado únicamente a su supervisor, Selman Waksman, que llegó incluso a recibir en 1952 el premio Nobel por este motivo. El descubrimiento de la estreptomicina tuvo una gran repercusión y muchos investigadores centraron sus esfuerzos en la búsqueda de nuevos agentes antimicrobianos procedentes de actinobacterias. Es así como comienza el auge de este grupo de bacterias que tan poco interés había suscitado hasta entonces.

Durante las siguientes décadas (especialmente entre los años 1950 y 1980), se descubrieron muchos antibióticos producidos por diversas especies de actinomicetos, fue la llamada “Edad de Oro” de los antibióticos. Como consecuencia los actinomicetos se convirtieron en el grupo de microorganismos más utilizado en la industria farmacéutica (Hopwood, 2007) (Figura 1).

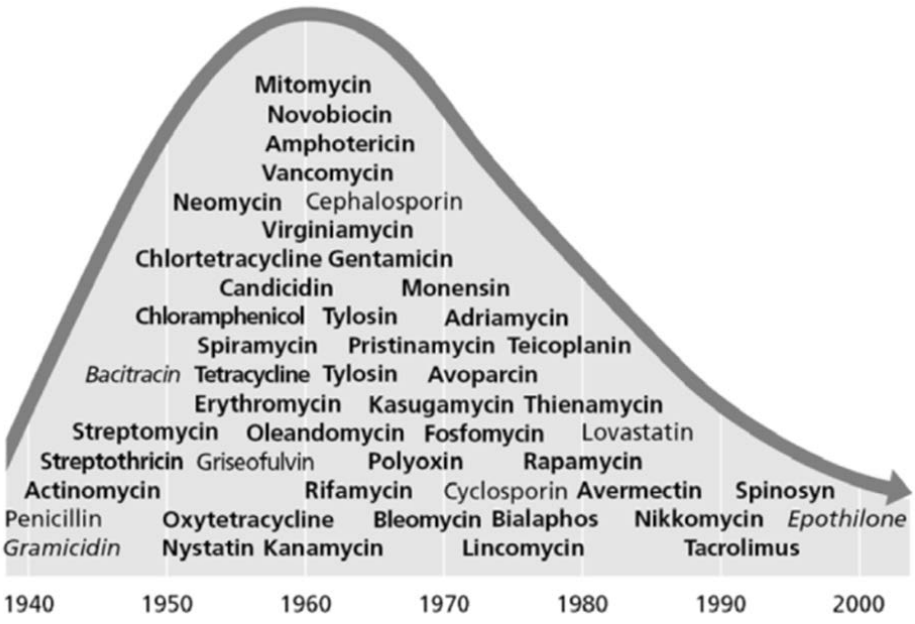

Fig. 1. Descubrimiento de antibióticos y otros productos naturales a lo largo de los años. En negrita aparecen los compuestos producidos por actinomicetos (Hopwood, 2007).

1.3 Características generales del género *Streptomyces*

Streptomyces es el género de bacterias más estudiado dentro del filo Actinobacteria. Actualmente, de acuerdo al "Bergey's Manual of Systematic Bacteriology" hay más de 500 especies de *Streptomyces* descritas (W. Whitman et al., 2012). El primer *Streptomyces* secuenciado fue *Streptomyces coelicolor* A3(2), esta es la especie de *Streptomyces* más estudiada y es considerada la cepa modelo del género (Bentley et al., 2002).

El género *Streptomyces* engloba bacterias filamentosas, con crecimiento micelial que recuerda al crecimiento característico de los hongos. Son bacterias Gram positivas (Gram, 1884) y fundamentalmente aerobias. Poseen un cromosoma lineal de gran tamaño (generalmente

mayor de 8 Mb) y su genoma tiene un alto contenido en GC (69-78%). Estos microorganismos están ampliamente distribuidos en la naturaleza siendo el suelo su hábitat natural más común donde son capaces de descomponer gran cantidad de compuestos orgánicos (saprófitos), principalmente plantas (Hagedorn, 1976; Hodgson, 2000).

Tal como se detallará en los siguientes apartados, una característica destacable del género *Streptomyces* es que tienen un ciclo de vida complejo, con procesos de muerte celular programada (MCP), diferenciación morfológica y esporulación y son considerados modelos procarióticos de multicelularidad (Chater, 1984). Todo esto hace que el estudio de *Streptomyces* tenga gran interés en la investigación básica.

Por otro lado y desde el punto de vista biotecnológico, la importancia de estos microorganismos radica en su capacidad para producir gran diversidad de metabolitos secundarios con actividades biológicas variadas, tales como antitumorales, inmunosupresores, antibióticos, herbicidas, inhibidores enzimáticos, pigmentos, aromas etc. (Challis & Hopwood, 2003; Thompson et al., 2002).

2. Ciclo de vida de *Streptomyces*

2.1 Ciclo de vida en medio sólido

El ciclo de vida de *Streptomyces* se describió en cultivos sólidos de laboratorio (placas de Petri) ya que en estas condiciones *Streptomyces* tiene un ciclo de vida completo que culmina con la esporulación de las hifas.

El ciclo de vida tradicional de *Streptomyces* describía como tras la germinación de las esporas, se forma una red de hifas ramificadas que penetran y solubilizan los desechos orgánicos mediante la acción de

enzimas hidrolíticos extracelulares, formado así el llamado micelio sustrato o vegetativo. (Chater, 1984) (Figura 2). Este micelio sustrato crece y se ramifica hasta que en un determinado momento, en respuesta a la carencia de nutrientes y a otras señales, se activa la expresión de determinados genes implicados en el desarrollo del micelio aéreo que crece nutriéndose del micelio sustrato en una especie de canibalismo (Chater, 1984; Miguelez et al., 1999). El micelio aéreo emerge del micelio sustrato y comienza a crecer en el aire para lo cual necesita recubrirse de una serie de cubiertas hidrofóbicas (Claessen et al., 2006; Flardh & Buttner, 2009). En este punto, en el que hay un gran aporte de nutrientes por parte del micelio sustrato, la bacteria es más susceptible de ser colonizada por otros microorganismos y para evitarlo, *Streptomyces* comienza a sintetizar compuestos antimicrobianos (Flardh & Buttner, 2009; McCormick & Flardh, 2012)**.** Finalmente las hifas de micelio aéreo se diferencian curvándose en su extremo y formando septos de pared gruesos que dan lugar a largas cadenas de esporas unigenómicas (Claessen et al., 2006; Flardh & Buttner, 2009). Estas esporas se liberan al medio siendo este el modo de dispersión de estos organismos. Las esporas permanecen latentes hasta que, bajo las condiciones adecuadas, germinan dando lugar al micelio sustrato que iniciará de nuevo el ciclo (Figura 2). Ambos micelios, sustrato y aéreo son multinucleados, es decir, tienen septos esporádicos en sus hifas que separan fragmentos multigenómicos. Las esporas serían por tanto, la única fase con compartimentos unigenómicos (Claessen et al., 2006; Flardh & Buttner, 2009).

Durante la última década, nuestro grupo de investigación realizó un estudio exhaustivo del ciclo de desarrollo de *Streptomyces* en el que se analizaron los cambios morfológicos y bioquímicos que acompañan la diferenciación. Se consiguió ampliar el ciclo de desarrollo tradicional al encontrar un estadio nuevo que había pasado desapercibido debido a que

en condiciones de laboratorio es muy transitorio (Manteca & Sanchez, 2009).

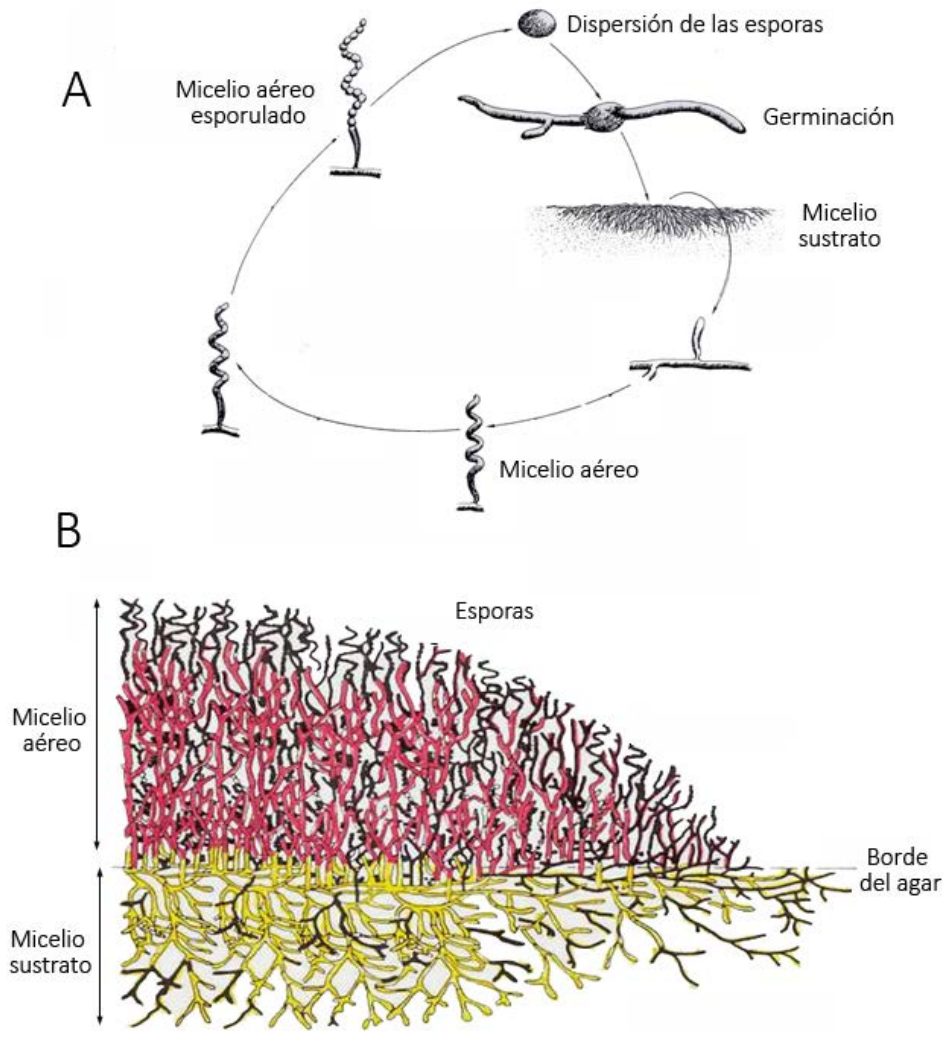

Fig 2. A. Ciclo de desarrollo clásico de *Streptomyces* en cultivos sólidos Adaptado de Kieser et al., (2000). B. Esquema de un corte transversal de la capa de micelio. Adaptado de Kieser et al., (2000).

Esta nueva fase, llamada primer micelio (MI), precede a la fase de micelio sustrato, y consiste en un micelio joven, totalmente compartimentalizado (Figura 3). El MI sufre un proceso de MCP muy ordenado en el que se alternan segmentos vivos y muertos dentro de la misma hifa (Manteca et al., 2005a; Manteca et al., 2005b). Los segmentos viables de este micelio comienzan a crecer y se diferencian a un micelio multinucleado, llamado segundo micelio (MII), que se corresponde con el micelio sustrato en tiempos tempranos o con el micelio aéreo una vez que empieza a expresar las cubiertas hidrofóbicas y a crecer en el aire. Finalmente se produce la fase de esporulación de parte de las hifas de micelio aéreo. La fase de MII (sustrato y aéreo) se correlaciona con la producción de metabolitos secundarios (Manteca et al., 2006; Manteca et al., 2005a; Manteca et al., 2005b), (Figura 3).

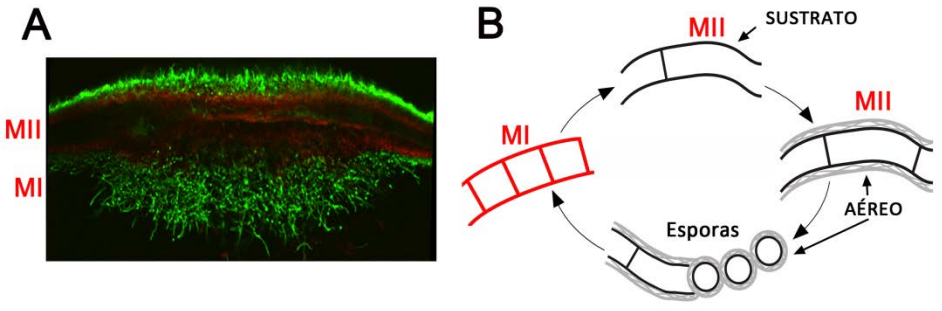

Fig 3. A. Corte transversal de una colonia de *Streptomyces antibioticus* marcada con SYTO9 y yoduro de propidio observada al microscopio confocal. B. Esquema del desarrollo de *Streptomyces*. Las nuevas fases del desarrollo descritas por nuestro grupo de investigación (MI y MII) están marcadas en rojo. Adaptado de (Yague et al., 2012)).

Durante esta tesis doctoral se ha medido la frecuencia de compartimentalización del MI (compartimentos con una longitud media de 1µm). También se ha conseguido caracterizar la ultraestructura de los mismos. Los tabiques de MI están formados por membranas celulares sin

pared celular, algo inédito en microbiología, que implica la existencia de un mecanismo de división celular por caracterizar (véase capítulo 2b).

2.2 Ciclo de vida en medio líquido

A pesar de que la mayoría de las fermentaciones industriales se realizan en cultivos líquidos (biorreactores), el ciclo de vida de *Streptomyces* en estas condiciones ha sido poco estudiado. Esto es debido a que en medio líquido la mayor parte de las cepas de *Streptomyces* no forman micelio aéreo ni esporulan, por lo que en el contexto del ciclo tradicional se asumía que no había diferenciación. En consecuencia, los metabolitos secundarios serían producidos por el micelio sustrato tras una detención transitoria del crecimiento que precede a una diferenciación fisiológica de este micelio sustrato (Pamboukian & Facciotti, 2004; Stocks & Thomas, 2001).

El nuevo modelo de desarrollo elaborado por nuestro grupo de investigación en medio sólido se puede aplicar también a cultivos líquidos: un micelio compartimentalizado (MI) sufre un proceso de MCP y se diferencia a un micelio multinucleado (MII) (Figura 4). La detección transitoria del crecimiento se corresponde con la MCP del MI, y la fase de producción con el desarrollo del MII, al igual que sucedía en cultivos sólidos (Manteca et al., 2008). De esta forma se demostró que en cultivos líquidos, en contra de lo que se creía tradicionalmente, sí existe diferenciación, y esta diferenciación se correlaciona con la producción de metabolitos secundarios (Manteca et al., 2008), (Figura 4). Esta fue la primera vez que pudo correlacionarse la producción (diferenciación fisiológica) con la diferenciación morfológica (MII) (Manteca et al., 2008).

El estudio del desarrollo de estas bacterias en cultivos líquidos, especialmente en biorreactores, tiene gran interés desde el punto de vista

biotecnológico debido a su posible aplicación en la mejora y optimización de las fermentaciones industriales de *Streptomyces* (véase capítulo 3).

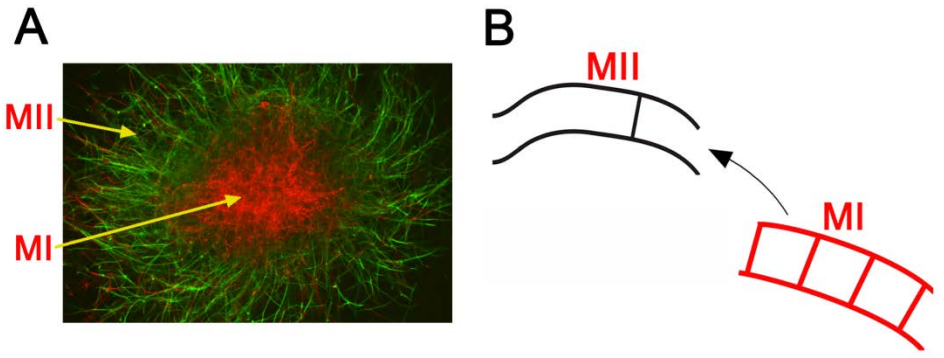

Fig 4. A. Imagen de microscopía confocal de un pellet de *Streptomyces antibioticus* en medio líquido marcado con SYTO9 y ioduro de propidio. B. Esquema del nuevo ciclo de desarrollo de *Streptomyces* en medio líquido. Adaptado de Yague et al., (2012).

2.3 Ciclo de vida en condiciones naturales (suelos)

En las condiciones de laboratorio se ha observado una fase de MI muy corta, especialmente en cultivos sólidos (unas 12 horas, aunque el tiempo exacto depende de la cepa de *Streptomyces* y del medio de cultivo). Esto puede ser debido a que la alta densidad celular alcanzada en estas situaciones provoca una aceleración de los procesos de muerte celular, diferenciación y esporulación; en definitiva, las condiciones de laboratorio son artificiales y generan artefactos en comparación con la naturaleza. En condiciones naturales se ha descrito un crecimiento discontinuo y un desarrollo limitado de las colonias (Williams, 1985).

En nuestro grupo de investigación, se llevaron a cabo experimentos en los que se recreaban estas condiciones naturales utilizando tierra irrigada con medios de cultivo pobres, inoculada con bajas densidades de esporas (Manteca & Sanchez, 2009). En estas condiciones se observó que la germinación de las esporas ocurre de forma lenta (no antes de 7 días) y

asincrónica (aún quedaban esporas sin germinar a los 20 días de cultivo), además el micelio no llega a formar *"pellets"* densos y permanece en fase de MI durante el periodo analizado (un mes), sin detectarse procesos de muerte, desarrollo de MII ni esporulación (Manteca & Sanchez, 2009) (Figura 5). Debido a esto, se ha propuesto que el MI es el auténtico micelio vegetativo de *Streptomyces* en los suelos naturales, siendo la fase multinucleada (MII) una fase transitoria que facilita la división del material genómico que precede a la esporulación (Manteca & Sanchez, 2009; Yague et al., 2013a).

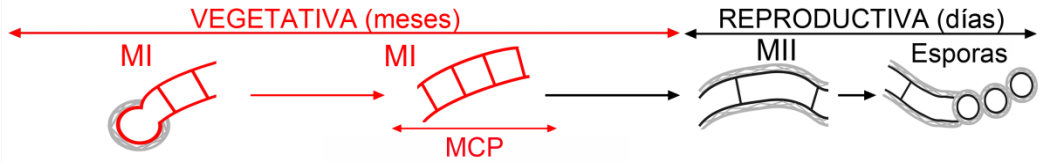

Fig. 5. Esquema propuesto del desarrollo de *Streptomyces* en condiciones naturales. La fase vegetativa (MI), en rojo, es la predominante. La fase reproductora (MII), en negro, es una fase transitoria. Adaptado de Yague et al., (2013a).

2.4 Muerte celular programada en *Streptomyces*

La MCP se puede definir como cualquier tipo de muerte celular ordenada que implique la activación de reguladores y efectores específicos de este proceso (Engelberg-Kulka et al., 2006). La MCP se ha descrito en bacterias de diferentes taxones como *Bacillus* y *Echerichia coli* (Engelberg-Kulka et al., 2006), *Anabaena* (Ning et al., 2002), *Caulobacter (Bos et al., 2012; Hochman, 1997)*, *Streptococcus* (Guiral et al., 2005), *Staphylococcus* (Chatterjee et al., 2010), y *Myxobacteria* (Sogaard-Andersen & Yang, 2008). En general, las rutas biomoleculares que controlan la MCP en bacterias, así como su función biológica no se conocen bien. Sólo en algunos casos, como los sistemas toxina-antitoxina de *E.coli*, los procesos de competencia

y esporulación en *Bacillus subtilis* (ambos revisados en Engelberg-Kulka et al., 2006), o los procesos de competencia en *Streptococcus pneumoniae* (Guiral et al., 2005) la MCP está bien caracterizada. Los mecanismos reguladores de estas MCPs son diferentes en cada caso.

Streptomyces tiene dos rondas de MCP en cultivos sólidos. Una primera ronda que afecta al MI y precede a la diferenciación del MII (Manteca et al., 2007; Manteca et al., 2006), y una segunda ronda de muerte que precede a la formación de micelio aéreo y esporulación (Manteca et al., 2006; Miguelez et al., 1999). Ambos eventos de muerte celular son programados, ya que implican un patrón morfológico muy ordenado (Manteca et al., 2005a; Miguelez et al., 1999), así como la activación de enzimas hidrolíticos encargados del desmantelamiento celular (Cal et al., 1996; Manteca et al., 2007; Manteca et al., 2006; Nicieza et al., 1999). El número de rondas de MCP depende de las condiciones de cultivo: en cultivos sólidos confluentes hay dos (Manteca et al., 2006); en colonias aisladas, tras un primer ciclo de germinación, MI, MCP, MII y esporulación, las esporas germinan de nuevo (probablmente por la difusión de nutrientes del medio de cultivo) y se repiten sucesivos ciclos de desarrollo habiendo múltiples rondas de MCP (Manteca & Sanchez, 2009); en cultivos líquidos (Manteca et al., 2008) hay una única PCD. Tal como se apuntó arriba, no debemos perder la perspectiva de que los cultivos de laboratorio son en cierto modo artefactos, y lo que es común a todos los cultivos de *Streptomyces* es la existencia de un MI que sufre una MCP y se diferencia a un MII productor de metabolitos secundarios destinado a esporular. La fase de MII se alarga cuando los nutrientes son abundantes, y sufre una o más rondas de MCP cuando hay nuevos agotamientos nutricionales (Manteca et al., 2008; Manteca et al., 2006; Manteca & Sanchez, 2009).

Algunos autores han considerado que las bacterias de ciclo de vida complejo, como es el caso de *Streptomyces*, son el origen evolutivo de algunos de los dominios proteicos implicados en los procesos de apoptosis de eucariotas (Koonin & Aravind, 2002). Es necesario un mayor estudio para llegar a conocer este posible origen, así como el papel de estos procesos en la biología de estas bacterias (Yague et al., 2013a).

3. Regulación del desarrollo de *Streptomyces*

La regulación del ciclo de desarrollo de *Streptomyces* requiere complejos mecanismos de señalización que dirigen su diferenciación morfológica. A continuación, se detallan las principales rutas de regulación conocidas en cada una de las fases del ciclo de *Streptomyces* (esquematizadas en la Figura 6).

3.1 Germinación

La regulación de la germinación es un proceso poco estudiado ya que tradicionalmente se ha prestado mucha más atención a las fases de esporulación y producción de antibióticos.

La germinación de las esporas es la primera fase del desarrollo y consiste a su vez en tres etapas: oscurecimiento, hinchamiento y emergencia del tubo germinativo (Hardisson et al., 1978). La fase de oscurecimiento requiere aporte exógeno de cationes divalentes (Ca^{2+}, Mg^{2+} o Fe^{2+}) y energía obtenida de las reservas de la espora (Salas et al., 1983).

Diversos estudios indican que Ca^{2+} juega un papel importante en la regulación de diferentes procesos del desarrollo y en concreto en la germinación (Wang et al., 2008). Se ha descrito que durante la

esporulación tiene lugar la acumulación de calcio en las cubiertas de las esporas y se libera durante esta primera fase de oscurecimiento (Salas et al., 1983). La fase de hinchamiento requiere una fuente exógena de carbono y durante la última fase, cuando tiene lugar la emergencia del tubo germinativo, se necesita más aporte de carbono y nitrógeno (Hardisson et al., 1978).

Una de las claves de la regulación de la germinación está en conocer cómo se mantiene la latencia en las esporas. En 1985 Grund y Ensign descubrieron la existencia de inhibidores de la germinación, sustancias de bajo peso molecular que inhiben la actividad ATPasa, inhibiendo con ello el crecimiento y la respiración en las esporas latentes. (Grund & Ensign, 1985). Estos inhibidores fueron caracterizados como germicidas por Petersen et al., (1993). También se ha descrito que los niveles de AMPc en las esporas están implicados en la regulación de la salida de la latencia (Susstrunk et al., 1998). NepA, una proteína hidrofóbica de bajo peso molecular que forma parte estructural de la pared celular de las esporas, también tiene un papel importante en el mantenimiento de la latencia de las esporas bajo condiciones desfavorables (de Jong et al., 2009). Guijarro et al., (1983) describieron un patrón de degradación de proteínas característico de la germinación. En un trabajo reciente en el que se analiza el transcriptoma de las esporas en diferentes puntos de la germinación, se observó que las esporas latentes cuentan con un amplio repertorio de ARNm. Cuando se activa la germinación, gran parte de este ARNm se degrada. Se ha observado que esta degradación puede ser inducida por calor o por activación de ARNasas intracelulares (Bobek et al., 2014). Además se ha demostrado que la germinación requiere la acción de numerosos factores sigma (Bobek et al., 2014). Muchos de estos factores sigma estaban relacionados con las respuestas a situaciones de estrés por lo que parece que el proceso de

germinación comparte características con estas respuestas a condiciones adversas. Esto no sorprende ya que la germinación supone una alteración de las condiciones estables en las que se encontraban las esporas (Bobek et al., 2014).

La reactivación del metabolismo en las esporas latentes y las etapas inmediatamente posteriores a la salida de la latencia también están reguladas. En el momento en el que se activa la germinación, se ha visto un gran aumento en la expresión de determinados genes, sobre todo genes relacionados con el metabolismo de lípidos y sistemas de transporte de membrana. En las fases siguientes se activan enzimas hidrolíticos que degradan la pared celular (Haiser et al., 2009). Noens et al., (2007) identificaron la proteína SsgA como una proteína necesaria para marcar los puntos de la pared celular donde va a tener lugar la emergencia del tubo germinativo.

Aunque como hemos visto existe información importante acerca de la regulación de la germinación, aún hay mucho por descubrir para llegar a entender las rutas bioquímicas que regulan este proceso. Tal como se expondrá más adelante, esta tesis doctoral ha contribuido a profundizar en la comprensión de los mecanismos de control de la maduración de las paredes de las esporas de *Streptomyces*, así como los procesos de hinchamiento que preceden la emisión del tubo germinativo (véase capítulo 2a).

3.2 Estadios tempranos del desarrollo: MI compartimentalizado, diferenciación del MII multinucleado

La principal diferencia morfológica entre el MI y el MII es que el MI está completamente compartimentalizado, mientras que el MII es multinucleado con tabiques esporádicos (Manteca et al., 2005a). La

principal diferencia fisiológica entre el MI y el MII es la baja activación del metabolismo secundario en el MI y la activación del mismo en el MII (Manteca et al., 2010a; Manteca et al., 2010b; Yague et al., 2013b; Yague et al., 2014).

La tabicación de las hifas de *Streptomyces* ha sido ampliamente estudiada en el contexto del ciclo de desarrollo tradicional (micelio sustrato, aéreo y esporulación). Jakimowicz & van Wezel., (2012) describieron la existencia de dos tipos de septos en *Streptomyces*: septos de micelio vegetativo (sustrato y aéreo) y septos de esporulación. Ambos tipos de septos tienen diferentes características y su formación está regulada por diferentes mecanismos (Willemse et al., 2011). Sin embargo, la tabicación del MI permanecía básicamente inexplorada. Tal como se comenta más adelante (capítulo 2b), en esta tesis se ha caracterizado la ultraestructura de los tabiques de MI, los cuales están formados por membranas celulares sin pared, lo que es inédito en bacterias.

Como se ha comentado anteriormente, nuestro grupo de investigación ha sido pionero en el estudio de las fases tempranas del desarrollo, primero demostrando que hay una correlación estrecha entre la producción de metabolitos secundarios y la diferenciación del MII (Manteca et al., 2008), y después demostrando mediante experimentos de proteómica y transcriptómica, una diferenciación fisiológica: los genes y proteínas del metabolismo secundario y de la formación de las cubiertas hidrofóbicas características del micelio aéreo están regulados al alza en el MII e inhibidos en el MI (Manteca et al., 2010a; Manteca et al., 2010b; Yague et al., 2013b; Yague et al., 2014) (Tabla 1).

Aún falta mucho trabajo para caracterizar las rutas biomoleculares que controlan la transición MI-MII. Tal como se comentará en el capítulo 1, en esta tesis doctoral se han realizado experimentos de proteómica

cuantitativa de las fases de MI y MII que han triplicado el número de proteínas identificadas y cuantificadas anteriormente por (Manteca et al., 2010a; Manteca et al., 2010b). Se han encontrado proteínas muy interesantes potencialmente relacionadas con la división celular y la regulación del metabolismo secundario diferencialmentet expresadas durante las fases de MI y MII (véase trabajo experimental, capítulo 1).

3.3 Diferenciación del micelio aéreo

La transición de micelio sustrato (MII temprano) a micelio aéreo (MII tardío) ha sido muy estudiada en el contexto del ciclo tradicional de *Streptomyces* (Figura 6). Los análisis de cepas mutantes bloqueadas en diferentes estadios del proceso de formación de las cubiertas hidrofóbicas del micelio aéreo, mutantes "*bald"* (calvos), han llevado a identificar los genes *bald* como genes responsables de la regulación de estos procesos. Estos genes regulan la activación de la *"sky pathway"* que controla la producción de las proteínas encargadas de la formación de las cubiertas hidrofóbicas del micelio aéreo: SapB, chaplinas y rodlinas. También se conoce bastante sobre las señales que desencadenan la diferenciación fisiológica del micelio aéreo. Así determinados factores como la disminución de los nutrientes, las reservas de ppGpp y GTP disponibles, la fuente de carbono utilizada o la señalización extracelular, afectan a la decisión de formar el micelio aéreo. Existen varias revisiones donde se describe en detalle esta regulación (Claessen et al., 2006; McCormick & Flardh, 2012).

Como es de esperar, los genes implicados en la formación de las cubiertas hidrofóbicas están regulados al alza en el MII (Tabla 1), especialmente en las fases tardías (micelio aéreo) (Yague et al., 2013b). Esto mismo se ha confirmado en los experimentos de proteómica cuantitativa realizados en esta tesis doctoral (véase capítulo 1).

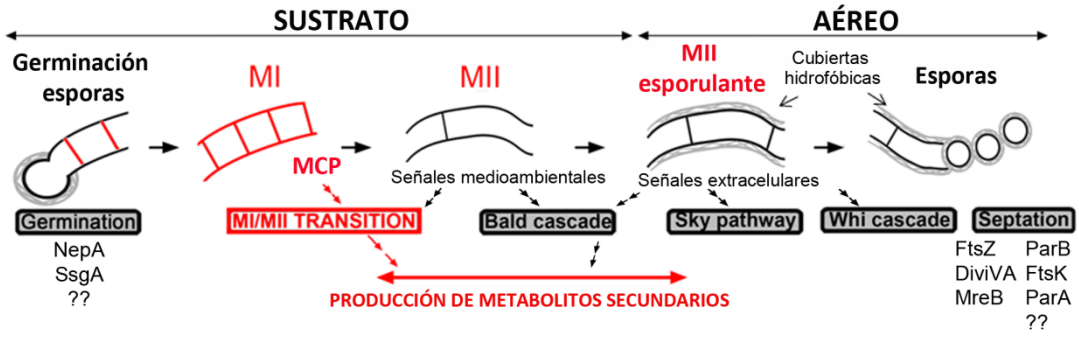

Fig. 6. Principales rutas biomoleculares conocidas de los procesos de diferenciación en *Streptomyces.* Los mecanismos de regulación de las fases pre-esporulantes han sido ignorados tradicionalmente. Adaptado de Yague et al., (2013a).

Tabla 1.

Algunos de los genes clave del desarrollo de *Streptomyces* bien caracterizados por la comunidad científica. Estos genes incluyen reguladores de la síntesis de antibióticos, diferenciación del micelio aéreo y de la esporulación. Adaptado de Claessen et al., (2006); van Wezel & McDowall, (2011); Yague et al., (2013b).

Gen	ID	Referencia
Reguladores negativos de metabolismo secundario expresados al alza en el MI		
cprB	SCO6312	(Onaka et al., 1998)
rrdA	SCO1104	(Ou et al., 2009)
	SCO1712	(Lee et al., 2010)
Reguladores positivos de metabolismo secundario expresados al alza en el MII		
actII-orf4	SCO5085	(Gramajo et al., 1993)
Red	SCO5877	(Feitelson et al., 1985)
dasR	SCO5231	(Rigali et al., 2008)
atrA	SCO4118	(Uguru et al., 2005)
absA1/2	SCO3225-SCO3226	(Anderson et al., 2001)
relA	SCO1513	(Chakraburtty et al., 1996)
rshA	SCO5794	(Sun et al., 2001)
rplK	SCO4648	(Ochi, 1990)
rpoB	SCO4654	(Lai et al., 2002)
cprA	SCO6071	(Onaka et al., 1998)

absR1/2	SCO6992-SCO6993	(Park et al., 2000)
Esa	SCO7699	(Wang et al., 2007)
Genes cuya mutación reporta un fenotipo *bld* al alza en el MI		
bldH (adpA)	SCO2792	(Takano et al., 2003)
Genes cuya mutación reporta un fenotipo bld al alza en el MII		
bldB	SCO5723	(Champness, 1988)
bldC	SCO4091	(Hunt et al., 2005)
bldD	SCO1489	(Elliot et al., 1998)
bldG	SCO3549	(Bignell et al., 2000)
bldK	SCO5112-SCO5116	(Akanuma et al., 2011)
bldM	SCO4768	(Molle & Buttner, 2000)
bldN	SCO3323	(Bibb et al., 2000)
Genes implicados en la formación de cubiertas hidrofóbicas al alza en el MII		
chpC	SCO1674	(Claessen et al., 2003)
chpH	SCO1675	(Claessen et al., 2003)
chpE	SCO1800	(Claessen et al., 2003)
chpG	SCO2699	(Claessen et al., 2003)
chpF	SCO2705	(Claessen et al., 2003)
chpA	SCO2716	(Claessen et al., 2003)
chpD	SCO2717	(Claessen et al., 2003)
chpB	SCO7257	(Claessen et al., 2003)
rdlA	SCO2718	(Claessen et al., 2003)
rdlB	SCO2719	(Claessen et al., 2003)
Genes de esporulación regulados al alza en el MII		
whiB	SCO3034	(Davis & Chater, 1992)
whiD	SCO4767	(Ryding et al., 1999)
whiG	SCO5621	(Mendez & Chater, 1987)
whiE	SCO5314-SCO5621	(Davis & Chater, 1990)
whiH	SCO5819	(Davis & Chater, 1990)
ssgA	SCO3926	(Kawamoto et al., 1997)
ssgB	SCO1541	(Kormanec & Sevcikova, 2002)
parA	SCO3886	(Kim et al., 2000)
parB	SCO3887	(Kim et al., 2000)
mreB	SCO2611	(Burger et al., 2000)
Mbl	SCO2451	(Heichlinger et al., 2011)

3.4 Esporulación

La última fase del desarrollo de *Streptomyces* (en medio sólido) consiste en la producción de esporas a partir de la célula apical de una hifa aérea, llamada también célula esporogénica (Kelemen et al., 1995). Entre la célula esporogénica apical y la célula subapical se encuentra el septo basal cuya formación es un evento clave en el inicio de la esporulación y permite que determinados genes del desarrollo se expresen específicamente en la célula esporogénica (McCormick & Flardh, 2012).

Al igual que la regulación de la formación del micelio aéreo, las rutas biomoleculares que desencadenan la esporulación están muy estudiadas. Se han aislado diversos mutantes afectados en la diferenciación morfológica, incapaces de formar esporas maduras. Entre estos destacan los mutantes *"white"* (blancos), los cuales tienen afectado el proceso de esporulación en diferentes estadios y no llegan a formar esporas maduras con su pigmento gris característico. Algunos genes *whi* activan la expresión de *ftsZ* que es un gen muy estudiado por su papel en la división celular de *Streptomyces*, principalmente durante la esporulación (McCormick et al., 1994). La proteína FtsZ es el principal componente de la maquinaria de división en *Streptomyces* pero existen otras proteínas que intervienen en la regulación de este proceso. Las más importantes son SsgA y SsgB: dos proteínas de la familia SALP con importante papel en morfogénesis y control de la división celular (Kawamoto et al., 1997; Sevcikova & Kormanec, 2003); y las proteínas ParA y ParB requeridas para la segregación del cromosoma (Kim et al., 2000). El modelo de la regulación del ensamblaje de la maquinaria de división celular necesaria para la esporulación está representado en la figura 7. Como ya habíamos visto en el caso de la germinación, SsgA es una proteína que se localiza en los sitios donde van a tener lugar procesos de remodelación de pared. Esta proteína

inicia también el proceso de esporulación localizándose en determinados puntos a lo largo de las hifas esporogénicas del micelio aéreo marcando así los lugares donde se formará un tabique. En ese momento ParA se encuentra recluido en la punta de la hifa. A continuación, SsgB se sitúa en los puntos donde se encuentra SsgA y al mismo tiempo ParA se extiende en forma de filamentos a lo largo de la hifa. En presencia de ParA, ParB forma complejos sobre el ADN que aún no está condensado. Después se ensambla FtsZ en forma de filamentos en espiral a lo largo de la hifa uniéndose a la membrana celular en los puntos donde se encontraba SsgB, y finalmente FtsZ adquiere una conformación de anillo ("*Z-ring*"). Esto es seguido de la condensación y segregación del cromosoma y formación de los septos de esporulación formados por membrana y pared celular (Flardh & Buttner, 2009; Jakimowicz & van Wezel, 2012; Willemse et al., 2011) (Figura 7).

Una vez que tiene lugar la septación, el siguiente paso es el engrosamiento de la pared. En este proceso intervienen proteínas del llamado complejo de síntesis de pared donde las proteínas MreB y Mbl son las más representativas (Heichlinger et al., 2011). También intervienen en la esporulación proteínas cuya función es mantener la integridad génica dentro de la espora como las proteínas asociadas a nucleoides Dps o HupS (Facey et al., 2009; Salerno et al., 2009). Por último WhiE se encarga de la síntesis del pigmento gris que se deposita en la espora madura (Davis & Chater, 1990). Tras la maduración de las esporas SsgA se sitúa a los lados de los septos marcando los futuros sitios de germinación (Willemse et al., 2011) (Figura 7).

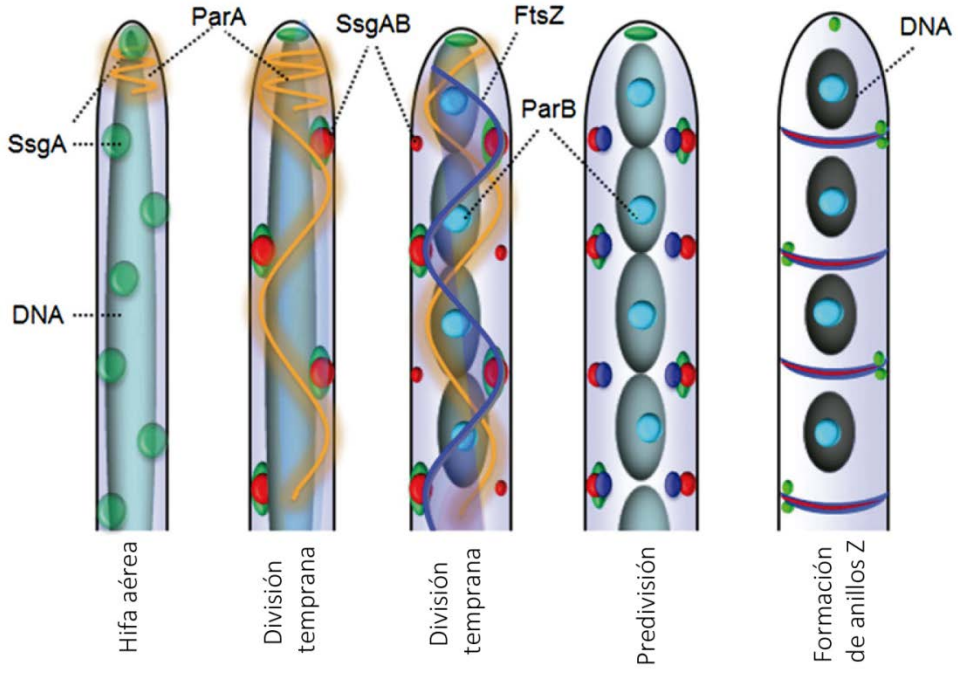

Fig 7. Modelo de regulación de la maquinaria de división celular que controla la formación de anillos Z formados durante la esporulación. Adaptado de Willemse et al., (2011).

Como es de esperar, los genes de división celular específicos de esporulación están expresados al alza en las fases de MII (Tabla 1), especialmente en las fases de MII tardío (Yague et al., 2013b). Esto mismo se ha corroborado en los experimentos de proteómica realizados en esta tesis doctoral (capítulo 1). Tal como se describirá más adelante, en esta tesis se demostró la existencia de proteínas de división celular no específicas de la esporulación, como por ejemplo FtsZ, reguladas al alza durante las fases de MI, como es de esperar para un micelio totalmente compartimentalizado (véase capítulo 1).

4. Aplicaciones industriales de la diferenciación de *Streptomyces.*

4.1 Búsqueda de nuevos metabolitos secundarios (*"screening"*)

Tal como se introdujo anteriormente, la búsqueda de nuevos metabolitos secundarios fue muy productiva durante la llamada "Edad de oro de los antibióticos." A finales del siglo XX, cada vez se hacía más difícil encontrar nuevos fármacos y el "screening" a partir de la naturaleza fue mayoritariamente sustituido por aproximaciones de ingeniería genética como la síntesis combinatorial.

Al mismo tiempo que se ha estancado el descubrimiento de nuevos metabolitos secundarios, las resistencias de los microorganismos a los antibióticos existentes están aumentando drásticamente, y como consecuencia, existen algunas infecciones extremadamente difíciles de tratar. Este escenario supone un gran peligro para la humanidad ya que se corre el riesgo de volver a una situación parecida a la que había antes del descubrimiento de los antibióticos donde existía una alta mortalidad por infecciones. Aunque existen métodos para frenar esta crisis, como las mejoras en los procedimientos sanitarios, el uso racional de los antibióticos disponibles y el uso de terapias alternativas (como fagos, vacunas, etc.), el descubrimiento de nuevos antibióticos es una prioridad ya que es la mejor opción para luchar contra las resistencias (Coates et al., 2011).

En la última década los procesos de *"screening"* se están retomando, y poco a poco van apareciendo nuevos compuestos bioactivos como oxazolidonas, lipopéptidos, mutilinas, tres prometedores grupos de compuestos que pueden ser usados como "esqueletos químicos" para la síntesis de nuevos antibióticos (Figura 8). Estos compuestos se

descubrieron hace dos décadas, pero sus aplicaciones clínicas han sido exploradas recientemente (Fischbach & Walsh, 2009). Otros antibióticos y "esqueletos químicos" están siendo descubiertos como la platensimicina, aislada de *Streptomyces platensis* (Allahverdiyev et al., 2013), o la teixobactina, un antibiótico aislado recientemente de bacterias no cultivables (Ling et al., 2015). En la última década, sólo dos antibióticos han sido llevados a la clínica para el tratamiento de enfermedades sistémicas: daptomicina, un lipopéptido (Hair & Keam, 2007) y linexolid, una oxazolidona (Zappia et al., 2007).

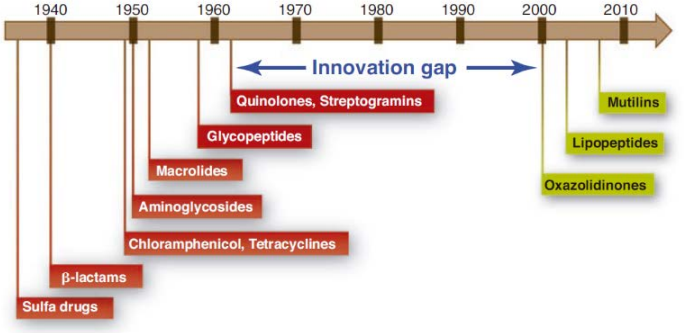

Fig. 8. Descubrimientos de los antibióticos más importantes a lo largo del tiempo. Véase también figura 1. (Fischbach & Walsh, 2009).

La mayoría de los estreptomicetos producen de 2 a 5 metabolitos secundarios en el laboratorio. No obstante, análisis genómicos recientes han revelado que los actinomicetos, incluidas las especies que no producen ningún compuesto bioactivo detectable en el laboratorio, tienen en su genoma una media de 30 rutas para la producción de metabolitos secundarios (Genilloud, 2014), es decir, existe una gran cantidad de cepas cuyo potencial biosintético está aún por explorar. En la actualidad muchos grupos de investigación y compañías biotecnológicas están poniendo sus esfuerzos en tratar de activar estas rutas crípticas.

Hay muchos grupos de investigación trabajando en la búsqueda de inductores (*"elicitors"*) que activan o reprimen específicamente rutas

biosintéticas: nutrientes como la glucosa, xilosa, pequeñas moléculas como el N-acetil glucosamina, fosfatos, etc. (Liu et al., 2013) (Figura 9). Por lo que uno de los enfoques para llevar a cabo este nuevo "screening" e intentar activar rutas biosintéticas que no pudieron ser activadas en los procesos clásicos de "screening", consistiría en modificar los medios de cultivo utilizando este tipo de moléculas reguladoras (Liu et al., 2013).

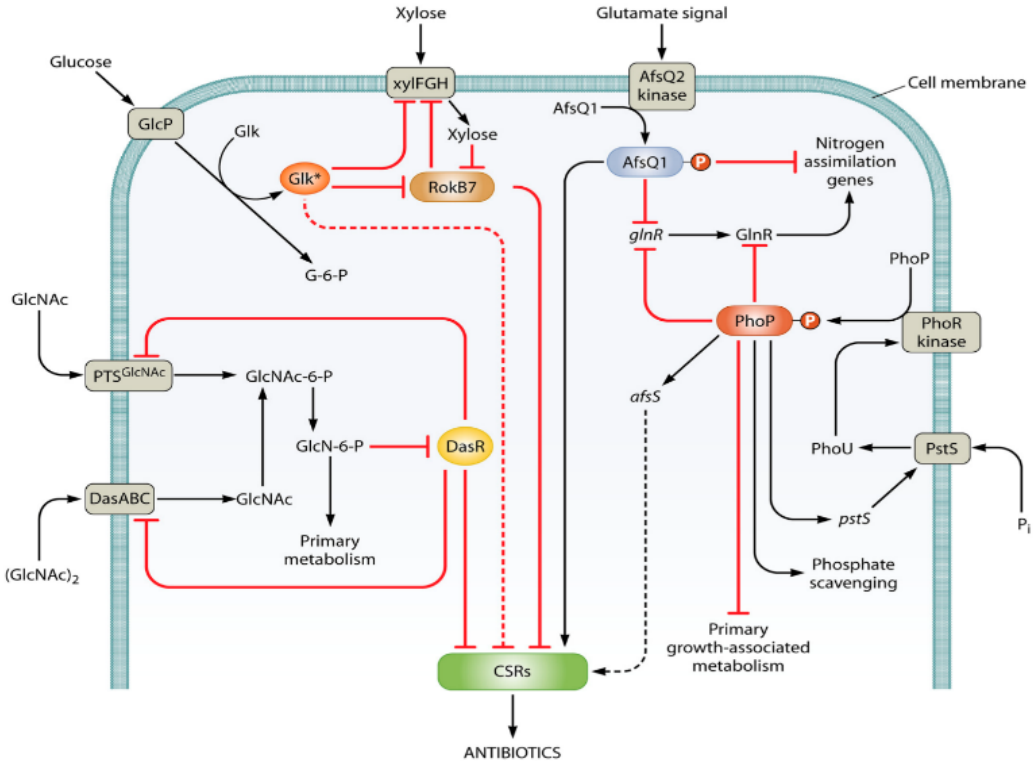

Fig. 9. Esquema de los nutrientes y señales que son reguladores de la producción de antibióticos en *S. coelicolor* (Liu et al., 2013).

Otra estrategia utilizada en la actualidad para la activación de rutas crípticas es la realización de co-cultivos de diferentes especies, intentando reproducir con ello lo que ocurre en la naturaleza donde los microorganismos de diferentes especies co-existen formando complejas comunidades microbianas. Con esto se ha visto que se puede conseguir

una mejora en la producción de compuestos ya conocidos y/o la acumulación de algunos compuestos crípticos que no son detectados en condiciones normales de laboratorio (Marmann et al., 2014). Todas estas y otras estrategias de activación de rutas crípticas son llevadas a cabo en el contexto del ciclo de vida tradicional y puestas a punto mediante optimización empírica. Sin embargo, no se está teniendo en cuenta la diferenciación del MII que aparece con el nuevo modelo de desarrollo de *Streptomyces* (Figura 10). Como se introdujo arriba, la fase de MII es la fase productora de metabolitos secundarios por lo que la diferenciación de este micelio puede ser una de las claves para activar la producción. Este nuevo enfoque está por el momento inexplorado, pero puede complementar las otras estrategias: no hay producción de metabolitos secundarios sin diferenciación de MII, pero existen rutas biosintéticas que además de la diferenciación del MII necesitan señales específicas para su activación. Un abordaje multidisciplinar será posiblemente la opción de futuro para abordar los procesos de búsqueda de nuevos metabolitos secundarios a partir de cepas naturales de estreptomicetos.

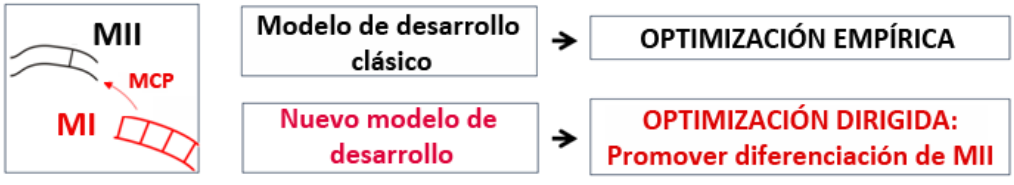

Fig. 10. Optimización del desarrollo de *Streptomyces* durante el *"screening"*. Ciclo de desarrollo tradicional (en negro): no hay diferenciación y la optimización es empírica. Nuevo modelo de desarrollo (en rojo): la optimización está dirigida hacia la diferenciación del MII.

En esta tesis doctoral se ha explorado la aplicabilidad del ciclo de desarrollo de *Streptomyces* (la diferenciación de un MII productor de

metabolitos secundarios) a la optimización de las fermentaciones en biorreactores a escala piloto (véase capítulo 3).

5. Síntesis y remodelación de la pared celular

5.1 Características y composición de la pared celular de *Streptomyces*

La pared celular de las bacterias es una estructura compleja cuya función es proteger a los organismos del entorno, pero permitiendo el paso selectivo de nutrientes al interior y deshechos al exterior de las células. En 1884 Christian Gram desarrolló una tinción que permite clasificar a las bacterias en dos grupos: Gram negativas y Gram positivas. Ambos grupos se diferencian en la composición de su pared celular (Gram, 1884) (Figura 11).

Las bacterias Gram negativas tienen una pared celular más compleja que consta principalmente de tres capas: una membrana externa, una pared de peptidoglicano y la membrana citoplasmática o membrana interna. Entre las dos membranas existe un compartimento acuoso llamado periplasma. Otra característica típica de las Gram negativas es que en su membrana externa tienen lipopolisacáridos con un importante papel como barrera.

Las bacterias Gram positivas, a diferencia de las Gram negativas, no tienen membrana externa en su pared. Además, la malla de peptidoglicano es mucho más gruesa, siendo el componente mayoritario de la pared. Este peptidoglicano se encuentra atravesado por polímeros llamados ácidos teitoicos (Silhavy et al., 2010).

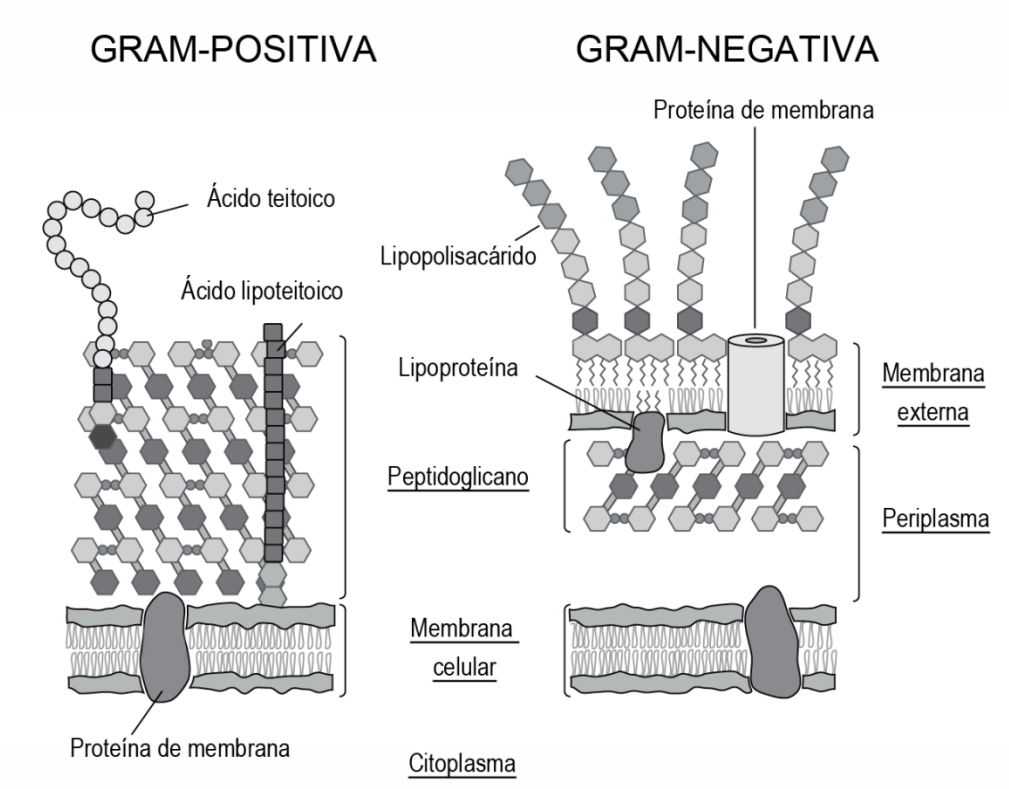

Fig. 11. Esquema comparativo de la estructura de la pared celular de Gram positivas y Gram negativas. Adaptado de Silhavy et al., (2010)

Streptomyces forma parte del grupo de las bacterias Gram positivas por lo que el peptidoglicano es el componente más importante de su pared. El peptidoglicano es un polímero lineal estructurado en capas que forman una red tridimensional. Cada cadena de peptidoglicano está formada por un muropéptido que consiste en la repetición de un disacárido: el ácido N-acetilmurámico (NAM) y la N-acetilglucosamina (NAG) unidos por enlace glicosídico β-(1,4). Cada molécula de NAM tiene unida una cadena peptídica, que puede contener de tres a cinco aminoácidos. Los muropéptidos se unen entre sí por enlaces entre estas cadenas peptídicas llamados enlaces *"crosslinking"*. Los aminoácidos que

participan en estos enlaces cambian entre distintas especies, por lo que puede usarse como criterio taxonómico (Schleifer & Kandler, 1972).

En el caso de *Streptomyces coelicolor,* la cadena peptídica unida a las moléculas de NAM consiste en un pentapéptido formado por los aminoácidos: L-alanina (L-Ala), ácido D-isoglutámico (D-iglu), ácido L,L-diaminopimélico (L,LA2pm) y dos D-alaninas terminales (D-Ala-D-Ala) (Figura 12A). El L,LA2pm está unido por su grupo amino a una glicina (Pethe et al., (2010), lo que genera una ramificación de la estructura troncal del pentapéptido. Aunque esta es la estructura principal, existen polimorfismos en la composición de los monoméros de muropéptido que forman el peptidoglicano de *S. coelicolor* (Figura 12A). Uno de estos polimorfismos consiste en que parte del NAM está N-deacetilado (NAM-Ac). Además las cadenas laterales de aminoácidos pueden consistir en dipéptidos, tripéptidos, tetrapéptidos o pentapéptidos. Por último, el α-carboxilo del D-iglu de la segunda posición de la cadena lateral de aminoácidos está parcialmente amidado (Figura 12A). También existen polimorfismos en los enlaces "*crosslinking"* debido a la coexistencia de enlaces generados por D,D-transpeptidasas (enlaces 4 -3) y L,D-transpeptidasas (enlaces 3-3) (Hugonnet et al., 2014) (Figura 12B).

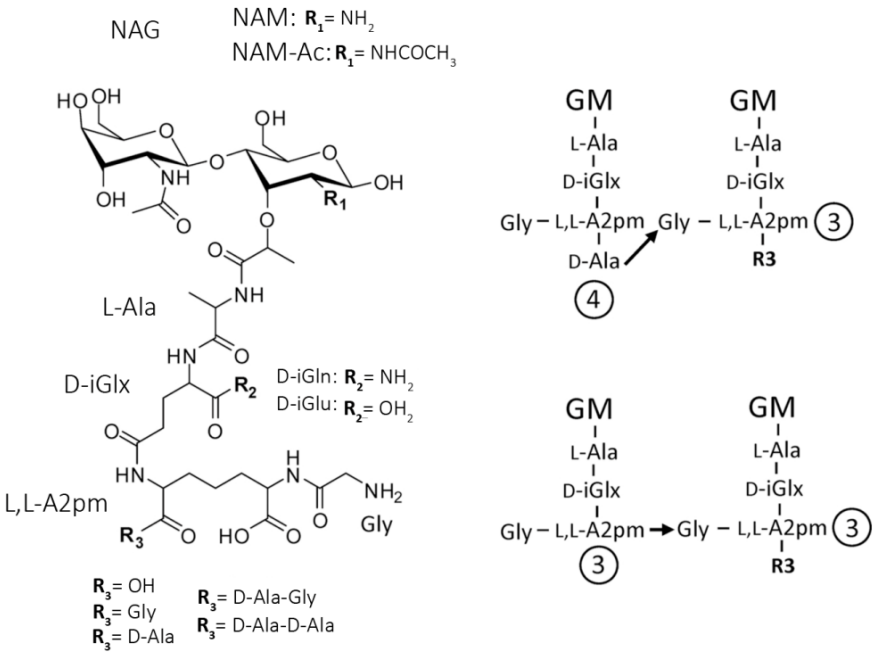

Fig. 12. Estructura del peptidoglicano de *S. coelicolor.* A. Tres tipos de polimorfismos en los monómeros de muropéptido. B. Dos polimorfismos en dímeros de muropéptidos. Adaptado de Hugonnet et al., (2014)

5.2 Proteínas de unión a penicilina: PBPs

Las PBPs, del inglés "*penicillin binding proteins",* son una familia de proteínas con un origen evolutivo común cuya función es sintetizar y remodelar la malla de peptidoglicano. Una característica que comparten todas ellas es que su actividad es inhibida por antibióticos β-lactámicos como la penicilina. Estas proteínas tienen actividad aciltransferasa y existen varios tipos según las reacciones que catalizan (Ghosh et al., 2008) (Figura 13):

- **Transglicosilasas**: catalizan la polimerización de las cadenas de peptidoglicano formadas por NAG y NAM.
- **Transpeptidasas**: catalizan la formación de los enlaces "*crosslinking"* entre las cadenas de peptidoglicano. En el caso de *S.*

coelicolor, estos enlaces se crean entre la D-Ala de la cuarta posición de la cadena lateral de aminoácidos de una cadena de peptidoglicano y la Gly del L,L-A2pm de la otra cadena liberando en el proceso la D-Ala terminal de la primera cadena.

- **Carboxipeptidasas**: eliminan la D-Ala terminal del pentapéptido de la cadena lateral de aminoácidos.
- **Endopeptidasas**: hidrolizan los enlaces "*crosslinking".*

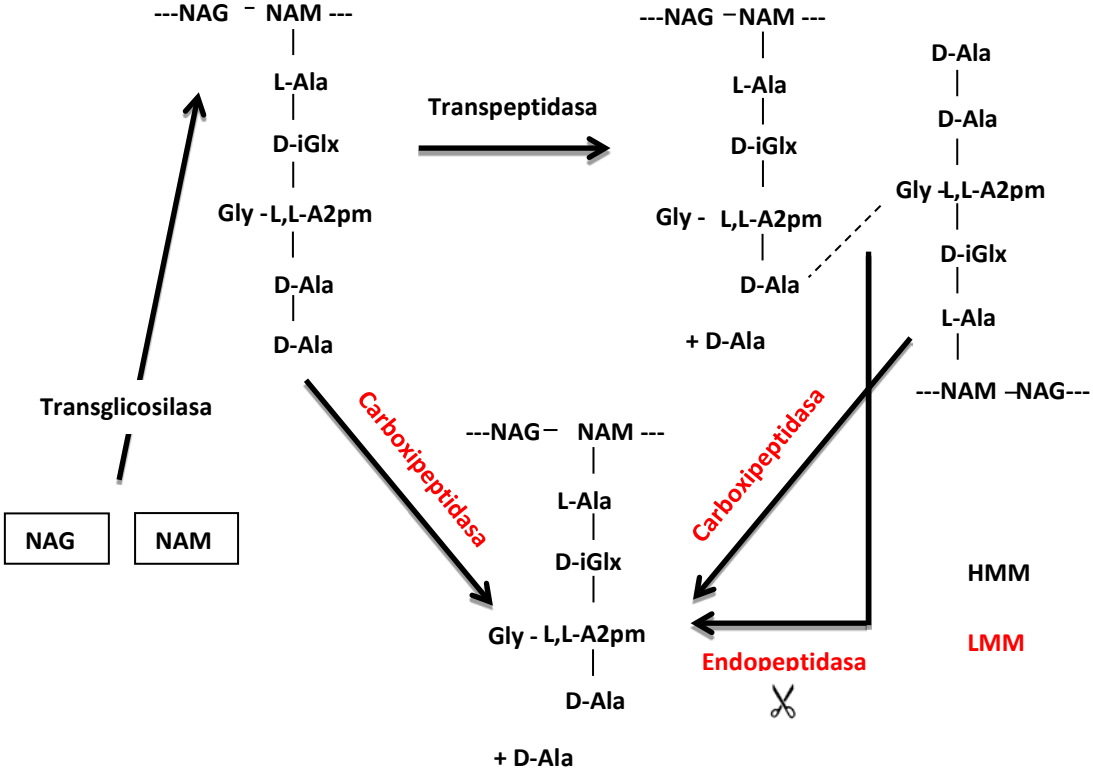

Fig. 13. Diagrama de los diferentes tipos de PBPs indicando la actividad que lleva a cabo cada una de ellas en la síntesis y remodelación del peptidoglicano de *S. coelicolor*. Línea discontínua: enlaces *"crosslinking"*. En negro aparecen las PBPs de alto peso molecular (HMM-PBPs) y en rojo las PBPs de bajo peso molecular (LMM-PBPs).

Las PBPs se clasifican en función de su peso molecular. Las de alto peso molecular: HMM-PBPs (*High Molecular Mass PBPs*) se dividen a su vez en dos tipos: las de clase A consisten en enzimas bifuncionales que poseen dos dominios, uno transglicosilasa y otro transpeptidasa, que les permiten llevar a cabo ambas acciones de forma independiente; y las de clase B son transpeptidasas monofuncionales. Las HMM-PBPs son esenciales para la bacteria ya que se encargan de la síntesis del peptidoglicano. Las PBPs de bajo peso molecular: LMM-PBPs (*Low Molecular Mass PBPs)* son carboxipeptidasas o endopeptidasas monofuncionales y suelen encontrarse ancladas a la membrana. LMM-PBPs generalmente no son esenciales y se encargan de regular la cantidad de enlaces "*crosslinking"* del peptidoglicano (Nemmara et al., 2011; Ogawara, 2015).

En general, las bacterias tienen múltiples PBPs con actividades redundantes. Las HMM-PBPs son las más estudiadas debido a que son esenciales para la viabilidad de la bacteria. Las Actinobacterias tienen una media de cinco genes que codifican para HMM-PBPs por genoma. En el caso de *Streptomyces coelicolor* el número asciende a trece: cuatro de clase A y nueve de clase B (Tabla 2) (Ogawara, 2015). Los genes que codifican para algunas de estas PBPs se encuentran muy próximos a genes de proteínas de la familia SEDS ("*shape, elongation, división and sporulation"*). Las proteínas SEDS son proteínas necesarias para el crecimiento, división y viabilidad celular. Se cree que la asociación de PBPs y SEDS en determinadas regiones génicas implica una relación funcional. Las parejas SEDS-PBPs colaborarían facilitando la remodelación del peptidoglicano que ocurre durante las fases de crecimiento y división (Meeske et al., 2016). *Streptomyces coelicolor* contiene cuatro "*clusters"* SEDS y cada uno de ellos incluye una transpeptidasa (HMM-PBPs clase B) (Mistry et al., 2008) (Figura. 14 y tabla 2).

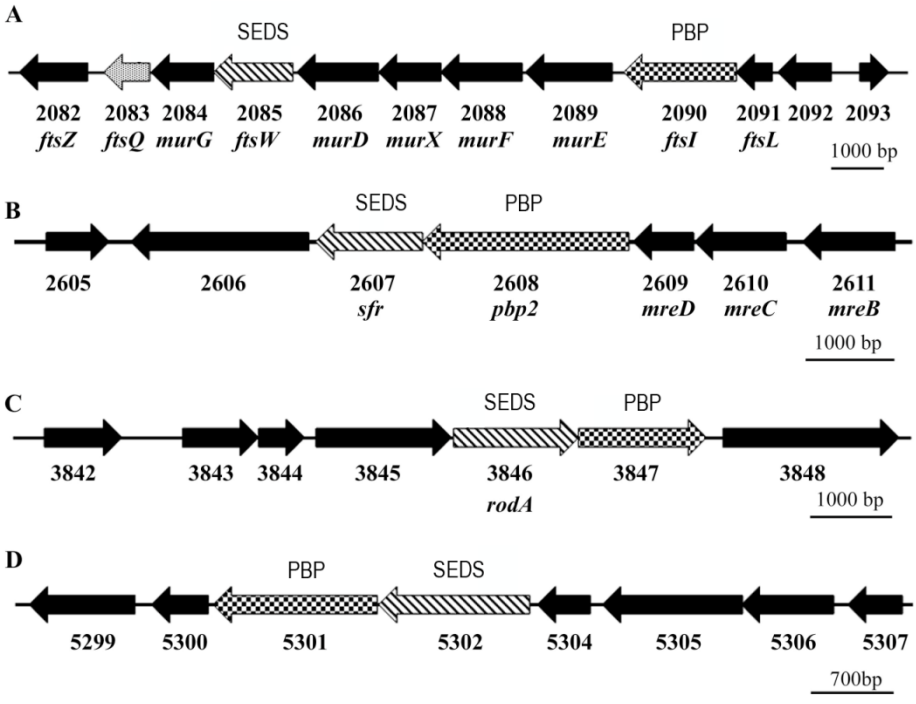

Fig. 14. Organización génica de los cuatro "*clusters"* de SEDS en *Streptomyces coelicolor*. En cada "*cluster"* está indicado el gen que codifica para la proteína SEDS en patrón rayado y el gen de la PBP asociada en patrón de cuadros. Adaptado de (Mistry et al., 2008).

Tabla 2

13 genes que codifican para HMM-PBPs en *S. coelicolor*. En negrita se indican los genes que se encuentran en "*clusters* SEDS" y el gen que codifica para la proteína SEDS a la que se asocian (Mistry et al., 2008; Ogawara, 2015).

HMM-PBPs en *S. coelicolor*		
Gen	**Tipo de PBP**	**SEDS asociado**
SCO2897	HMM-A	-
SCO3580	HMM-A	-
SCO3901	HMM-A	-
SCO5039	HMM-A	-
SCO1875	HMM-B	-
SCO2090 (*ftsI*)	**HMM-B**	**SCO2085 (*ftsW)***
SCO2608 (*pbp2)*	**HMM-B**	**SCO2607 (*sfr)***

SCO3156	HMM-B	-
SCO3157	HMM-B	-
SCO3771	HMM-B	-
SCO3847	**HMM-B**	**SCO3846 (RodA)**
SCO4013	HMM-B	-
SCO5301	**HMM-B**	**SCO5302**

Las proteínas LMM-PBPs son consideradas dispensables para el crecimiento y la viabilidad. Debido a esto, estas proteínas están poco estudiadas. Esta tesis doctoral ha contribuido a conocer más sobre la función biológica de este grupo de proteínas mediante la caracterización del gen SCO4439 que codifica para una carboxipeptidasa (véase capítulo 2a).

5.3 La pared celular como diana de antibióticos

Los antibióticos actúan frente a dianas celulares específicas en las bacterias a las que se enfrentan. Muchos de ellos tienen como diana la pared celular bacteriana. Estos antibióticos afectan a la síntesis del peptidoglicano de la pared y provocan con ello la muerte de la bacteria.

Dentro de este grupo de antibióticos los más conocidos son los β-lactámicos (como la penicilina) que actúan uniéndose a las PBPs e inhibiendo su actividad. Otro grupo de antibióticos que también actúan inhibiendo la síntesis del peptidoglicano son los glucopéptidos (como la vancomicina o la teicoplanina). Su mecanismo de acción consiste en la unión del antibiótico a la D-alanil-D-alanina (D-Ala-D-Ala) terminal de la cadena lateral de aminoácidos impidiendo con ello que la transpeptidasa lleve a cabo la formación de los enlaces "*crosslinking*" (Reynolds, 1989) (Fig. 15A).

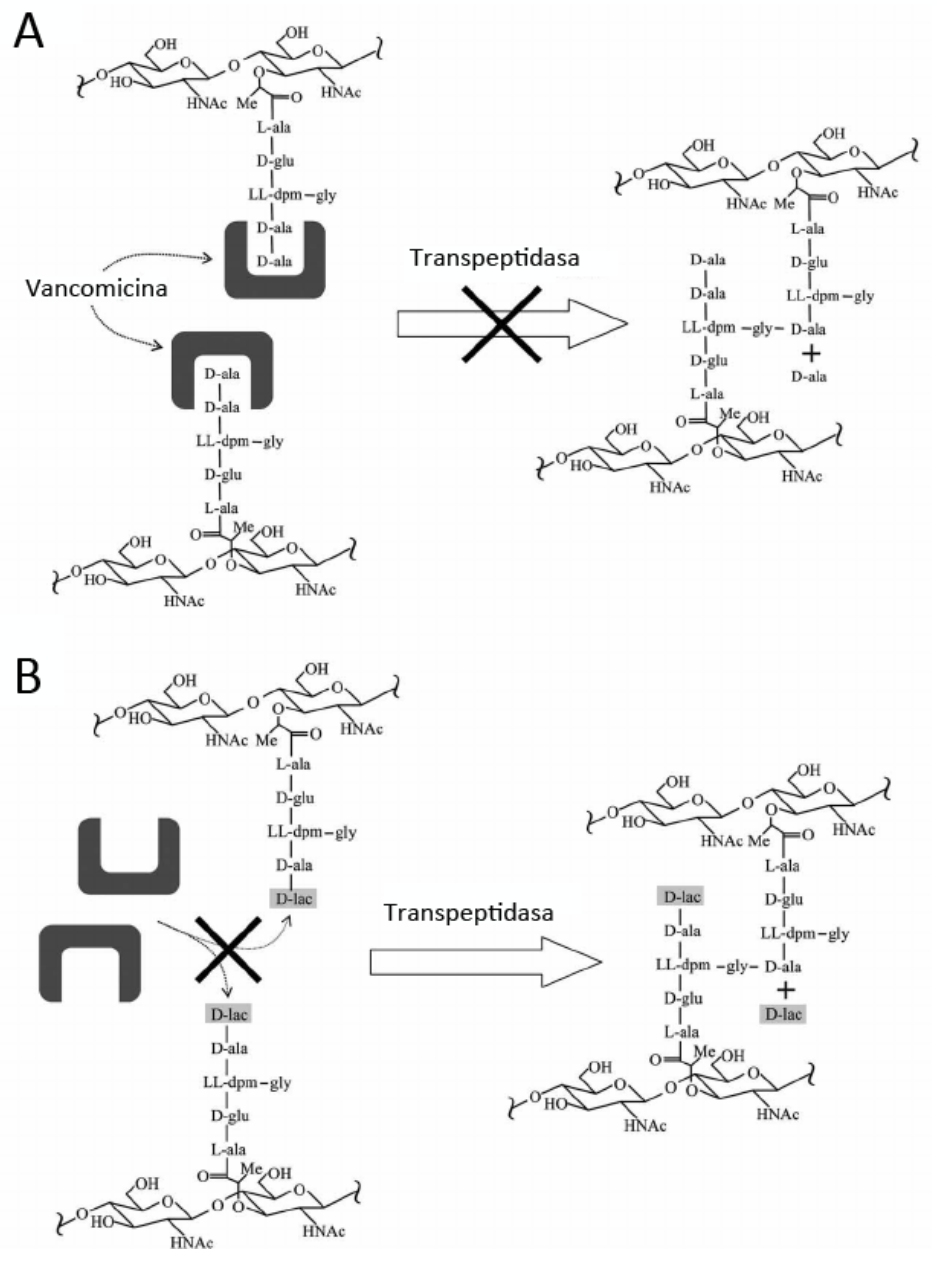

Fig. 15. A. Mecanismo de acción del antibiótico glicopéptido vancomicina. B. Principal mecanismo de resistencia a vancomicina. Adaptado de Hong et al., (2008).

Frente a estos mecanismos de acción, las bacterias han desarrollado sus propios sistemas de defensa. Los mecanismos de resistencia a estos

antibióticos es un tema de gran interés en los últimos años debido al aumento de patógenos resistentes causantes de infecciones nosocomiales. Uno de los más estudiados es la vancomicina. Este antibiótico se ha considerado durante más de cuarenta años el mejor tratamiento para cepas de *Staphylococcus aureus* resistentes a meticilina, principal causante de muerte por infecciones adquiridas en hospitales, pero su uso excesivo ha llevado a la aparición de cepas de *S. aureus* resistentes a vancomicina (Chang et al., 2003).

Los mecanismos de resistencia a glucopéptidos han sido muy estudiados sobre todo en actinomicetes productores de estos antibióticos como *Streptomyces toyocaensis* y *Actinoplanes teichomyceticus* donde la activación de esta resistencia previene la autotoxicidad (Hong et al., 2008). El mecanismo más común de resistencia a vancomicina consiste en la conversión del dipéptido D-Ala-D-Ala terminal de la cadena lateral de aminoácidos del peptidoglicano en D-Ala-D-lactato (D-Lac). La afinidad de la vancomicina por D-Ala-D-lac es mil veces menor que por D-Ala-D-Ala (Fig. 15B).

Esto es posible gracias a la activación de los genes *van*. El gen *vanH* codifica para una deshidrogenasa que cataliza la conversión de piruvato en D-Lac, *vanA* codifica para una D-Ala-D-Lac ligasa y *vanX* codifica para una DD-dipeptidasa que rompe el dipéptido D-Ala-D-Ala remanente. La activación de la transcripción de estos genes sólo ocurre en presencia de vancomicina y está regulada por el sistema de dos componentes VanR-VanS. El receptor quinasa (VanS) se une a la vancomicina y activa al regulador de respuesta VanR que a su vez activa la transcripción del operón vanHAX. El número de genes presentes en el "*cluster*" de resistencia puede variar, pero el núcleo siempre consiste en estos cinco genes *vanSRHAX* (Hong, Hutchings et al. 2008).

Streptomyces coelicolor fue el primer microrganismo no patógeno y no productor de vancomicina en el que se han encontrado genes de resistencia a vancomicina (Fig.16) (Hong et al., 2004). El "*cluster"* de resistencia en *S. coelicolor* consiste en siete genes divididos en cuatro unidades de transcripción: *vanRS* (SCO3589-90), *vanJ* (SCO3592), *vanK* (SCO3593) y *vanHAX* (SCO3594-96). Este "*cluster"* contiene dos genes: *vanK* y *vanJ* que no habían sido descritos en otros "*clusters"* de resistencia a vancomicina. La proteína VanK pertenece a la familia de proteínas Fem que son peptidiltransferasas no ribosómicas cuya función es añadir los aminoácidos que forman ramificaciones en la estructura troncal del pentapéptido; en concreto VanK se encarga de unir la ramificación de glicina a la cadena del pentapéptido cuando el aminoácido terminal es D-Lac en lugar de D-Ala (Hong et al., 2004). VanJ es una proteína de membrana que a pesar de estar codificada en el "*cluster"* de genes *van*, se ha visto que no es necesaria para generar la resistencia a vancomicina. Sin embargo, parece que está involucrada en la resistencia a teicoplanina (Novotna et al., 2012).

Existen muchos estudios enfocados a aumentar el conocimiento de estos mecanismos de resistencia. Recientemente se ha demostrado que la resistencia a vancomicina en *S. coelicolor* depende, al menos en parte, de la concentración de fosfato inorgánico (Pi) en el medio (Santos-Beneit & Martıín, 2013). En los últimos años se ha caracterizado también una nueva D-D-carboxipeptidasa involucrada en la resistencia a glucopéptidos en *Nonomuraea sp.* (Binda et al., 2012). En esta tesis doctoral se ha caracterizado la actividad y función biológica de SCO4439, una D-D-carboxipeptidasa de *S. coelicolor*. Se ha visto que esta proteína está relacionada con la resistencia a los antibióticos glucopéptidos vancomicina y teicoplanina (véase capítulo 2a).

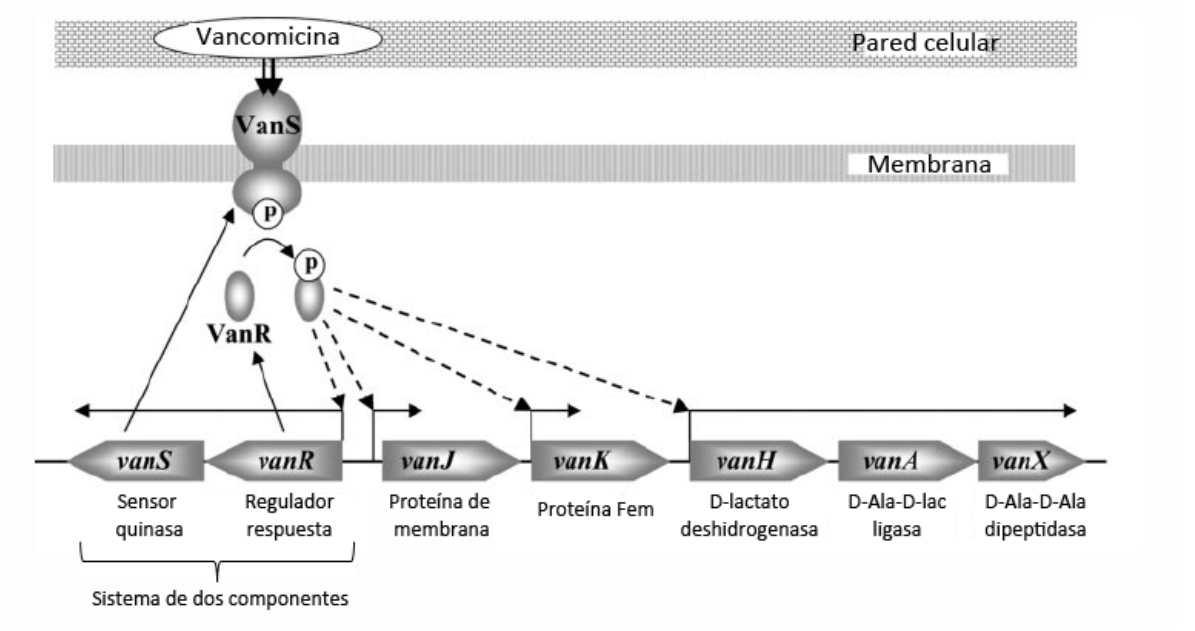

Fig. 16. Organización y regulación del "*cluster"* de genes *van* de *S. coeliolor* que confiere resistencia a vancomicina. Adaptado de Hong et al., (2005).

6. Biología de sistemas: fundamentos en proteómica

Durante las últimas décadas el desarrollo de proyectos de secuenciación de ADN, como el Proyecto Genoma humano, ha llevado al desarrollo de nuevas técnicas en el campo de la biotecnología. Estas técnicas han permitido un mayor entendimiento de los sistemas biológicos a nivel molecular. Sin embargo, no podemos considerar a los organismos como compartimentos moleculares aislados. Debido a esto, se ha desarrollado un nuevo enfoque en el que se plantea una visión global de los procesos biológicos. Esto ha dado lugar a la llamada era "ómica". El sufijo –oma significa "conjunto de", y las técnicas "ómicas" cubren las nuevas aproximaciones de análisis masivo de los procesos biológicos. Debido al gran volumen de información que se genera con este tipo de aproximaciones a gran escala, son necesarias potentes técnicas

estadísticas e informáticas que nos ayuden a interpretar los datos obtenidos, por lo que la bioinformática se convierte en imprescindible detrás del desarrollo de cualquier ciencia "ómica" y es necesaria para la integración de las mismas.

Las principales "ómicas" desarrolladas durante los últimos años son: la **genómica** (estudia el contenido, la organización, la función y la evolución de la información molecular del ADN contenida en los genomas); la **transcriptómica** (estudia el conjunto de ARNm que existe en una célula, tejido u órgano de forma que se muestra qué genes se están expresando en un momento dado); la **proteómica** (es el estudio a gran escala de las proteínas, en particular de su abundancia, estructura y función) y la **metabolómica** (estudia los metabolitos, es decir, las moléculas de bajo peso molecular que se encuentran en los sistemas biológicos en un momento dado).

La proteómica y fosfoproteómica de *Streptomyces* han sido una parte fundamental de esta tesis doctoral, por lo que esta introducción sobre las "ómicas" se restringirá a la proteómica.

6.1 Proteómica

Tal como se adelantaba arriba, la proteómica consiste en el estudio del proteoma de las células. El término "proteoma" viene de la fusión de "proteína" y "genoma" y fue acuñado por Marc Wilkins en 1994 (Wilkins, 2009). La proteómica es un campo de estudio muy importante para comprender los procesos biológicos ya que las proteínas son los efectores principales de las rutas metabólicas de las células.

6.1.1 Evolución de la proteómica

La proteómica clásica se desarrolla mediante el uso de geles bidimensionales (2D) y posterior identificación de las proteínas por su

"huella peptídica" (Figura 17). En un primer paso, la mezcla de proteínas se separa en geles 2D en función de su tamaño y su punto isoeléctrico; de esta forma cada punto (*"spot")* se corresponde con una proteína. Cada una de estas proteínas se digiere con tripsina que corta en secuencias concretas dando un patrón diferente en cada proteína; esto es lo que se conoce como huella peptídica. El análisis de los fragmentos trípticos de cada proteína se lleva a cabo mediante espectrometría de masas (MALDI-TOF) que permite separar cada fragmento en función de su masa/carga. Finalmente, las proteínas se identifican gracias a una base de datos que incluye todos los posibles fragmentos trípticos de cada proteína del organismo analizado en base a la secuencia de su ADN cromosómico. Aunque estas técnicas siguen dando muy buenos resultados, tienen importantes limitaciones siendo el tiempo una de las más importantes sobre todo si se quieren realizar experimentos de proteómica a gran escala.

Estas técnicas de proteómica clásica, basadas en geles 2D, siguen usándose en estudios proteómicos a pequeña/mediana escala en diversos organismos incluyendo *Streptomyces* (Hesketh et al., 2007; Kim et al., 2005; Rodriguez-Garcia et al., 2007; Wu et al., 2016).

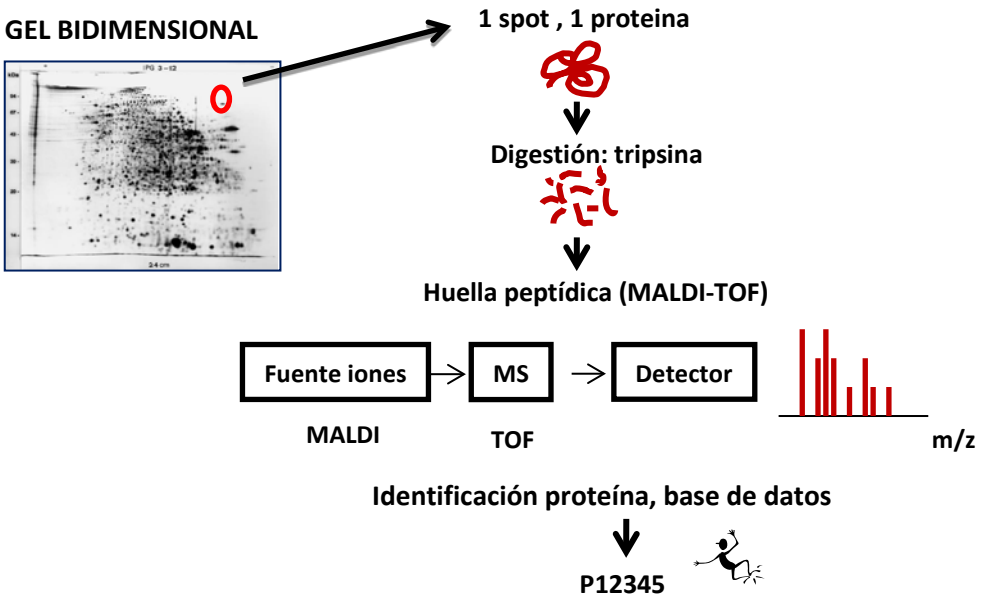

Fig. 17. Esquema en el que se representa el fundamento de la "proteómica clásica".

Los avances llevados a cabo en los últimos tiempos en las técnicas de cromatografía y espectrometría de masas han llevado al desarrollo de las técnicas de proteómica libres de gel que consisten en técnicas de nano-HPLC combinadas con espectrometría de masas en tándem (LC-MS/MS). Estas técnicas han revolucionado el campo de la proteómica ya que permiten el análisis de muestras complejas con una gran rapidez en comparación con las técnicas de proteómica clásica. El fundamento se esquematiza en la figura 18. El extracto de proteínas de partida se digiere con tripsina. Una vez digerido, la mezcla de fragmentos trípticos se separa en un nano HPLC en función de sus características fisicoquímicas; este paso es necesario para fraccionar la muestra de partida en muestras más sencillas. Cada fracción cromatográfica se ioniza mediante un electrospray y se introduce en el primer espectrómetro de masas (MS1) donde se separan los diferentes péptidos en función de su masa/carga. Una vez

separados los péptidos, el equipo es capaz de elegir un solo péptido y llevarlo a una celda de colisión donde es fraccionado en multitud de fragmentos. Estos fragmentos entran en el segundo espectrómetro de masas (MS2) donde se separan permitiendo deducir la secuencia de aminoácidos de los péptidos, que finalmente, gracias a las bases de datos, nos lleva a identificar las proteínas de partida.

Durante los últimos años se han desarrollado grandes avances en las técnicas de LC-MS/MS que han llevado al diseño de instrumentos muy potentes, con gran sensibilidad y resolución. También se ha avanzado muchísimo en herramientas bioinformáticas que permitan gestionar toda esta información.

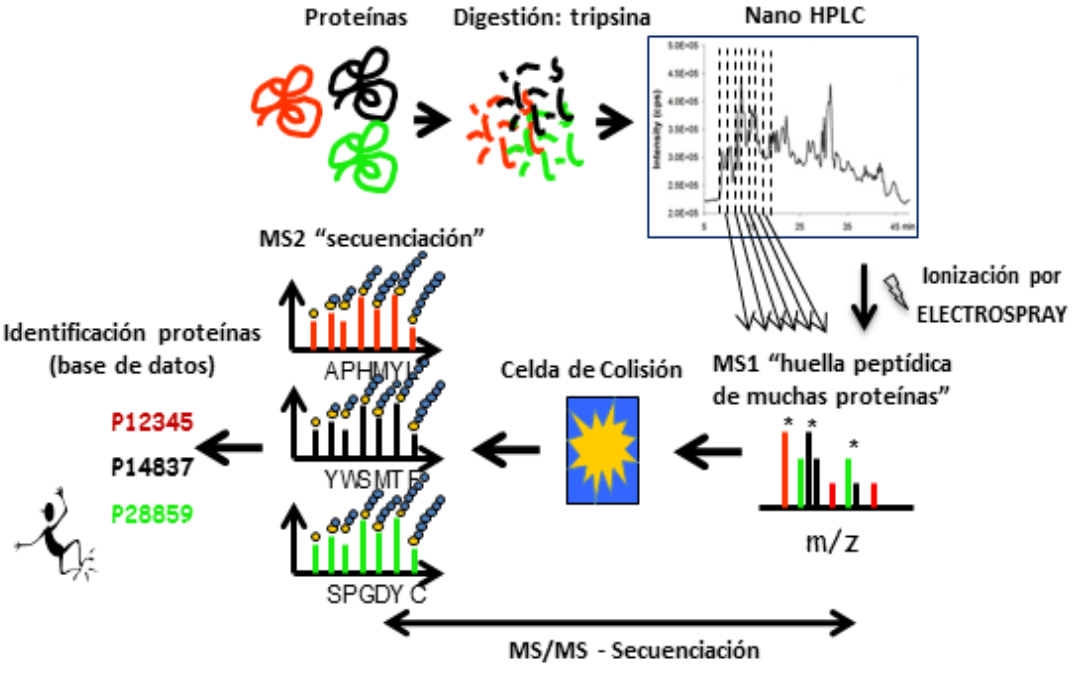

Fig. 18. Esquema en el que se representa el fundamento de las técnicas de "proteómica avanzada" libre de gel (LC-MS/MS).

6.1.2 Proteómica cuantitativa

Una vez que las proteínas han sido identificadas, puede ser útil determinar la cantidad de cada proteína presente en la muestra ya sea de forma absoluta o relativa. Las técnicas de proteómica de hoy en día permiten realizar estos estudios cuantitativos de los proteomas en experimentos de proteómica a gran escala libres de gel.

Una de las técnicas más utilizadas actualmente en proteómica cuantitativa es la cuantificación relativa mediante marcaje isobárico. Estos marcadores consisten en isótopos estables de la misma molécula. La masa total de las diferentes moléculas de marcaje es la misma, lo que cambia es la distribución de esta masa. Estas moléculas constan de dos elementos principales: el "*mass reporter"* que es la parte que permite diferenciar una molécula de otra por pequeñas diferencias en la masa y el "*mass normaliser"* que es la parte que compensa las diferencias de masa del "*mass reporter"* haciendo que la masa total sea en todas las moléculas la misma. Ambos elementos están unidos por un enlace que tiene tendencia a romperse en las condiciones de fragmentación usadas en el espectrómetro de masas. De esta forma, aunque todos los reactivos tengan la misma masa, al fragmentarse se generan *"reporters"* de distinta masa que permiten identificar la muestra de partida.

El fundamento de esta técnica se esquematiza en la figura 19. Tras la digestión de las muestras proteicas con tripsina, los péptidos resultantes de cada una de ellas se marcan con uno de los reactivos de marcaje isobárico. Una vez marcada cada muestra con un reactivo diferente, se mezclan en una misma muestra. El siguiente paso es inyectar esa mezcla en el LC-MS/MS. En el MS1 se separan los diferentes péptidos. Cada uno de estos péptidos es llevado a la celda de colisión donde se fragmentan y es en esta fragmentación donde se rompe el enlace del marcador isobárico

que libera la parte del "*mass reporter*". Finalmente, el MS2 además de identificar el péptido, permite cuantificar qué cantidad de ese péptido procede de cada muestra gracias a los pesos moleculares e intensidades de los iones "*reporter*" (Figura 19). Esta sería una cuantificación relativa ya que permite comparar la intensidad de un mismo péptido en las diferentes muestras.

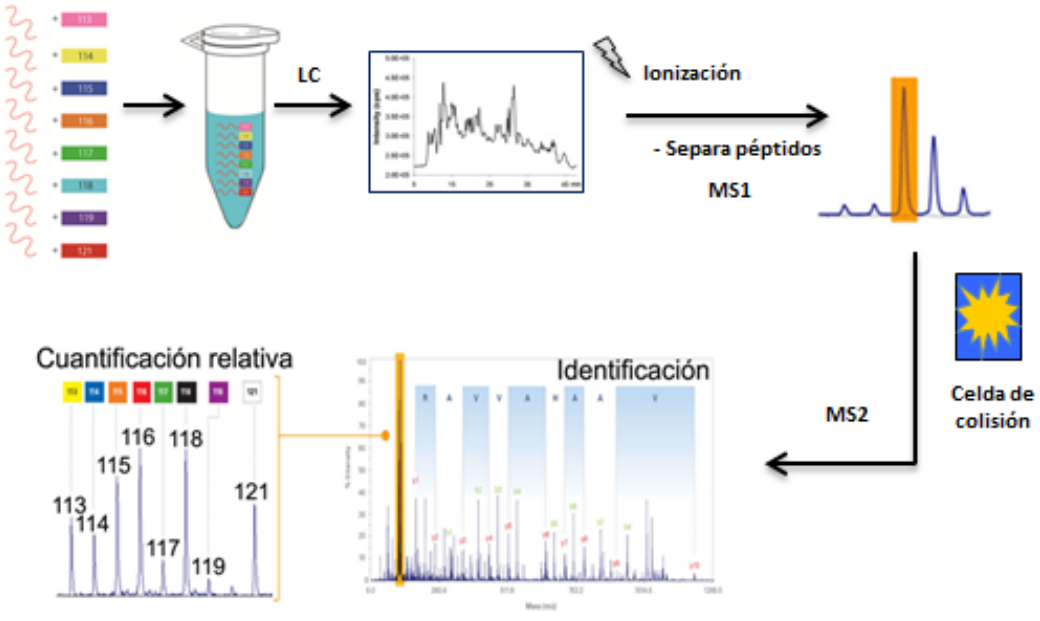

Fig. 19. Esquema en el que se representa el fundamento de la técnica de proteómica cuantitativa mediante marcaje de masa isobárico (iTRAQ o TMT).

Existen varios tipos de marcaje de masa isobárico. Los más utilizados son el iTRAQ y el TMT. El marcaje iTRAQ ("*Isobaric tags for absolute and relative quantification*") permite el marcaje de hasta 8 muestras diferentes ya que existen 8 isótopos diferentes de la molécula (8plex). Por otro lado, el TMT ("*Tandem mass tags*") permite marcar hasta 10 muestras diferentes (10plex). Esta es la principal ventaja del TMT frente al iTRAQ. Sin embargo las diferencias de masa entre los diferentes isótopos en TMT son

muy pequeñas (6mDa), mucho menores que en el caso del iTRAQ (1Da) por lo que se requieren espectrómetros de masa con alta resolución y precisión que puedan resolver estos iones (Chahrour et al., 2015; Rauniyar & Yates, 2014).

Existen pocos estudios a gran escala de proteómica cuantitativa en *Streptomyces*. Los primeros trabajos en los que se caracteriza la variación del proteoma durante el desarrollo fue llevada a cabo por Jayapal et al., (2008); Manteca et al., (2010a); Manteca et al., (2010b). Más adelante Gubbens et al., (2012) analizó la variación del proteoma bajo diferentes condiciones nutricionales. En este último trabajo se cuantificó la variación de 2000 proteínas, que corresponde al 25,6% del proteoma de *S. coelicolor.* Esta cifra constituyó un récord en proteómica cuantitativa de *Streptomyces*, sólo superado por el trabajo de proteómica cuantitativa realizado en esta tesis doctoral (véase capítulo 1).

6.1.3 Modificaciones postraduccionales: fosfoproteómica

Las modificaciones postraduccionales de una proteína son cambios químicos ocurridos en ésta después de su síntesis por los ribosomas. Estas modificaciones juegan un papel muy importante en casi todos los procesos celulares. Existen diferentes tipos de modificaciones postraduccionales. Las más comunes son: glicosilación, fosforilación, ubiquitinación y acilación.

Las técnicas actuales de proteómica permiten estudiar y caracterizar estas modificaciones. Para ello, previo al análisis por LC-MS/MS es necesario enriquecer la muestra en proteínas con la modificación de interés. Se han desarrollado diferentes técnicas de enriquecimiento dependiendo del tipo de modificación. En esta introducción nos centraremos en la fosfoproteómica, que es la técnica que se usó en esta tesis (véase capítulo 1).

La fosfoproteómica estudia el conjunto de proteínas fosforiladas o fosfoproteoma de una célula, tejido u organismo. La fosforilación de proteínas en residuos de serina (Ser), treonina (Thr), tirosina (Tyr) e histidina (His) es una de las modificaciones postraduccionales más importantes en la naturaleza ya que está implicada en la regulación de multitud de procesos celulares. Esto hace que existan gran cantidad de estudios de fosfoproteómica, sobre todo en eucariotas. En procariotas la fosforilación en histidina es la más frecuente. Sin embargo, es lábil a los ácidos y, por tanto, indetectable con la mayoría de las metodologías usadas en proteómica. La fosforilación de Ser/Thr/Tyr es mucho menos frecuente en procariotas que en eucariotas lo que hace que el estudio de fosfoproteómica en bacterias sea un reto hoy en día. Debido a esto, optimizar las técnicas de enriquecimiento en fosfoproteínas en procariotas es especialmente importante.

Existen multitud de técnicas de fosfoenriquecimiento, algunas de las más usadas son cromatografía de afinidad con metal inmovilizado (IMAC) (Thingholm & Jensen, 2009) y enriquecimiento por dióxido de titanio (TiO2) (Thingholm et al., 2006). Durante los últimos años, utilizando estas dos técnicas o variantes de las mismas, se han realizado estudios de fosfoproteómica a gran escala en diferentes organismos procariotas: *E. coli* (Lim et al., 2015; Macek et al., 2008; Soares et al., 2013), *Streptococcus pneumonia* (Sun et al., 2010), *Klebsiella pneumoniae* (Lin et al., 2009), *Lactococcus lactis* (Soufi et al., 2008), *Pseudomonas* (Ravichandran et al., 2009), *Bacillus subtilis* (Macek et al., 2007; Ravikumar et al., 2014), *Halobacterium salinarum* (Aivaliotis et al., 2009), *Corynebacterium acetobutylicum* (Bai & Ji, 2012), *Streptomyces coelicolor* (Manteca et al., 2011; Parker et al., 2010), *Mycobacterium tuberculosis* (Prisic et al., 2010), *Listeria monocytogenes* (Misra et al., 2011), *Helicobacter pylori* (Ge et al., 2011), *Rhodopseudomomas palustris* (Hu et al., 2012), *Thermus*

termophilus (Takahata et al., 2012), *Acinetobacter baumanii* (Soares et al., 2014), *Staphylococcus aureus* (Basell et al., 2014) y *Saccharopolyspora erythraea* (Licona-Cassani et al., 2014). Todos ellos parten de grandes cantidades de proteína y llegan a detectar baja cantidad de fosfopéptidos (Tabla 3). El que mayor eficiencia muestra en este sentido es el trabajo realizado por (Manteca et al., 2011). Esto es gracias a que en este estudio se optimizó el fosfoenriquecimiento con TiO2 realizando un enriquecimiento previo mediante precipitación con fosfato cálcico (CPP), lo que cuadriplicó el número de fosfopéptidos identificados (Manteca et al., 2011)

Tabla 3

Comparación de fosfoproteomas publicados de diferentes organismos, incluyendo *S. coelicolor*. Está indicada la cantidad total de proteína usada para el análisis y el número total de fosfopéptidos, fosfoproteínas y sitios de fosforilación identificados. El trabajo de Manteca et al. (2011) (en negrita), en el que se realiza un preenriquecimiento con CPP, es el más eficiente.

	Bacteria	Proteína (mg)	Fosfoproteínas	Fosfopéptidos	Sitios de fosforilación	Referencia
Gram +	***S. coelicolor***	**0.3**	**127**	**260**	**289**	**(Manteca et al., 2011)**
	S. coelicolor	50	40	44	46	Parker et al., 2010
	S. erythraea	10	88	109	n.r.	Licona-Cassani et al., 2014
	B. subtilis	10	78	103	78	Macek et al., 2007
	B. subtilis	12	139	177	144	Ravikumar et al., 2014
	C. acetobutylicum	2	61	82	107	Bai & Ji, 2012
	L. lactis	20	63	102	79	Soufi et al., 2008
	M. tuberculosis	n.r.	301	380	500	Prisic et al., 2010
	S. pneumoniae	1	84	102	163	Sun et al., 2010

	L. monocytogenes	10	112	155	143	(Misra et al., 2011)
	L. monocytogenes	8	191	256	242	(Misra et al., 2011)
	S. aureus	50	108	n.r.	76	(Basell et al., 2014)
Gram -	*E. coli*	20	79	105	81	Macek et al., 2008
	K. pneumoniae	30	81	117	93	Lin et al., 2009
	P. aeruginosa	1.2	39	57	61	Ravichandran et al., 2009
	P. putida	1.2	59	56	55	Ravichandran et al., 2009
	H. pylori	n.r.	67	82	126	Ge et al., 2011
	R. palustris (Ch)	2	54	100	63	Hu et al., 2012
	R. palustris (Ph)	2	42	74	59	Hu et al., 2012
	T. thermophilus	100	48	52	46	Takahata et al., 2012
	E. coli	9.8	133	n.r.	108	Soares et al., 2013
	E. coli	10	n.r	34	n.r.	Lim et al., 2015
	A. baumanii Abh12O-A2	9	70	n.r.	80	Soares et al., 2014
	A. baumanii ATCC 17879	9	41	n.r.	48	Soares et al., 2014
Archaea	*H. salinarum*	20	26	42	31	Aivaliotis et al., 2009
Eukarya	*H. sapiens*	6	7832	>50000	38229	(Sharma et al., 2014)

Los estudios de fosfoproteómica cuantitativa en bacterias son escasos y en nuestro conocimiento sólo hay seis trabajos de este tipo: un trabajo de cuantificación sin marcaje ("label-free") en *S. coelicolor* (Manteca et al., 2011); tres estudios de cuantificación mediante marcaje de los aminoácidos del medio de cultivo con isótopos estables (SILAC) realizados en *E. coli* (Soares et al., 2013), *Bacillus subtilis* (Ravikumar et al., 2014) y *Listeria monocytogenes* (Misra et al., 2014) y por último dos

trabajos en los que la cuantificación se hace mediante monitorización de reacción seleccionada (SRM) realizados en *E.coli* (Lim et al., 2015) y en *Saccharopolyspora erythraea* (Licona-Cassani et al., 2014).

Streptomyces coelicolor contiene 47 proteínas quinasas de tipo eucariótico predichas que son el doble de las que hay en otras bacterias conocidas como *E.coli* o *Bacillus subtilis*, lo que hace de *Streptomyces* un buen modelo para estudiar la fosforilación en bacterias. En esta tesis se llevó a cabo un estudio de fosfoproteómica cuantitativa en *S. coelicolor* siendo esta la primera vez que se realiza fosfoproteómica cuantitativa utilizando marcaje de masa isobárico (TMT) en bacterias (véase capítulo 1).

OBJETIVOS

Los objetivos globales de esta tesis son caracterizar las rutas biomoleculares que regulan los procesos de diferenciación y MCP en *Streptomyces,* centrándose principalmente en las fases no contempladas en el ciclo de vida tradicional; y analizar estos procesos de diferenciación en fermentaciones industriales a escala piloto.

Para ello se establecieron cuatro objetivos que se corresponden con los cuatro capítulos que forman parte de esta tesis:

1. **Analizar los cambios en el proteoma y fosfoproteoma durante la diferenciación de *S. coelicolor*.**

   Manuscrito 1:

   Rioseras B, Shliaha PV, Gorshko V, Yagüe P, López-García MT, Gonzalez-Quiñonez N, Rogowska-Wrzesinska A, Jensen ON, Manteca Á. "Proteome and phosphoproteome variations accompanying *Streptomyces coelicolor* differentiation in solid sporulating cultures". In preparation.

2. **Estudiar las modificaciones de la pared celular que tienen lugar durante las fases de esporulación y germinación.**

   Manuscrito 2:

   Rioseras B, Yagüe P, López-García MT, Gonzalez-Quiñonez N, Binda E, Marinelli F, Manteca A. 2016. "Characterization of SCO4439, a D-alanyl-D-alanine carboxypeptidase involved in spore cell wall maturation, resistance, and germination in *Streptomyces coelicolor*". Sci Rep. 6:21659.

3. **Caracterizar los procesos de división celular y compartimentalización durante la fase vegetativa temprana (fase de MI).**

Manuscrito 3:

Yagüe P, Willemse J, Koning RI, **Rioseras B**, López-García MT, Gonzalez-Quiñonez N, Lopez-Iglesias C, Shliaha PV, Rogowska-Wrzesinska A, Koster AJ, Jensen ON, van Wezel GP, Manteca A. 2016. "Subcompartmentalization by cross-membranes during early growth of *Streptomyces hyphae*". Nat Commun. 7:12467

4. **Analizar los procesos de desarrollo, diferenciación y producción de antibiótico en fermentaciones industriales a escala piloto (biorreactores de 2L).**

Manuscrito 4:

Rioseras B, López-García MT, Yagüe P, Sánchez J, Manteca A. 2014. "Mycelium differentiation and development of *Streptomyces coelicolor* in lab-scale bioreactors: Programmed cell death, differentiation, and lysis are closely linked to undecylprodigiosin and actinorhodin production". Bioresour Technol. 151:191-198.

TRABAJO EXPERIMENTAL

CAPTÍTULO 1

Análisis de los cambios en el proteoma y fosfoproteoma durante la diferenciación de *S. coelicolor*.

Como se introdujo anteriormente, el nuevo ciclo de desarrollo de *Streptomyces* incluye una nueva fase (MI) que hasta entonces había pasado desapercibida (Manteca & Sanchez, 2009). Durante la última década nuestro grupo de investigación realizó varios trabajos en los que se comparan los transcriptomas y proteomas de esta nueva fase con los de las fases de micelio ya conocidas tradicionalmente (MII sustrato y aéreo) (Manteca et al., 2010a; Manteca et al., 2010b; Manteca et al., 2011; Yague et al., 2013b; Yague et al., 2014). El rango dinámico de los trabajos de transcriptómica fue muy bueno, cuantificándose la variación de un 50% del transcriptoma de *Streptomyces* (Yague et al., 2013b), sin embargo, en el caso de la proteómica sólo se llegó a un 8% del proteoma (Manteca et al., 2010a; Manteca et al., 2010b), y en el caso de las fosfoproteómica no se pudo cuantificar la abundancia de los fosfopéptidos y fosfoproteínas (Manteca et al., 2011).

Este trabajo se planteo con el fin de mejorar los resultados obtenidos en los trabajos previos de proteómica y fosfoproteómica. Esta mejora fue posible principalmente debido a que durante los últimos años han tenido lugar importantes mejoras en las técnicas e instrumentos utilizados.

Conocer las diferencias en el proteoma y fosfoproteoma a lo largo del desarrollo puede ser muy útil para identificar proteínas clave en la regulación del desarrollo.

Este objetivo se aborda en una publicación:

Manuscrito 1:

Rioseras B, Shliaha PV, Gorshko V, Yagüe P, López-García MT, Gonzalez-Quiñonez N, Rogowska-Wrzesinska A, Jensen ON, Manteca A. "Proteome and phosphoproteome variations accompanying *Streptomyces coelicolor* differentiation in solid sporulating cultures". In preparation.

Proteome and phosphoproteome variations accompanying *Streptomyces coelicolor* differentiation in solid sporulating cultures

Beatriz Rioseras[1,a], Pavel V Shliaha[2,a], Vladimir Gorshkov[2], Paula Yagüe[1], María T López-García[1], Nathaly Gonzalez-Quiñonez[1], Adelina Rogowska-Wrzesinska[2], Ole N Jensen[2,b] & Ángel Manteca[1,b]

Streptomyces **is a multicellular bacterium with a complex developmental cycle. It is one of the bacteria with the largest number of genes encoding for Ser/Thr/Tyr kinases, and constitutes an outstanding model for the study bacterial Ser/Thr/Tyr phosphorylation. Here we report the first isobaric-tag labelling quantitative phosphoproteomic study in bacteria, specifically in *Streptomyces coelicolor*. The non-phosphorylated proteome was used as reference to normalise phosphoproteomic quantitative data. The variation in the abundance of 3462 non-phosphorylated proteins (44.3% of *S. coelicolor* proteome) was quantified along differentiation. 91 phosphopeptides and 89 phosphorylation sites from 47 phosphoproteins were identified. 59 peptides from 34 proteins were differentially phosphorylated during development, including peptides from key regulatory proteins as DasR (SCO5231) or RarA (SCO1630), as well as cell-division proteins as DivIVA (SCO2077) or FtsZ (SCO2082). 13 non-regulatory proteins and 19 proteins with unknown function were also differentially phosphorylated during development. This work reports the largest database about proteome variations during *Streptomyces* development, as well as the first quantitative database of Ser/Thr/Tyr phosphorylation variations accompanying *Streptomyces* differentiation. Data are available via ProteomeXchange with identifier PXD005558.**

Streptomyces is a Gram-positive soil bacterium of great importance for biotechnology given their ability to produce a large array of bioactive compounds, including antibiotics, anticancer agents, immunosuppressants, as well as industrial enzymes (1). Streptomyces has a complex morphogenesis which includes hypha differentiation and sporulation. After spore germination, a fully compartmentalized mycelium (MI) (2) initiates development until it undergoes an ordered programmed cell death (PCD) (3) and differentiates to a second multinucleated mycelium (substrate mycelium, early MII) which starts to express the chaplin and rodlin genes encoding the proteins constituting the hydrophobic coats necessary to growth into the air (aerial mycelium; late MII) (4). At the end of the cycle, there is hypha septation and sporulation.

Limited number of publications reported proteomics analysis of Streptomyces. The first works aimed to characterize proteome variations during development were performed by Jayapal et al. (5) and Manteca et al. (6, 7). Later, Gubbens et al. (8) analysed Streptomyces proteome variations under different nutritional conditions, reporting the most efficient quantitative proteomic work in Streptomyces so far (2000 proteins, 25.6% of *S. coelicolor* proteome).

Reversible protein phosphorylation at serine, threonine, and tyrosine is a well-known dynamic post-translational modification with stunning regulatory and signalling potential in eukaryotes (9). In contrast, the extent and biological function of Ser/Thr/Tyr protein phosphorylation in bacteria is poorly defined.

1 Área de Microbiología, Departamento de Biología Funcional e IUOPA, Facultad de Medicina, Universidad de Oviedo, 33006 Oviedo, Spain.
2 Department of Biochemistry and Molecular Biology and VILLUM Center for Bioanalytical Sciences, University of Southern Denmark, Campusvej 55, DK-5230, Odense M, Denmark.
[a] These authors contributed equally to this work
[b] These authors contributed equally to this work

The abbreviations used are: LC/MS/MS, Liquid Chromatography-Mass Spectrometry-Mass Spectrometry; PCD, programmed cell death; CPP, calcium phosphate precipitation; TMT, tandem mass tag.

Phosphorylation in bacteria is dramatically lower than in eukaryotes, making bacterial phosphoproteomics challenging. Several large-scale Ser/Thr/Tyr phosphoproteome studies in bacteria have been reported recently: for E. coli (10), Streptococcus pneumonia (11), Klebsiella pneumoniae (12), Lactococcus lactis (13), Pseudomonas (14), Bacillus subtilis (15), Halobacterium salinarum (16) , Corynebacterium acetobutylicum (17), *Streptomyces coelicolor* (18, 19), Mycobacterium tuberculosis (20), Listeria monocytogenes (21), Helicobacter pylori (22), Rhodopseudomomas palustris (23), Thermus termophilus (24), Acinetobacter baumanii (25), and Staphylococcus aureus (26). Most of the bacterial phosphoproteomic studies used large amounts of protein (milligrams) obtained during the vegetative growth to detect relatively low number of phosphopeptides (Table I). This precludes application of isobaric mass tagging quantitation strategies, since labelling such large amount of peptides is prohibitively expensive. Hence quantitative phosphoproteomics is even harder, and in our knowledge, there were only six quantitative phosphoproteomic studies in bacteria: the label-free quantitative phosphoproteomics performed in *S. coelicolor* (18); the stable isotope labelling by amino acids in cell culture (SILAC) works performed in E. coli (27), B. subtillis (28) and L. monocytogenes (29); and the scheduled reaction monitoring analyses performed in E. coli (30) and S. erythraea (31).

Streptomyces coelicolor, the model Streptomyces strain (32), has 47 predicted eukaryotic-like protein kinases, twice the number of kinases predicted from genomes of other well characterized bacteria, including E. coli and Bacillus subtilis, and constitutes an outstanding model for the study bacterial Ser/Thr/Tyr phosphorylation (18). Here we investigated the changes of *S. coelicolor* proteome and phosphoproteome during differentiation in solid sporulating cultures at three timepoints (hour 16, 30 and 65). To our knowledge results presented here, constitute the first isobaric-tag labelling quantitative phosphoproteomic study in bacteria. The developmental stages analysed by proteomics, were identical to those analysed by transcriptomics previously (33), which allowed us to make unprecedented direct comparison between the *S. coelicolor* proteome and transcriptome.

EXPERIMENTAL PROCEDURES

Bacterial Strains and Media - *S. coelicolor* M145 strain was used in this study (32). Solid cultures were grown on Petri dishes (8.5 cm) with 25 mL of solid GYM medium (glucose, yeast/malt extract) (34) that were covered with cellophane disks, inoculated with 100 µL of a spore suspension (1 x 107 viable spores/mL), and incubated at 30 ºC.

Sampling of S. coelicolor cells throughout the Differentiation Cycle - The mycelial lawns of *S. coelicolor* M145 grown on cellophane disks were scraped off at different time points using a plain spatula. Samples were lysed by boiling in 2% SDS, 50 mM pH 7 Tris-HCl, 150 mM NaCl, 10 mM MgCl2, 1 mM EDTA, 7 mMβ-mercaptoethanol, EDTA-free Protease Inhibitor Cocktail Tablets from Roche, and 1% phosphatase inhibitor mixtures 1 and 2 (Sigma); sample viscosity was reduced by sonication (MSE soniprep 150, in four cycles of 10 s, on ice); cell debris were discarded after centrifugation at 20,000gs for 10 minutes; the sample was cleaned by precipitation with acetone/ethanol (sample/EtOH/acetone 1:4:4 v/v/v overnight at -20 ºC; washing with EtOH/acetone/H2O 2:2:1 v/v/v); resuspended in water; dialyzed against large volumes of water (1 h at 4 ºC with four water changes); quantified by the (35); lyophilized in aliquots of 100 µg; and stored at -80 ºC.

Protein digestion and analysis of the proteolysis - Lyophilized proteins were dissolved in 8 M urea 100 mM TEAB buffer. Protein concentrations were measured by bicinchoninic acid assay and adjusted to 2 mg of protein per mL. Samples were reduced with 5 mM DTT at RT for 1 hour; S-alkylated with 15 mM iodoacetamide (15-30 minutes at RT in darkness); the alkylation reaction was stopped adding DTT up to 10mM; 300-µg of protein were digested using a combined trypsin/LysC digestion protocol (36); samples were

TABLE I.

Comparison of *S. coelicolor* phosphoproteome with other Published Prokaryotic and human phosphoproteomes. Notice that the two experiments performed in our lab (18) using CPP pre-enrichment were the most efficient ones.

	Bacterium	Protein (mg)[1]	Phospho proteins	Phospho peptides	Phosphorylation sites	Reference
Gram +	*S. coelicolor*	0.1	47	91	72	This work
	S. coelicolor	0.3	127	260	289	(18)
	S. coelicolor	50	40	44	46	(19)
	S. erythraea	10	88	109	n.r.	(31)
	B. subtilis	10	78	103	78	(15)
	B. subtilis	12	139	177	144	(28)
	C. acetobutylicum	2	61	82	107	(17)
	L. lactis	20	63	102	79	(13)
	M. tuberculosis	n.r.	301	380	500	(20)
	S. pneumoniae	1	84	102	163	(11)
	L. monocytogenes	10	112	155	143	(21)
	L. monocytogenes	8	191	256	242	(29)
	S. aureus	50	108	n.r.	76	(26)
Gram -	*E. coli*	20	79	105	81	(10)
	K. pneumoniae	30	81	117	93	(12)
	P. aeruginosa	1.2	39	57	61	(14)
	P. putida	1.2	59	56	55	(14)
	H. pylori	n.r.	67	82	126	(22)
	R. palustris (Ch)	2	54	100	63	(23)
	R. palustris (Ph)	2	42	74	59	(23)
	T. thermophilus	100	48	52	46	(24)
	E. coli	9.8	133	n.r.	108	(27)
	E. coli	10	n.r	34	n.r.	(30)
	A. baumanii Abh12O-A2	9	70	n.r.	80	(25)
	A. baumanii ATCC 17879	9	41	n.r.	48	(25)
Archaea	*H. salinarum*	20	26	42	31	(16)
Eukarya	*H. sapiens*	6	7832	>50000	38229	(87)

N.r. Not reported. 1 The total amount of protein used for all the MS/MS or 2D gel experiments is indicated.

desalted using Oasis HLB solid reverse-phase columns (Waters).

TMT labelling - Samples were labelled using TMT-10-plex reagent (ThermoFisher). The 30- and 65-hour samples were analysed in biological triplicate, and the 16-hour samples were analysed in quadruplicate. Peptide concentration was quantified by amino acid analysis (37). For each condition, 60 µg of peptides was labelled with 0.5 mg of TMT-10-plex reagent following the manufacturer's protocol. The samples were then combined.

Phosphoenrichment - Phosphopeptides were pre-enriched using calcium phosphate precipitation (CPP) as previously described Zhang et al. and Manteca et al. (18, 38). 100 µg of TMT labelled peptides were precipitated using CPP and desalted using reverse phase chromatography

(POROS R3 resin), prior to TiO2 enrichment (18). The optimal proportion between TiO2 beads and peptides was tested using 100 µg of CPP pre-enriched TMT labelled peptides and different amounts of TiO2 beads.

LC-MS/MS - 50 µg of TMT labelled peptides were fractionated by hydrophilic interaction liquid chromatography (HILIC) to generate twelve fractions. Each of the fractions was analysed by LC-MS/MS on EasyLC system (Thermo) coupled to Orbitrap-Fusion-LUMOS. The LC aqueous mobile phase contained 0.1% (v/v) formic acid in water, and the organic mobile phase contained 0.1% (v/v) formic acid in 95% (v/v) acetonitrile. Before injection the trap and analytical columns were pre-equilibrated with 15 and 3.5µls buffer A respectively. The samples were injected on a custom 3-cm trap column (100-µM internal diameter silica tubing packed with Reprosil 120 C18 5-µM particles) and desalted with 18 µl of buffer A. Separation was performed on a home-made 20-cm column (75-µM internal diameter silica tubing packed with Reprosil 120 C18 3-µM particles) with a pulled emitter at 250 nL min-1. For total proteome analysis separation was performed with 1-8% gradient over 3 minutes, 8 to 28% in 80min, 28 to 40% in 10 minutes and 40 to 100% in 5 minutes, the column was then kept at 100% for 8 minutes. For phosphopeptide analysis peptides were separated with 1 to 34% buffer B in 60 minutes, 34 to 100% in 5 minutes, the column was then kept at 100% for 8 minutes.

The eluted peptides were analyzed on an Orbitrap Fusion mass spectrometer in data-dependent mode. The MS1 spectrum was acquired on an Orbitrap mass analyzer at 400-1600 mass range 120.000 resolution with an AGC target of 5e5 (60 ms maximum injection time). For MS2 scans, peptides were isolated with a quadrupole using a 1.2-Da isolation window and fragmented at 40% normalized collision energy. AGC was set at 5e4 (maximum injection time 120ms), and dynamic exclusion was 20 sec.

Raw data were deposited in the ProteomeXchange database (accession numbers PXD005558).

Data analysis - Data were analysed in Proteome Discoverer 2.1 software (see supplementary materials for full set of parameters). Database search was performed with Mascot 2.3.2 using *Streptomyces coelicolor* uniprot database (retrieved on 06.03.15). Methionine oxidation was set as variable modification, while Cys carbamidomethylation, TMT6plex (K), TMT6plex (N-term). Peptides were validated by mascot percolator with 0.01 PEP threshold. Precursor and fragment mass tolerance was 10ppm and 0.02Da respectively. For phosphopeptide analysis phosphorylation position was validated by ptmRS.

Peptide spectrum matches with total summed reporter intensities of less than 4e5 were not considered for quantitation due to the high level of noise in the quantitation data. The quantification results of peptide spectrum matches were converted to peptide-level quantitation, which in turn was converted into protein quantitation using an R script (39). Only proteins with two or more quantified peptides were considered. This resulted in quantitation of 3468 proteins. Proteins were analysed for differential expression using the limma package in R (40). P values were adjusted for multiple comparison using the R stats package.

Protein abundances of the reproductive stages (MII) were normalised against the vegetative stage (MI). The fold change of the MII stages with respect to the MI was estimated using the average TMT abundances from three or four biological replicates.

Phosphopetide abundances were normalized against the MI stage, and further normalized against the abundance of the non-phosphorylated peptide, in order to correct differences due to changes in protein abundances instead to real changes in phosphorylation levels (see methods). Given the nature of isobaric mass tagging experiments it is possible to observe different ratio suppression levels (underestimation of the relative change due to co-fragmentation of co-eluting ions with similar m/z) (41) at phosphopeptide and protein level quantitation. Hence normalisation of a phosphopeptide on protein level might result in artificial changes. To account for this, we also report whether the direction of changes is the same at phosphopeptide and protein level at the three developmental stages analysed (Supplemental table 2).

Data processing - Proteins were classified manually into functional categories according to

their annotated functions in the Gene Bank database, publications and by homology/functions according to the Gene Ontology, the Conserved Domain, and the KEGG Pathway databases. When a protein was involved in the synthesis of any secondary metabolite, it was classified in the secondary metabolism group, even if it fitted with additional categories. When a protein was involved in cell division regulation, it was included in cell division, instead of the category of regulatory proteins.

RESULTS

Streptomyces coelicolor culture and phosphoenrichment- Proteome and phosphoproteome variations were analysed at three key developmental stages: MI (16-hours), MII (30-hours), and sporulating MII (65-hours) (4) (Fig. 1A) (see methods for details).

The TiO2 beads and peptides ratio is one of the key parameters in phosphoproteomics that needs to be optimized for each sample and organism (42). In our experiments, the best phosphoenrichment efficiency (48% ± 2 phosphopeptides) was obtained using 0.15 mg TiO2 beads per 100 µg of TMT labelled peptides (Fig. 1B) This is lower than what was previously estimated by Engholm-Keller for mammalian cultures, which is expected given much higher amount of phosphopeptides in eukarytotes compared to bacteria (42).

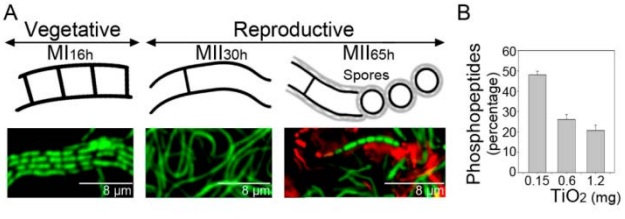

FIG. 1. **Sample preparation**. (A) *S. coelicolor* hyphae stained with SYTO 9 and propidium iodide observed under the confocal microscope at the MI (16-hours), substrate mycelium (MII_{30h}) and sporulating aerial mycelium (MII_{65h}) stages. Notice the PCD. (B) Analysis of the proteolysis during development (percentage of tryptic peptides over time. (C) Optimization of the TiO_2 bead amount per 100µg of TMT labelled peptides. Error bars correspond to the S.D. from three biological replicates.

Identification and quantification of Streptomyces coelicolor proteins general overview- A total of 3461 proteins (44.3% of *S. coelicolor* proteome) fulfilled the criteria used for protein identification and quantification (see methods for details) (Supplemental Table 1; see protein abundances heat maps in Supplemental Fig. 1). Protein TMT abundances were highly consistent across the biological replicates analysed, with an average correlation coefficient of 0.91 and a median coefficient of variation of 6.5% (Fig. 2A-C). Protein variation between developmental stages (normalized against the MI stage, MII30h/MI16h and MII65h/MI16h ratios, see Methods) (red/blue lines in Fig. 2D), were far more variable than between biological replicates (MI16h/MI16h, MII30h/MII30h, MII65h/MII65h, grey lines in Fig. 2D), indicating a good reproducibility between biological replicates, and a correlation between protein abundance variations and differentiation (Fig. 2D). As previously reported (18) discrepancies between MI and MII protein abundances were greater at the sporulating stage (MII65h, red lines in Fig. 2D) than at the substrate mycelium phase (MII30h, blue lines in Fig. 2D).

Due to remarkably low variability of quantitation, overall 3144 (90.6%) proteins showed a statistically significant change between at least two of the conditions (q-value of less than 0.01). In order to focus in the most outstanding we picked 1350 proteins that were both statistically significantly changing and were down- or up-regulated at least two times (log2 ratio MII/MI lower than -1 or higher than 1).As a control, the ratios between biological replicates (MI16h/MI16h, MII30h/MII30h, MII65h/MII65h) were calculated, and they were always inside the ±1 interval (non-significant variations; grey lines in Fig. 2D). 2111 proteins showed non-significant variation between MI and MII (Fig. 2E), while 1350 proteins showed significant variations with respect to the MI at least in one of the MII stages analysed (MII30h or MII65h) (Fig. 2F,G). Importantly 1142 proteins were up- or down-regulated in both MII stages (30- and 65-hours) (Fig. 2F), evidencing that the proteome of the substrate mycelium (MII30h) and sporulating aerial mycelium (MII65h) are highly similar and different to the MI stage and validating choosing MI timepoint as a reference in this stdudy. Only 208 proteins showed opposite differences at the MII30h or the MII65h (Fig. 2G). As expected, proteins showing the biggest differences in their abundances between the substrate (MII30h) and the aerial sporulating mycelia (MII65h) included proteins involved in aerial mycelium hydrophobic coats formation and sporulation (see below, Table II).

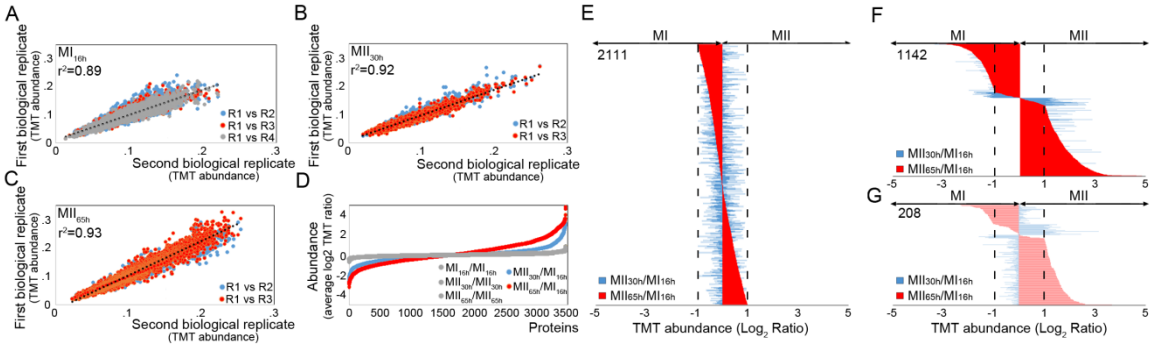

FIG. 2. **Quantitative proteomic data analysis**. (A-C) Correlation of TMT abundances between biological replicates. Coefficient of regressions are shown. (D) Variation of TMT ratios (average from biological replicates) of the 3461 proteins quantified between different (MII/MI, blue and red lines), and the same (MI/MI and MII/MII, gray lines) developmental phases. (E-G) TMT ratios (log2 MII/MI) of the 3461 proteins identified and quantified: (E) proteins without significant variations (abundances inside the ± 1 interval); (F) proteins with significant variations at least in one of the MII stages analysed with respect to the MI and up- or down-regulated in both MII stages analysed; (G) proteins with significant variations at least in one of the MII stages analysed with respect to the MI and opposite differences at the MII_{30h} or the MII_{65h}. Dashed lines indicate the limit for considering abundance variations as significant (log2 abundances greater than ±1).

Clustering of proteins with similar abundance trends - With the aim of identifying proteins with similar abundance profiles, the fuzzy c-means algorithm with a Euclidean distance matrix (43) was used (Fig. 3, Supplemental Table 1). 858 proteins from the 1350 proteins showing significant variations (Fig. 2F, G) were assigned to 5 clusters showing distinctive abundance profiles (Fig. 3).

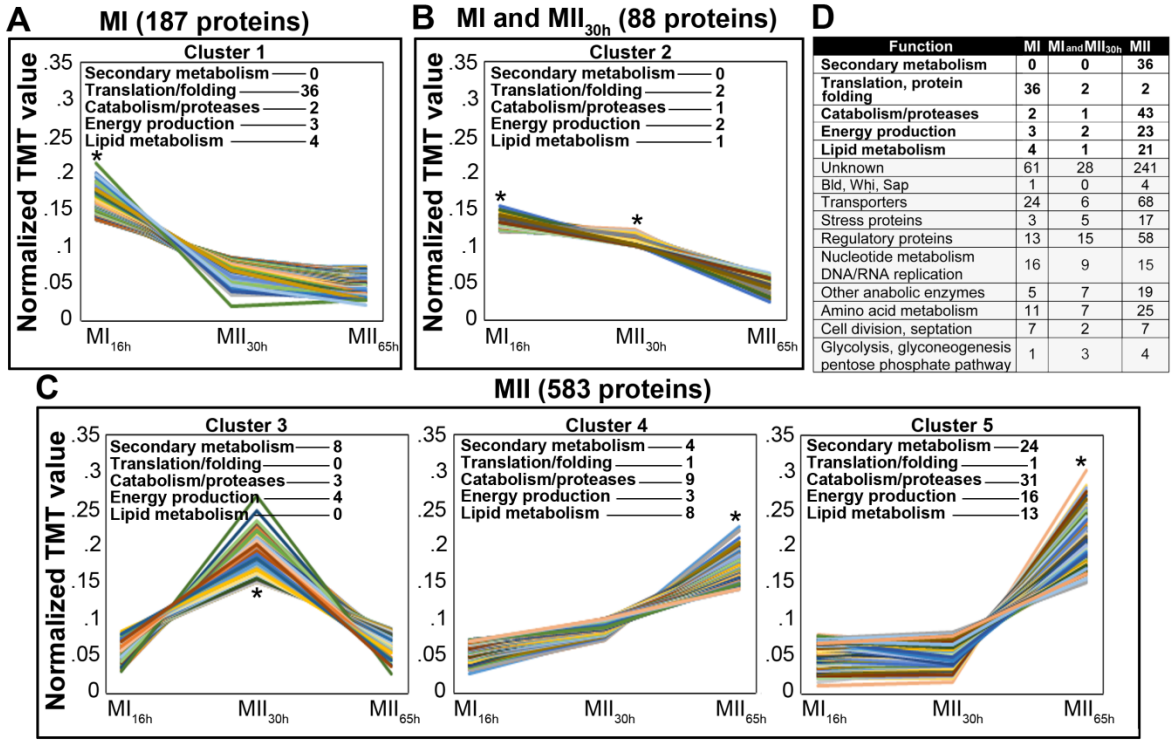

D

Function	MI	MI and MII30h	MII
Secondary metabolism	**0**	**0**	**36**
Translation, protein folding	**36**	**2**	**2**
Catabolism/proteases	**2**	**1**	**43**
Energy production	**3**	**2**	**23**
Lipid metabolism	**4**	**1**	**21**
Unknown	61	28	241
Bld, Whi, Sap	1	0	4
Transporters	24	6	68
Stress proteins	3	5	17
Regulatory proteins	13	15	58
Nucleotide metabolism DNA/RNA replication	16	9	15
Other anabolic enzymes	5	7	19
Amino acid metabolism	11	7	25
Cell division, septation	7	2	7
Glycolysis, glyconeogenesis pentose phosphate pathway	1	3	4

Fig. 3. **Cluster analysis** (classification by fuzzy c-means approach) of *S. coelicolor* protein expression patterns. Proteins clustered were those significantly quantified at least in one of the developmental phases analysed (see methods). (A) Cluster 1, proteins up-regulated at the MI16h stage; (B) Cluster 2, proteins up-regulated at MI16h and MII30h; (C) Clusters 3-5, proteins up-regulated at the MII stage; (D) The number of proteins for each functional category in cluster 1, cluster 2 and clusters 3-5 is indicated. Developmental time points with significant differences in their abundances (p-value lower than 0.01) are labelled by an asterisk. The number of proteins for key functional categories is indicated over the graphs.

187 proteins were up-regulated at the MI stage (Fig. 3A), 88 at the MI and MII30h (Fig. 3B) and 583 at the MII stages (Fig. 3C). All proteins involved in secondary metabolism (actinorhodin, CPK biosynthesis, deoxysugar synthases) were included in clusters 3-5 (up-regulated at the MII), while most proteins involved in protein synthesis (translation/protein folding) were up-regulated at the MI (cluster 1) (Fig. 3); proteins involved in energy production (krebs cycle, oxidative phosphorylation) and lipid metabolism, were mostly up-regulated at the sporulating stages (MII65h, cluster 5) (Fig. 3).

Similarities and differences between MI and MII proteomes - The MI and MII proteomes were compared grouping the 1350 proteins showing significant variations (Fig. 2F,G) into functional categories (Fig. 4, see methods for details). As described above (Fig. 2E-G), the MI stage was used as reference, and protein abundances were shown as the log2 MII/MI.

Proteins involved in secondary metabolite biosynthesis were up-regulated at the MII stages, but with different trends in function of the specific compound (Fig. 4A) (Table II). Proteins involved in CPK (SCO6273-SCO6286) and coelichelin (SCO0489-SCO0499) biosynthesis were up-regulated at the MII30h (up to 6.5-fold with respect to the MI, blue bars in Fig. 4A), indicating that CPK and coelichelin production is repressed in the aerial mycelium (MII65h red bars in Fig. 4A). SCO6286, a CPK biosynthesis repressor, was in fact up-regulated (3.4-fold at the MII65h) (Fig. 4A). All proteins involved in actinorhodin synthesis (SCO5071-SCO5092), as well as deoxysugar synthases (SCO0381-SCO0401) putatively involved in secondary metabolite biosynthesis (44), were up-regulated (up to 24.2-fold) at the later stages of MII (Fig. 4A). The abundance of the proteins involved in calcium-dependent antibiotic (CDA) biosynthesis (SCO3210-SCO3249) didn't change during the MI and MII stages (Fig. 4A). CDA genetic cluster includes SCO3225 and SCO3226, a two-component system repressing CDA biosynthesis (45), which showed similar abundances at the MI and MII stages, indicating a constitutive repression of CDA production under the culture conditions used in this work.

Proteins involved in the regulation of the aerial mycelium hydrophobic coat formation and sporulation (bald, whi, wbl, sap proteins) showed different abundances between MI and MII (Fig. 4B) (Table II). Key bald proteins preceding aerial mycelium formation, as BldC (SCO4091), BldD (SCO1489) or BldKA (SCO5112) were down-regulated at the MII stage (up to 0.3-fold). Key white genes as WhiE ORFs VI and VIII (SCO5315, SCO5321) controlling spore pigmentation (46), or WhiH (SCO5819), controlling hypha septation accompanying sporulation (47), were significantly up-regulated at the sporulating aerial mycelium (MII65h) (up to 3.7-fold). Other proteins regulating sporulation as BldB (SCO5723), SapA (SCO0409) (47), were also significantly up-regulated at the MII65h (up to 3.2-fold). BldN (SCO3323), a sigma factor required for aerial mycelium formation and sporulation (48) was significantly up-regulated at the MII30h and MII65h (2.8- and 3.7-fold respectively). Uncharacterized proteins as SCO3424, a BldB homologue, or SCO3897, SCO4301, SCO6476, SCO6638, SCO6717, possible BldA targets (they harbour Leu encoded by TTA) (49) had also different abundances during development (Fig. 4B) (Table II).

The abundance of 60 proteins involved in cell-division were quantified (Fig. 4B). 22 proteins were reported before as involved cell division regulation, while the other 37 proteins putatively involved in cell division, show homologies with cell-division proteins, but in our knowledge, there is not any report characterising them (Supplemental table 1). Among the well characterized proteins the following demonstrated significant change and a change of at least two fold: CrgA (SCO3854), a sporulation cell-division protein (50) and HupS (SCO5556), a nucleoid-associated protein (51). CrgA was up-regulated at the MII65h (2.6-fold) and HupS was down-regulated at the MII30h and MII65h (0.25-fold and 0.3-fold respectively) (Table II).

Interestingly, as discussed below, some key cell division proteins that did not passed the two fold umbral considered in this work, were differentially expressed during development. Six were more abundant (up to 1.7-fold) at the sporulation stage than at the MI: SffA (SCO1416) (52), ParJ (SCO1662) (53), SepF (SCO2079) (54), SCO4114 (55), SmC (SCO5577) (56), SCO5750 (FtsK homolog) (57), all of them reported as involved in sporulation. 13 cell-division proteins that not passed the two fold umbral, were down-

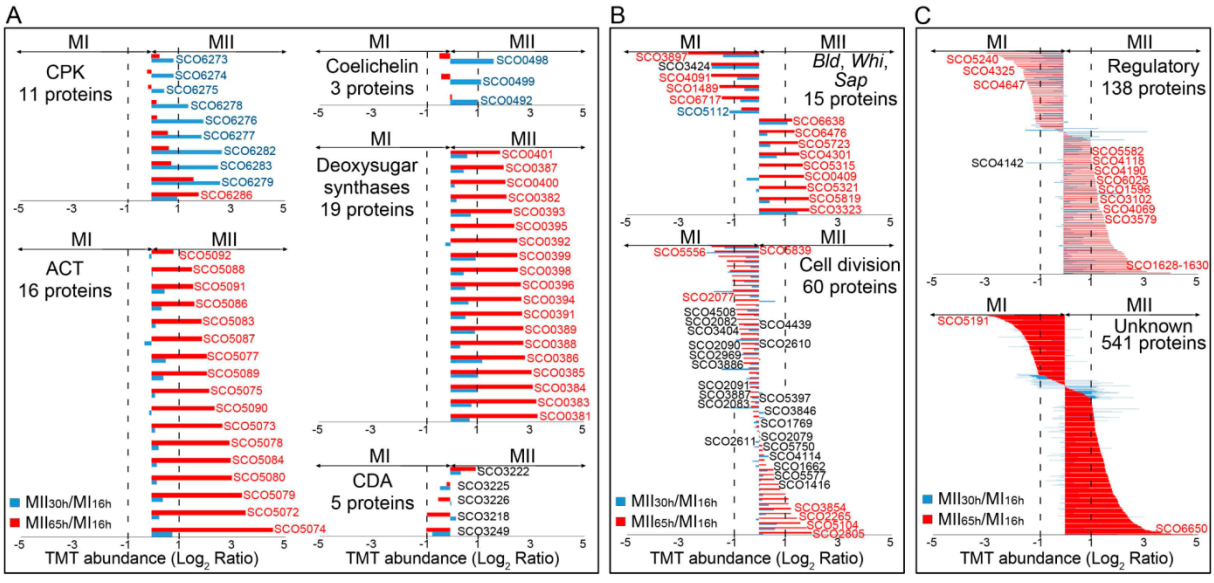

FIG. 4. **Protein abundance values (logarithm of TMT ratio values) for the main functional groups of proteins.** (A) Secondary metabolism; (B) Bld, Whi, Sap and cell division proteins; (C) Regulatory and unknown proteins. The SCO numbers of the proteins described in the text are indicated. Dashed lines indicate the limit for considering abundance variations as significant (log2 abundances greater than ±1).

regulated at the MII stages (up to 0.57-fold): FtsZ (SCO2082), the key effector of bacterial cell division (58); DivIVA (SCO2077), one of the proteins regulating apical growth in Streptomyces (59); SCO4508, a FtsK-related protein (57); SCO2090 and SCO2091, FtsL transpeptidase homologues involved in Streptomyces cell-division (60); ParA (SCO3886), and ParB (SCO3887), reported to be involved in sporulation (61); FtsQ (SCO2083), a protein required for sporulaton (62); ScpB (SCO1769) affecting the nucleoid morphology during early stages of sporulation (56); MreB and C (SCO2610 and SCO2611) (63); SCO4439 DD-CPase (64); and Scy (SCO5397), involved in polarized growth (65).

37 uncharacterized proteins putatively related with cell-division were also identified: (Supplemental Table 1) (Table II). These proteins include proteins harbouring domains related with sporulation as SCO2265, SCO2805, or SCO5104; a protein harbouring a putative murein hydrolase activator NlpD domain (SCO5839); or proteins related with cell-division, as SCO3404 (FtsH homolog), and SCO2969 (FtsE homolog) (Table II).

138 regulatory proteins (transcriptional regulators, kinases, etc.) had different abundances at least in one of the MII stages with respect to the MI (Fig. 4C). As in the case of other functional categories, most of these proteins were up- (positive values) or down-regulated (negative values) at the MII30h and MII65h with respect to the MI (Fig. 4C). The unique protein with significant opposite abundances at the MII30h (0.4-fold) and MII65h (2.1-fold) with respect to the MI, was PstS (SCO4142) (Table II), a phosphate-binding protein that forms part of the high-affinity phosphate transport system encoded by the pst operon (66). Among the rest of regulatory proteins the following were involved in differentiation (Table II): ScbR (SCO6265), a γ-butyrolactone binding protein regulating morphological differentiation and secondary metabolism (67); Nsda (SCO5582), a BldD target regulating morphological differentiation and secondary metabolism (68); RarA-C "restoration of aerial mycelium formation'' proteins (SCO1628-SCO1630) (69); WblA (SCO3579) and WblE (SCO5240), two regulators of development (70); SarA (SCO4069), a protein influencing sporulation and secondary metabolism (71); PkaE (SCO3102), an inhibitor of actinorhodin production (72); OhkA (SCO1596), a regulator of secondary metabolism and morphological differentiation (73); DevA (SCO4190), a GntR-Like transcriptional regulator controlling aerial mycelium development (74); AtrA (SCO4118), an activator of actinorhodin biosynthetic gene expression (75); NusG (SCO4647), a transcription antiterminator regulating secondary metabolism (76) and CspB (SCO4325), a secondary metabolism repressor (77). Most of these 138

TABLE II.

Averaged TMT protein abundances (from at least three biological replicates) of the substrate mycelium (MII_{30h}) and sporulating aerial mycelium (MII_{65h}) with respect to the MI stage (16-hours). The ratio between MII/MI is shown in the logarithm (log2) and lineal forms. Cl, clusters of proteins with similar abundance profiles. N.S. Not significant. The proteins discussed in the text are indicated. Only abundances over the significance threshold used in this work (more than two-fold up or down-regulated) are shown, with the exception of cell division proteins, whose abundances below the 2-fold threshold are shown and discussed in the manuscript.

Category	SCO nº	Cl	Function	Log 2 (MII_{30h}/MI)	Log 2 (MII_{65h}/MI)	Fold-change (MII_{30h}/MI)	Fold-change (MII_{65h}/MI)
Secondary metabolism	SCO6286	4	CPK repressor	0.9	1.8	1.9	3.4
	SCO6276	3	CPK biosynthesis	1.9	n.s.	3.7	n.s.
	SCO6277	3		1.9	n.s.	3.7	n.s.
	SCO6278	3		1.4	n.s.	2.6	n.s.
	SCO6279	n.s.		2.6	1.6	6	3
	SCO6282	3		2.7	n.s.	6.5	n.s.
	SCO6283	3		2.6	n.s.	6	n.s.
	SCO0492	3	Coelichelin biosynthesis	1.1	n.s.	2.1	n.s.
	SCO0498	3		1.6	n.s.	3	n.s.
	SCO0499	3		1.2	n.s.	2.3	n.s.
	SCO5072	5	ACT biosynthesis	n.s.	3.6	n.s.	12.1
	SCO5073	5		n.s.	2.7	n.s.	6.5
	SCO5074	5		n.s.	4.6	n.s.	24.2
	SCO5075	5		n.s.	2.2	n.s.	4.6
	SCO5077	n.s.		n.s.	2.1	n.s.	4.3
	SCO5078	5		n.s.	3	n.s.	8
	SCO5079	5		n.s.	3.4	n.s.	10.5
	SCO5080	5		n.s.	3	n.s.	8
	SCO5083	5		n.s.	1.9	n.s.	3.7
	SCO5084	5		n.s.	3	n.s.	8
	SCO5086	n.s.		n.s.	1.6	n.s.	3
	SCO5087	5		n.s.	1.9	n.s.	3.7
	SCO5088	5		n.s.	1.6	n.s.	3
	SCO5089	n.s.		n.s.	2.1	n.s.	4.3
	SCO5090	5		n.s.	2.4	n.s.	5.3
	SCO5091	4		n.s.	1.6	n.s.	3
	SCO5092	5		n.s.	n.s.	n.s.	n.s.
	SCO0381	5	Deoxysugar synthases	n.s.	3.3	n.s.	9.8
	SCO0382	n.s.		n.s.	2.1	n.s.	4.3
	SCO0383	5		n.s.	3.3	n.s.	9.8
	SCO0384	5		1	3.1	2	8.6
	SCO0385	5		1	3.1	2	8.6
	SCO0386	5		n.s.	2.8	n.s.	7
	SCO0387	n.s.		n.s.	2	n.s.	4
	SCO0388	5		n.s.	2.8	n.s.	7
	SCO0389	5		n.s.	2.8	n.s.	7
	SCO0391	5		n.s.	2.7	n.s.	6.5
	SCO0392	4		n.s.	2.6	n.s.	6.1
	SCO0393	n.s.		n.s.	2.3	n.s.	4.9
	SCO0394	5		n.s.	2.7	n.s.	6.5
	SCO0395	n.s.		n.s.	2.4	n.s.	5.3
	SCO0396	5		n.s.	2.7	n.s.	6.5
	SCO0398	5		n.s.	2.6	n.s.	6.1
	SCO0399	4		n.s.	2.6	n.s.	6.1

	SCO0400	n.s.		n.s.	2.1	n.s.	4.3
	SCO0401	n.s.		n.s.	1.9	n.s.	3.7
	SCO3218	n.s.	CDA biosynthesis	n.s.	n.s.	n.s.	n.s.
	SCO3222	4		n.s.	n.s.	n.s.	n.s.
	SCO3225	n.s.		n.s.	n.s.	n.s.	n.s.
	SCO3226	n.s.		n.s.	n.s.	n.s.	n.s.
	SCO3249	1		n.s.	n.s.	n.s.	n.s.
Bald/whi Sap	SCO0409	5	SapA	n.s.	1,.7	n.s.	3.2
	SCO1489	n.s.	BldD	n.s.	-1.5	n.s.	0.3
	SCO3323	n.s.	BldN	1.5	1.9	2.8	3.7
	SCO3424	1	BldB homologue	-1.8	-1.8	0.3	0.3
	SCO4091	n.s.	BldC	n.s.	-1.8	n.s.	0.3
	SCO5112	n.s.	BldKA	-1.1	n.s.	0.5	n.s.
	SCO5315	5	WhiE ORFVI	n.s.	1.6	n.s.	3
	SCO5321	5	WhiE ORFVIII	n.s.	1.8	n.s.	3.5
	SCO5723	n.s.	BldB	n.s.	1.5	n.s.	2.8
	SCO5819	n.s.	WhiH	n.s.	1.9	n.s.	3.7
	SCO3897	1	Possible targets for bldA regulation	-1.4	-2.7	0.4	0.2
	SCO4301	4		n.s.	1.5	n.s.	2.8
	SCO6476	n.s.		n.s.	1.4	n.s.	2.6
	SCO6638	n.s.		1	1.3	2	2.5
	SCO6717	n.s.		n.s.	-1.4	n.s.	0.4
Cell division[1]	SCO1416	5	SffA	0.03	0.8	1	1.7
	SCO1662	n.s.	ParJ	0.33	0.55	1.3	1.5
	SCO1769	n.s.	ScpB	-0.2	-0.1	0.9	0.9
	SCO2077	n.s.	DivIVA	-0.3	-0.9	0.8	0.5
	SCO2079	n.s.	SepF	0.1	0.02	1.1	1
	SCO2082	2	FtsZ	-0.2	-0.8	0.9	0.57
	SCO2083	n.s.	FtsQ	-0.1	-0.3	0.9	0.8
	SCO2090	2	FtsL homolog	-0.2	-0.6	0.9	0.7
	SCO2091	1	FtsL homolog	-0.4	-0.4	0.8	0.8
	SCO2265	1	Hypothetical protein	0.7	1.6	1.6	3
	SCO2610	2	MreC	-0.2	-0.7	0.9	0.6
	SCO2611	n.s.	MreB	-0.1	0.04	0.9	1
	SCO2805	5	ObgE	0.2	2	1.1	4
	SCO2969	1	FtsE homolog	-0.7	-0.6	0.6	0.7
	SCO3404	n.s.	FtsH homolog	0.07	-0.8	1	0.6
	SCO3854	5	CrgA	-0.11	1.4	0.9	2.6
	SCO3886	n.s.	ParA	-0.3	-0.6	0.8	0.7
	SCO3887	2	ParB	-0.1	-0.3	0.9	0.8
	SCO4114	n.s.	Sporulation associated protein	0.4	0.2	1.3	1.1
	SCO4439	n.s.	DD-CPase	-0.4	-0.7	0.8	0.6
	SCO4508	n.s.	FtsK homolog	-0.4	-0.9	0.8	0.5
	SCO5104	1	SpoIIE	0.6	1.8	1.5	3.5
	SCO5397	n.s.	Scy	-0.3	-0.3	0.8	0.8
	SCO5556	1	HupS	-2	-1.7	0.25	0.3

	SCO5577	n.s.	SmC	0.08	0.6	1	1.5
	SCO5750	n.s.	FtsK	-0.2	0.1	0.9	1.1
	SCO5839	4	NlpD	-1.3	-1.8	0.41	0.3
Regulatory	SCO1596	n.s.	OhkA	n.s.	1.5	n.s.	2.8
	SCO1628	4	RarC	1.6	3.1	3	8.6
	SCO1629	n.s.	RarB	n.s.	2.6	n.s.	6.1
	SCO1630	5	RarA	n.s.	3	n.s.	8
	SCO3102	5	PkaE	n.s.	1.5	n.s.	2.8
	SCO3579	n.s.	WblA	1.1	1.6	2.1	3
	SCO4069	n.s.	SarA	n.s.	1.5	n.s.	2.8
	SCO4118	4	AtrA	n.s.	1.1	n.s.	2.1
	SCO4142	n.s.	PstS	-1.4	1.1	0.4	2.1
	SCO4190	5	DevA	n.s.	1.3	n.s.	2.5
	SCO4325	n.s.	CspB	n.s.	-2.2	n.s.	0.2
	SCO4647	n.s.	NusG	n.s.	-1.9	n.s.	0.3
	SCO5240	n.s.	WblE	n.s.	-2.6	n.s.	0.2
	SCO5582	4	Nsda	n.s.	1.1	n.s.	2.1
	SCO6265	n.s.	ScbR	1.6	1.5	3	2.8
Unknown	SCO5191	1	Hypothetical protein	-3.4	-3	0.09	0.12
	SCO6650	5	Hypothetical protein	n.s.	4.8	n.s.	27.8

[1] In the case of cell division proteins, variations inside the ±1 interval (not significant), are shown.

putative regulatory proteins with significant differences in their abundance between the MI and MII show homologies with regulatory proteins, but in our knowledge, they remain uncharacterised (Supplemental Table 1).

541 uncharacterized proteins without any clear homology, showed significant differences at least in one of the MII stages analysed with respect to MI (Fig. 4C). As discussed below, these proteins constitute a huge database of potential regulators and effectors of differentiation (Supplemental Table 1). For example, SCO5191 was down-regulated 0.09 and 0.12-fold at the MII30h and MII65h, or SCO6650, up-regulated 28-fold at the MII65h.

Comparison between S. coelicolor transcriptomics and proteomics datasets - The expression of the genes encoding for 1885 proteins identified and quantified in this study has been quantified previously by transcriptomics in *S. coelicolor* cultures performed under the same developmental conditions (33). The comparison between the relative protein and transcript abundances

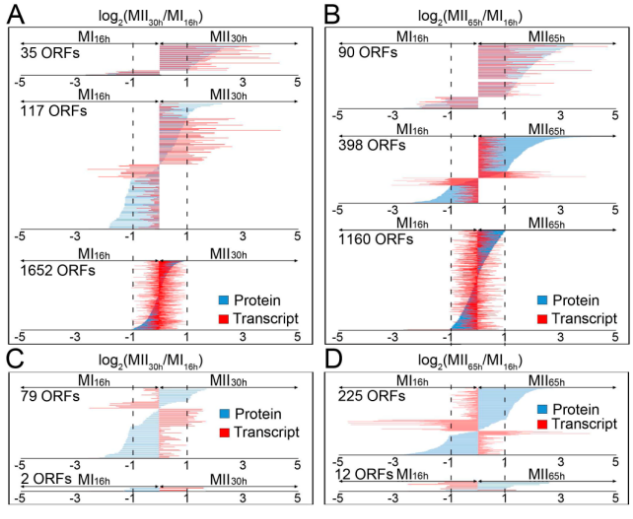

FIG. 5. **Comparison between *S. coelicolor* proteome and transcriptome.** Abundance values of the ORFs identified by proteomics (this work) and transcriptomics (33) were compared. (A) and (B) proteins and transcripts with similar trends (up- or down- regulated in the MII with respect to the MI). (C) and (D) proteins a nd transcripts with opposite trends (positive protein abundance and negative transcript abundance or vice versa). (A) and (C) MII_{30h}/MI_{16h}; (B) and (D) MII_{65h}/MI_{16h}. Proteins (blue bars); transcripts (red bars). Dashed lines indicate the limit for considering abundance variations as significant (log2 abundances greater than ±1).

expressed as log2 MII/MI is shown in Figure 5. Most proteins and transcripts showed comparable abundances in the MII30h (Fig. 5A) and MII65h (Fig. 5B): 35 and 90 proteins/transcripts were up-regulated or down-regulated more than two-fold at the MII; 117 and 398 proteins/transcripts had similar trends but their variation was significant only in one of the two molecules analysed (transcript or protein); 1652 and 1160 proteins/transcripts did not differ significantly (log 2 abundances within ±1 interval). 81 and 237 proteins/transcripts (4.3% and 12.6% of all the proteins/transcripts quantified) showed divergent abundances (positive protein abundance and negative transcript abundance or vice versa) at the MII30h (Fig. 5C) or MII65h (Fig. 5D), however only 2 and 12 of these proteins/transcripts (0.1% and 0.6% of the total) had significant opposite differences (Fig. 5C, D).

Streptomyces coelicolor phosphoproteome - 89 unique phosphorylation sites (52% Ser, 48% Thr, 0% Tyr) from 91 phosphopeptides and 47 phosphoproteins were identified and their abundances quantified along three developmental stages (MI16h, MII30h, and MII65h) (Fig. 6) (see phosphopeptide TMT abundance heat maps in Supplemental Fig. 2; and abundances in Supplemental Table 2). There is a clear and striking up-regulation of phosphorylation at MII. Phosphopetide abundances were normalized against the MI stage, and further normalized against the abundance of the non-phosphorylated peptide, in order to correct differences due to changes in protein abundances instead to real changes in phosphorylation levels (see methods). In order to focus in the most reliable phosphoproteome differences, only a small fraction of the phosphopeptides that passed the abundance expression test, those showing at least double or half abundance changes between MII and MI at least in one of the MII stages analysed, were considered as differently phosphorylated: 59 phosphopeptides, 3 up-regulated at the MI stage, one up-regulated at the MII30h, 40 up-regulated at the MII65h, 14 up-regulated at MII30h and MII65h and one down-regulated at the MII30h and up-regulated at the MII65h (Fig. 6A) (Supplemental Table 2). As discussed below, 52 of these 59 phosphopeptides showed opposite abundance trends at the phosphopeptide and protein levels, making quantification artefacts due to the ion ratio suppression intrinsic to the isobaric mass tagging labelling used (41), highly improbable. Seven of these 59 phosphopeptides showed similar trends at the phosphopeptide and protein levels, but as described above, with more than twice abundance variation, making ion ratio suppression also improbable (Supplemental Table 2).

18 phosphopeptides from 12 regulatory proteins were identified (Fig. 6B) (Table III). A phosphopeptide from RarA (SCO1630), a protein involved in the regulation of aerial mycelium differentiation (69), was down-regulated in the MII30h (0.4-fold). 8 phosphopeptides from regulatory proteins were up-regulated at the MII65h: a phosphopeptide from SCO7463 putative histidine kinase, up-regulated 8-fold; a phosphopeptide from DasR (SCO5231), a pleiotropic regulator (78), up-regulated 3.5-fold; a phosphopeptide from the rho transcription terminator factor SCO5357, up-regulated 3-fold; a phosphopeptide from PspA (SCO2168), a phage shock protein (79), up-regulated 3-fold; a phosphopeptide from DevA (SCO4190), a GntR-like transcriptional regulator required for aerial mycelium development (74), up-regulated 2.8-fold; and 3 phosphopeptides from the pleiotropic regulator SCO5544 (80), up-regulated 2.3-, 2.3- and 2.8-fold respectively. 3 phosphopeptides from regulatory proteins were up-regulated at the MII30h and MII65h; a phospopeptide from the SCO4232 putative transcriptional regulator, up-regulated 2- and 4-fold respectively; and two phosphopeptides from SCO5544 up-regulated up to 13.9-fold (Table III). Only a phosphopeptide from regulatory proteins was differentially phosphorylated during the two MII stages analysed with respect to the MI: that from SCO0204, an orphan response regulator (81) whose expression is affected by the sporulation-specific cell division activator SsgA, was down-regulated at the MII30h (0.2-fold) and up-regulated at the MII65h (4.9-fold) (Table III). The other 5 phosphopeptides from regulatory proteins didn't show significant variations between the MI and MII stages analysed (Fig. 6B) (Supplemental Table 2).

5 phosphopeptides from 5 proteins involved in cell division and cell wall synthesis were identified (Fig. 6C) (Supplemental Table 2). Two of them were up-regulated at the MII65h: a phosphopeptide from FtsZ (SCO2082), the key tubulin-like bacterial division protein (58), up-

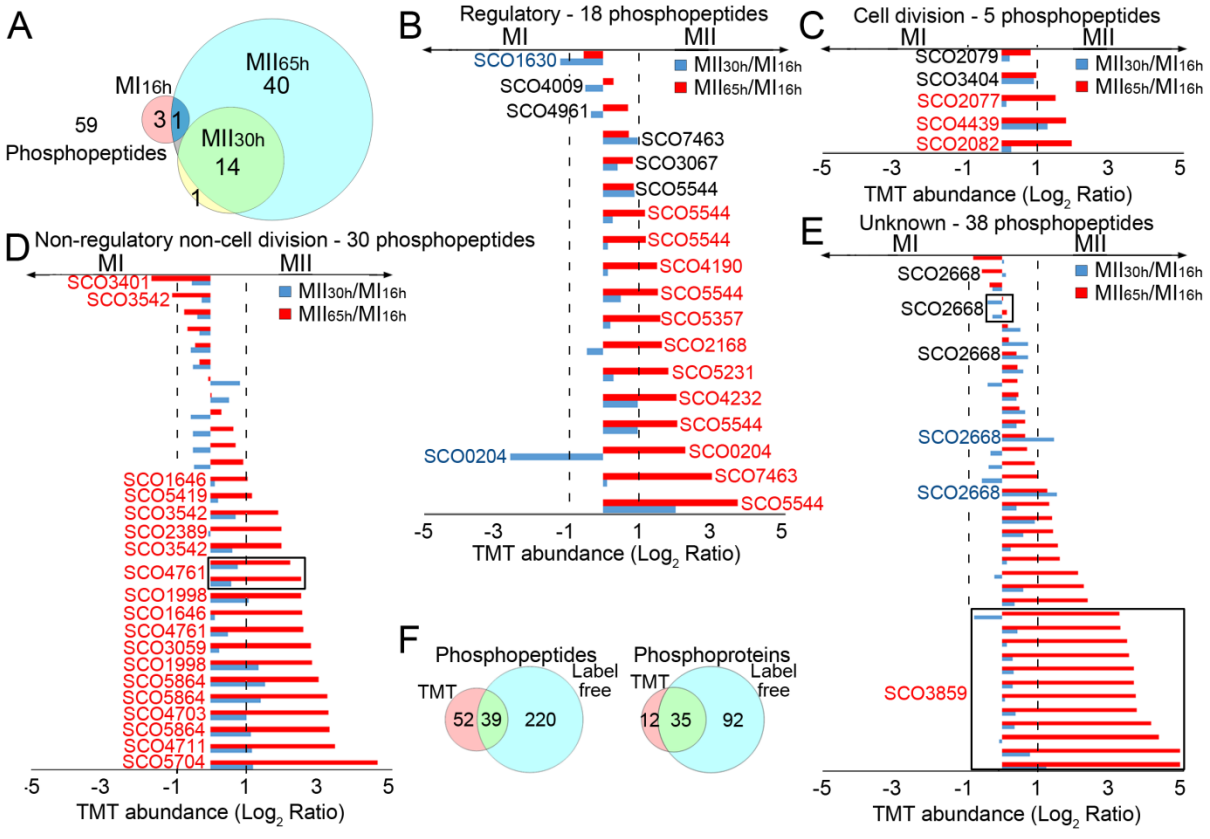

Fig. 6. ***S. coelicolor*** **phosphoproteome.** (A) Venn diagram showing the distribution of the peptides differentially phosphorylated during development (log2 TMT ratios normalized by the non-phosphorylated peptides greater than ±1, see Methods). (B-E) Phosphopeptide abundance values. The SCO numbers of the proteins described in the text are indicated (F) Comparison between TMT phosphorproteomics (this work) and label free proteomics (18).

regulated 4-fold; and one from DivIVA (SCO2077), one of the proteins regulating apical growth in Streptomyces, which was demonstrated to be regulated by phosphorylation (59), up-regulated 2.8-fold (Table III). A phosphopeptide from SCO4439, a D-alanyl-D-alanine carboxypeptidase involved in spore cell wall maturation, spore resistance, germination and mycelial resistance to vancomycin and teicoplanin (64), was up-regulated at the MII30h (2.5-fold) and MII65h (3.5-fold) (Table III). Two phosphopeptides from the cell division proteins identified didn't show significant variations between the MI and MII: SCO3404, a FtsH homolog with unknown function, and SepF (SCO2079) (54), one of the proteins included into the Streptomyces division and cell wall (dcw) cluster (Table III).

30 phosphopeptides from 15 proteins with no regulatory nor cell division functions (Fig. 6D) (Supplemental Table 2). Two phosphopeptides were down regulated at the MII65h with respect to the MI: one from SCO3401, a putative hydroxymethyldihydropteridine pyrophosphokinase, down-regulated 0.3-fold; and another one from SCO3542, a putative thymidine monophosphate kinase detected before as phosphorylated (18, 19), down-regulated 0.3-fold (Table III). Ten phosphopeptides from non-regulatory/non-cell division proteins were up-regulated at the MII65h: a phoshopeptide from phosphoribosylaminoimidazole carboxylase catalytic subunit PurE (SCO3059), up-regulated 7-fold; three phosphopeptides from chaperonin GroES (SCO4761) up-regulated 4.9, 5.7, and 6.1-fold; two phosphopeptides from SCO3542, up-regulated 3.7 and 4-fold; a phosphopeptide from SCO5419 putative thioredoxin, up-regulated 2.3-fold; a phosphopeptide from acyl carrier protein SCO2389, up-regulated 4-fold; and two phosphopeptides from proteasome-associated protein SCO1646, up-regulated 2.1 and 6-fold (Table III). Eight phosphopeptides from non-regulatory / non-cell division proteins were up-regulated at MII30h and MII65h: a

TABLE III

Averaged TMT phosphopeptide abundances (from at least three biological replicates) of the substrate mycelium (MII_{30h}) and sporulating aerial mycelium (MII_{65h}) with respect to the MI stage (16-hours), of the phosphopeptides and phosphoproteins discussed in the manuscript. See Supplemental Table 2 for a description of the rest of the phosphopeptides. The ratio between MII/MI is shown in the logarithm (log2) and lineal forms. The proteins discussed in the text are indicated. Only abundances over the significance threshold used in this work (more than two-fold up or down-regulated) are shown, with the exception of cell division proteins, whose abundances below the 2-fold threshold are shown and discussed in the manuscript.

Category	SCO nº	Phosphopeptide	Log 2 (MII_{30h}/ MI)	Log 2 (MII_{65h}/ MI)	Fold-change (MII_{30h}/MI)	Fold-change (MII_{65h}/MI)
Regulatory	SCO0204	AH**pS**EQGDNTGSPVR	-2.6	2.3	0.2	4.9
	SCO1630	AHQES**pS**SNEPAHAPADDEGNLK	-1.2	n.s.	0.4	n.s.
	SCO2168[1]	QAIEGGQGQGEA**pS**P**S**QSQQPQDTPR	n.s.	1.6	n.s.	3
	SCO4190	ALQEDGLLTNV**pS**K	n.s.	1.5	n.s.	2.8
	SCO4232	AEALLDEVLA**pS**	1	2	2	4
	SCO5231	STDVSSAENEGGA**pT**VR	n.s.	1.8	n.s.	3.5
	SCO5357	VNASAEQAAPADDAP**pS**ER	n.s.	1.6	n.s.	3
	SCO5544	GHDEPDSSR**pT**DR	n.s.	1.2	n.s.	2.3
	SCO5544	GHDEPD**pS**SRTDR	n.s.	1.2	n.s.	2.3
	SCO5544	RDESQD**pT**GQYAQPGQNQYDAR	n.s.	1.5	n.s.	2.8
	SCO5544	GHDEPDS**pS**RTDRTPR	1	2.1	2	4.3
	SCO5544	GHDEPD**pS**p**S**RTDRTPR	2	3.8	4	13.9
	SCO7463	TSDTPGASSEGHEV**pS**	n.s.	3	n.s.	8
Cell division	SCO2077	QLETQADD**pS**LAPPR	0.1	1.5	1.1	2.8
	SCO2079	IAEGGFFNQ**pS**	0.2	0.8	1.2	1.8
	SCO2082	VTVIAAGFDGGQPP**pS**K	0.3	2	1.2	4
	SCO3404	STTVEPAPAPERAPEDRPE**pS**	0.9	1	1.9	2
	SCO4439	DGDADGYDGPPPVDQP**pT**AVFK	1.3	1.8	2.5	3.5
Non-regulatory/Non-cell division	SCO1646	A**pT**RSTEEVEEQAQDAQASEDLK	n.s.	1.1	n.s.	2.1
	SCO1646	ApTR**pS**TEEVEEQAQDAQASEDLK	n.s.	2.6	n.s.	6
	SCO1998	AAAEGVD**pT**AGAAPAASGGGGGGSYSSEGGD NSGALASDEALAALR	1.1	2.5	2.1	5.6
	SCO1998	AAAEGVDTAGAAPAASGGGGGGSYSSEGGDN **pS**GALASDEALAALR	1.3	2.9	2.5	7.5
	SCO2389	SFTDDLDVD**pS**LSMVEVVVAAEER	n.s.	2	n.s.	4
	SCO3059	EFQQDLNDQA**pT**EK	n.s.	2.8	n.s.	7
	SCO3401	SAPFAQGPSDPTVQPVPASVIEQVDAADT**pT**L SNPK	n.s.	-1.6	n.s.	0.3
	SCO3542	EESPAEEAQDR**pT**R	n.s.	-1.6	n.s.	0.3
	SCO3542	ELPQIDPDQAPP**pS**R	n.s.	1.9	n.s.	3.7
	SCO3542	ELPQIDPDQAPP**pS**RR	n.s.	2	n.s.	4
	SCO4703	AVD**pT**EGSEA	1	3.3	2	9.8
	SCO4711	SE**pS**NVTEETK	1.2	3.5	2.3	11.3
	SCO4761	IVVQPLDAEQ**pT**TASGLVIPDTAK	n.s.	2.3	n.s.	4.9
	SCO4761	IVVQPLDAEQTTA**pS**GLVIPDTAK	n.s.	2.5	n.s.	5.7
	SCO4761	IVVQPLDAEQT**pT**ASGLVIPDTAK	n.s.	2.6	n.s.	6.1
	SCO5419	NVLAEEPGN**pT**EAK	n.s.	1.2	n.s.	2.3
	SCO5704	IDIRPDTEQPSDASPEQS**pS**GGRGE	1.2	4.7	2.3	26
	SCO5864	KTDDDVDSD**pS**LEELK	1.1	3.3	2.2	10.2
	SCO5864	TDDDVD**pS**DSLEELK	1.5	3	2.9	8.2
	SCO5864	KTDDDVD**pS**DSLEELK	1.4	3.3	2.7	9.7

N.S. Not significant. [1] Only one phosphorylation site exists in S13 or S14

phosphopeptide from SCO5704, NusA transcription elongation factor, up-regulated 2.3- and 26-fold; a phosphopeptide from the 30S ribosomal protein S17 (SCO4711), up-regulated 2.3- and 11.3-fold; a phosphopeptide form 50S ribosomal protein L4 (SCO4703), up-regulated 2- and 9.8-fold; 2 phosphopeptides from ribosomal protein RspA (SCO1998), up-regulated 5.6 and 7.5-fold; and 3 phosphopeptides from putative protease SCO5864, up-regulated up to 2.9-fold at MII30h and 10.2-fold at MII65h (Table III). The other ten phosphopeptides from non-regulatory / non-cell division proteins didn't show significant variations between the MI and MII (Fig. 6D) (Supplemental Table 2).

38 phosphopeptides from 15 proteins with unknown functions were identified (Fig. 6E) (Supplemental Table 2): 2 phosphopeptides were up-regulated at the MII30h and MII65h, 20 phosphopeptides at the MII65h, one phosphopeptide at the MII30h and 15 phosphopeptides did not show significant variations during development (Fig. 6E) (Supplemental Table 2). Interestingly, SCO3859 and SCO2668 were multiphosphorylated at 9 different positions each one (Supplemental Fig. 2).

As discussed below, TMT labelling, reduced the efficiency of Ser/Thr/Tyr phosphopeptide identification in *Streptomyces coelicolor* by 2.8-fold in comparison to label free phosphoproteomics (18) (Fig. 6F).

DISCUSSION

Previous proteomic works reported the quantification of the changes of the 8% (6, 7), and 25% (8) of *S. coelicolor* proteome. Here, we quantified the variation of 3461 proteins, 44.3% of S. coelicolor proteome. All proteins currently known to be involved in secondary metabolism were highly up-regulated at the MII stages (CPK, ACT, deoxysugar synthases), with the exception of CDA and coelichelin, which are not produced ("cryptic") under the experimental conditions used in this work; most proteins involved in primary metabolism, especially those involved in protein synthesis (translation and protein folding) were up-regulated at the MI, while proteins involved in the generation of the energy (krebs cycle, oxidative phosphorylation) and the precursors (lipid metabolism, amino acid metabolism, pentose phosphate pathway) necessary for secondary metabolism, were up-regulated in MII; the most important differences between MII30h (substrate mycelium) and MII65h (aerial mycelium), were in the proteins involved in the regulation of hydrophobic cover formation and sporulation (Bld, Whi, SapA, RarA-C) (see above and Figs. 3 and 4). All these data corroborate that MI is the vegetative mycelium, growing actively and synthetizing proteins, while MII is the differentiated mycelium producing secondary metabolites (6, 7). Specific regulators and elicitors regulate the activation or repression of specific secondary metabolite pathways at the MII stages (substrate and aerial mycelia) (82). For instance, AtrA (SCO4118), the activator of actinorhodin biosynthetic genes (75) is up-regulated at the MII65h, activating actinorhodin production, while PkaE (SCO3102) a repressor of actinorhodin production (72) was up-regulated at the MII30h, blocking production; SCO6286, a CPK repressor (83), was up-regulated at the MII65h, blocking CPK biosynthesis during the aerial mycelium stage; SCO3225 and SCO3226, a two-component system repressing CDA biosynthesis showed similar abundances at the MI and MII stages, repressing CDA production under the culture conditions used in this work. Surprisingly, none of the proteins involved in undecylprodigiosin biosynthesis were detected in this or our previous proteomic studies (6, 7), indicating that, for some unknown reason; the same was happening with rodlins and chaplins, the proteins forming the hydrophobic coats of the aerial mycelium, in this case probably due to their high hydrophobicity.

138 regulatory proteins, most of them uncharacterized, and 541 putative proteins without any clear homology, showed differential abundances during the MI and MII (Fig. 4C). These proteins constitute the most complete proteomic database described so far about potential regulators and effectors of Streptomyces differentiation to be characterized.

The existence of a new kind of cell division based in cross-membranes without

detectable peptidoglycan in the MI hyphae was recently demonstrated (2, 84). FtsZ (SCO2082), the key effector of bacterial cell division, including the massive cell-divison accompanying Streptomyces sporulation (58), participates in cross-membrane formation, but FtsZ is not essential, as cross-membranes also exist in the FtsZ-null mutant (2, 84). Despite the fact that most cell-division proteins quantified in this work did not pass the umbral considered as significant (more than twice variation), as it was described for FtsZ (2, 84), several of them were more abundant at the MI than at the sporulating MII (Table II, Supplemental Table 1), suggesting a role in the MI cross-membrane based cell division, as it was described for FtsZ (2). These proteins constitute a good starting point to study the mechanisms controlling cross-membrane cell division in Streptomyces.

The abundance of 1885 proteins (this work) and transcripts (33) (25% of *S. coelicolor* proteome/transcriptome), was compared. Most of them, 95.7% and 88% respectively, had a good agreement at the MII30h and MII65h (Fig. 5A, B), which reveals that differences between the developmental stages (MI, vegetative; MII, reproductive) are much greater than the variability generated by differences in the transcript/protein turnovers, or by the methodological variability intrinsic to proteomic and transcriptomic methodologies.

This work reports the first isobaric mass tagging based quantitative phosphoproteomic work in bacteria. The existence of a dramatic increase in Ser/Thr/Tyr protein phosphorylation accompanying Streptomyces differentiation (MII differentiation) and sporulation was demonstrated: 95% of all the phosphopeptides showing differential abundances during development were up-regulated at the MII stage and 93% at the MII65h (Fig. 6A). This result demonstrates an important role of Ser/Thr/Tyr phosphorylation in the regulation of sporulation, as suggested in our previous label-free phosphoproteomic work (18). TMT labelling interfered in some way with the CPP-TiO2 phosphoenrichment, reducing phosphopeptide yields by 2.8-fold with respect to label-free phosphoproteomics (Fig. 6F). This can be consequence, at least in part, to the high difference in the MI and MII phosphorylation levels. After TMT labelling and sample mixing, the global phosphorylation level is decreased under the umbral in which TiO2 enrichment is not efficient, due the low phosphorylation in the MI sample. The existence of an umbral from which TiO2 phosphoenrichment shows a dramatic efficiency loss was demonstrated before comparing TiO2 phosphoenrichments from CPP pre-enriched/no pre-enriched samples (18). At present, there is not any methodology optimizing phosphopeptide identification and quantification in Streptomyces or other bacteria. Consequently, microbiologists should choose between label-free proteomics and have high yields of phosphopeptide identification (at MII stages) or label-based proteomics and have high reliability in the abundance quantification, but lower dynamic range.

91 phosphopeptides from 47 phosphoproteins were identified. As detailed above, the umbral for considering phosphopeptide variations significant, was fixed in two-fold up- or down-regulated, reporting 59 phosphopeptides from 34 proteins differentially phosphorylated during development (Supplemental Table 2). These phosphopeptides only included a small fraction of the phosphopeptides that passed the differential expression test, and most of them had opposite abundance trends along the three developmental stages analysed in comparison to the non-phosphopeptides (Supplemental Table 2), making methodological drawbacks, as ion ratio suppression (underestimation of the relative change due to co-fragmentation of co-eluting ions with similar m/z) (Ow et al., 2009) (41) highly improbable. Proteins differentially phosphorylated during development included key regulatory proteins as DasR (SCO5231) or RarA (SCO1630). Cell-division proteins as DivIVA (SCO2077) or FtsZ (SCO2082) were highly phosphorylated during the MII65h stage, suggesting a role of this phosphorylation in the regulation of the cell-division accompanying sporulation. Non-regulatory/non cell division proteins and proteins without known function were also differentially phosphorylated during development. With very few exceptions as in the cases of DivIVA, whose phosphorylation by the

AfsK kinase was demonstrated to regulate the assembly of apical polarisomes (59), or the transcriptional regulators AbsA2 (SCO3226) and AfsR (SCO4426) whose activities were described to be regulated by phosphorylation (85, 86), the biological role of the phosphorylation of these proteins remains uncharacterized.

Overall, this work reports the largest database about proteome variations during Streptomyces development, as well as the first quantitative database of Ser/Thr/Tyr phosphorylation variations accompanying Streptomyces differentiation.

Acknowledgements - We thank the European Research Council (ERC Starting Grant; Strp-differentiation 280304), and the Spanish "Ministerio de Economía y Competitividad" (MINECO; BIO2015-65709-R) for financial support. Nathaly Gonzalez-Quiñonez was funded by a Severo Ochoa fellowship (FICYT, Consejería de Educación y Ciencia, Spain). Thanks to Beatriz Gutierrez Magan (Universidad de Oviedo, Dpto. Biología Funcional, Área de Microbiología) for her laboratory assistance.

REFERENCES

1. Hopwood, D. A. (2007) *Streptomyces in nature and medicine: the antibiotic makers.*, Oxford University Press Ed., New York
2. Yague, P., Willemse, J., Koning, R. I., Rioseras, B., Lopez-Garcia, M. T., Gonzalez-Quinonez, N., Lopez-Iglesias, C., Shliaha, P. V., Rogowska-Wrzesinska, A., Koster, A. J., Jensen, O. N., van Wezel, G. P., and Manteca, A. (2016) Subcompartmentalization by cross-membranes during early growth of Streptomyces hyphae. *Nature communications* **7**, 12467
3. Manteca, A., Fernandez, M., and Sanchez, J. (2006) Cytological and biochemical evidence for an early cell dismantling event in surface cultures of Streptomyces antibioticus. *Res Microbiol* **157**, 143-152
4. Yague, P., Lopez-Garcia, M. T., Rioseras, B., Sanchez, J., and Manteca, A. (2013) Pre-sporulation stages of Streptomyces differentiation: state-of-the-art and future perspectives. *FEMS microbiology letters* **342**, 79-88
5. Jayapal, K. P., Philp, R. J., Kok, Y. J., Yap, M. G., Sherman, D. H., Griffin, T. J., and Hu, W. S. (2008) Uncovering genes with divergent mRNA-protein dynamics in *Streptomyces coelicolor. PloS one* **3**, e2097
6. Manteca, A., Jung, H. R., Schwammle, V., Jensen, O. N., and Sanchez, J. (2010) Quantitative proteome analysis of *Streptomyces coelicolor* Nonsporulating liquid cultures demonstrates a complex differentiation process comparable to that occurring in sporulating solid cultures. *Journal of proteome research* **9**, 4801-4811
7. Manteca, A., Sanchez, J., Jung, H. R., Schwammle, V., and Jensen, O. N. (2010) Quantitative proteomics analysis of *Streptomyces coelicolor* development demonstrates that onset of secondary metabolism coincides with hypha differentiation. *Molecular & cellular proteomics : MCP* **9**, 1423-1436
8. Gubbens, J., Janus, M., Florea, B. I., Overkleeft, H. S., and van Wezel, G. P. (2012) Identification of glucose kinase-dependent and -independent pathways for carbon control of primary metabolism, development and antibiotic production in *Streptomyces coelicolor* by quantitative proteomics. *Molecular microbiology* **86**, 1490-1507
9. Pawson, T., and Scott, J. D. (2005) Protein phosphorylation in signaling--50 years and counting. *Trends Biochem Sci* **30**, 286-290
10. Macek, B., Gnad, F., Soufi, B., Kumar, C., Olsen, J. V., Mijakovic, I., and Mann, M. (2008) Phosphoproteome analysis of E. coli reveals evolutionary conservation of bacterial Ser/Thr/Tyr phosphorylation. *Molecular & cellular proteomics : MCP* **7**, 299-307
11. Sun, X., Ge, F., Xiao, C. L., Yin, X. F., Ge, R., Zhang, L. H., and He, Q. Y. (2010) Phosphoproteomic analysis reveals the multiple roles of phosphorylation in pathogenic bacterium Streptococcus pneumoniae. *Journal of proteome research* **9**, 275-282
12. Lin, M. H., Hsu, T. L., Lin, S. Y., Pan, Y. J., Jan, J. T., Wang, J. T., Khoo, K. H., and Wu, S. H. (2009) Phosphoproteomics of Klebsiella pneumoniae NTUH-K2044 reveals a tight link between tyrosine phosphorylation and virulence.

Molecular & cellular proteomics : MCP **8**, 2613-2623
13. Soufi, B., Gnad, F., Jensen, P. R., Petranovic, D., Mann, M., Mijakovic, I., and Macek, B. (2008) The Ser/Thr/Tyr phosphoproteome of Lactococcus lactis IL1403 reveals multiply phosphorylated proteins. *Proteomics* **8**, 3486-3493
14. Ravichandran, A., Sugiyama, N., Tomita, M., Swarup, S., and Ishihama, Y. (2009) Ser/Thr/Tyr phosphoproteome analysis of pathogenic and non-pathogenic Pseudomonas species. *Proteomics* **9**, 2764-2775
15. Macek, B., Mijakovic, I., Olsen, J. V., Gnad, F., Kumar, C., Jensen, P. R., and Mann, M. (2007) The serine/threonine/tyrosine phosphoproteome of the model bacterium Bacillus subtilis. *Molecular & cellular proteomics : MCP* **6,** 697-707
16. Aivaliotis, M., Macek, B., Gnad, F., Reichelt, P., Mann, M., and Oesterhelt, D. (2009) Ser/Thr/Tyr protein phosphorylation in the archaeon Halobacterium salinarum--a representative of the third domain of life. *PloS one* **4**, e4777
17. Bai, X., and Ji, Z. (2012) Phosphoproteomic investigation of a solvent producing bacterium Clostridium acetobutylicum. *Applied microbiology and biotechnology* **95**, 201-211
18. Manteca, A., Ye, J., Sanchez, J., and Jensen, O. N. (2011) Phosphoproteome analysis of Streptomyces development reveals extensive protein phosphorylation accompanying bacterial differentiation. *Journal of proteome research* **10**, 5481-5492
19. Parker, J. L., Jones, A. M., Serazetdinova, L., Saalbach, G., Bibb, M. J., and Naldrett, M. J. (2010) Analysis of the phosphoproteome of the multicellular bacterium *Streptomyces coelicolor* A3(2) by protein/peptide fractionation, phosphopeptide enrichment and high-accuracy mass spectrometry. *Proteomics* **10**, 2486-2497
20. Prisic, S., Dankwa, S., Schwartz, D., Chou, M. F., Locasale, J. W., Kang, C. M., Bemis, G., Church, G. M., Steen, H., and Husson, R. N. (2010) Extensive phosphorylation with overlapping specificity by Mycobacterium tuberculosis serine/threonine protein kinases. *Proceedings of the National Academy of Sciences of the United States of America* **107**, 7521-7526
21. Misra, S. K., Milohanic, E., Ake, F., Mijakovic, I., Deutscher, J., Monnet, V., and Henry, C. (2011) Analysis of the serine/threonine/tyrosine phosphoproteome of the pathogenic bacterium Listeria monocytogenes reveals phosphorylated proteins related to virulence. *Proteomics* **11**, 4155-4165
22. Ge, R., Sun, X., Xiao, C., Yin, X., Shan, W., Chen, Z., and He, Q. Y. (2011) Phosphoproteome analysis of the pathogenic bacterium Helicobacter pylori reveals over-representation of tyrosine phosphorylation and multiply phosphorylated proteins. *Proteomics* **11**, 1449-1461
23. Hu, C. W., Lin, M. H., Huang, H. C., Ku, W. C., Yi, T. H., Tsai, C. F., Chen, Y. J., Sugiyama, N., Ishihama, Y., Juan, H. F., and Wu, S. H. (2012) Phosphoproteomic analysis of Rhodopseudomonas palustris reveals the role of pyruvate phosphate dikinase phosphorylation in lipid production. *Journal of proteome research* **11**, 5362-5375
24. Takahata, Y., Inoue, M., Kim, K., Iio, Y., Miyamoto, M., Masui, R., Ishihama, Y., and Kuramitsu, S. (2012) Close proximity of phosphorylation sites to ligand in the phosphoproteome of the extreme thermophile Thermus thermophilus HB8. *Proteomics* **12**, 1414-1430
25. Soares, N. C., Spat, P., Mendez, J. A., Nakedi, K., Aranda, J., and Bou, G. (2014) Ser/Thr/Tyr phosphoproteome characterization of Acinetobacter baumannii: comparison between a reference strain and a highly invasive multidrug-resistant clinical isolate. *J Proteomics* **102**, 113-124
26. Basell, K., Otto, A., Junker, S., Zuhlke, D., Rappen, G. M., Schmidt, S., Hentschker, C., Macek, B., Ohlsen, K., Hecker, M., and Becher, D. (2014) The phosphoproteome and its physiological dynamics in Staphylococcus aureus. *Int J Med Microbiol* **304**, 121-132
27. Soares, N. C., Spat, P., Krug, K., and Macek, B. (2013) Global dynamics of the Escherichia coli proteome and phosphoproteome during growth in minimal medium. *Journal of proteome research* **12**, 2611-2621
28. Ravikumar, V., Shi, L., Krug, K., Derouiche, A., Jers, C., Cousin, C., Kobir, A., Mijakovic, I., and Macek, B. (2014) Quantitative phosphoproteome analysis of Bacillus subtilis

reveals novel substrates of the kinase PrkC and phosphatase PrpC. *Molecular & cellular proteomics : MCP* **13**, 1965-1978
29. Misra, S. K., Moussan Desiree Ake, F., Wu, Z., Milohanic, E., Cao, T. N., Cossart, P., Deutscher, J., Monnet, V., Archambaud, C., and Henry, C. (2014) Quantitative proteome analyses identify PrfA-responsive proteins and phosphoproteins in Listeria monocytogenes. *Journal of proteome research* **13**, 6046-6057
30. Lim, S., Marcellin, E., Jacob, S., and Nielsen, L. K. (2015) Global dynamics of Escherichia coli phosphoproteome in central carbon metabolism under changing culture conditions. *J Proteomics* **126**, 24-33
31. Licona-Cassani, C., Lim, S., Marcellin, E., and Nielsen, L. K. (2014) Temporal dynamics of the Saccharopolyspora erythraea phosphoproteome. *Molecular & cellular proteomics : MCP* **13**, 1219-1230
32. Kieser, T., Bibb, M. J., Buttner, M. J., Chater, K. F., and Hopwood, D. A. (2000) *Practical Streptomyces genetics.*, John Innes Foundation Ed., Norwich
33. Yague, P., Rodriguez-Garcia, A., Lopez-Garcia, M. T., Martin, J. F., Rioseras, B., Sanchez, J., and Manteca, A. (2013) Transcriptomic analysis of *Streptomyces coelicolor* differentiation in solid sporulating cultures: first compartmentalized and second multinucleated mycelia have different and distinctive transcriptomes. *PloS one* **8**, e60665
34. Novella, I. S., Barbes, C., and Sanchez, J. (1992) Sporulation of Streptomyces antibioticus ETHZ 7451 in submerged culture. *Canadian journal of microbiology* **38**, 769-773
35. Bradford, M. M. (1976) A rapid and sensitive method for the quantitation of microgram quantities of protein utilizing the principle of protein-dye binding. *Anal Biochem* **72**, 248-254
36. Glatter, T., Ludwig, C., Ahrne, E., Aebersold, R., Heck, A. J., and Schmidt, A. (2012) Large-scale quantitative assessment of different in-solution protein digestion protocols reveals superior cleavage efficiency of tandem Lys-C/trypsin proteolysis over trypsin digestion. *Journal of proteome research* **11**, 5145-5156
37. Hojrup, P. (2015) Analysis of Peptides and Conjugates by Amino Acid Analysis. *Methods Mol Biol* **1348**, 65-76
38. Zhang, X., Ye, J., Jensen, O. N., and Roepstorff, P. (2007) Highly Efficient Phosphopeptide Enrichment by Calcium Phosphate Precipitation Combined with Subsequent IMAC Enrichment. *Molecular & cellular proteomics : MCP* **6**, 2032-2042
39. Polpitiya, A. D., Qian, W. J., Jaitly, N., Petyuk, V. A., Adkins, J. N., Camp, D. G., 2nd, Anderson, G. A., and Smith, R. D. (2008) DAnTE: a statistical tool for quantitative analysis of -omics data. *Bioinformatics* **24**, 1556-1558
40. Ritchie, M. E., Phipson, B., Wu, D., Hu, Y., Law, C. W., Shi, W., and Smyth, G. K. (2015) limma powers differential expression analyses for RNA-sequencing and microarray studies. *Nucleic Acids Res* **43**, e47
41. Ow, S. Y., Salim, M., Noirel, J., Evans, C., Rehman, I., and Wright, P. C. (2009) iTRAQ underestimation in simple and complex mixtures: "the good, the bad and the ugly". *Journal of proteome research* **8**, 5347-5355
42. Engholm-Keller, K., Birck, P., Storling, J., Pociot, F., Mandrup-Poulsen, T., and Larsen, M. R. (2012) TiSH--a robust and sensitive global phosphoproteomics strategy employing a combination of TiO2, SIMAC, and HILIC. *J Proteomics* **75**, 5749-5761
43. Schwammle, V., and Jensen, O. N. (2010) A simple and fast method to determine the parameters for fuzzy c-means cluster analysis. *Bioinformatics* **26**, 2841-2848
44. Bentley, S. D., Chater, K. F., Cerdeno-Tarraga, A. M., Challis, G. L., Thomson, N. R., James, K. D., Harris, D. E., Quail, M. A., Kieser, H., Harper, D., Bateman, A., Brown, S., Chandra, G., Chen, C. W., Collins, M., Cronin, A., Fraser, A., Goble, A., Hidalgo, J., Hornsby, T., Howarth, S., Huang, C. H., Kieser, T., Larke, L., Murphy, L., Oliver, K., O'Neil, S., Rabbinowitsch, E., Rajandream, M. A., Rutherford, K., Rutter, S., Seeger, K., Saunders, D., Sharp, S., Squares, R., Squares, S., Taylor, K., Warren, T., Wietzorrek, A., Woodward, J., Barrell, B. G., Parkhill, J., and Hopwood, D. A. (2002) Complete genome sequence of the model actinomycete *Streptomyces coelicolor* A3(2). *Nature* **417**, 141-147
45. Anderson, T. B., Brian, P., and Champness, W. C. (2001) Genetic and transcriptional analysis of absA, an antibiotic gene cluster-linked two-component system that

regulates multiple antibiotics in *Streptomyces coelicolor*. *Molecular microbiology* **39**, 553-566
46. Kelemen, G. H., Brian, P., Flardh, K., Chamberlin, L., Chater, K. F., and Buttner, M. J. (1998) Developmental regulation of transcription of whiE, a locus specifying the polyketide spore pigment in *Streptomyces coelicolor* A3 (2). *Journal of bacteriology* **180**, 2515-2521
47. Chater, K. F. (2001) Regulation of sporulation in *Streptomyces coelicolor* A3(2): a checkpoint multiplex? *Current opinion in microbiology* **4**, 667-673
48. Bibb, M. J., Molle, V., and Buttner, M. J. (2000) sigma(BldN), an extracytoplasmic function RNA polymerase sigma factor required for aerial mycelium formation in *Streptomyces coelicolor* A3(2). *Journal of bacteriology* **182**, 4606-4616
49. Chandra, G., and Chater, K. F. (2008) Evolutionary flux of potentially bldA-dependent Streptomyces genes containing the rare leucine codon TTA. *Antonie van Leeuwenhoek* **94**, 111-126
50. Del Sol, R., Mullins, J. G., Grantcharova, N., Flardh, K., and Dyson, P. (2006) Influence of CrgA on assembly of the cell division protein FtsZ during development of *Streptomyces coelicolor.* *Journal of bacteriology* **188**, 1540-1550
51. Salerno, P., Larsson, J., Bucca, G., Laing, E., Smith, C. P., and Flardh, K. (2009) One of the two genes encoding nucleoid-associated HU proteins in *Streptomyces coelicolor* is developmentally regulated and specifically involved in spore maturation. *Journal of bacteriology* **191**, 6489-6500
52. Ausmees, N., Wahlstedt, H., Bagchi, S., Elliot, M. A., Buttner, M. J., and Flardh, K. (2007) SmeA, a small membrane protein with multiple functions in Streptomyces sporulation including targeting of a SpoIIIE/FtsK-like protein to cell division septa. *Molecular microbiology* **65**, 1458-1473
53. Ditkowski, B., Troc, P., Ginda, K., Donczew, M., Chater, K. F., Zakrzewska-Czerwinska, J., and Jakimowicz, D. (2010) The actinobacterial signature protein ParJ (SCO1662) regulates ParA polymerization and affects chromosome segregation and cell division during Streptomyces sporulation. *Molecular microbiology* **78**, 1403-1415
54. Letek, M., Fiuza, M., Ordonez, E., Villadangos, A. F., Ramos, A., Mateos, L. M., and Gil, J. A. (2008) Cell growth and cell division in the rod-shaped actinomycete Corynebacterium glutamicum. *Antonie van Leeuwenhoek* **94**, 99-109
55. Li, W., Ying, X., Guo, Y., Yu, Z., Zhou, X., Deng, Z., Kieser, H., Chater, K. F., and Tao, M. (2006) Identification of a gene negatively affecting antibiotic production and morphological differentiation in *Streptomyces coelicolor* A3(2). *Journal of bacteriology* **188**, 8368-8375
56. Dedrick, R. M., Wildschutte, H., and McCormick, J. R. (2009) Genetic interactions of smc, ftsK, and parB genes in *Streptomyces coelicolor* and their developmental genome segregation phenotypes. *Journal of bacteriology* **191**, 320-332
57. Wang, L., Yu, Y., He, X., Zhou, X., Deng, Z., Chater, K. F., and Tao, M. (2007) Role of an FtsK-like protein in genetic stability in *Streptomyces coelicolor* A3(2). *Journal of bacteriology* **189**, 2310-2318
58. Flardh, K. (2003) Growth polarity and cell division in Streptomyces. *Current opinion in microbiology* **6**, 564-571
59. Hempel, A. M., Cantlay, S., Molle, V., Wang, S. B., Naldrett, M. J., Parker, J. L., Richards, D. M., Jung, Y. G., Buttner, M. J., and Flardh, K. (2012) The Ser/Thr protein kinase AfsK regulates polar growth and hyphal branching in the filamentous bacteria Streptomyces. *Proceedings of the National Academy of Sciences of the United States of America* **109**, E2371-2379
60. Bennett, J. A., Aimino, R. M., and McCormick, J. R. (2007) *Streptomyces coelicolor* genes ftsL and divIC play a role in cell division but are dispensable for colony formation. *Journal of bacteriology* **189**, 8982-8992
61. Jakimowicz, D., Zydek, P., Kois, A., Zakrzewska-Czerwinska, J., and Chater, K. F. (2007) Alignment of multiple chromosomes along helical ParA scaffolding in sporulating Streptomyces hyphae. *Molecular microbiology* **65**, 625-641
62. McCormick, J. R., and Losick, R. (1996) Cell division gene ftsQ is required for efficient sporulation but not growth and viability in *Streptomyces coelicolor* A3(2). *Journal of bacteriology* **178**, 5295-5301
63. Kleinschnitz, E. M., Heichlinger, A., Schirner, K., Winkler, J., Latus, A., Maldener, I.,

Wohlleben, W., and Muth, G. (2011) Proteins encoded by the mre gene cluster in *Streptomyces coelicolor* A3(2) cooperate in spore wall synthesis. *Molecular microbiology* **79**, 1367-1379
64. Rioseras, B., Yague, P., Lopez-Garcia, M. T., Gonzalez-Quinonez, N., Binda, E., Marinelli, F., and Manteca, A. (2016) Characterization of SCO4439, a D-alanyl-D-alanine carboxypeptidase involved in spore cell wall maturation, resistance, and germination in *Streptomyces coelicolor. Scientific reports* **6**, 21659
65. Holmes, N. A., Walshaw, J., Leggett, R. M., Thibessard, A., Dalton, K. A., Gillespie, M. D., Hemmings, A. M., Gust, B., and Kelemen, G. H. (2013) Coiled-coil protein Scy is a key component of a multiprotein assembly controlling polarized growth in Streptomyces. *Proceedings of the National Academy of Sciences of the United States of America* **110**, E397-406
66. Santos-Beneit, F., Rodriguez-Garcia, A., Sola-Landa, A., and Martin, J. F. (2009) Cross-talk between two global regulators in Streptomyces: PhoP and AfsR interact in the control of afsS, pstS and phoRP transcription. *Molecular microbiology* **72**, 53-68
67. Hsiao, N. H., Nakayama, S., Merlo, M. E., de Vries, M., Bunet, R., Kitani, S., Nihira, T., and Takano, E. (2009) Analysis of two additional signaling molecules in *Streptomyces coelicolor* and the development of a butyrolactone-specific reporter system. *Chemistry & biology* **16**, 951-960
68. den Hengst, C. D., Tran, N. T., Bibb, M. J., Chandra, G., Leskiw, B. K., and Buttner, M. J. (2010) Genes essential for morphological development and antibiotic production in *Streptomyces coelicolor* are targets of BldD during vegetative growth. *Molecular microbiology* **78**, 361-379
69. Komatsu, M., Takano, H., Hiratsuka, T., Ishigaki, Y., Shimada, K., Beppu, T., and Ueda, K. (2006) Proteins encoded by the conservon of *Streptomyces coelicolor* A3(2) comprise a membrane-associated heterocomplex that resembles eukaryotic G protein-coupled regulatory system. *Molecular microbiology* **62**, 1534-1546
70. Fowler-Goldsworthy, K., Gust, B., Mouz, S., Chandra, G., Findlay, K. C., and Chater, K. F. (2011) The actinobacteria-specific gene wblA controls major developmental transitions in *Streptomyces coelicolor* A3(2). *Microbiology* **157**, 1312-1328
71. Ou, X., Zhang, B., Zhang, L., Dong, K., Liu, C., Zhao, G., and Ding, X. (2008) SarA influences the sporulation and secondary metabolism in *Streptomyces coelicolor* M145. *Acta biochimica et biophysica Sinica* **40**, 877-882
72. Urabe, H., Ogawara, H., and Motojima, K. (2015) Expression and characterization of *Streptomyces coelicolor* serine/threonine protein kinase PkaE. *Bioscience, biotechnology, and biochemistry* **79,** 855-862
73. Lu, Y., He, J., Zhu, H., Yu, Z., Wang, R., Chen, Y., Dang, F., Zhang, W., Yang, S., and Jiang, W. (2011) An orphan histidine kinase, OhkA, regulates both secondary metabolism and morphological differentiation in *Streptomyces coelicolor*. *Journal of bacteriology* **193**, 3020-3032
74. Hoskisson, P. A., Rigali, S., Fowler, K., Findlay, K. C., and Buttner, M. J. (2006) DevA, a GntR-like transcriptional regulator required for development in *Streptomyces coelicolor*. *Journal of bacteriology* **188**, 5014-5023
75. Uguru, G. C., Stephens, K. E., Stead, J. A., Towle, J. E., Baumberg, S., and McDowall, K. J. (2005) Transcriptional activation of the pathway-specific regulator of the actinorhodin biosynthetic genes in *Streptomyces coelicolor. Molecular microbiology* **58**, 131-150
76. Meng, L., Yang, S. H., Palaniyandi, S. A., Lee, S. K., Lee, I. A., Kim, T. J., and Suh, J. W. (2011) Phosphoprotein affinity purification identifies proteins involved in S-adenosyl-L-methionine-induced enhancement of antibiotic production in *Streptomyces coelicolor*. *The Journal of antibiotics* **64**, 97-101
77. Mikulik, K., Khanh-Hoang, Q., Halada, P., Bezouskova, S., Benada, O., and Behal, V. (1999) Expression of the Csp protein family upon cold shock and production of tetracycline in Streptomyces aureofaciens. *Biochem Biophys Res Commun* **265**, 305-310
78. Rigali, S., Titgemeyer, F., Barends, S., Mulder, S., Thomae, A. W., Hopwood, D. A., and van Wezel, G. P. (2008) Feast or famine: the global regulator DasR links nutrient stress to antibiotic production by Streptomyces. *EMBO reports* **9**, 670-675

79. Vrancken, K., Van Mellaert, L., and Anne, J. (2008) Characterization of the Streptomyces lividans PspA response. *Journal of bacteriology* **190**, 3475-3481
80. Takano, H., Hashimoto, K., Yamamoto, Y., Beppu, T., and Ueda, K. (2011) Pleiotropic effect of a null mutation in the cvn1 conservon of *Streptomyces coelicolor* A3(2). *Gene* **477**, 12-18
81. Wang, W., Shu, D., Chen, L., Jiang, W., and Lu, Y. (2009) Cross-talk between an orphan response regulator and a noncognate histidine kinase in *Streptomyces coelicolor*. *FEMS microbiology letters* **294**, 150-156
82. Liu, G., Chater, K. F., Chandra, G., Niu, G., and Tan, H. (2013) Molecular regulation of antibiotic biosynthesis in streptomyces. *Microbiology and molecular biology reviews : MMBR* **77**, 112-143
83. Gottelt, M., Kol, S., Gomez-Escribano, J. P., Bibb, M., and Takano, E. (2010) Deletion of a regulatory gene within the cpk gene cluster reveals novel antibacterial activity in *Streptomyces coelicolor* A3(2). *Microbiology* **156**, 2343-2353
84. Celler, K., Koning, R. I., Willemse, J., Koster, A. J., and van Wezel, G. P. (2016) Cross-membranes orchestrate compartmentalization and morphogenesis in *Streptomyces*. *Nature communications* **7**, ncomms11836
85. McKenzie, N. L., and Nodwell, J. R. (2007) Phosphorylated AbsA2 negatively regulates antibiotic production in *Streptomyces coelicolor* through interactions with pathway-specific regulatory gene promoters. *Journal of bacteriology* **189**, 5284-5292
86. Sawai, R., Suzuki, A., Takano, Y., Lee, P. C., and Horinouchi, S. (2004) Phosphorylation of AfsR by multiple serine/threonine kinases in *Streptomyces coelicolor* A3(2). *Gene* **334**, 53-61
87. Sharma, K., D'Souza, R. C., Tyanova, S., Schaab, C., Wisniewski, J. R., Cox, J., and Mann, M. (2014) Ultradeep human phosphoproteome reveals a distinct regulatory nature of Tyr and Ser/Thr-based signaling. *Cell reports* **8**, 1583-1594

CAPÍTULO 2

Modificaciones de la pared celular que tienen lugar durante las fases de esporulación y germinación.

En este trabajo se estudian los cambios que tienen lugar en la pared celular de las esporas, principalmente durante la germinación, debidos a la acción de una LMM-PBP que se demostró que participa en la formación y remodelación del peptidoglicano: una D-alanil-Dalanina carboxipeptidasa codificada por el gen SCO4439. El estudio de la función biológica de esta proteína nos llevó a caracterizar estadios de la germinación desconocidos hasta entonces.

Este objetivo se aborda en una publicación:

Manuscrito 2:

Rioseras B, Yagüe P, López-García MT, Gonzalez-Quiñonez N, Binda E, Marinelli F, Manteca A. 2016. "Characterization of SCO4439, a D-alanyl-D-alanine carboxypeptidase involved in spore cell wall maturation, resistance, and germination in *Streptomyces coelicolor*". Sci Rep. 6:21659.

SCIENTIFIC REPORTS

OPEN

Characterization of SCO4439, a D-alanyl-D-alanine carboxypeptidase involved in spore cell wall maturation, resistance, and germination in *Streptomyces coelicolor*

Received: 22 October 2015
Accepted: 28 January 2016
Published: 12 February 2016

Beatriz Rioseras[1], Paula Yagüe[1], María Teresa López-García[1], Nathaly Gonzalez-Quiñonez[1], Elisa Binda[2,3], Flavia Marinelli[2,3] & Angel Manteca[1]

This work contributes to the understanding of cell wall modifications during sporulation and germination in *Streptomyces* by assessing the biological function and biochemical properties of SCO4439, a D-alanyl-D-alanine carboxypeptidase (DD-CPase) constitutively expressed during development. SCO4439 harbors a DD-CPase domain and a putative transcriptional regulator domain, separated by a putative transmembrane region. The recombinant protein shows that DD-CPase activity is inhibited by penicillin G. The spores of the *SCO4439::Tn5062* mutant are affected in their resistance to heat and acid and showed a dramatic increase in swelling during germination. The mycelium of the *SCO4439::Tn5062* mutant is more sensitive to glycopeptide antibiotics (vancomycin and teicoplanin). The DD-CPase domain and the hydrophobic transmembrane region are highly conserved in *Streptomyces*, and both are essential for complementing the wild type phenotypes in the mutant. A model for the biological mechanism behind the observed phenotypes is proposed, in which SCO4439 DD-CPase releases D-Ala from peptidoglycan (PG) precursors, thereby reducing the substrate pool for PG crosslinking (transpeptidation). PG crosslinking regulates spore physical resistance and germination, and modulates mycelium resistance to glycopeptides. This study is the first demonstration of the role of a DD-CPase in the maturation of the spore cell wall.

Streptomycetes are mycelial microorganisms characterized by their complex developmental cycles, including programmed cell death (PCD) and hyphae differentiation, which leads to aerial mycelium formation and sporulation[1,2]. Streptomycetes are important industrial bacteria producing approximately two-thirds of clinical antibiotics, as well as a large number of eukaryotic cell differentiation inducers and inhibitors[3]. Most of these bioactive compounds are specialized metabolites[4], the production of which is regulated, at least in part, by hyphal differentiation[5]. *Streptomyces* development, is activated by extracellular signals, including nutritional stimuli or cell density (quorum sensing), and is regulated by complex signaling pathways that are only partially known[5–7]. The best-characterized stages of *Streptomyces* development are those related to aerial mycelium and sporulation. Several key regulatory networks controlling these stages have been characterised (bald, sky or white pathways, reviewed in Flärdh and Buttner[1]). Despite this, the regulation of aerial mycelium and sporulation remains incompletely understood, and new genes and proteins regulating these important processes, are still being discovered[8].

[1]Área de Microbiología, Departamento de Biología Funcional and IUOPA, Facultad de Medicina, Universidad de Oviedo, 33006 Oviedo, Spain. [2]Department of Biotechnology and Life Sciences, University of Insubria, via J. H. Dunant 3, 21100 Varese, Italy. [3]"The Protein Factory" Research Center, Politecnico of Milano, ICRM CNR Milano and University of Insubria, 21100 Varese, Italy. Correspondence and requests for materials should be addressed to A.M. (email: mantecaangel@uniovi.es)

Stages preceding aerial mycelium, including spore germination and differentiation in liquid non-sporulating cultures, are even less characterized and comprehended[2,9].

D-alanyl-D-alanine carboxypeptidases (DD-CPases) are members of the penicillin binding proteins (PBPs), a family of proteins inhibited by ß-lactam antibiotics involved in peptidoglycan (PG) synthesis and remodelling. The PBPs constitute a family of acyltransferases with a common evolutionary origin and a common substrate (the D-Ala-D-Ala dipeptides present in the pentapeptide stems of PG precursors), that are collectively known as DD-peptidases. DD-peptidases include transglycosylases, which catalyze the polymerization of glycan chains composed of N-acetylglucosamine (NAG) and N-acetylmuramic acid (NAM); DD-CPases, which remove the terminal D-alanine from muramyl pentapeptide; transpeptidases, which catalyze the cross-link formation between one D-Ala of one PG strand and one amino acid of the other strand; and endopeptidases, which cleave the cross-linked peptide side-chains[10]. The DD-peptidases are classified on the basis of their molecular mass, amino acid sequence and enzyme activity at high molecular mass (HMM) and low molecular mass (LMM)[11–13]. HMM DD-peptidases are usually bifunctional transglycosylases/transpeptidases (also classified as class A), or monofunctional transpeptidases (class B) anchored to membranes. LMM DD-peptidases are monofunctional carboxypeptidases or endopeptidases, and the majority are also anchored to membranes (class C). LMM DD-peptidases are usually not essential, and they are not found in most studies and reviews on PBPs[13].

Most bacteria have multiple PBPs with varying degrees of redundant activity. A phylogenetic analysis revealed that Actinobacteria have an average of five HMM DD-peptidases per genome; this number doubled only in streptomycetes (13 DD-peptidases in the case of *S. coelicolor*)[13]. Many DD-peptidases belong to the SEDS (shape, elongation, division, and sporulation) clusters of genes involved in PG synthesis and remodeling and are essential for growth, cell division, and cellular viability. DD-peptidases that are not included in the SEDS clusters are considered dispensable for growth and viability[10], and their biological function remains poorly investigated. *Streptomyces coelicolor* harbors four SEDS clusters[14], that include four transpeptidases (SCO2090, SCO2608, SCO3847 and SCO5301).

This work contributes characterizing the biological function of the largely ignored redundant and non-essential LMM DD-peptidases by studying the activity and role of *SCO4439*, a gene encoding a putative DD-CPase. *SCO4439* is a very unusual DD-CPase that is highly conserved in streptomycetes and is therein fused with a putative transcriptional regulator domain (see below). *SCO4439* was found to be slightly over-expressed during the aerial mycelium and sporulation stages[15], however, its biological role remained unclear.

Results

Mutation of *SCO4439* affects spore swelling during germination, increases spore resistance to acid/heating and reduces the glycopeptide resistance. Cosmid D6.2.B06_046 harboring a copy of *SCO4439* interrupted by Tn5062 was used to obtain the *S. coelicolor SCO4439::Tn5062* mutant using the methodology developed by Fernández-Martínez *et al.*[16]. The early stages of *SCO4439::Tn5062* mutant spore germination were similar to those in the *S. coelicolor* wild strain (Fig. 1a–h); however *SCO4439::Tn5062* mutant showed a clear and distinctive phenotype at later stages, consisting of a dramatic increase in spore swelling (Fig. 1k,l) with respect to the wild-type strain (Fig. 1i,j).

The kinetics of spore germination in the *S. coelicolor* wild type and in the *SCO4439::Tn5062* mutant were studied by using time-lapse confocal microscopy (Fig. 1m,n and Supplementary Movies 1 and 2). The spores of the *S. coelicolor* parental strain swelled until they reached a diameter of $2.3 \pm 0.4\,\mu m$ (5-hour culture), before the emergence of the germ tube, which coincided with a deswelling and a consequent reduction of the spore diameter (from $2.3 \pm 0.4\,\mu m$ at 5-hours to $1.2 \pm 0.4\,\mu m$ at 8-hours) (Fig. 1m,r). At early time points, the swelling of the spores of the *SCO4439::Tn5062* mutant was slower than the swelling of the spores of the wild strain (compare 5 hour-time in Fig. 1m,n), but they continued to swell after the emergence of the germ tube, reaching a diameter that was the double that of the wild type spores ($3.2\,\mu m \pm 0.4\,\mu m$) before deswelling and reducing the spore diameter (Fig. 1n,r). Another difference between the wild type and the *SCO4439::Tn5062* mutant was that, after germination and deswelling, the cell membrane permeability inside the spores remained intact in the wild type strain (SYTO9 staining, Fig. 1o), but not in the *SCO4439::Tn5062* mutant (PI staining, Fig. 1p). The increase in spore swelling affected 100% of the *SCO4439::Tn5062* mutant spores at 15–18 hours (average diameter of $3.1 \pm 0.4\,\mu m$, Fig. 1r).

Contrary to expectations[16], DNA sequencing demonstrated that the insertion of Tn5062 into cosmid D6.2.B06_046 generated a deletion. Tn5062 was inserted at position 640 of *SCO4439* and 669 of *SCO4440*, generating a loss of 1,641 bp, which affected the 5′-terminus of *SCO4439* and most of the *SCO4440* open reading frame (ORF) (schematized in Fig. 2a). The deletion of the 5′-terminus of *SCO4439* may affect the expression of *SCO4437* and *SCO4438* (both located downstream of *SCO4439*), whereas the deletion of *SCO4440* may affect the expression of *SCO4441* and *SCO4442* (Fig. 2a). To identify the gene responsible for the observed phenotype, plasmid pMS82[17] was used to introduce different fragments of the *SCO4437-SCO4442* chromosomal region, into the *SCO4439::Tn5062* mutant strain (schematized in Fig. 2b). The only DNA fragments complementing the wild-type phenotype were those including *SCO4439,* as was the case for plasmid pBRB3 (compare Fig. 2c with Fig. 1k,l) (Supplementary Movie 3). Similar results were obtained in the *SCO4439::Tn5062* mutant harboring plasmid pBRB2 but not in the mutant strain harboring plasmid pBRB1 (data not shown).

As introduced above, the *SCO4439* gene was previously reported to be slightly over-expressed during aerial mycelium and sporulation in microarray-based transcriptomic analyses; however differences in expression were too low to be considered significant[15] (Fig. 2e). In this work, RT-PCR analyses confirmed the expression pattern of *SCO4439* (Fig. 2e).

The spore resistance profiles of the *SCO4439::Tn5062* mutant and the wild type strains were compared (Fig. 3). Lysozyme treatment increases germination, and sonication kills 99% of the spores in the *S. coelicolor* wild strain. The *SCO4439* mutation did not affect resistance to the lysozyme, to sonication or to freezing

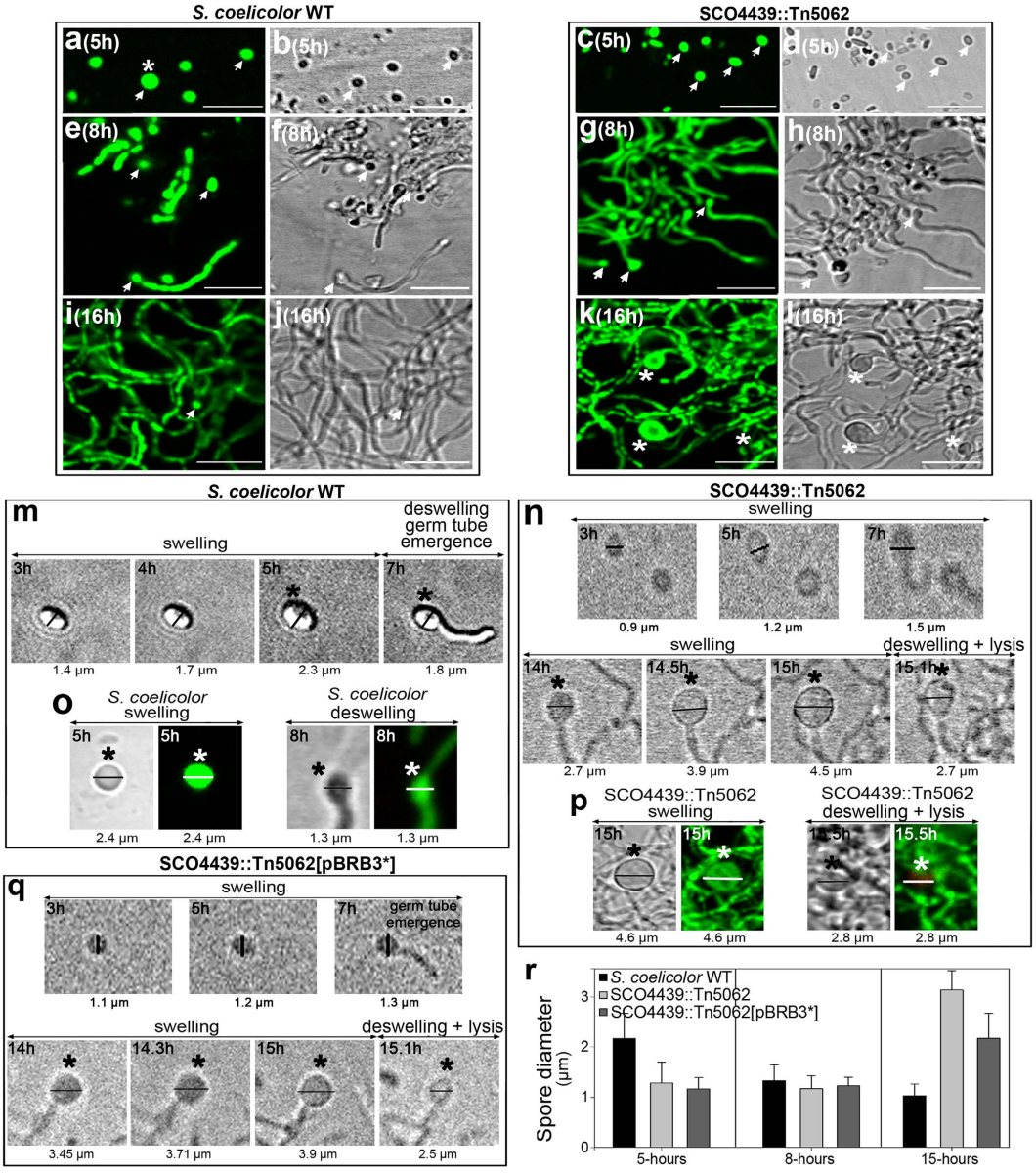

Figure 1. Analysis of the germination stages in *S. coelicolor* wild type and in *S. coelicolor SCO4439::Tn5062* mutant. (**a–l**) Confocal laser-scanning fluorescence microscopy analysis (SYTO9/PI staining) of the *S. coelicolor* wild type (left panel) and *SCO4439::Tn5062* mutant (right panel). The same samples were observed using the fluorescence (left pictures) or interference contrast modes (right pictures). Bars indicate 8 µm (**m,n**) Time-lapse confocal microscopy (interference contrast mode) of the germination of spores from the wild type and of the *SCO4439::Tn5062* mutant, respectively. Spore diameters are indicated. (**o,p**) Confocal laser-scanning fluorescence microscopy analysis (SYTO9/PI staining) and interference contrast images of spore swelling and spore deswelling stages in the wild type and *SCO4439::Tn5062* mutant, respectively. (**q**) Time-lapse confocal microscopy of the germination of spores from the *SCO4439::Tn5062* mutant harboring the *SCO4439** mutated gene (SCO4439::Tn5062[pBRB3*] strain). Time-lapse experiments were limited to 12 hours (see Methods for details). Arrows indicate spores. Asterisks indicate swelled spores. (**r**) Quantification of the spore diameters (average ± SD) of the wild type, *SCO4439::Tn5062* mutant, and *SCO4439::Tn5062*[pBRB3*] strain at 5, 8 and 15 hours.

(Fig. 3a–c) but increased fivefold the spore resistance to acid and heating compared with the parental strain and the *SCO4439::Tn5062* complemented mutant (Fig. 3d,e).

Mycelium resistance to glycopeptides (vancomycin and teicoplanin) was reduced in the *SCO4439::Tn5062* mutant (minimum inhibitory concentrations of 110 and 0.7 µg/ml, respectively), in respect to the *S. coelicolor* wild type strain (minimum inhibitory concentrations 140 and 0.9 µg/ml) (Fig. 3f).

SCO4439 harbors two protein domains separated by a putative hydrophobic transmembrane region. *SCO4439* encodes a multi-domain protein harboring a DD-CPase (conserved domain database

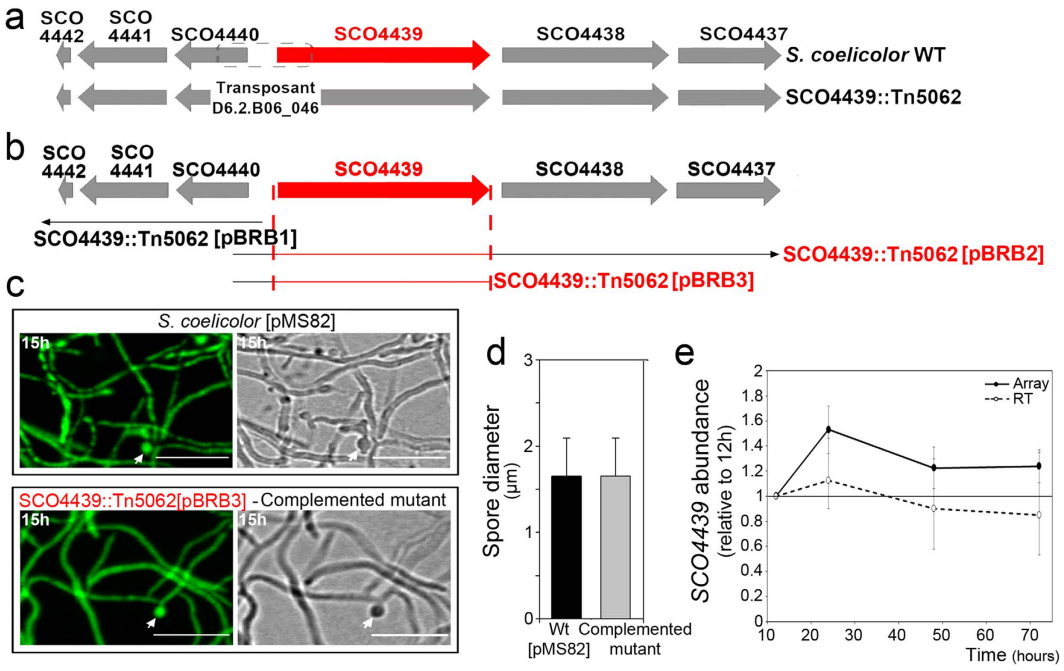

Figure 2. Complementation of the wild-type phenotype in the *SCO4439::Tn5062* mutant, and *SCO4439* gene expression during development. (**a**) Scheme of the *SCO4437-SCO4442* region in the wild type and the *SCO4439::Tn5062* mutant. The dashed line indicates the chromosome deletion generated by the transposon insertion. (**b**) Scheme illustrating the fragments introduced into the mutant strain using plasmids pBRB1, pBRB2 and pBRB3. Fragments that complemented the phenotype in the mutant strain are highlighted in red. (**c**) Confocal laser fluorescence microscopy analysis of the *S. coelicolor* wild-type strain harboring pMS82 (control), and the *S. coelicolor SCO4439::Tn5062* mutant strain harbouring pBRB3 (complementation of the phenotype is also observed with pBRB2 but not with pBRB1). Samples were observed using the fluorescence (left pictures) or interference contrast modes (right pictures). Arrows indicate spores. (**d**) Quantification of spore diameters (average ± SD) in the wild type harboring pMS82 and in the *SCO4439::Tn5062* mutant harboring pBRB3. (**e**) *SCO4439* gene abundance at 12, 24, 48 hours (aerial mycelium) and 72 hours (spores). Data represent the fold change with respect to the 12 hour time point (qRT-PCR and microarray values). Microarray data are from Yagüe *et al.*[2].

accession COG1686), and a putative transcriptional regulator (conserved domain database accession PHA03307) (Fig. 4a). According to the Phobius software prediction (http://phobius.sbc.su.se/), these two domains are separated by a putative transmembrane region (Fig. 4a). The DD-CPase domain and the putative hydrophobic transmembrane domain are highly conserved in the *Streptomyces* genus (70% average similarity in *Streptomyces*) and actinomycetes in general (data not shown). The conservation of the transcriptional regulatory domain is substantially lower (44% average similarity in *Streptomyces*), and this domain is not present in other actinomycetes.

Different fragments of the *SCO4439* gene were introduced into the *SCO4439::Tn5062* mutant strain, using pMS82 as the integrative carrier vector (see Materials and Methods for details and scheme in Fig. 4a). The only fragments that complemented the wild-type phenotype were those containing both, the transmembrane and DD-CPase domains (data not shown).

Amino acid sequence alignment of the *S. coelicolor* DD-CPase domain (Fig. 4b) showed an overall high identity with the orthologous proteins from the six model *Streptomyces* strains analyzed, including the triad of "SxxK", "SxN" and "KTG" motifs that characterize the "SxxK" superfamily of penicillin-binding DD-peptidases[11]. Interestingly, a replacement of Leu_{684} by Pro (randomly generated by PCR, see Methods) partially blocked the phenotype complementation in spore swelling in the *SCO4439::Tn5062* mutant (Fig. 1q). As discussed below, the maximum spore-swelling of the *SCO4439::Tn5062* mutant strain harboring the mutated *SCO4439** gene (*SCO4439::Tn5062* [pBRB3*] strain) was 3.9 μm (Fig. 1q), which is an intermediate value between the wild type (2.3 μm) and the *SCO4439:Tn5062* mutant (4.5 μm) spore diameters (Fig. 1m,n,q,r; Supplementary Movie 4).

SCO4439 carboxypeptidase activity. The SCO4439 protein and its mutated version SCO4439* (mutation replacing Leu_{684} with Pro_{684}, see above) were over-expressed in *E. coli*, and purified using His-tag affinity chromatography (Fig. 5a). The identity of the overproduced proteins was confirmed via peptide mass fingerprinting (data not shown).

The enzymatic activities of the purified SCO4439 and SCO4439* were assayed on D-Ala-D-Ala dipeptide and on the tripeptide N_{α},N_{ε}-diacetyl-L-Lys-D-Ala-D-Ala, which mimics the terminal portions of the PG pentapeptide precursors[17,18]. SCO4439 and SCO4439* cleaved the D-Ala from the tripeptide and, to a lesser extent, from the dipeptide D-Ala-D-Ala. Thus, they showed a significantly higher DD-CPase activity than DD-dipeptidase activity (Fig. 5b). The enzyme activity of the mutated SCO4439* was half that of the non-mutated protein (Fig. 5b and

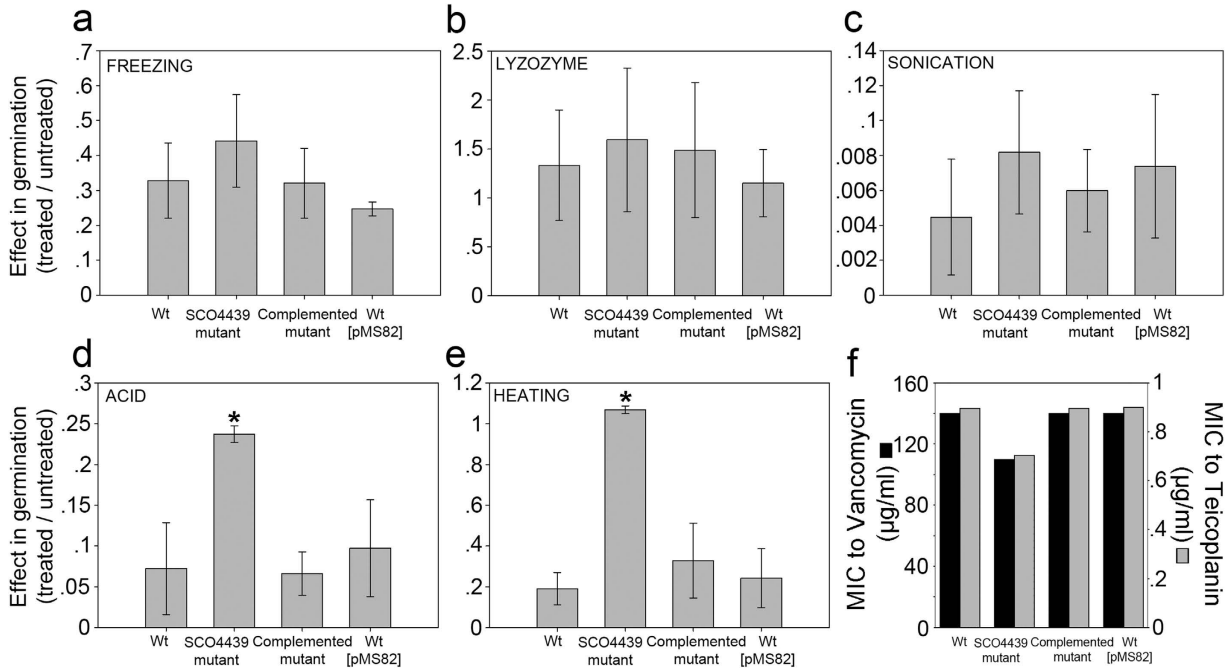

Figure 3. Spore resistance to physicochemical stresses and mycelium resistance to glycopeptides (vancomycin and teicoplanin). (**a**) Spore resistance to freezing. (**b**) lysozyme. (**c**) sonication. (**d**) acid. (**e**) heating. (**f**) Minimum inhibitory concentrations of vancomycin and teicoplanin towards *S. coelicolor*. The (1) effect on germination of the treated spores with respect to the untreated spores, and the (2) MIC values were estimated for the *S. coelicolor* wild-type strain (wt), *SCO4439::Tn5062* mutant (SCO4439 mutant), *SCO4439::Tn5062* complemented with pBRB3 (complemented mutant) and the control wild type strain harboring pMS82 (wt pMS82). Note that lysozyme treatment increased germination in all strains. Asterisks indicate a significant increase in resistance to acid and heating in the mutant strain. Percentages of germination are the average ± SD of three replicates; MIC values were estimated using three biological replicates; SD = 0.

discussed below). As expected, due to the presence of the canonical Ser-x-x-Lys motif present in SCO4439, the enzyme activity was inhibited by penicillin G (IC_{50} of 1 mM, Fig. 5c). As a control, no DD-CPase/DD-dipeptidase activity was detectable in the *E.coli* host transformed with the empty expression vectors (data not shown).

The DD-CPase/DD-dipeptidase activity of SCO4439 was then assayed in extracts from wild type *S. coelicolor,* the *SCO4439::Tn5062* mutant, and the complemented mutant. The DD-CPase/DD-dipeptidase activity was always detectable in insoluble fractions (membranes and cell wall debris) from the *S. coelicolor* wild-type strain and the complemented mutant, but not in those from the *S. coelicolor SCO4439::Tn5062* mutant (Fig. 5d,e). There was no detectable activity in the cytosolic fractions from any of the two strains (data not shown). Interestingly, the specific DD-CPase enzymatic activity was slightly higher at the early time points after germination (16 hours) than in the substrate (30 hours) or aerial (72 hours) mycelium stages (Fig. 5d). As expected, incubation of the insoluble fractions with penicillin G abolished the enzyme's activity (data not shown).

The spore PG crosslinking index (ratio between cross-linked glycine and total glycine) was estimated by adapting the 1-fluoro-2,4-dinitrobenzene (FDNB) method originally described for *Bacillus*[19] to *Streptomyces* (see Methods for details) (Fig. 5f). As discussed below, the spores of the *S. coelicolor SCO4439::Tn5062* mutant had 20% more crosslinking than the spores of the wild type strain. Interestingly, the PG crosslinking of the *SCO4439::Tn5062* harboring the mutated *SCO4439** gene (*SCO4439::Tn5062* [pBRB3*]) were at an intermediate level in PG crosslinking between the *SCO4439::Tn5062* mutant and the wild type strain (10% more crosslinking than the spores of the wild type strain; Fig. 5f).

PG synthesis during spore swelling and germination. Peptidoglycan synthesis during spore germination and swelling was analyzed using fluorescent BODIPY-vancomycin[20] (Fig. 6). BODIPY-vancomycin preferentially stains nascent PG, the staining of which protrudes above the areas in which there is no PG synthesis[20]. No PG synthesis occurred during the spore germination and swelling early stages in the wild and complemented strains, at least in the amount detectable by BODIPY-vancomycin staining (Fig. 6). Only at the latest stages of spore swelling, some areas of PG synthesis become detectable in the swelled spores of the mutant strain (Fig. 6j).

Discussion

The aim of this work was the characterization of SCO4439, a DD-CPase constitutively expressed during development (Fig. 2e), and whose enzymatic activity is present during all developmental stages analyzed (Fig. 5d). The best characterized DD-peptidases are those belonging to the SEDS genes involved in PG synthesis/remodeling which are essential for growth, cell division, and viability. However, with very few exceptions, the biological role

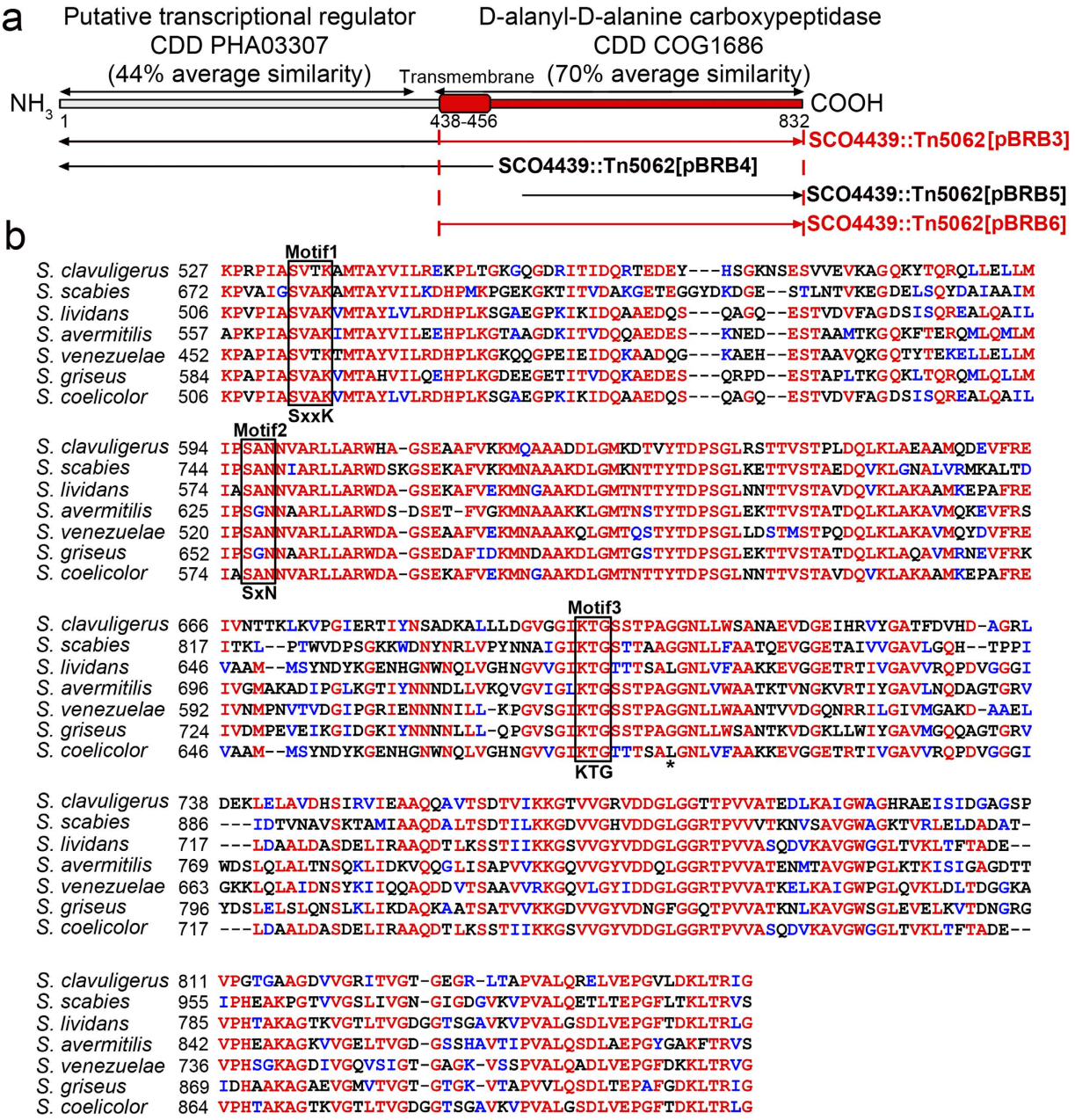

Figure 4. Structure of SCO4439 and orthologous proteins in the *Streptomyces* genus. (**a**) Scheme indicating the structure of the SCO4439 protein. Conserved database domain (CDD) references and their average similarities in the *Streptomyces* genus are indicated. *SCO4439* fragments introduced in plasmids pBRB3, pBRB4, pBRB5 and pBRB6 are shown schematically. Fragments that complemented the phenotype in the mutant strain are highlighted in red. (**b**) Sequence alignment of the DD-CPase domain of SCO4439 (*S. coelicolor*) and their orthologs in other model streptomycetes. Conserved "SxxK", "SxN" and "KTG" motifs that characterize the "SxxK" superfamily of DD-peptidases are indicated. An asterisk indicates the Leu_{684} whose replacement by Pro partially blocks complementation of the wild type phenotype in the *SCO4439::Tn5062* mutant.

of other redundant DD-peptidases, not included in the SEDS clusters, such as SCO4439, remains unknown[19,21]. SCO4439 is not essential for growth; however its mutation resulted in a dramatic increase in both spore resistance to acid/heating and swelling during germination.

DD-CPases are usually anchored to cell membranes at their N-terminus, and their active sites are exposed to the periplasmic space in which they catalyze the final stages of cell wall biosynthesis[11]. SCO4439 is very unusual, because in addition to the DD-CPase domain, it harbors an additional putative transcriptional regulator domain. Other DD-CPases, including most HMM DD-CPases, are multi domain proteins and harbor glycosyl transferase domains involved in cell wall maturation[11]. However, to our knowledge, SCO4439 is the first DD-CPase that is associated with a putative transcriptional regulatory domain. SCO4439 has a high molecular mass of 84 kDa, resulting in its classification as an HMM DD-CPase. However, the DD-peptidase domain of

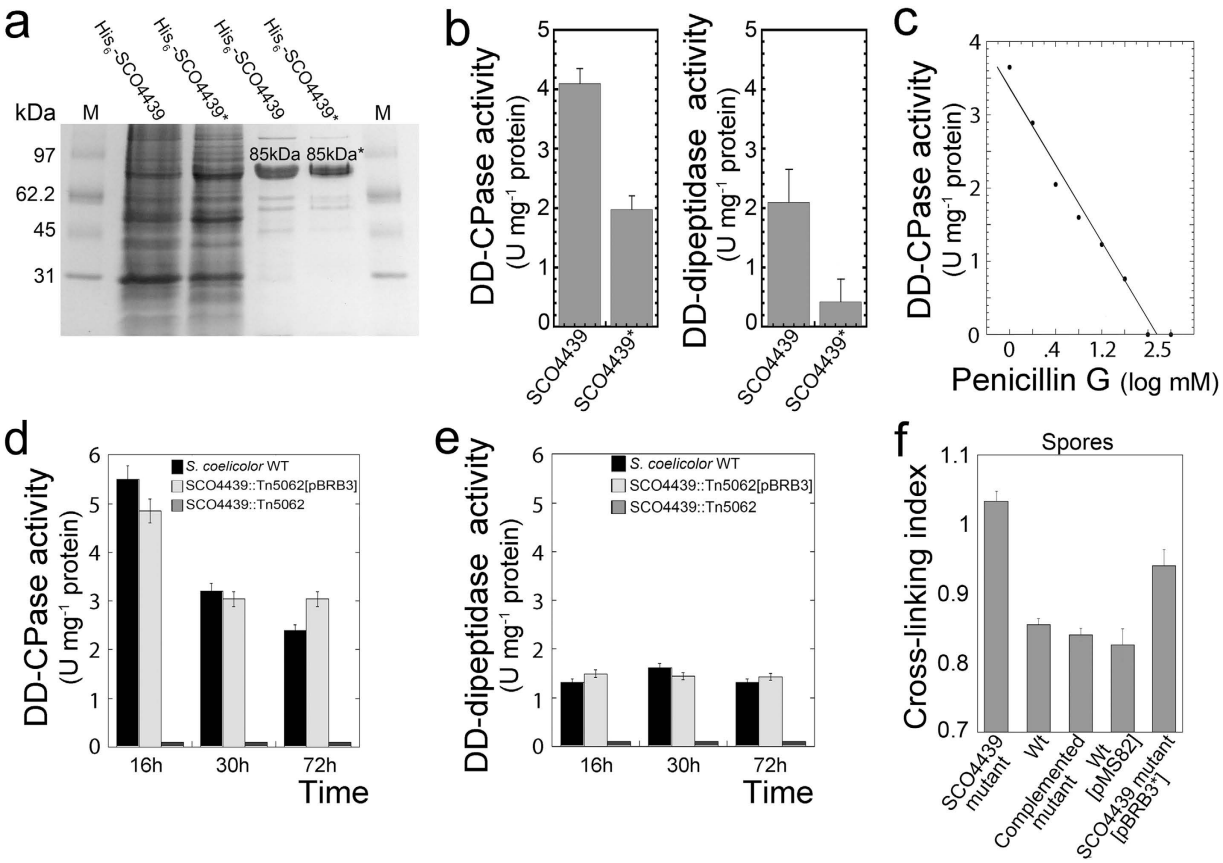

Figure 5. Purification of recombinant His_6-SCO4439/ His_6-SCO4439*, SCO4439 activity and cellular localization. (**a**) Coomassie-stained SDS-PAGE gel of overproduced His_6-SCO4439 and His_6-SCO4439* (substitution of Leu_{684} for Pro_{684}). M, molecular weight markers. Lane 1, *E. coli* JM109 producing His_6-SCO4439 (45 μg). Lane 2, *E. coli* JM109 producing His_6-SCO4439* (45 μg). Lane 3, purified His_6-SCO4439 (4 μg). Lane 4 purified His_6-SCO4439* (4 μg). (**b**) DD-CPase and DD-dipeptidase activities of His_6-SCO4439 and His_6-SCO4439*. Enzyme activity values (units per mg of pure recombinant protein) are the average ± SD of three replicates. (**c**) His_6-SCO4439 penicillin inhibition curve. (**d**,**e**) DD-CPase and DD-dipeptidase activity (units per mg of total protein) detected in insoluble fractions (membrane and cell wall debris) of *S. coelicolor* wild type and of *SCO4439::Tn5062* mutant strains. (**f**) PG crosslinking in the spores of the *SCO4439::Tn5062* mutant (SCO4439 mutant), *S. coelicolor* wild type (wt), *SCO4439::Tn5062* complemented with pBRB3 (complemented mutant), the control wild type strain harboring pMS82 (wt pMS82), and the *SCO4439::Tn5062* mutant complemented with pBRB3* (SCO4439 mutant [pBRB3*]). Values are the means ± SD of two biological replicates, and four technical replicates.

SCO4439 is homologous to LMM DD-peptidases and exhibits the DD-CPase activity that is peculiar to LMM DD-peptidases[11]. The putative transmembrane domain of SCO4439 is located in the middle of the protein, separating the DD-CPase and the putative transcriptional regulator domains, which is also unusual. The (1) Phobius prediction of the protein structure, (2) the presence of DD-CPase activity only in *S. coelicolor* insoluble fractions (membranes and cell wall debris) (Fig. 5d) and (3) the presence of the essential nature of the transmembrane domain for biological activity (Fig. 4a) suggest that the DD-CPase domain is exposed to the periplasmic space, whereas the putative transcriptional regulatory domain is likely located on the cytosol side of the cell membrane. Further work is required to understand the biological function, if any, of the putative transcriptional regulatory domain located at the N-terminus of SCO4439. The presence of this domain in all SCO4439 orthologs suggests that it may have a relevant function (Fig. 4). In contrast, its relatively low conservation (44% average similarity), its exclusive occurrence in streptomycetes, and finally, its unessential role in complementing the spore germination and resistance phenotypes in the *SCO4439::Tn5062* mutant may indicate that this domain has not an essential function.

Spore germination comprises a succession of distinctive steps that were organized by Hardisson *et al.*[22] into three stages: darkening, swelling, and germ tube emergence (Fig. 7). The biomolecular mechanisms controlling these stages remain poorly characterized[23–25]. There are two examples of proteins known to be involved in *Streptomyces* spore germination. NepA was described as a structural cell wall protein involved in the maintenance of spore dormancy in *S. coelicolor*[26]. SsgA was identified as a protein marking cell-wall sites in which germination takes place[27]. The phenotype of the *SCO4439::Tn5062* mutant observed in this work indicates the existence of a new stage that includes the deswelling of the spores once they cannot resist further swelling. The occurrence of

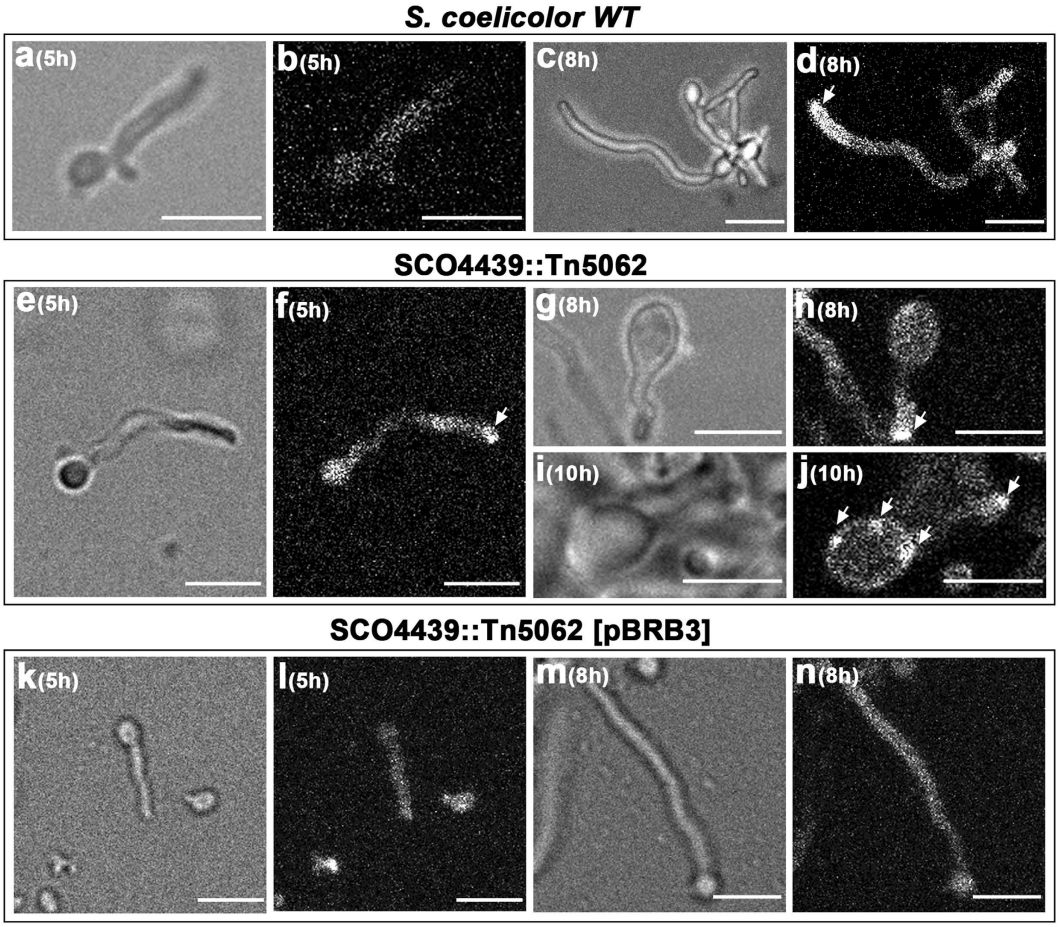

Figure 6. Nascent-PG synthesis during germination. (**a**–**d**) *S. coelicolor* wild type. (**e**–**j**) *SCO4439::Tn5062* mutant. (**k**–**n**), (*SCO4439::Tn5062*[pBRB3] complemented strain. GYM liquid cultures were stained with BODIPY-vancomycin, and observed at the confocal microscope. The interference contrast mode (left pictures) and fluorescent images (right pictures) are shown. Arrows indicate nascent PG. Developmental time points are indicated. Scale bars represent 4 μm.

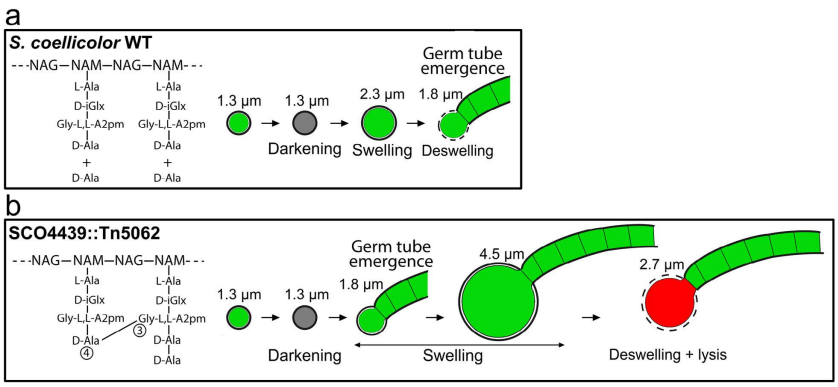

Figure 7. Model for the biological function of SCO4439. (**a**) *S. coelicolor* wild type. (**b**) *SCO4439::Tn5062.* Classical germination stages: darkening, swelling and germ tube emergence[24]. The proposed spore deswelling stage is indicated. Green illustrates the membrane-intact cells (SYTO 9 staining); red indicates propidium iodide (PI) permeable cells (lysis). D-iGlx, D-*iso*-glutamine or D-*iso*-glutamic acid. See text for details.

this stage was demonstrated via time-lapse microscopy in both the wild type and the *SCO4439::Tn5062* mutant (Supplementary Movies 1 and 2; Fig. 1m,n). In the wild-type strain, spore deswelling coincided with germ tube emergence, whereas the spores of the *SCO4439::Tn5062* mutant continued to swell after the emergence of the germ tube (Fig. 7). In the partially complemented *SCO4439::Tn5062* mutant (the strain complemented with the *SCO4439** mutated gene), spore swelling persisted also after germ tube emergence, but the maximum swelling

was lower than in the mutant (maximum spore diameter of 3.9 μm vs. the 4.6 μm reached in the mutant; Fig. 1p,q; Supplementary Movies 2 and 4).

The proposed biomolecular model to account for the observed phenotypes in the *SCO4439::Tn5062* mutant is schematized in Fig. 7. Accordingly, a deficiency in SCO4439 DD-CPase increments the pool of available transpeptidase substrates (PG pentapeptides), thereby enhancing the activity of these enzymes and promoting the formation of PG crosslinks. Spores with highly crosslinked PG are more resistant to heating and acid and swell more slowly at early germination time points, but they can reach greater dimensions before lysing due to osmotic shock (Fig. 7). The mutation in SCO4439 that replaces Leu_{684} with Pro_{684}, halved the native DD-CPase activity, and when the *SCO4439** gene was introduced into the *SCO4439::Tn5062* mutant, the phenotype was only partially restored. This demonstrates that spore swelling during germination is proportional to SCO4439 DD-CPase activity. The model proposed in Fig. 7 would also be valid for new PG synthetized in the *SCO4439::Tn5062* mutant after spore germination, at the latest stages of the swelling, which will have more cross-linking than the wild strain.

Streptomyces mutants created in germination such as *SCO4439::Tn5062*, represent a key tool that provides insight into this process. Up to now, the osmotic mechanism controlling spore swelling is largely unknown. Germ tube emergence is marked by SsgA[27], and uncharacterized lytic enzymes regulate the splitting of the spore covers at this germination point[28]. Spore swelling may facilitate the emergence of the germ tube[22], and germ tube emergence coincides with the end of the swelling in the *S. coelicolor* wild type strain (Fig. 1m). The dramatic swelling of the spores in the *SCO4439::Tn5062* mutant after germ tube emergence suggests that the high osmotic pressure in the spore cytoplasm feeds this swelling. In the weaker spores of the wild-type strain (low PG crosslinking), spore swelling culminate with the emergence of the germ tube. However, spores of the *SCO4439::Tn5062* mutant have higher PG crosslinking, and the swelling continues after the emergence of the germ tube. In this scenario, the cells likely still detect the high osmotic pressure that in normal conditions would indicate the absence of germination, thus they increase swelling and osmotic pressure to facilitate germination (Fig. 7). Further work is required to fully comprehend this phenomenon. Interestingly, some studies have already suggested a role for PBPs in spore germination in other sporulating bacteria such as *Bacillus.* Neyman and Buchanan[29] and Murray *et al.*[30] described how some DD-peptidases are expressed differentially during *Bacillus* sporulation and germination, and Buchanan and Gustafson[31] showed that *dacB* mutants produce spores with unusual resistance to chemicals and heating in *Bacillus*.

The lack of the DD-CPase activity in *SCO4439::Tn5062* mutant strain increases the pool of PG pentapeptide, the terminal D-Ala-D-Ala dipeptides of which are the molecular target of glycopeptide antibiotics[32]. Consequently, the mycelium of the *SCO4439::Tn5062* mutant was more sensitive to vancomycin and teicoplanin than the mycelium of the wild-type strain (Fig. 3f). *S. coelicolor* resistance to vancomycin (but not to teicoplanin), was described to be due to the canonical set of *vanRSHAX* genes induced by vancomycin (but not by teicoplanin) that are responsible for replacing the terminal D-Ala-D-Ala dipeptides with the resistant D-Ala-D-Lac dipeptides[33,34]. Recent work demonstrated that other enzymes (VanY-like) contribute to glycopeptide resistance in actinomycetes by removing the last D-Ala from the PG-pentapeptide precursors[34,35]. Interestingly, these enzymes are membrane-associated LMW DD-CPases with a minor activity on dipeptides and are in some cases inhibited by β-lactams[35,36].

The *SCO4439* DD-CPase gene is constitutively expressed (Fig. 2e), whereas the specific DD-CPase enzymatic activity decreases during development (from 5 U/mg protein at 16 hours, to 3 U/mg protein at 72 hours) (Fig. 5d). This can be a consequence, that, at later time points, most of the mycelium suffers a programmed cell death[1,2] disrupting cell membrane integrity and experiencing an increasing proteolytic activity. Loss of DD-CPase activity may be due to the increasing protein instability in the above conditions. Anyhow, the occurrence of other specific post-translational modifications regulating the DD-CPase activity cannot be ruled out.

Overall, this work demonstrates that the SCO4439 DD-CPase regulates the proportion of PG crosslinking in the spore cell walls, a process that is critical for the regulation of spore germination. The *SCO4439* DD-CPase gene is constitutively expressed, and its activity is present in the *Streptomyces* vegetative hyphae. However, its biological role in the mycelium (beyond the increase of resistance to glycopeptide antibiotics) remains unknown. Knowledge of the biological role of the genes involved in antimicrobial resistance is important to understand the evolution of resistance in nature.

Methods

Bacterial strains and media. Bacterial strains are listed in Table 1. *Streptomyces coelicolor* M145 was the reference strain and was used to generate the mutants. Petri dishes (8.5 cm) with 25 ml of solid GYM medium (glucose, yeast/malt extract)[37] were covered with cellophane disks, inoculated with 100 μl of a fresh spore suspension (1×10^7 viable spores/ml), and incubated at 30 °C. Spores were obtained from SFM solid cultures[38].

Escherichia coli strains were grown at 37 °C in solid (2% agar) or liquid 2xTY medium[39] supplemented with the appropriate antibiotics (Table 1).

Disruption of *SCO4439*. The transposon insertion single-gene knockout library created by Prof. P. Dyson's research group[16] was used for mutagenesis of *SCO4439*. Cosmid D6.2.B06 was used to construct the *SCO4439::Tn5062* mutant strain (Table 1). Gene disruption was carried out by obtaining double cross-overs via conjugation using *E. coli* ET12567/pUZ8002 as a donor strain and following the protocol described in Kieser *et al.*[38]. Mutant strains were confirmed using Southern blotting with chromosomal DNA digested with *SalI*. Southern hybridization was carried out using established procedures with the digoxigenin-labeled 3442-bp Tn5062 *PvuII* fragment from plasmid pQM5062[40] as a probe.

Complementation of *SCO4439::Tn5062* mutation. The integrative plasmid pMS82[41] was used to introducedifferent fragments from the *SCO4437-SCO4442* chromosomal region into the *SCO4439::Tn5062*

Strain, plasmid, cosmid	Description	Reference
Bacterial strains		
S.coelicolor M145	SCP1$^-$ SCP2$^-$	38
S.*coelicolor SCO4439::Tn5062*	*SCO4439*-40::Tn5062, Am^R	This study
E. coli TOP10	F- mcrA Δ(mrr-hsdRMS-mcrBC) φ80lacZΔM15 ΔlacX74 nupG recA1 araD139 Δ(ara-leu)7697 galE15 galK16 rpsL(Str^R) endA1 λ$^-$	Invitrogen
E. coli JM109 (DE3)	*E. coli* JM109 containing a chromosomal copy of the gene for T7 RNA polymerase	Promega
E. coli ET12567	dam-13::Tn9, dcm-6	52
E. coli ET12567/pUZ8002	*E. coli* ET12567 containing plasmid pUZ8002, a not self-transmissible plasmid which can mobilize other plasmids	53
Plasmids & cosmids		
pQM5062	Plasmid containing *eGFP* Tn5062	40
pMS82	Cloning vector, Hyg^R	41
pBRB1	SCO4440-4442 harbouring its own promoter cloned into pMS82/*SpeI*/*EcoRV*, Hyg^R	This study
pBRB2	SCO4437-4439 harbouring its own promoter cloned into pMS82/*SpeI*/*EcoRV*, Hyg^R	This study
pBRB3	*SCO4439* harbouring its own promoter cloned into pMS82/*Spe*I/*Eco*RV, Hyg^R	This study
pBRB3*	*SCO4439* harbouring its own promoter containing a mutation (Leu$_{684}$ was changed by Pro) and cloned into pMS82/*Spe*I/*Eco*RV, Hyg^R	This study
pCR™-Blunt II-TOPO®	Zero Blunt®TOPO® PCR Cloning Kit, Km^R	Invitrogen
pTOPO4439	*SCO4439* harbouring its own promoter cloned into pCR™-Blunt II-TOPO®, Km^R	This study
pTOPO4439-P-N	pTOPO4439 digested with *Nru*I and *Spe*I (filled blunt) and religated, Km^R	This study
pTOPO4439-P-C	pTOPO4439 digested with *Afe*I and *Nru*I and religated, Km^R	This study
pTOPO4439-P	*SCO4439* promoter cloned into Blunt TOPO, Km^R	This study
pTOPO4439-T-C	Transmembrane region and carboxyl end of *SCO4439* cloned into pCR™-Blunt II-TOPO®, Km^R	This study
pTOPO4439-P-T-C	pTOPO4439-P digested with EcoRV/NdeI and cloned in pTOPO-4439-T-C digested with *EcoRV*/*Nde*I, Km^R	This study
pBRB4	Fragment *EcoRV*/*Hind*III from pTOPO4439-P-N cloned in *Hind*III and *Kpn*I (filled blunt) of vector pMS82, Hyg^R	This study
pBRB5	Fragment *EcoRV*/*SpeI* from pTOPO4439-P-C cloned in *EcoRV*/*Spe*I of pMS82/*Spe*I/*EcoRV*, Hyg^R	This study
pBRB6	Fragment *EcoRV*/*Spe*I from TOPO4439-P-T-C cloned in *EcoRV*/*Spe*I of pMS82/*Spe*I/*EcoRV*, Hyg^R	This study
pET11a	Cloning/expression vector, Ap^R	Novagen
pBRB7	His-SCO4439 cloned in pET11a/*Nde*I/*BamHI*, Ap^R	This study
pBRB7*	His-SCO4439 containing a mutation (Leu$_{684}$ was changed by Pro) cloned in pET11a/*Nde*I/*BamHI*, Ap^R	This study
D6.2.B06	D6 cosmid carrying D6.2.B06 transposant	18
Primers		
BRB1F	5′AAAAAGATATCGTCTCGCGGACCGACAGC 3′	This study
BRB1R	5′CCCACTAGTAACTGGTCGAGAGGGCTCC 3′	This study
BRB2F	5′AAAAAGATATCACCGAGGTCGAGCGACTG 3′	This study
BRB2R	5′CCCACTAGTGCTCACCAGCGACAATGAGG 3′	This study
BRB3R	5′CCCACTAGTGTTTGGCGACGCTAGCAC 3′	This study
BRB6R	5′AACATATGCGCCAGCCGCGGATCAC 3′	This study
BRB6F	5′AACATATGACCACCCAGCAGCCGCTG 3′	This study
BRB7F	5′TTCATATGCATCATCATCATCATCATGTGGCCCGGGAGGACG 3′	This study
BRB7R	5 GGGGATCCGTTTGGCGACGCTAGCAC 3′	This study
SCO4848F	5′ CGTCGTATCCCCTCGGTTG 3′	This study
pMS82R	5′ GAGCCGGGAAAGCTCATTCA 3′	This study
SCO4439-qRTPCR-F	5′ GGCGTTCGTGGAGAAGATG 3′	This study
SCO4439-qRTPCR-R	5′ CTCACCGTCGTGTTGTTCAG 3′	This study

Table 1. Bacterial strains, plasmids and primers used in this study. The pairs of primers used to amplify fragments cloned in plasmids pBRB1-7 and pTOPO4439-P-N-T-C are described in the Materials and Methods section.

mutant. Fragments were amplified via PCR using Phusion High-Fidelity DNA Polymerase (Thermo), and were then cloned into pCR™-Blunt II-TOPO®. The sequences were checked via DNA sequencing using the M13 universal primers prior to subcloning them into pMS82. The following plasmids were constructed (Table 1): pBRB1 containing the *SCO4440-SCO4442* fragment amplified with primers BRB1F/BRB1R; pBRB2 containing

the *SCO4437-SCO4439* fragment amplified with primers BRB2F/BRB2R; pBRB3 containing *SCO4439* amplified with primers BRB2F/BRB3R. One of the amplified *SCO4439* fragments cloned in pCR™-Blunt II-TOPO® had a mutation generated during the PCR that replaced Leu_{684} with Pro; this mutation was also cloned into pMS82 generating plasmid pBRB3*. In all cases, primers were designed to hybridize at least 250 bps before the ATG of the ORFs to encompass the promoter region.

Three additional pMS82-derived plasmids were constructed containing different parts of the multidomain *SCO4439* gene: one harboring the *SCO4439* N-terminus and the other two harboring two regions of the *SCO4439* C-terminus. The *SCO4439*-N-terminus truncated gene was generated in two steps: first, the whole *SCO4439* gene was amplified with primers B2F/B3R and cloned into pCR™-Blunt II-TOPO®, selecting for the plasmid in which the C-terminus of the *SCO4439* gene was orientated to the *Spe*I side of the pCR™-Blunt II-TOPO® (pTOPO4439); second, the DD-CPase domain was deleted by digesting pTOPO4439 with *Nru*I and *Spe*I, the *Spe*I cohesive end was filled with the Klenow DNA polymerase, and the plasmid was religated to generate pTOPO4439-P-N. A stop codon (TAG) from the *Spe*I restriction site was formed in the correct ORF. Two C-terminus constructions were performed, one including the 5′ region of the gene (promoter and RBS) followed by the DD-CPase domain (*SCO4439*-P-C), and the second including the 5′ region followed by both the transmembrane and DD-CPase domains (*SCO4439*-P-T-C). *SCO4439*-P-C was generated by digesting pTOPO4439 with *Afe*I and *Nru*I, and re-ligating the plasmid. pTOPO4439-P-C, lacked the *Afe*I-*Nru*I fragment (the putative transcriptional regulatory and transmembrane domains) but conserved the 5′-region and the open reading frame. *SCO4439*-P-T-C was created in three steps: first the 5′ region was amplified with primers BRB2F/BRB6R and cloned into pCR™-Blunt II-TOPO® (pTOPO4439-P); second, the *SCO4439* C-terminus (including the transmembrane and DD-CPase domains) was amplified with BRB3R/BRB6F and cloned into pCR™-Blunt II-TOPO®, and the plasmid in which the *Nde*I (introduced in primer BRB6F) orientated to the *Eco*RV side of the pCR™-Blunt II-TOPO® was selected, to generate pTOPO4439-T-C; and third, the promoter region was released from pTOPO4439-P with *Eco*RV-*Nde*I and cloned into pTOPO-T-C digested with the same enzymes to generate pTOPO4439-P-T-C. pTOPO4439-P-T-C conserved the open reading frame of the transmembrane and DD-CPase domains. The three truncated genes were subcloned into pMS82, generating plasmids pBRB4, pBRB5 and pBRB6 (Table 1).

The seven pMS82-derived plasmids (pBRB1-pBRB6 and pBRB3*) were independently conjugated into the *SCO4439::Tn5062* strain as indicated above. The integration of these plasmids into the pMS82 integration site (gene *SCO4848*)[41] was verified by PCR using primers SCO4848F (hybridizing with the *SCO4848* gene) and pMS82R (hybridizing with pMS82). Plasmid integration was confirmed via the generation of a 617-bp amplicon.

Viability staining. Culture samples were obtained and processed for microscopy at various incubation durations, as previously described[42]. The cells were stained with propidium iodide and SYTO 9 (LIVE/DEAD BacLight Bacterial Viability Kit, Invitrogen, L-13152). The samples were observed under a Leica TCS-SP8 confocal laser-scanning microscope at wavelengths of 488 nm and 568 nm excitation and 530 nm (green) or 640 nm (red) emissions[42]. More than 30 images were analyzed for each developmental time point in a minimum of three independent cultures. For spore diameter quantification, the images were calibrated with Image J, and the diameter of at least 100 spores was quantified for each strain and developmental time point (Supplementary Figs S1 and S2). These images included pictures from at least three biological replicates.

Time-lapsed (live) imaging. Initially spores were incubated on GYM medium; after 6 hours of incubation, the samples were cut out and inverted into uncoated m-dishes (Ibidi GmbH). The lid was turned so it was supported on the vents, allowing gas exchange, and sealed off by two layers of Parafilm to prevent medium drying. The samples were incubated at 30 °C and imaged with a Leica TCS-SP8 confocal laser-scanning microscope. Images were taken using the interference contrast mode (unstained samples) every 10 minutes for 12 hours. Time-lapse images were processed with Image J. Time lapse experiments were limited to 12 hours because prolonged incubations dry the culture medium and interfere with hyphal growth.

RNA extraction and Real-Time Quantitative Reverse Transcription PCR (qRT-PCR). Total RNA samples from three biological replicates of each developmental time point were obtained. Approximately 100 mg of mycelia (fresh weight) were scraped from the GYM-cellophane medium using a plain spatula. Five hundred microliters of RNA Protect Bacteria reagent (Qiagen) were added to the mycelia to provide immediate RNA stabilization. The extraction was carried out using the RNeasy Mini Kit (Qiagen). The lysis step was made using Fast-Prep (MP™ Biomedicals) with two 30-s force 6.5 cycles, with 1 minute on ice between each run. A phenol acid extraction was performed immediately prior to applying the samples to the column. Treatments with DNase I (Qiagen) and TURBO DNA-freeTM kit (Ambion) were performed to eliminate possible chromosomal DNA contamination. RNA integrity was verified using a 2100 Bioanalyzer (Agilent).

Quantitative RT-PCR (qRT-PCR) was performed as previously described by Yagüe *et al.*[15]. Relative quantification of gene expression was calculated using the (REST) software tool[43]. Primer efficiencies were measured using different dilutions of genomic DNA as templates.

Resistance of spores to sonication, lysozyme, mild acid, heating and freezing. Freshly prepared suspensions of spores were prepared at a concentration of 10^8 spores/ml in sterile distilled water, and subjected to different treatments as detailed below. Germination of the spores prior to and after treatment were analyzed by plating and quantifying the number of colony-forming units. All quantifications were performed in triplicate, and the data correspond to the average ± SD of the replicates.

For sonication, 2 ml of spores were treated in an MSE Soniprep (six cycles of 15 seconds of sonication, 1 minute on ice). For lysozyme incubation, 1 ml of spores was treated with a concentration of 50 μg/ml freshly prepared

lysozyme (Sigma-Aldrich, L6876) and incubated at 37 °C for 30 minutes. For mild acid treatment, 0.2 ml of spores were incubated with 0.1 N of HCl for 5 minutes at 25 °C; acid was neutralized via 20-fold dilution in 50 mM potassium phosphate buffer (pH 7.1). For heating, the spores were heated at 55 °C for 90 minutes. For freezing, the spores were stored at −20 °C for 24 hours.

Determination of the minimum inhibitory concentration (MIC). Minimum inhibitory concentrations (MICs) of teicoplanin and vancomycin (Sigma-Aldrich V1130 and T0578) were determined in GYM by adding increasing concentrations of glycopeptides. The inoculum was 10^5 spores/plate, and the plates were incubated at 30 °C until colonies appeared. The MIC was the lowest concentration of the antibiotic that inhibited the visible growth of *S. coelicolor*[44,45]. The experiments were performed in triplicate, and were highly reproducible with a variation of zero.

***SCO4439* and *SCO4439** gene overexpression and protein purification.** The *SCO4439* and *SCO4439** (SCO4439 mutated in Leu_{684}) genes were amplified with primers BRB7F/BRB7R from pBRB3/pBRB3* and cloned into the expression vector pET11a (Novagen) to generate pBRB7/pBRB7*. A His_6 tag was included at the 5′-terminus of the BRB7F primer. The *SCO4439/SCO4439** genes were overexpressed in *E. coli* JM109 (DE3) using the MagicMedia *E. coli* Expression Medium (Invitrogen K6803). The expression was performed at 18 °C for 36 hours following the manufacturer's protocol. The cells were harvested via centrifugation, resuspended in buffer A (20 mM sodium phosphate, 0.5 M NaCl, 40 mM imidazole, complete EDTA-free Protease Inhibitor Cocktail Tablets from Roche, pH 7.4) and ruptured using Fast-Prep (MP™ Biomedicals) with $\leq$106 μm beads (Sigma-Aldrich, G8893) and three 20-s force 6.5 cycles, with 1 minute on ice between each run. Finally, the samples were centrifuged at 7,740 × *g* for 15 minute at 4 °C. The resulting supernatant fraction was centrifuged at 100,000 × g for 1 hour at 4 °C, and the supernatant was used for protein purification.

Recombinant His_6-SCO4439/ His_6-SCO4439* were purified using 1 ml HisTrap HP affinity columns from GE Healthcare (reference 17-5247-01). Buffer A, described above, was used as a binding buffer; the elution buffer was similar but contained 500 mM imidazole. The protein was purified using an Amersham Pharmacia FPLC (LCC 500 plus controller and two P500 pumps). Purification was performed at 4 °C using a flow of 1 ml per minute, a 20 ml linear elution gradient, and collecting fractions of 500 μl. Fractions were analyzed via SDS-PAGE Coomassie gels, and those containing the overproduced protein were combined, quantified by Bradford[46], and used for further experiments.

Mass spectrometry analysis. The identity of the overproduced protein was confirmed via peptide mass fingerprinting. The overproduced purified His_6-SCO4439 protein was manually excised from a 1D Coomassie gel, and the proteins were digested following the method of Havlis *et al.*[47], and analyzed using a 4800 Proteomics Analyzer matrix-assisted laser desorption ionization time-of-flight (MALDI-TOF/TOF) mass spectrometer (AB Sciex). Protein identification, was performed using Mascot v. 2.2.04.

Assay of DD-dipeptidase and DD-carboxypeptidase activities. Enzymatic activities were assayed as reported previously[35,45] by measuring the release of D-Ala from commercially available dipeptide (D-Ala-D-Ala, 10 mM; Sigma-Aldrich, A0912) and tripeptide (N_α,N_ε-diacetyl-L-Lys-D-Ala-D-Ala, 10 mM; Sigma-Aldrich, D9904) in the reaction buffer (100 mM Tris-HCl, pH 7.2), together with different amounts of the purified recombinant His_6-SCO4439 or His_6-SCO4439*. The release of D-Ala was followed spectrophotometrically with a D-amino acid oxidase (Sigma-Aldrich, A5222)-peroxidase (Sigma-Aldrich 77332) coupled reaction that oxidized the colorimetric substrate 4-aminoantipyrine (Sigma-Aldrich 06800) to chinonemine in the presence of phenol solution (Sigma-Aldrich P4557)[35,48]. One unit of enzyme activity is defined as the amount of enzyme that produced 1 μmol D-Ala per minute from the tripeptide as substrate; this value must be halved when the dipeptide is used as substrate. To measure the inhibition of DD-CPase/DD-dipeptidase activity, the protein was incubated with increasing concentrations (from 0 to 5 mM) of penicillin G (Sigma-Aldrich, P3032) for 15 minutes at 37 °C and then added to the assay mixtures. All measurements were performed in triplicate, and the data correspond to the means ± SD.

Cellular fractioning. *S. coelicolor* and the *SCO4439::Tn5062* mutant were grown in solid GYM medium as described above for 16, 30 and 72 hours at 30 °C. The mycelium collected from cellophane discs were suspended in 2 ml of 0.9% NaCl per gram of cells (wet weight). All of the following manipulations were carried out at 0 to 4 °C, and all solutions contained proteinase inhibitors (0.19 mg/ml phenylmethanesulfonyl fluoride and 0.7 g/ml pepstatin, both purchased from Sigma-Aldrich P7626 and P5318), unless otherwise stated. Mycelia were fragmented by sonication with a Sonics Vibra-Cell VCX 130. Sonication was carried out for 5 minutes on ice with cycles of 30 seconds with an amplitude of 90% (90% of 60 Hz), and breaks of 10 seconds. The samples were then centrifuged at 39,000 × *g* for 15 minutes, and the supernatants (cytoplasmic fractions) were collected. Alkaline extraction of the insoluble fraction (membranes and cell wall debris) was carried out by adapting a previously developed protocol for extracting membrane-bound proteins in enterococci by Kariyama *et al.*[49] and recently adapted to *Streptomyces* by Binda *et al.*[43]. The sedimented pellets were resuspended in ice-cold distilled water; immediately prior to centrifugation (28,000 × *g* for 15 minutes at 4 °C), the pH was adjusted to 12 by adding an appropriate volume of 2.5 N NaOH. Immediately after centrifugation, the supernatants (resuspended insoluble fractions) were neutralized to pH 7 by adding 0.5 M sodium acetate (pH 5.4)[35,36,45]. Enzymatic activities in the cytosolic fractions and the re-suspended insoluble fractions were assayed as previously reported[36,45].

FDNB determination of spore PG crosslinking. The protocol described by Atrih *et al.*[50] to analyze the PG crosslinking in the spores of *Bacillus* was adapted to *S. coelicolor*. The protocol for PG extraction was modified as follows: spores were collected from solid SFM media[38]; the concentration of spores used for extraction

was 3 mg (dry weight) per ml of extraction buffer; FDNB treatment was performed using 200 μl of the extracted spore cell walls. This protocol works for the analysis of the PG from *Streptomyces* spores, but not for mycelium, perhaps due to the difficulty to homogenize the dense pellets of the mycelium, making PG poorly accessible to the extraction and FDNB treatment.

Glycine and diaminopimelic acid (Dpm) were measured via high-performance liquid chromatography using pre-column derivatization with *o*-phthaldehyde (OPA) and UV detection (338 nm). The chromatographic equipment used included the Agilent 1100 HPLC System: a G1312A binary pump, G1329A autosampler, and G1315B-Diode Array Detector. Data collection and integration were performed using Software Chem Station LC 3D. The column used was a 250 × 3.9 mm, 100 Å, Symmetry C18 (5 μm) (WAT046980) from Waters. The binding buffer (10 mM Na_2HPO_4, 40 mM boric acid, pH 8.15) and the elution buffer (MeOH:ACN:H_2O; 45:45:10, v/v/v) were filtered (0.45 μm) prior to use. Samples were eluted in an increasing gradient of elution buffer (20% for 1.9 minutes, 70% for 13 minutes; 100% for 2.7 minutes) with a flow of 1ml /minute. The column temperature was 40 °C, the injection volume 20 μl, and the detection of the amino acids was at 338 nm. Pure glycine and Dpm (both from Sigma-Aldrich) were used as standards.

The crosslinking index defined by Atrih *et al.*[50] is based on the difference between the Dpm measured in the FDNB-treated and untreated samples. FDNB treatment is performed prior to PG hydrolysis and blocks NH groups of the Dpm residues that have not formed crosslinks. NH groups blocked with FDNB cannot react with the derivative reagent used for HPLC UV detection. *S. coelicolor* differs from *Bacillus*, and PG crosslinking is formed by Gly instead of Dpm[51]. Consequently, in this work, the crosslinking index was calculated as the ratio between the cross-linked Gly (Gly detected in the FDNB-treated samples) and total Gly (Gly detected in the non-treated samples). Dpm was used to normalize the glycine measurements (expressed as a ratio to Dpm).

Bioinformatic analyses. Transmembrane topology of the SCO4439 gene was analyzed using Phobius software (http://phobius.sbc.su.se/).

Orthologous sequences to SCO4439 from other streptomycetes were obtained from the databases at the National Center for Biological Information (http://www.ncbi.nlm.nih.gov). The accession numbers of the selected sequences were: WP_016326920 (*S. lividans*), NP_824958 (*S. avermitilis*), YP_006878621 (*S. venezuelae*), WP_013002845 (*S. scabies*), YP_001825771 (*S. griseus*), and WP_003961441 (*S. clavuligerus*). The DD-CPase domains of the proteins were aligned using MUSCLE software, and amino acid similarities were estimated by using Lalign software (http://www.ch.embnet.org/software/LALIGN_form.html).

Fluorescent vancomycin staining. Nascent PG synthesis was stained in *Streptomyces* liquid cultures growing in GYM medium[37], inoculated with spores at a concentration of 1×10^7 viable spores/ml, and incubated at 30 °C and 200 rpm for 5 and 8 hours. The samples were stained as previously described[20]. BODIPY-vancomycin (Invitrogen V34850) was mixed with an equal amount of unlabeled vancomycin (Sigma SBR00001). The vancomycin and BODIPY-vancomycin mixtures were added to the cultures at final concentrations of 1 μg/ml and incubated for 20 minutes. Cells were fixed for 15 minutes at room temperature using PBS (0.14 M NaCl, 2.6 mM KCl, 1.8 mM KH_2PO_4 and 10 mM Na_2HPO_4) containing 2.8% paraformaldehyde and 0.0045% glutaraldehyde, and observed under a Leica TCS-SP8 confocal laser scanning microscope at 505 nm excitation and 513 nm emission wavelengths.

References

1. Flärdh, K. & Buttner, M. J. *Streptomyces* morphogenetics: dissecting differentiation in a filamentous bacterium. *Nat. Rev. Microbiol.* **7,** 36–49 (2009).
2. Yagüe, P., López-García, M. T., Rioseras, B., Sánchez, J. & Manteca, A. Pre-sporulation stages of Streptomyces differentiation, state-of-the-art and future perspectives. *FEMS Microbiol. Lett.* **342,** 79–88 (2013).
3. Hopwood, D. A. *Streptomyces* in nature and medicine: The antibiotic makers. Oxford University Press, New York (2007).
4. Davies, J. Specialized microbial metabolites: functions and origins. *J. Antibiot. (Tokyo)* **66,** 361–364 (2014).
5. van Wezel, G. P. & McDowall, K. J. The regulation of the secondary metabolism of *Streptomyces*: new links and experimental advances. *Nat. Prod. Rep.* **28,** 1311–1333 (2011).
6. Chater, K. F., Biro, S., Lee, K. J., Palmer, T. & Schrempf, H. (2010) The complex extracellular biology of *Streptomyces*. *FEMS Microbiol. Rev.* **34,** 171–198.
7. McCormick, J. R. & Flärdh, K. Signals and regulators that govern *Streptomyces* development. *FEMS Microbiol. Rev.* **36,** 206–231 (2012).
8. Salerno, P. *et al.* Identification of new developmentally regulated genes involved in *Streptomyces coelicolor* sporulation. *BMC Microbiol.* **13,** 281 (2013).
9. van Dissel, D., Claessen, D. & van Wezel, G. P. Morphogenesis of *Streptomyces* in submerged cultures. *Adv. Appl. Microbiol.* **89,** 1–45 (2014).
10. Ghosh, A. S., Chowdhury, C. & Nelson, D. E. Physiological functions of D-alanine carboxypeptidases in *Escherichia coli*. *Trends Microbiol.* **16,** 309–317 (2008).
11. Goffin, C. & Ghuysen, J. M. Biochemistry and comparative genomics of SxxK superfamily acyltransferases offer a clue to the mycobacterial paradox: presence of penicillin-susceptible target proteins versus lack of efficiency of penicillin as therapeutic agent. *Microbiol. Mol. Biol. Rev.* **66,** 702–738 (2002).
12. Pratt, R. F. Substrate specificity of bacterial DD-peptidases (penicillin-binding proteins). *Cell Mol. Life. Sci.* **65,** 2138–2155 (2008).
13. Ogawara, H. Penicillin-binding proteins in Actinobacteria. *J. Antibiot. (Tokyo)*. **68,** 223–245 (2015).
14. Mistry, B. V., Del Sol, R., Wright, C., Findlay, K. & Dyson, P. FtsW is a dispensable cell division protein required for Z-ring stabilization during sporulation septation in *Streptomyces coelicolor*. *J. Bacteriol.* **190,** 5555–5566 (2008).
15. Yagüe, P. *et al.* Transcriptomic analysis of *Streptomyces coelicolor* differentiation in solid sporulating cultures: first compartmentalized and second multinucleated mycelia have different and distinctive transcriptomes. *Plos One* **8,** e60665 (2013b).
16. Fernández-Martínez, L. T. *et al.* A transposon insertion single-gene knockout library and new ordered cosmid library for the model organism *Streptomyces coelicolor* A3(2). *Antonie Van Leeuwenhoek* **99,** 515–522 (2011).
17. Rasmussen, J. R. & Strominger, J. L. Utilization of a depsipeptide substrate for trapping acyl-enzyme intermediates of penicillin-sensitive D-alanine carboxypeptidases. *Proc. Natl. Acad. Sci. USA* **75,** 84–88 (1978).

18. Treviño, J. *et al.* New insights into glycopeptide antibiotic binding to cell wall precursors using SPR and NMR spectroscopy. *Chemistry* **10,** 7363–7372 (2014).
19. Sanders, A. N. & Pavelka, M. S. Phenotypic analysis of *Escherichia coli* mutants lacking L,D-transpeptidases. *Microbiology* **159,** 1842–1852 (2013).
20. Daniel, R. A. & Errington, J. Control of cell morphogenesis in bacteria: two distinct ways to make a rod-shaped cell. *Cell.* **113,** 767–776 (2003).
21. Schoonmaker, M. K., Bishai, W. R. & Lamichhane, G. Nonclassical transpeptidases of *Mycobacterium tuberculosis* alter cell size, morphology, the cytosolic matrix, protein localization, virulence, and resistance to β-lactams. *J. Bacteriol.* **196,** 1394–1402 (2014).
22. Hardisson, C., Manzanal, M. B., Salas, J. A. & Suárez, J. E. Fine structure, physiology and biochemistry of arthrospore germination in *Streptomyces antibioticus*. *J. Gen Microbiol.* **105,** 203–214 (1978).
23. Bobek, J., Strakova, E., Zikova, A. & Vohradsky, J. Changes in activity of metabolic and regulatory pathways during germination of S. coelicolor. *BMC Genomics*. **15,** 1173 (2014).
24. Strakova, E. *et al.* Systems insight into the spore germination of Streptomyces coelicolor. *J. Proteome Res.* **4,** 525–536 (2013).
25. Bobek, J., Strakova, E., Zikova, A. & Vohradsky, J. Changes in activity of metabolic and regulatory pathways during germination of S. coelicolor. *BMC Genomics*. **15,** 1173 (2014).
26. de Jong, W. *et al.* NepA is a structural cell wall protein involved in maintenance of spore dormancy in Streptomyces coelicolor. *Mol. Microbiol.* **71,** 1591–1603 (2009).
27. Noens, E.E. *et al.*, Loss of the controlled localization of growth stage-specific cell-wall synthesis pleiotropically affects developmental gene expression in an ssgA mutant of Streptomyces coelicolor. *Mol. Microbiol.* **64,** 1244–1259 (2007).
28. Haiser, H. J., Yousef, M. R. & Elliot, M. A. Cell wall hydrolases affect germination, vegetative growth, and sporulation in Streptomyces coelicolor. *J. Bacteriol.* **191,** 6501–6512 (2009).
29. Neyman, S. L. & Buchanan, C. E. Restoration of vegetative penicillin-binding proteins during germination and outgrowth of *Bacillus subtilis* spores: relationship of individual proteins to specific cell cycle events. *J. Bacteriol.* **161,** 164–168 (1985).
30. Murray, T., Popham, D. L. & Setlow, P. Identification and characterization of *pbpC*, the gene encoding *Bacillus subtilis* penicillin-binding protein 3. *J. Bacteriol.* **178,** 6001–6005 (1996).
31. Buchanan, C. E. & Gustafson, A. Mutagenesis and mapping of the gene for a sporulation-specific penicillin-binding protein in *Bacillus subtilis*. *J. Bacteriol.* **174,** 5430–5435 (1992).
32. Cooper, M. A. & Williams, D. H. Binding of glycopeptide antibiotics to a model of a vancomycin-resistant bacterium. *Chem. Biol.* **6,** 891–899 (1999).
33. Hong, H. J. *et al.* Characterisation of an inducible vancomycin resistance system in *Streptomyces coelicolor* reveals a novel gene (*vanK*) required for drug resistance. *Mol. Microbiol.* **52,** 1107–1121 (2004).
34. Schäberle, T. F. *et al.* Self-resistance and cell wall composition in the glycopeptide producer Amycolatopsis balhimycina. *Antimicrob Agents Chemother* **55,** 4283–4289 (2011).
35. Binda, E., Marcone, G. L., Pollegioni, L. & Marinelli, F. Characterization of VanY(n), a novel D,D-peptidase/D,D-carboxypeptidase involved in glycopeptide antibiotic resistance in *Nonomuraea* sp. ATCC 39727. *FEBS J.* **279,** 3203–3213 (2012).
36. Marcone, G. L., Binda, E., Carrano, L., Bibb, M. & Marinelli, F. The relationship between glycopeptide production and resistance in the actinomycete *Nonomuraea* sp. ATCC 39727. *Antimicrob. Agents Chemother.* **58,** 5191–5201 (2014).
37. Novella, I. S., Barbes, C. & Sánchez, J. Sporulation of *Streptomyces antibioticus* ETHZ 7451 in liquid culture. *Can J Microbiol* **38,** 769–773 (1992).
38. Kieser, T., Bibb, M. J., Buttner, M. J., Chater, K. F. & Hopwood, D. A. Growth and Preservation of *Streptomyces*. In Practical Streptomyces Genetics, Chapter 2, pp. 43–61. Norwich, UK: The John Innes Foundation (2000).
39. Hong, H. J., Hutchings, M. I., Hill, L. M. & Buttner, M. J. The role of the novel Fem protein VanK in vancomycin resistance in *Streptomyces coelicolor*. *J. Biol. Chem.* **280,** 13055–13061 (2005).
40. Bishop, A., Fielding, S., Dyson, P. & Herron, P. Systematic insertional mutagenesis of a streptomycete genome: a link between osmoadaptation and antibiotic production. *Genome Res.* **14,** 893–900 (2004).
41. Gregory, M. A., Till, R. & Smith, M. C. Integration site for *Streptomyces* phage phiBT1 and development of site-specific integrating vectors. *J. Bacteriol.* **185,** 5320–5323 (2003).
42. Manteca, A., Alvarez, R., Salazar, N., Yague, P. & Sanchez, J. Mycelium differentiation and antibiotic production in liquid cultures of St*reptomyces coelicolor*. *Appl. Environ. Microbiol.* **74,** 3877–3886 (2008).
43. Pfaffl, M. W., Horgan, G. W. & Dempfle, L. Relative expression software tool (REST) for group-wise comparison and statistical analysis of relative expression results in real-time PCR. *Nucleic. Acids Res.* **30,** e36 (2002).
44. Andrews, J. M. Determination of minimum inhibitory concentrations. *J. Antimicrob. Chemother.* **48,** 5–16 (2001).
45. Binda, E., Marcone, G. L., Berini, F., Pollegioni, L. & Marinelli, F. *Streptomyces* spp. as efficient expression system for a D,D-peptidase/D,D-carboxypeptidase involved in glycopeptide antibiotic resistance. *BMC Biotechnol* **13,** 24 (2013).
46. Bradford, M. M. A rapid and sensitive for the quantitation of microgram quantitites of protein utilizing the principle of proteindye binding. *Anal Biochem* **72,** 248–254 (1976).
47. Havlis, J., Thomas, H., Sebela, M. & Shevchenko, A. Fast-response proteomics by accelerated in-gel digestion of proteins. *Anal. Chem.* **75,** 1300–1306 (2003).
48. Granier, B. *et al.* Serine-type D-Ala-D-Ala peptidases and penicillin-binding proteins. *Methods Enzymol.* **244,** 249–266 (1994).
49. Kariyama, R., Massidda, O., Daneo-Moore, L. & Shockman, G. D. Properties of cell wall-associated DD-carboxypeptidase of Enterococcus hirae (Streptococcus faecium) ATCC 9790 extracted with alkali. *J. Bacteriol.* **172,** 3718–3724 (1990).
50. Atrih, A., Zöllner, P., Allmaier, G. & Foster, S. J. Structural analysis of Bacillus subtilis 168 endospore peptidoglycan and its role during differentiation. *J. Bacteriol.* **178,** 6173–6183 (1996).
51. Hugonnet, J. E. *et al.* Peptidoglycan crosslinking in glycopeptide-resistant Actinomycetales. *Antimicrob. Agents Chemother*. **58,** 1749–1756 (2014).
52. MacNeil, D. J. *et al.* Analysis of *Streptomyces avermitilis* genes required for avermectin biosynthesis utilizing a novel integration vector. *Gene* **111,** 61–68 (1992).
53. Flett, F., Mersinias, V. & Smith, C. P. High efficiency intergeneric conjugal transfer of plasmid DNA from *Escherichia coli* to methyl DNA-restricting streptomycetes. *FEMS Microbiol. Lett.* **155,** 223–229 (1997).

Acknowledgements

This research was funded by an ERC Starting Grant (Strp-differentiation 280304). Our thanks to Beatriz Gutiérrez Magán (Universidad de Oviedo, Dpto. Biología Funcional, Área de Microbiología) for laboratory assistance, Paul Dyson and Meirwyn Evans (Swansea University) for providing the disrupted cosmids, Carlos Barreiro and Mar Calonge (INBIOTEC, Leon) for the mass spectrometry and amino acid analyses, Maggie Smith (University of York) for providing the pMS82 plasmid, and Nature Publishing Group Language Editing service for proof-reading the text.

Author Contributions

B.R., P.Y., M.T.L.G., N.G.Q. and E.B. performed the experiments; B.R., P.Y., E.B., F.M. and A.M. assisted with data analysis; all authors contributed to the critical discussion of the manuscript; B.R., F.M. and A.M. conceived, designed the work and wrote the manuscript. All authors read and approved the final manuscript.

Additional Information

Supplementary information accompanies this paper at http://www.nature.com/srep

Competing financial interests: The authors declare no competing financial interests.

How to cite this article: Rioseras, B. *et al.* Characterization of SCO4439, a D-alanyl-D-alanine carboxypeptidase involved in spore cell wall maturation, resistance, and germination in *Streptomyces coelicolor*. *Sci. Rep.* **6**, 21659; doi: 10.1038/srep21659 (2016).

This work is licensed under a Creative Commons Attribution 4.0 International License. The images or other third party material in this article are included in the article's Creative Commons license, unless indicated otherwise in the credit line; if the material is not included under the Creative Commons license, users will need to obtain permission from the license holder to reproduce the material. To view a copy of this license, visit http://creativecommons.org/licenses/by/4.0/

CAPÍTULO 3

Mecanismos de división celular y compartimentalización durante la fase vegetativa temprana (Fase de MI).

Como hemos visto en la introducción, las bacterias del género *Streptomyces* se consideran un modelo de bacterias multicelulares. Su crecimiento micelial implica que en la fase vegetativa se formen largas hifas multinucleadas con algún tabique esporádico. La tabicación de las hifas de *Streptomyces* ha sido ampliamente estudiada en el contexto del ciclo de desarrollo tradicional (septos de micelio sustrato y aéreo), y sobre todo en las fases de esporulación (septos de esporulación) donde se forman cadenas de esporas unigenómicas a partir de hifas de micelio aéreo. Ambos tipos de septos tienen diferentes características y su formación está regulada por diferentes mecanismos (Willemse et al., 2011). Sin embargo, la tabicación del MI permanecía prácticamente inexplorada.

En este apartado nos planteamos analizar los mecanismos de división y compartimentalización de las hifas durante la fase de MI. Para ello se ha caracterizado la ultraestructura de los tabiques de MI, la regulación de la compartimentalización en esta fase y la alteración de la permeabilidad de la membrana durante los procesos de MCP.

Este objetivo se aborda en una publicación:

Manuscrito 3:

Yagüe P, Willemse J, Koning RI, **Rioseras B**, López-García MT, Gonzalez-Quiñonez N, Lopez-Iglesias C, Shliaha PV, Rogowska-Wrzesinska A, Koster AJ, Jensen ON, van Wezel GP, Manteca A. 2016. "Subcompartmentalization by cross-membranes during early growth of *Streptomyces* hyphae". Nat Commun. 7:12467

nature COMMUNICATIONS

ARTICLE

Received 19 Aug 2015 | Accepted 5 Jul 2016 | Published 12 Aug 2016

DOI: 10.1038/ncomms12467 OPEN

Subcompartmentalization by cross-membranes during early growth of *Streptomyces* hyphae

Paula Yagüe[1], Joost Willemse[2], Roman I. Koning[3], Beatriz Rioseras[1], María T. López-García[1], Nathaly Gonzalez-Quiñonez[1], Carmen Lopez-Iglesias[4,†], Pavel V. Shliaha[5], Adelina Rogowska-Wrzesinska[5], Abraham J. Koster[3], Ole N. Jensen[5], Gilles P. van Wezel[2,6] & Ángel Manteca[1]

Bacteria of the genus *Streptomyces* are a model system for bacterial multicellularity. Their mycelial life style involves the formation of long multinucleated hyphae during vegetative growth, with occasional cross-walls separating long compartments. Reproduction occurs by specialized aerial hyphae, which differentiate into chains of uninucleoid spores. While the tubulin-like FtsZ protein is required for the formation of all peptidoglycan-based septa in *Streptomyces*, canonical divisome-dependent cell division only occurs during sporulation. Here we report extensive subcompartmentalization in young vegetative hyphae of *Streptomyces coelicolor*, whereby 1 μm compartments are formed by nucleic acid stain-impermeable barriers. These barriers possess the permeability properties of membranes and at least some of them are cross-membranes without detectable peptidoglycan. Z-ladders form during the early growth, but cross-membrane formation does not depend on FtsZ. Thus, a new level of hyphal organization is presented involving unprecedented high-frequency compartmentalization, which changes the old dogma that *Streptomyces* vegetative hyphae have scarce compartmentalization.

[1] Área de Microbiología, Departamento de Biología Funcional e IUOPA, Facultad de Medicina, Universidad de Oviedo, 33006 Oviedo, Spain. [2] Molecular Biotechnology, Institute of Biology, Leiden University, Sylviusweg 72, P.O. Box 9502, 2300RA Leiden, The Netherlands. [3] Department of Molecular Cell Biology, Leiden University Medical Centre, PO Box 9600, 2300RC Leiden, The Netherlands. [4] Crio-Microscòpia Electrònica. Centres Científics i Tecnològics, Universitat de Barcelona, 08028 Barcelona, Spain. [5] Department of Biochemistry and Molecular Biology and VILLUM Center for Bioanalytical Sciences, University of Southern Denmark, Campusvej 55, DK-5230, Odense M, Denmark. [6] Microbial Ecology, Netherlands Institute for Ecology (NIOO-KNAW), PO Box 50, 6700AB Wageningen, The Netherlands. † Present address: Nanoscopy Division of the Maastricht MultiModal Molecular Imaging Institute (M4i) Maastricht University, Maastricht 6211 LK, The Netherlands. Correspondence and requests for materials should be addressed to P.Y. (email: yaguepaula@uniovi.es) or to A.M. (email: mantecaangel@uniovi.es).

Streptomycetes are filamentous Gram-positive bacteria that are of great importance for biotechnology given their ability to produce a large array of natural products, including antibiotics, anticancer agents and immunosuppressants, as well as a plethora of industrial enzymes[1,2].

The *Streptomyces* life cycle has largely been studied during the growth of surface-grown cultures[3–8] (Fig. 1). The life cycle starts with the germination of a spore, which expands out via tip growth and hyphal branching to form a vegetative mycelium consisting of multinucleate compartments[3]. When dispersal is required, for example, after nutrient depletion, the vegetative mycelium eventually differentiates into a new so-called aerial mycelium, which grows into the air. The aerial hyphae are also initially multinucleated, but these eventually develop sporogenic structures that differentiate into chains of unigenomic spores[4]. The lysis of the substrate mycelium and, later, the early aerial mycelium, exhibits the hallmarks of programmed cell death (PCD), with the involvement of specific lytic enzymes (nucleases, proteases and muramidases)[5,6]. New features affecting early development have been described over the last decade[7,8]. An early compartmentalized mycelium (MI) undergoes an early PCD-like process affecting the substrate and aerial hyphae[6]. Remarkably, live and dying cells are alternately observed in the MI hyphae[6]. The lifespan of this young mycelium is very short under laboratory conditions, but it is likely the predominant mycelium in cultures grown under natural conditions, such as in non-amended soils[7]. The substrate and aerial hyphae in the MII phase[6] are physiologically different from those in the MI phase. MI corresponds to the vegetative mycelium, whereas the substrate and aerial mycelia are the reproductive stages driving towards sporulation[8]. Secondary metabolism is typically restricted to the MII phase[8].

The study of cell division in *Streptomyces* has primarily focused on sporulation-specific cell division, in which ladders of Z-rings are formed, resulting in chains of spores[4]. In contrast, during vegetative growth, the hyphae are compartmentalized by occasional cross-walls, which delimit adjacent elongated compartments containing multiple copies of the chromosome. Consequently, streptomycetes are rare examples of multicellular bacteria[9,10]. During both sporulation and vegetative growth, the GTPase FtsZ polymerizes to form a dynamic ring-like structure known as the Z-ring[11,12]. Surprisingly, in the model organism *Streptomyces coelicolor* A3(2), *ftsZ* is required for cell division (and thus for sporulation) but not for growth, and the deletion of *ftsZ* results in hyphae that are devoid of septa[13]. The process of vegetative cell division differs mechanistically from canonical division, as illustrated by the fact that many of the other canonical cell division genes (for example, *ftsI, ftsL* and *ftsW*) are required for sporulation but not for cross-wall formation[14,15]. Recently, a novel mechanism of cell division was established in vegetative hyphae of *Streptomyces*, based on membranous structures instead of peptidoglycan-based cross-walls[16].

So far, the mechanisms of cell division and hyphal compartmentalization during early vegetative growth (MI stage) have been poorly characterized. Here we provide insights into the ultrastructure of MI hyphae, the regulation of MI compartmentalization, and the kinetics of membrane permeability alteration during PCD in *Streptomyces*. Our data also reveal a surprisingly high frequency of subcompartmentalization of the MI hyphae by cross-membranes.

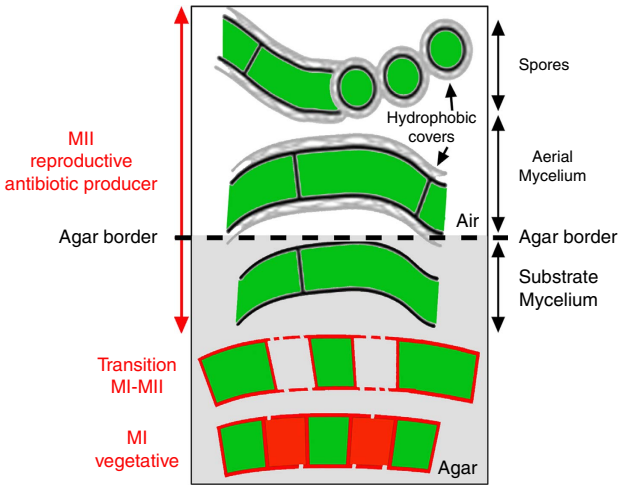

Figure 1 | Development of *Streptomyces* on solid agar plates. The *Streptomyces* developmental cycle[3–8] along the transverse axis of the plate is illustrated (the agar border is indicated with a dashed line). Discontinuities in hyphal membranes represent changes in membrane permeability in dying cells. Red and green colours represent PI fluorescence (dying cells) and SYTO9 fluorescence (live cells), respectively. The traditional nomenclature for substrate and aerial mycelia is indicated in black letters (right); the new nomenclature for MI and MII stages is indicated in red letters (left).

Results

MI hyphae exhibit differential membrane permeability. PCD leads to changes in the membrane permeability of cells and to the alternation of propidium iodide (PI) membrane-permeable and non-permeable cellular segments (Fig. 2a) in the same continuous hyphae[6] (compare fluorescence and phase-contrast images in Supplementary Fig. 1). The average size of MI segments demonstrating differences in permeability was 1.1 ± 0.38 and 0.9 ± 0.25 for PI- and SYTO9-stained segments, respectively, and compartmentalization affected 100% of the analysed hyphae (Fig. 2a; Supplementary Fig. 1). In addition to SYTO9 and PI, we used the non-permeable nucleic acid stain YOPRO-1, which selectively stains eukaryotic apoptotic cells[17]. YOPRO-1 permits the visualization of cells with altered selective permeability that have not yet undergone complete lysis and are therefore not stained by PI[18]. We applied this new technique here to determine whether partial lysis (as observed in eukaryotic apoptotic cells) also occurs in *Streptomyces*. Cells that were stained with PI were also stained with YOPRO-1 (Fig. 2b), whereas live cells were not stained (compare Fig. 2a with Fig. 2b). However, when the samples were processed for microscopy in a more rapid manner (within seconds instead of minutes), the dying cells in the MI hyphae were stained only with YOPRO-1 and not with PI (Supplementary Fig. 2), resembling eukaryotic apoptosis. The average size of the segments stained with SYTO9, PI, and YOPRO-1 at the MI stage was 1.1 ± 0.41 µm (Fig. 2a,b), similar to the spacing observed during sporulation-specific compartmentalization (0.99 ± 0.16 µm) (Fig. 2e). At later time points (transition MI-MII, 18 h), SYTO9-stained cells (live cells) grew as multinucleated compartments, and the average compartment size increased from 1.0 µm (Fig. 2a,b, curves in black) to 1.5 ± 0.55 µm (Fig. 2c, curves in red). Dying cells were no longer stained with either PI or YOPRO-1, most likely due to the complete DNA degradation, but compartmentalization was still observed, and the average length of these unstained segments (18 h; average size of 0.91 ± 0.17 µm) (Fig. 2c) was the same as that observed in early dying cells stained with PI (Fig. 2a,b). The regular pattern of cellular segments with differential, alternating permeabilities to PI and YOPRO-1 in the same hyphae indicates the existence of permeability barriers to these two vital stains separating cellular segments in the MI hyphae.

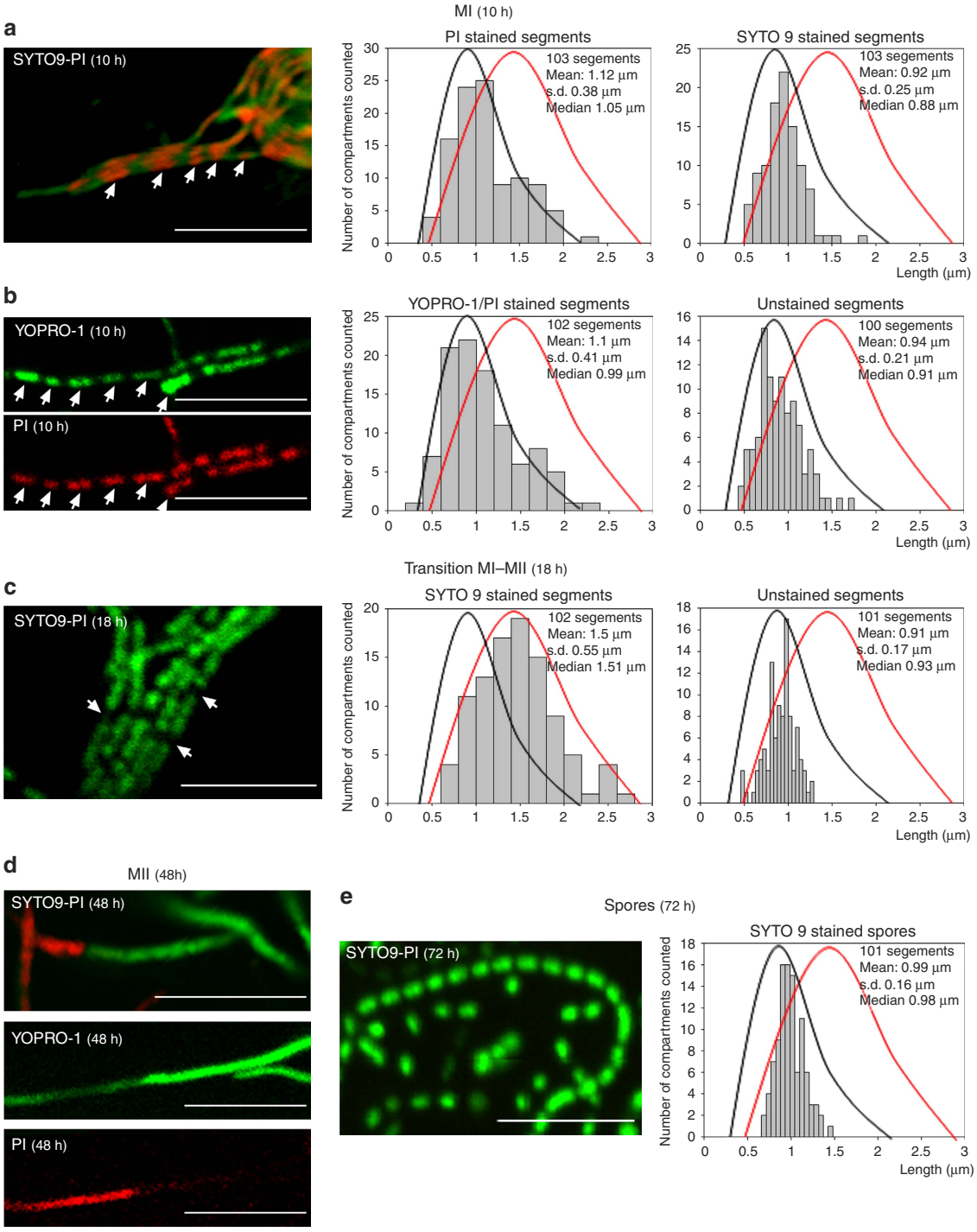

Figure 2 | Confocal laser scanning fluorescence microscopy analysis of *S. coelicolor* growing on GYM agar. (**a**) SYTO9 (green) and PI (red) staining (MI, 10 h). (**b**) YOPRO-1 (green) and PI (red) staining (MI, 10 h). (**c**) SYTO9-PI staining (transition from MI to MII, 18 h). (**d**) SYTO9-PI staining and YOPRO-1-PI (MII, 48 h). YOPRO-1 and PI were usezd simultaneously; notice that not all of the hyphae stained with YOPRO-1 were stained with PI. (**e**) SYTO9-PI staining (spores, 72 h). The scale bars correspond to 8 µm. The arrows in **a**–**c** highlight dying cells in 'MI' and 'transition MI-MII' hyphae. Histograms of the stained and unstained segments are shown. Two distributions were observed: one from the MI stained and unstained segments in **a** and **b** and from the unstained segments in **c** (black lines), and the second from the living segments stained with SYTO9, which begin to enlarge as multinucleated hyphae in **c** (red lines).

A regular pattern of permeable and non-permeable cells was not observed during the MII stage, once the dying MI cells disintegrated[6], while live cells grew out to form non-septated multinucleated hyphae (Fig. 2d). This indicates that the regular pattern of YOPRO-1/PI staining observed in the MI hyphae is attributable to the nature of this mycelium, which differs from that of the MII hyphae.

During the last developmental stages, the hyphae compartmentalized into spores with an average diameter of 0.99 ± 0.16 µm and a size distribution comparable to that of the MI segments (compare Fig. 2a–c with Fig. 2e). Sporulating septa consisted of very thick cell walls that were not stained by nucleic acid-binding stains and were observed as unstained regions (Fig. 2e; notice that the length of the unstained regions

corresponding to thick cell walls is much shorter than that of the unstained regions corresponding to MI cellular segments).

Visualization of compartmentalization by electron microscopy. To obtain detailed insight into the discontinuities along the MI mycelium (12 h), the hyphae were analysed by performing cryo-correlative light/electron microscopy (cryo-CLEM; Fig. 3a–d) and high-pressure freezing and freeze substitution electron microscopy (Fig. 3e,f). Two types of cells/compartments were observed to alternate and contained either weakly FM5-95-stained and electron-dense cytoplasm, or strongly FM5-95-stained and electron-lucent cytoplasms (Fig. 3b–d). In the latter, vesicles and membrane invaginations were frequently observed (arrows in Fig. 3). Samples for cryo-CLEM were flash-frozen within milliseconds in liquid ethane, without chemical fixation, minimizing the possibility that the membranous structures observed may have been the result of chemical artifacts[18,19].

Two types of barriers delimiting MI cellular segments were detected: cross-membranes without detectable peptidoglycan under the tested conditions (Fig. 3e); and peptidoglycan-based cross-walls (Fig. 3f).

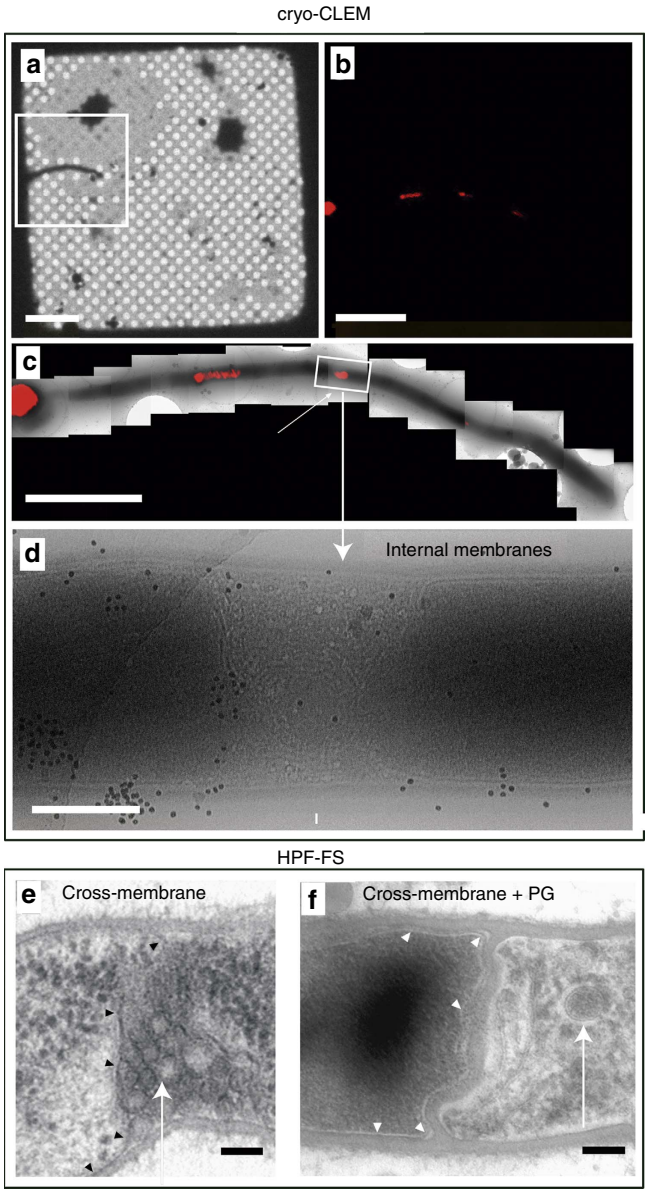

Figure 3 | Cryo-correlative light and electron microscopy (cryo-CLEM) and high-pressure freezing and freeze substitution (HPF-FS) of 12-hour MI hyphae of *S. coelicolor* grown on GYM agar. (**a**–**d**) Cryo-CLEM. (**a**) Phase-contrast mode, (**b**,**c**) FM5-95 (red) staining, (**d**) electron microscopy. (**e**,**f**) HPF-FS electron microscopy, (**e**) cross-membrane without cell wall, (**f**) cross-membrane with a thick cell wall. Arrows indicate internal cross-membranes in the form of membrane vesicles and membrane arrays. Arrowheads indicate cross-membranes continuous with the extracellular membrane delimiting cellular segments. Scale bars: (**a**) 20 µm, (**b**) 5 µm, (**c**) 4 µm, (**d**) 500 nm, (**e**) and (**f**) 100 nm.

FtsZ expression and Z-ring formation in MI hyphae. MI is a transitory stage in laboratory cultures, and has been ignored in most studies examining *Streptomyces* development. However, previous transcriptome analysis of RNA isolated from young hyphae of *S. coelicolor* suggested that *ftsZ* is overexpressed at this stage of the life cycle[8]. We performed quantitative reverse transcription–PCR (qRT–PCR) analysis of RNA isolated from solid-grown cultures on GYM agar plates to show that *ftsZ* transcript levels are higher after spore germination (MI, 15 h) and are even higher those observed during sporulation (that is, 63–70 h; solid line in Fig. 4a). The lowest *ftsZ* transcript levels were observed at ~39 h, corresponding to the formation of multinucleated substrate/pre-sporulating aerial hyphae. *ftsZ* gene expression correlates well with FtsZ protein abundance (dashed line Fig. 4a), as quantified by tandem mass tag (TMT) protein labelling and LC-MS/MS. FtsZ was more abundant at the MI stage than during sporulation.

There is a strong correlation between the frequency of septation—and thus compartment sizes—and the expression level of FtsZ: high levels of FtsZ are required to support sporulation-specific cell division[20,21]. Therefore, we examined whether high *ftsZ* transcription and protein levels also correspond to the septation frequency during the earliest stages of growth after spore germination. The cellular localization of FtsZ-eGFP was analysed by performing confocal microscopy with *S. coelicolor* FM145, a derivative of the model strain M145 exhibiting low autofluorescence[22] (Fig. 4b,c; Supplementary Fig. 1 and Supplementary Movie 1). Z-ring formation begins with the development of dynamic spiral-like structures of FtsZ, which are visualized as transitory spots that move rapidly inside the mycelium, and do not cross the entire diameter of the hypha[11,12] (arrowheads in Fig. 4b, Supplementary Movie 1). These spots ultimately form Z-rings, which are more stable and cross the entire diameter of the hypha (arrows in Fig. 4b, Supplementary Movie 1). During the early MI stage, Z-rings formed asynchronously during MI growth (Supplementary Movie 1). Z-rings disappear once the septa are complete[23,24]; consequently, they could not be observed at the same developmental time point in a single image (Supplementary Movie 1). However, the maximum projection of images acquired during an overnight time-lapse experiment (Fig. 4c and Supplementary Fig. 1) revealed that the Z-rings in the Z-ladders were spaced at an average of 1.1 ± 0.48 µm in all of the MI hyphae (Fig. 4d and Supplementary Fig. 1). This spacing and regularity are highly similar to that observed during sporulation-specific cell division[24].

To analyse the relationship between the Z-rings observed in *S. coelicolor* FM145 expressing FtsZ-eGFP as well as the differences in the PI permeability observed in the MI, both techniques were combined, staining the *S. coelicolor* FM145 strain expressing FtsZ-eGFP with PI. Z-rings are transitory, and PI permeability barriers can only be visualized when dying cells (stained with PI) alternate with living cells (not stained with PI). Consequently, it was difficult to detect Z-rings at a discrete time

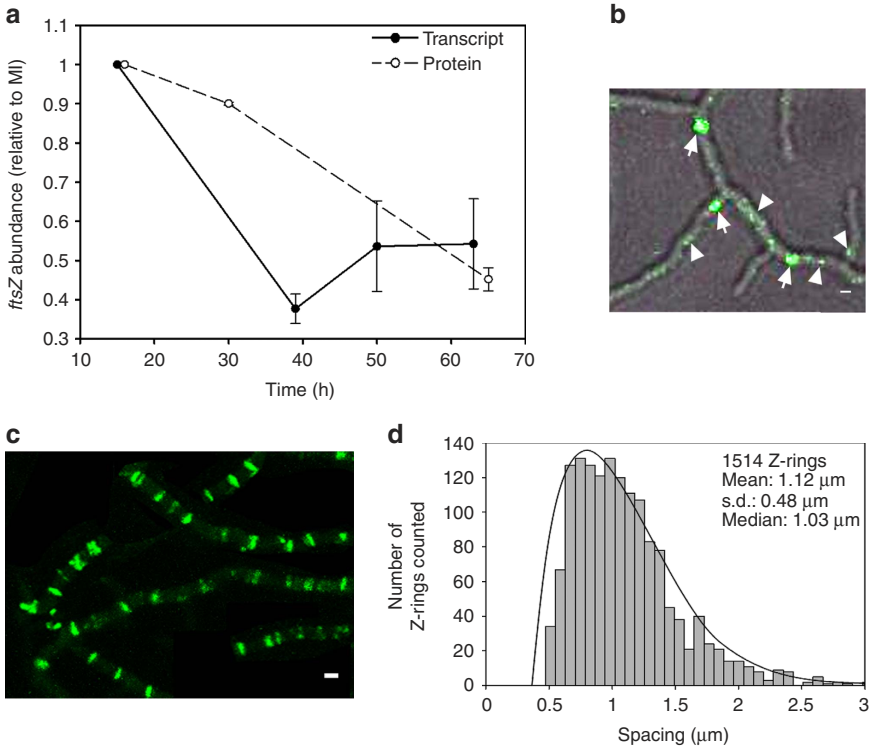

Figure 4 | *ftsZ* gene expression, protein abundance and cellular localization. (**a**) qRT-PCR analysis of *FtsZ* mRNA (solid line) and FtsZ protein abundance (dashed line). The average values of three biological replicates are presented (with SD). The MI sample (15 h in transcriptomics, 16 h in proteomics) was used for normalization and consequently has a value of 1 and an s.d. of 0. All abundance values were significantly different with respect to the 15-h sample (P value < 0.05; limma analysis[43] for protein; analysis of variance with Turkey's HSD *post hoc* analysis for transcript). (**b**) Z-ring formation shown by eGFP-FtsZ at early developmental time points of *S. coelicolor* grown on GYM agar plates (12 h). Fluorescence and phase-contrast images are overlaid. Arrowheads label transitory dynamic spiral-like structures that do not cross the entire diameter of the hyphae. Arrows label Z-rings. (**c**) Maximum projection of the time-lapse experiments (15 h); 100% of the hyphae had a regular pattern of Z-rings as indicated by eGFP-FtsZ (see Supplementary Movie 1 and Supplementary Fig. 1). (**d**) Spacing of the Z-rings. The spacing of a total of 1514 Z-rings was analyzed. Scale bars in **b** and **c** correspond to 1 µm.

point coinciding with the borders between a dying and a living cell (Supplementary Fig. 3). The colocalization of Z-rings with PI permeability barriers suggests that at least some of the Z-rings observed at the MI stage may contribute to the formation of permeability barriers separating PI permeable/impermeable segments.

Membrane permeability of the *ftsZ* mutant. SYTO9/PI and YOPRO-1/PI staining were applied to the *ftsZ* null mutant HU133 (McCormick *et al.*[13]). Surprisingly, the *ftsZ* mutant exhibited an alternating pattern of PI/YOPRO-1 permeable and impermeable segments comparable to that of the parental strain (Fig. 5). This pattern was observed at all time points in the mutant (the images shown in Fig. 5 correspond to a 48-h culture). The average size of the live segments, that is, those stained with SYTO9 but not with PI or YOPRO-1, was 0.85 µm ± 0.41 and 0.81 µm ± 0.36, respectively (red curves in Fig. 5), comparable to the sizes observed in the parental strain (see above and Fig. 2). As discussed below, the average length of dying cells, thta is, those stained with PI and YOPRO-1, was 1.83 µm ± 1.27 and 2.03 µm ± 1.3, respectively, with a maximum length of 6.12 µm (curves in black in Fig. 5), which was double the length observed in the parental strain. This pattern of PI/YOPRO1-permeable and -impermeable segments alternating in the same hypha was present in 100% of the mycelium (Supplementary Fig. 4).

Membrane and cell wall staining of *Streptomyces* hyphae. The lipophilic membrane colourant FM4-64 was used to stain hyphae of *S. coelicolor* M145 at the MI stage (Fig. 6a–d), and this staining was compared with HU133 (*ftsZ* mutant; Fig. 6e,f). As previously reported[7], FM4-64 stained the *S. coelicolor* hyphae heterogeneously, and only a fraction of the hyphae were stained (compare the hyphae observed by phase-contrast with those stained with FM4-64 in Fig. 6a). Two types of internal membranes were detected: sharp cross-membranes continuous with the extracellular membrane and delimiting cellular segments (arrows in Fig. 6b) and large spots stained with FM4-64 (arrowhead in Fig. 6c). At the MI stage, some hyphae exhibited a regular pattern of cross-membranes, and/or FM4-64 stained spots (Fig. 6d), but this pattern was not observed in all hyphae. As discussed below, FM4-64 could not be used to quantify the proportion of cross-membranes in the MI hyphae, because it does not stain all membranes under the conditions employed in this work. FM4-64 also stained internal membranes in the *ftsZ* null mutant (Fig. 6e,f). The two types of internal membranes described above were observed, but with an obvious difference: the large spots stained with FM4-64 were much larger in the *ftsZ* null mutant than in the parental strain (compare Fig. 6c with Fig. 6e).

Cell wall stains such as fluo-wheat germ agglutinin (fluo-WGA) and boron-dipyrromethene-vancomycin (BODIPY-vancomycin) stained 100% of the hyphae observed (Fig. 6g,j). Fluo-WGA stained the complete external hyphal walls and the cross-walls of the MI septa in the *S. coelicolor* parental strain (Fig. 6h). BODIPY-vancomycin stains nascent peptidoglycan[25], and most of the cell walls were not visualized with this stain (Fig. 6k,l). D-amino acid pulse labelling of cell walls[26] gave the

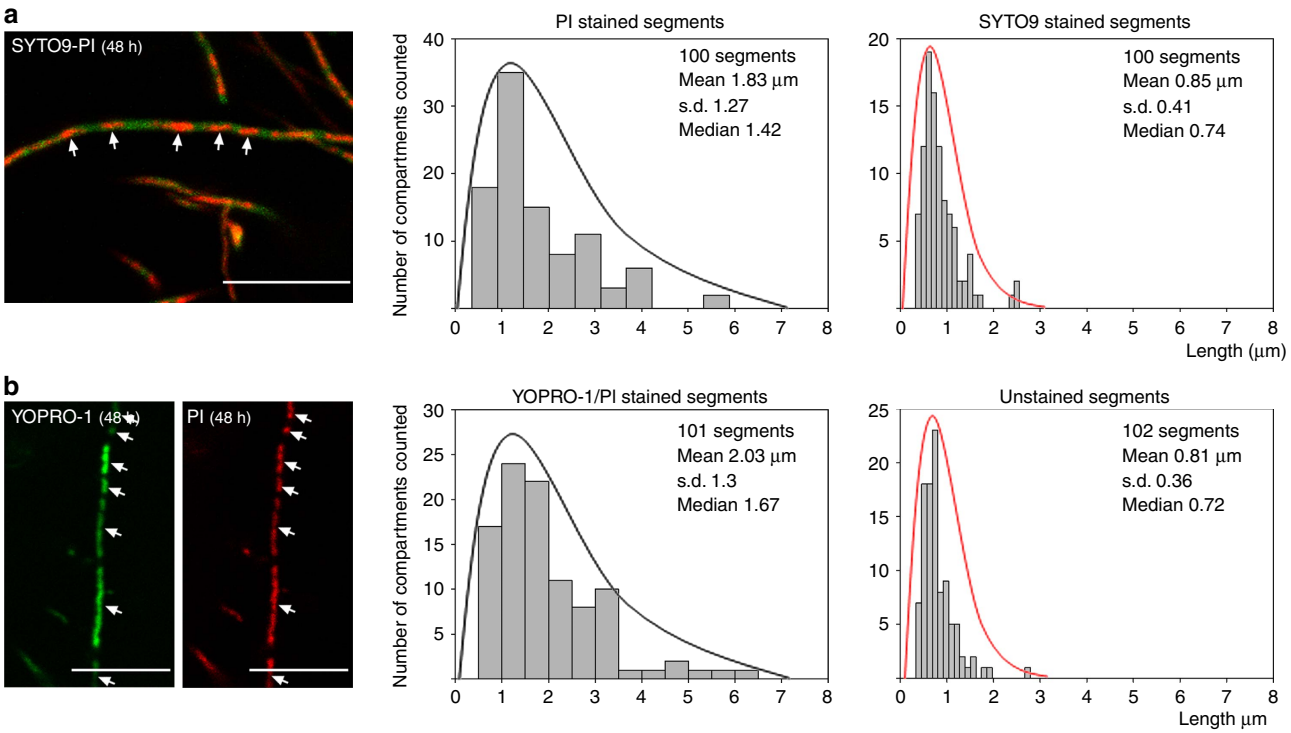

Figure 5 | Confocal laser scanning fluorescence microscopy analysis of the *ftsZ* mutant HU133. (**a**) SYTO9 (green) and PI (red) staining (48 h). (**b**) YOPRO-1 (green) and PI (red) staining (48 h). Histograms of the stained and unstained segments are shown. Two distributions were observed: one from viable segments stained with SYTO9 and not stained with YOPRO-1 or PI (red lines); the second from dying cells stained with YOPRO-1 and/or PI (black lines). The scale bars correspond to 8 µm.

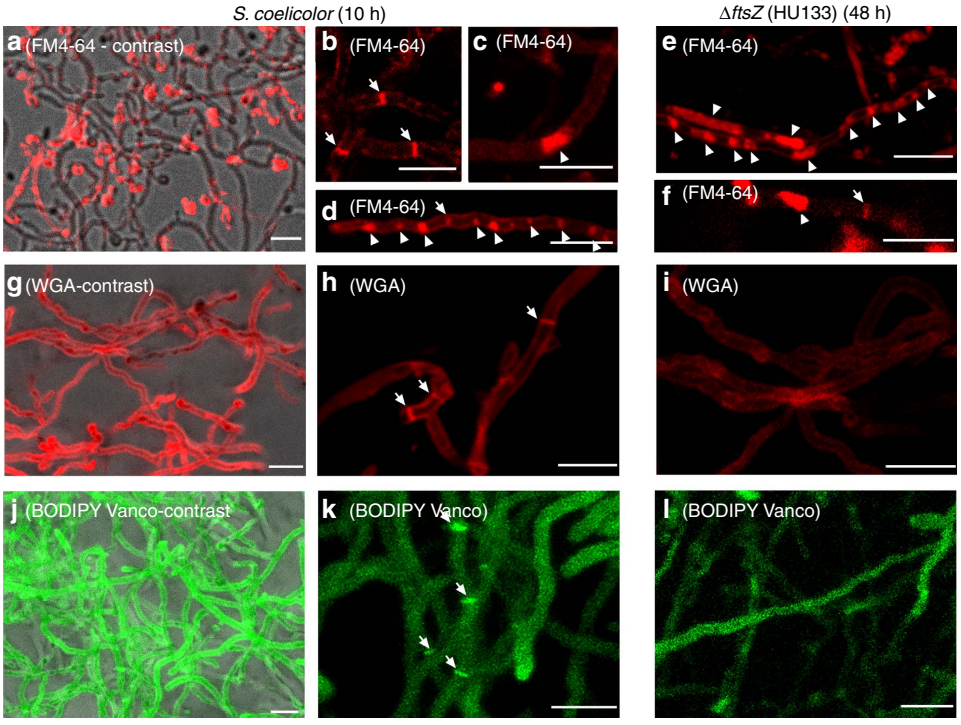

Figure 6 | Membrane and cell wall staining of *S. coelicolor* and its *ftsZ* mutant HU133. (**a**–**f**) FM4-64 staining (membranes). (**g**–**i**) WGA staining (cell wall). (**j**–**l**) BODIPY-vancomycin staining (nascent peptidoglycan). Fluorescent images in **a**, **g** and **j** correspond to the maximum projection 10-µm series overlaid with their respective phase-contrast images, showing 100% of the stained hyphae. Arrows indicate cross-membranes and cross-cell walls. Arrowheads indicate membrane cellular segments filled with membrane vesicles. Scale bars, 4 µm.

same results as those observed for fluo-WGA staining (Supplementary Fig. 5). The frequency of cross-walls stained with all cell wall colourants was lower than the frequency of the PI and YOPRO-1 permeability barriers as previously described (Fig. 2). Specifically, most of the permeability barriers separating PI/YOPRO-1-permeable and -impermeable segments do not have sufficient cell wall to be observed by fluorescence microscopy. The use of fluorescent D-amino acids combined with PI *in vivo* showed that septa (membranes with thick cell walls[15]) colocalize only with some of the PI permeability barriers (Supplementary Fig. 3). This provides further evidence that, at minimum, the PI permeability barriers colocalizing with cross walls in the MI correspond to cross-membranes. Fluo-WGA, fluorescent D-amino acids or BODIPY-vancomycin did not stain cross walls in the *ftsZ* null mutant (Fig. 6i,l), as expected for a mutant without cross walls[13].

S. coelicolor FM145 expressing FtsZ-eGFP was stained with FM4-64 (membrane stain) and HADA (cell wall stain), which indicated that at least a portion of the Z-rings colocalize with cross-walls and/or cross-membranes (Supplementary Fig. 3). As discussed below, Z-rings are transitory, and FM4-64 does not stain all membranes, but colocalization can be detected, providing further evidence that Z-rings may be involved in the formation of cross-membranes.

Compartmentalization correlates with protoplast formation. The ability to form protoplasts depends on the differentiation stage[27], and this feature can be used to distinguish MI-compartmentalized hyphae from MII-multinucleated hyphae because MII hyphae do not form many protoplasts, likely due to the instability of the large protoplasts formed by multinucleated hyphae[6]. We devised a method based on protoplast formation and flow cytometry measurements to quantify the number of protoplasts formed per unit of biomass. Protoplasts formed in high amounts during the MI stage (16 h), whereas their numbers progressively decreased during the MI and MII transition phase, and very few protoplasts were produced at the late MII stage (48 h) (Fig. 7a). The average protoplast size was 2.2 ± 1.13 µm, and there were no protoplasts with diameters larger than 5–6 µm (Fig. 7b; Supplementary Fig. 6). During the sporulation stages, unigenomic spores were readily obtained, but no protoplasts were observed (data not shown) because *Streptomyces* spores are resistant to lysozyme[28]. Protoplast formation correlated well with the compartmentalization observed in the MI but not MII hyphae (see above), thus providing a method to assess the degree of compartmentalization of the hyphae and to distinguish between the MI and MII phases.

The *ftsZ* null mutant (*S. coelicolor* HU133) formed protoplasts in numbers and with an average diameter (1.98 ± 0.8; Fig. 7c,d; Supplementary Fig. 6) comparable to those of the *S. coelicolor* parental strain at the MI stage. The *S. coelicolor ftsZ* null mutant grows very slowly, and its growth was therefore not comparable to the parental strain. *S. coelicolor* HU133 formed protoplasts at all time points (the protoplasts quantified in Fig. 7c,d were obtained from a 48-h culture).

Discussion

The alternation of PI/YOPRO1-permeable/impermeable segments in the MI hyphae demonstrates the existence of barriers impermeable to these viability stains, with the diffusion properties of membranes[6] (outlined in Fig. 8). The frequency of these permeability barriers is much higher than the frequency of septa formed by cross walls[3]. Here we applied cryo-CLEM and FM lipophilic styryl dyes (FM4-64/FM5-95) to reveal the existence of two types of internal membranes, which were not associated with

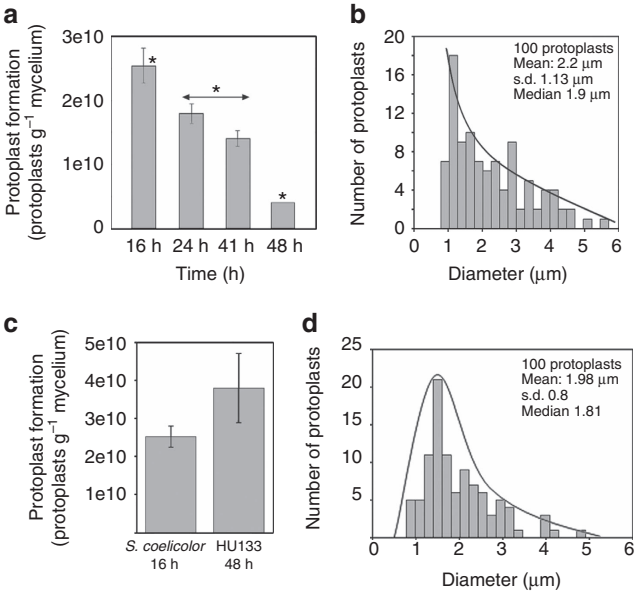

Figure 7 | Protoplast formation correlates with MI and compartmentalization in the *ftsZ* mutant HU133. (**a**,**b**) Protoplast formation in the *S. coelicolor* parental strain (presented as the number of protoplasts per gram of fresh mycelium) grown in GYM and a histogram of protoplast diameter at 10 h. Significant differences in protoplast formation (P value < 0.05; analysis of variance with Turkey's HSD *post hoc* analysis) with respect to the 16 h sample (MI) are labelled with an asterisk. (**c**,**d**) Protoplast formation in the Δ*FtsZ* HU133 mutant at 48 h of growth in GYM and histograms of protoplast diameter. The error bars indicate ± s.d. of three biological replicates.

detectable peptidoglycan: cross-membranes continuous with the extracellular membrane that delimit cellular segments and are difficult to be observed (Fig. 3 and Fig. 6b); and vesicles/membrane arrays, that are non-continuous with the extracellular membrane, and are easily visualized by CLEM (Fig. 3 and Fig. 6c). As discussed below, cross-membranes are also found in the *ftsZ* null mutant, which is not able to produce peptidoglycan-based septa[13]. Importantly, recent FRAP and CLEM/cryo-electron tomography experiments performed on liquid-grown mycelia, revealed the existence of impermeable cross-membranes compartmentalizing vegetative hyphae of *Streptomyces albus*, and their existence was also corroborated in *S. coelicolor*[16]. In the current work, experimentation was performed at the earliest stages of growth (MI stage) in solid-grown cultures of *S. coelicolor*, with the experiments aimed at quantifying the nature and the extent of hyphal compartmentalization. Our fluorescence and electron microscopy experiments failed to detect 1-µm spacing cross-membranes correlating with the 1-µm spacing permeability barriers observed with PI/YOPRO-1. This is most likely explained by the fact that fluorescence and electron microscopy do not permit the visualization of all *Streptomyces* membranes, as it happens in other microorganisms. For example, FM4-64 only stains vacuolar membranes in yeast[29], the inner membrane and membrane domains enriched in basic phospholipids in *E. coli*[30], the outer membrane in *Agrobacterium*[31] and under the conditions employed in this work, only a fraction of *S. coelicolor* hyphae (Fig. 6a). Next-generation electron microscopy methodologies, such as CLEM and cryo-electron tomography, are enabling the detection of novel internal structures in bacteria, including membranes, but the existence of further undetected structures cannot be dismissed (reviewed in Jensen *et al.*[32]). Interestingly, the use of fluorescent D-amino acids combined with PI *in vivo* showed that the membranes associated with cross walls (septa), can be detected as

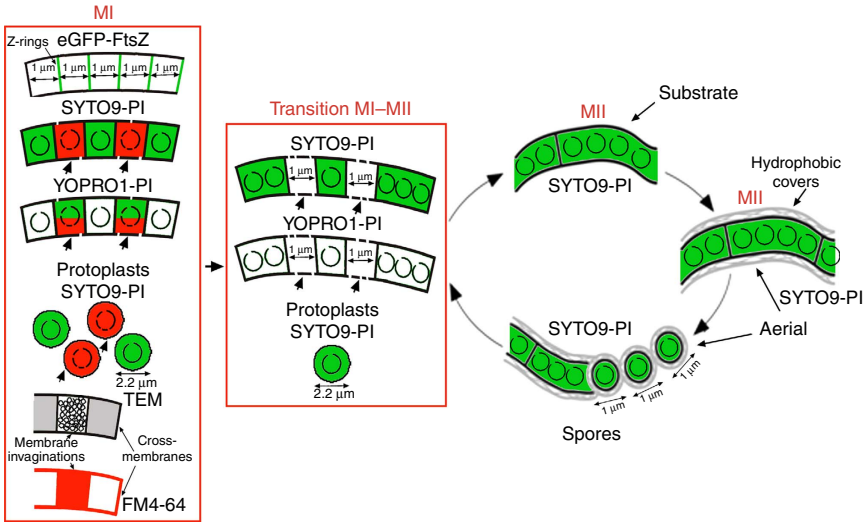

Figure 8 | Model of compartment formation and PCD in vegetative hyphae of *Streptomyces coelicolor*. Z-rings, cross-membranes, membrane invaginations/vesicles, and protoplasts are illustrated. Peptidoglycan walls (not shown in the scheme) are associated with some of the cross-membranes forming classical septa. Open circles inside compartments represent intact chromosomal DNA, and fragmented circles indicate degraded chromosomal DNA. Membrane discontinuities represent the changes in membrane permeability in dying cells. Red corresponds to PI fluorescence, and green corresponds to SYTO9 or YOPRO1 fluorescence. Arrows indicate dying cells; DNA is fully degraded in these cells during the transition from MI to MII and thus is not stained. FM4-64 labelling is illustrated in red.

PI permeability barriers colocalizing with cross walls (Supplementary Fig. 3). PI permeability barriers that are not associated with cross walls most likely also represent cross-membranes. The compartmentalization of MI hyphae correlates with the ability to form stable protoplasts, which again supports the existence of cross-membranes surrounding the compartments that are able to produce protoplasts (Fig. 7a,b). Further work employing new and improved microscopy techniques will be necessary to test whether all permeability barriers to PI and YOPRO-1 correspond to membranes.

In contrast to the cross-membranes delimiting cellular segments, internal membranous structures are easier to contrast against the cytoplasm of the MI hyphae, and were described long ago in *S. coelicolor* by Glauert and Hopwood[33] and in dying cells of *S. antibioticus* by Miguelez *et al*[5]. However, these authors applied chemical fixation, and thus they could not discard the possibility that these structures were chemical artifacts[5]; to this day, their discovery has remained unvalidated. Further work is necessary to characterize the biological function of vesicles/membrane invaginations in the MI hyphae, but their observation by cryo-electron microscopy supports the conclusion that they are not chemical artifacts. Celler *et al.*[16] recently observed internal membranous structures in vegetative hyphae using cryo-electron tomography and CLEM. The authors showed that large membrane assemblies are formed creating DNA-free zones, often (but not always) associated with initiation of septum formation, suggesting a role of these structures in protecting the DNA during the onset of vegetative cell division.

Two different types of septa exist in *Streptomyces*, both of which consist of peptidoglycan and membranes: the cross walls in the substrate and early aerial mycelia and the sporulation septa in sporulating aerial hyphae. Although their formation depends on FtsZ, the localization of the Z-rings is regulated by entirely different mechanisms during these two growth phases[14,15,34,35]. The compartmentalization of MI hyphae is comparable to that of sporulation-specific cell division, with the formation of ladders of Z-rings, with an average spacing of 1 µm. A proportion of the Z-rings observed in the MI colocalize with cross-membranes, and some colocalize with PI permeability barriers (Supplementary Fig. 3). These results indicate that Z-rings might contribute to the formation of at least some of the permeability barriers separating the 1-µm cellular segments and again suggest that PI permeability barriers correspond to the cross-membranes observed by CLEM. One of the most intriguing peculiarities of *Streptomyces* cell division is that *ftsZ* null mutants are viable, resulting in long non-septated branched vegetative hyphae[13]. Counterintuitively, the hyphae of the *ftsZ*-null mutant can be fragmented without loss of viability, suggesting that the release of their contents is somehow prevented[13]. Here we have provided evidence for the existence of cross-membranes in the *ftsZ*-null mutant (Fig. 6e,f). The formation of membranous- rather than peptidoglycan-based 'septa' that are not dependent on FtsZ is so far unique in bacteria. Interestingly, a somewhat analogous case is known in archaea: most Crenarchaea lack *ftsZ*, but some such as *Pyrobaculum islandicum*, produce cross-walls that consist of an S-layer rather than peptidoglycan[36]. Further work should characterize the role of FtsZ (if any) in the formation of cross-membranes and identify any possible differences between the cross-membranes formed in the presence or absence of *ftsZ*.

In summary, this work provides evidence for the existence of an unprecedented high-frequency compartmentalization in MI hyphae based on cross-membranes. Cross-membranes may have developed to support the multicellular life style of streptomycetes, enabling subcompartmentalization to provide an additional level of organization in the long hyphae. It will be very interesting to determine whether similar membrane-based compartmentalization also exists in other (multicellular) bacteria.

Methods

Strains and media. *Streptomyces coelicolor* M145 (ref. 37) was obtained from the John Innes Centre strain collection and its *ftsZ* null mutant HU133 (ref. 13) was obtained from the Harvard University strain collection. GYM (glucose, yeast and malt)[38] was used as the growth medium in both liquid and solid media. Agar plates were used with and without cellophane disks and were inoculated with 100 µl of an inoculum suspension (1×10^7 viable spores ml^{-1}), followed by incubation at 30 °C. The reduced autofluorescence strain *S. coelicolor* FM145 harbouring a plasmid expressing FtsZ-eGFP was previously described[22].

Real-time qRT-PCR. Total RNA was obtained by phenol extraction and using the RNeasy Midi Kit (Qiagen). RNA integrity was verified using a 2100 BioAnalyzer (Agilent). The RNAs used in real-time RT–PCR analysis were digested with the TURBO DNA-free kit (Ambion) to remove possible DNA contamination according to the manufacturer's instructions. Briefly, 50 µl of 200 ng µl^{-1} RNA solution was treated with DNase I at 37 °C for 30 min. The samples were mixed with 0.2 volumes of inactivation reagent, incubated for 5 min at room temperature and recovered by centrifugation.

One microgram of RNA was used as the template for complementary DNA (cDNA) synthesis using the High-Capacity cDNA Reverse Transcription Kit (Applied Biosystems) according to the manufacturer's specifications. The primers used for real-time PCR of *ftsZ* were 5′-GCAGCACCGCAGAACTAC-3′ and 5′-AGACCGACCTCGATCATCC-3′. Real-time PCR was performed on an ABI PRISM 7900 HT thermocycler (Applied Biosystems). The reactions contained 2 µl of cDNA diluted twofold, 10 µl of SYBR Green PCR Master Mix (Applied Biosystems) and 300 nM primers in a final volume of 20 µl. Three biological samples were analysed, and control reactions with RNA and water as templates were performed to verify the absence of DNA contamination and primer–dimer formation. The thermal profile was as follows: an initial stage at 50 °C for 2 min, a second stage at 95 °C for 10 min, a third stage of 40 cycles at 95 °C for 15 s and 60 °C for 1 min, and a final dissociation profile of 95 °C for 15 s, 60 °C for 15 s and 95 °C for 15 s to confirm the absence of primer dimers. Relative quantification of gene expression was performed using the ΔΔCt method[39]. *SCO3878*, which encodes the β-chain of DNA polymerase III, was used as an internal control to quantify the relative expression of the target gene employing experimental conditions as previously reported[8]. *SCO3878* was expressed constitutively under the conditions used in this work[8]. The reliability of the differences in the *ftsZ* expression levels was analysed by analysis of variance with Turkey's honest significant difference (HSD) *post hoc* analysis. Differences were considered as significant if their P value was ≤ 0.05.

FtsZ protein quantification. Protein was extracted from *Streptomyces* cultures at 16, 30 and 65 h as previously described[40]. The 30- and 65-h samples were analysed in biological triplicate, and the 16-h samples were analysed in quadruplicate. Protein pellets were resuspended in 8 M urea with 50 mM TEAB for bicinchoninic acid assay quantitation. A 300-µg quantity of protein was digested using a combined trypsin/LysC digestion protocol[41]. The samples were then desalted and subjected to amino acid analysis. For each condition, 60 µg of peptides was labelled with 0.5 mg of TMT-10-plex reagent (ThermoFisher) following the manufacturer's protocol. The samples were then combined, and 50 µg was fractionated by hydrophilic interaction liquid chromatography to generate 12 fractions, which were further fractionated on an EasyLC system (Thermo) with a 90-min gradient (0–35%). The LC aqueous mobile phase contained 0.1% (v/v) formic acid in water, and the organic mobile phase contained 0.1% (v/v) formic acid in 95% (v/v) acetonitrile. The samples were injected on a custom 3-cm trap column (100-µM internal diameter silica tubing packed with Reprosil 120 C18 5-µM particles) and desalted with 18 µl of buffer A. Separation was performed on a custom 20-cm column (75-µM internal diameter silica tubing packed with Reprosil 120 C18 3-µM particles) with a pulled emitter at 250 nl min^{-1}. The eluted peptides were analysed on an Orbitrap Fusion mass spectrometer in data-dependent mode. The MS1 spectrum was acquired on an Orbitrap mass analyser at 120,000 resolution with an AGC target of 5e5. For MS2 scans, peptides were isolated with a quadrupole using a 1.2-Da isolation window and fragmented at 35 and 40% normalized collision energy. AGC was set at 5e4, the maximum injection time was 120 ms and dynamic exclusion was 20 s. Data were processed with Proteome Discoverer 2.1 with Mascot as the search engine using the UniProt *S. coelicolor* database (retrieved on 06.03.15). Peptides were validated by Mascot Percolator with a threshold of 0.01 PEP. Peptide spectrum matches with total summed reporter intensities of $<4e5$ were not considered for quantitation due to the high level of noise in the quantitation data. The quantification results of peptide spectrum matches were converted to peptide-level quantitation, which in turn was converted into protein quantitation using an R script[42]. Only proteins with two or more quantified peptides were considered. This resulted in quantitation of 3,575 proteins (manuscript in preparation). FtsZ was quantified by 13 peptides (Supplementary Table 1). Proteins were analysed for differential expression using the limma package in R[43]. P values were adjusted for multiple comparison using the R stats package. Thus the reported Q values for the change in FtsZ expression were adjusted for multiple comparisons within the data set. The relative abundance (normalized as the ratio against the 16 h sample) was estimated using the TMT abundances from three biological replicates (Supplementary Table 1).

Viability staining. Culture samples were obtained and processed as previously reported[6] for excised cellophane or agar pieces and were stained a few minutes later. The LIVE/DEAD BacLight Bacterial Viability Kit (Invitrogen, L-13152) was employed for staining. This kit uses SYTO9 and PI, two DNA-binding colourants. SYTO9 penetrates intact membranes and stains viable cells green, whereas PI only penetrates bacteria with damaged membranes. At the concentrations used in the kit, PI displaces SYTO9 from DNA when both colourants are present in dying cells, staining cells red[44]. Samples were observed under a Leica TCS-SP2-AOBS and/or Leica TCS SP8 laser scanning microscope at wavelengths of 488 and 568 nm for excitation and 530 (green) or 630 nm (red) for emission. More than 100 images were analysed in a minimum of three independent culture analyses for each developmental condition.

Both YOPRO-1 (Invitrogen Y3603) and PI were used at concentrations of 5 µM. YOPRO-1 was observed by confocal microscopy using the same parameters described above for SYTO9.

Images were processed using Image J software. The lengths of at least 100 stained and unstained segments were quantified, and histograms of length distributions and statistical analyses were constructed using SigmaPlot 12.0.

Membrane staining. The lipophilic styryl dye, N-(3-triethylammoniumpropyl)-4-(p-diethylaminophenyl-hexatrienyl) pyridinium dibromide (FM4-64) (Molecular Probes, T-3166) was added directly to the culture medium at a final concentration of 1 mg ml^{-1} before the plates were poured. This concentration of FM4-64 does not affect growth. Samples were observed under a confocal laser scanning microscope at wavelengths of 550 nm for excitation and 700 nm for emission.

Cell wall staining. Cells were fixed for 15 min at room temperature using PBS (0.14 M NaCl, 2.6 mM KCl, 1.8 mM KH_2PO_4 and 10 mM Na_2HPO_4) containing 2.8% paraformaldehyde and 0.0045% glutaraldehyde. Texas Red WGA (Invitrogen W21405) was added at a concentration of 100 mg ml^{-1} in 2% BSA in PBS and the cells were incubated at room temperature for 3 h. BODIPY-vancomycin (Invitrogen V34850) was used at a concentration of 0.5 µg ml^{-1} in PBS for 15 min. The samples were washed with PBS and observed under a Leica TCS-SP8 confocal laser scanning microscope at excitation wavelengths of 595/505 and emission wavelengths of 615/513 for WGA and BODIPY-vancomycin, respectively.

Fluorescent D-alanine (HADA) was used as recommended by Kuru *et al.*[26]. Briefly, the HADA stock solution was prepared in dimethylsulphoxide at a concentration of 100 mM. In the case of the *S. coelicolor* parental strain, liquid cultures (0.5 ml) containing 500 µM HADA were inoculated with fresh spores (10^7 spores per ml) and incubated at 200 r.p.m.s. and 30 °C. The *ftsZ* null mutant did not grow in liquid cultures under our experimental conditions; instead it was grown in small (0.5 ml) solid GYM cultures with 500 µM HADA.

Time-lapsed live imaging. The spores were initially incubated on GYM medium, for six hours. Samples were then excised out and inverted into uncoated m-dishes (Ibidi GmbH). The lids were turned so they were supported on the vents to allow gas exchange and were then sealed with two layers of parafilm to prevent drying of the medium. The samples were incubated at 30 °C and imaged with a Zeiss Observer confocal microscope. Images were acquired every 45 min for 15 h. Excitation was performed with a 488-nm laser, and detection was performed with a 505–530 nm bandpass filter. To minimize focal drift, the microscope stage and imaging chamber were allowed to equilibrate for 60 min before imaging.

Time-lapse images were processed with ImageJ. Z-rings were detected using a Gaussian filter with a Sigma value of 2 followed by an Unsharp Mask filter with a radius of 3 and a mask weight of 0.6. Then, a Find Maxima process with a noise tolerance of 50 was used to obtain binary images of the Z-ring local maxima. Finally, the nearest distance between Z-rings was calculated using the Nearest Neighbourhood Distance plugin (Nnd; https://icme.hpc.msstate.edu/mediawiki/index.php/Nearest_Neighbor_Distances_Calculation_with_ImageJ).

Cryo-correlative light and electron microscopy. For cryo-CLEM, an EM grid was positioned on a *Streptomyces* culture during growth and was vitrified directly afterwards by plunging into liquid ethane using a Leica EM GP from RT at approximately 75% humidity with 1-second blotting. Plunge-frozen grids were used for correlative light and microscopy. Plunge-frozen EM grids containing *Streptomyces* were imaged using a fluorescence microscope equipped with CMS196 cryo light microscope stage (Linkam, Surrey, UK), in conjunction with a Zeiss Axio Imager M2. Cryo-EM was performed on a Tecnai 20 FEG operated at 200 kV (FEI Company). Images were recorded on a 2k × 2k camera mounted behind a GIF energy filter (Gatan) operated at a slit width of 20 eV.

High-pressure freezing and freeze substitution. To observe *S. coelicolor* cells by transmission electron microscopy (TEM), Epon-embedded thin sections were obtained as described by Frias *et al.*[45]. Briefly, bacterial cells were cryo-immobilized as quickly as possible using a Leica EMPact high-pressure freezer (Leica, Vienna, Austria). Frozen samples were freeze-substituted in a Leica EM automatic freeze substitution system (Leica, Vienna, Austria). The substitution was performed in pure acetone containing 2% (wt/vol) osmium tetroxide and 0.1% (wt/vol) uranyl acetate at 90 °C for 72 h. The temperature was gradually decreased (5 °C h^{-1}) to 4 °C, held constant for 2 h, and then finally increased to room temperature and maintained for 1 h. The samples were washed for 1 h in acetone at room temperature and infiltrated in a graded series of Epon-acetone mixtures: 1:3 for 2 h, 2:2 for 2 h, 3:1 for 16 h, and pure Epon 812 (Ted Pella, Inc.) for 30 h. The samples were embedded in fresh Epon and polymerized at 60 °C for 48 h. Ultrathin sections were cut with a Leica UCT ultramicrotome and mounted on Formvar carbon-coated copper grids. Sections were post-stained with 2% (wt/vol) aqueous uranyl acetate and lead citrate and examined with a Tecnai Spirit electron microscope (FEI Company, The Netherlands) at an acceleration voltage of 120 kV.

Mycelium protoplasting. Protoplasts were obtained according to the method described by Okanishi *et al.*[27], and Kieser *et al.*[37] with some modifications to ensure that the efficiency of protoplasting was close to 100% (as analysed by observing the disintegration of the hyphae by phase-contrast and confocal microscopy, Supplementary Fig. 6) and that there was no significant loss of protoplasts during manipulations, both of which are critical requirements for reproducible and significant flow cytometry measurements (see below).

Mycelia grown on cellophane discs were scraped off, and 60 mg of mycelia (fresh weight) were resuspended in 1.12 ml of buffer P (0.6% TES buffer pH 7.2, 103% sucrose) in a 2-ml Eppendorf tube. Lysozyme was added from a freshly prepared stock at a final concentration of 2 mg ml^{-1} and incubated for 30 min at 600 r.p.m. and 37 °C in an Eppendorf ThermoMixer. Protoplasts were drawn in and out twice in a 1-ml pipette, incubated for an additional 30 min, washed two times by sedimentation (1,000*g*) and resuspended in buffer P. After the final wash, the protoplasts were resuspended in 500 µl of buffer P.

The original buffer P described by Kieser *et al.*[37] included a trace element solution and other salts. These salts interfere with flow cytometry measurements, and consequently, it was necessary to use the modified buffer P described in this work, which only includes TES buffer and sucrose (K_2SO_4, $MgCl_2$ and the trace element solution were not added). The buffer P used in these experiments was filtered through a 0.2-µm filter.

Protoplast quantification. Protoplast samples were stained with SYTO9 and quantified directly by fluorescence microscopy using a Thoma chamber (depth: 0.02 mm) or a flow cytometer (Cytomics FC500, Beckman-Coulter, Inc., Miami, FL, USA). In all cases, protoplasts from two biological replicates were quantified. Both methodologies produced similar results, but only flow cytometry data were included in this work.

Flow cytometry measurements were performed using BD Trucount Tubes (reference 340334), containing 500 µl of protoplasts stained with SYTO9 (6 µM). The trigger signal was established with an FL1 detector (530/540 nm) with an adequate negative control (buffer P) and a biological control (BD Plasma Count, reference 338331). Absolute quantifications were performed by counting 10,000 of the standard beads included in the BD Trucount Tubes. The protoplast dilutions used for cytometry quantifications contained absolute protoplast numbers within the 5,000–10,000 range, which was close to the number of beads used as a standard. The number of protoplasts per µl was calculated based on the number of standard beads, and the number of protoplasts per mg of fresh weight was calculated based on the original fresh weight used to form the protoplasts (see above).

The reliability of the differences in the number of protoplasts formed was analysed by analysis of variance with Tukey's HSD *post hoc* analysis. Differences were considered significant if the *P* value was equal to or less than 0.05 (asterisks in Fig. 7a).

Data availability. The authors declare that the data supporting the findings of this study are available within the article and its supplementary information files or from the corresponding authors on request.

References

1. Bérdy, J. Bioactive microbial metabolites. *J. Antibiot. (Tokyo)* **58,** 1–26 (2005).
2. Hopwood, D. A. *Streptomyces in Nature and Medicine: The Antibiotic Makers* (Oxford University Press, 2007).
3. Barka, E. A. *et al.* Taxonomy, physiology, and natural products of actinobacteria. *Microbiol. Mol. Biol. Rev.* **80,** 1–43 (2015).
4. Flärdh, K. & Buttner, M. J. *Streptomyces* morphogenetics: dissecting differentiation in a filamentous bacterium. *Nat. Rev. Microbiol.* **7,** 36–49 (2009).
5. Miguelez, E. M., Hardisson, C. & Manzanal, M. B. Hyphal death during colony development in *Streptomyces antibioticus*: morphological evidence for the existence of a process of cell deletion equivalent to apoptosis in a multicellular prokaryote. *J. Cell. Biol.* **145,** 515–525 (1999).
6. Manteca, A., Fernandez, M. & Sanchez, J. Cytological and biochemical evidence for an early cell dismantling event in surface cultures of *Streptomyces antibioticus*. *Res. Microbiol.* **157,** 143–152 (2006).
7. Manteca, A. & Sanchez, J. *Streptomyces* development in colonies and soils. *Appl. Environ. Microbiol.* **75,** 2920–2924 (2009).
8. Yagüe, P. *et al.* Transcriptomic analysis of liquid non-sporulating *Streptomyces coelicolor* cultures demonstrates the existence of a complex differentiation comparable to that occurring in solid sporulating cultures. *PLoS ONE* **21,** e86296 (2014).
9. Wildermuth, H. Development and organization of the aerial mycelium in *Streptomyces coelicolor*. *J. Gen. Microbiol.* **60,** 43–50 (1970).
10. Claessen, D., Rozen, D. E., Kuipers, O. P., Sogaard-Andersen, L. & van Wezel, G. P. Bacterial solutions to multicellularity: a tale of biofilms, filaments and fruiting bodies. *Nat. Rev. Microbiol.* **12,** 115–124 (2014).
11. Bi, E. F. & Lutkenhaus, J. FtsZ ring structure associated with division in *Escherichia coli*. *Nature* **354,** 161–164 (1991).
12. de Boer, P., Crossley, R. & Rothfield, L. The essential bacterial cell-division protein FtsZ is a GTPase. *Nature* **359,** 254–256 (1992).
13. McCormick, J. R., Su, E. P., Driks, A. & Losick, R. Growth and viability of *Streptomyces coelicolor* mutant for the cell division gene *ftsZ*. *Mol. Microbiol.* **14,** 243–254 (1994).
14. McCormick, J. R. Cell division is dispensable but not irrelevant in *Streptomyces*. *Curr. Opin. Biotechnol.* **12,** 689–698 (2009).
15. Jakimowicz, D. & van Wezel, G. P. Cell division and DNA segregation in *Streptomyces*: how to build a septum in the middle of nowhere? *Mol. Microbiol.* **85,** 393–404 (2012).
16. Celler, K. *et al.* Cross-membranes orchestrate compartmentalization and morphogenesis in *Streptomyces*. *Nat. Commun.* **7,** 11836 (2016).
17. Idziorek, T., Estaquier, J., De Bels, F. & Ameisen, J. C. YOPRO-1 permits cytofluorometric analysis of programmed cell death (apoptosis) without interfering with cell viability. *J. Immunol. Methods* **185,** 249–258 (1995).
18. Vanhecke, D., Graber, W. & Studer, D. Close-to-native ultrastructural preservation by high pressure freezing. *Methods Cell. Biol.* **88,** 151–164 (2008).
19. Milne, J. L. & Subramaniam, S. Cryo-electron tomography of bacteria: progress, challenges and future prospects. *Nat. Rev. Microbiol.* **7,** 666–675 (2009).
20. Flärdh, K., Leibovitz, E., Buttner, M. J. & Chater, K. F. Generation of a non-sporulating strain of *Streptomyces coelicolor* A3(2) by the manipulation of a developmentally controlled *ftsZ* promoter. *Mol. Microbiol.* **38,** 737–749 (2000).
21. Willemse, J., Mommaas, A. M. & van Wezel, G. P. Constitutive expression of *ftsZ* overrides the *whi* developmental genes to initiate sporulation of *Streptomyces coelicolor*. *Antonie Van Leeuwenhoek* **101,** 619–632 (2012).
22. Willemse, J. & van Wezel, G. P. Imaging of *Streptomyces coelicolor* A3(2) with reduced autofluorescence reveals a novel stage of FtsZ localization. *PLoS ONE* **4,** e4242 (2009).
23. Jyothikumar, V., Tilley, E. J., Wali, R. & Herron, P. R. Time-lapse microscopy of *Streptomyces coelicolor* growth and sporulation. *Appl. Environ. Microbiol.* **74,** 6774–6781 (2008).
24. Schwedock, J., Mccormick, J. R., Angert, E. R., Nodwell, J. R. & Losick, R. Assembly of the cell division protein FtsZ into ladder like structures in the aerial hyphae of *Streptomyces coelicolor*. *Mol. Microbiol.* **25,** 847–858 (1997).
25. Daniel, R. A. & Errington, J. Control of cell morphogenesis in bacteria: two distinct ways to make a rod-shaped cell. *Cell* **113,** 767–776 (2003).
26. Kuru, E. *et al. In Situ* probing of newly synthesized peptidoglycan in live bacteria with fluorescent D-amino acids. *Angew. Chem. Int. Ed. Engl.* **51,** 12519–12523 (2012).
27. Okanishi, M., Suzuki, K. & Umezawa, H. Formation and reversion of Streptomycete protoplasts: Cultural condition and morphological study. *J. Gen. Microbiol.* **80,** 389–400 (1974).
28. DeJong, P. J. & McCoy, E. Qualitative analyses of vegetative cell walls and spore walls of some representative species of *Streptomyces*. *Can. J. Microbiol.* **12,** 985–994 (1966).
29. Vida, T. A. & Emr, S. D. A new vital stain for visualizing vacuolar membrane dynamics and endocytosis in yeast. *J. Cell. Biol.* **128,** 779–792 (1995).
30. Fishov, I. & Woldringh, C. L. Visualization of membrane domains in *Escherichia coli*. *Mol. Microbiol.* **32,** 1166–1172 (1999).
31. Zupan, J. R., Cameron, T. A., Anderson-Furgeson, J. & Zambryski, P. C. Dynamic FtsA and FtsZ localization and outer membrane alterations during polar growth and cell division in *Agrobacterium tumefaciens*. *Proc. Natl Acad. Sci. USA* **110,** 9060–9065 (2013).
32. Jensen, G. J. & Briegel, A. How electron cryotomography is opening a new window onto prokaryotic ultrastructure. *Curr. Opin. Struct. Biol.* **17,** 260–267 (2007).
33. Glauert, A. M. & Hopwood, D. A. A membranous component of the cytoplasm in *Streptomyces coelicolor*. *J. Biophys. Biochem. Cytol.* **6,** 515–516 (1959).
34. Traag, B. A. & van Wezel, G. P. The SsgA-like proteins in actinomycetes: small proteins up to a big task. *Antonie Van Leeuwenhoek* **94,** 85–97 (2008).
35. Willemse, J., Borst, J. W., de Waal, E., Bisseling, T. & van Wezel, G. P. Positive control of cell division: FtsZ is recruited by SsgB during sporulation of *Streptomyces*. *Genes Dev.* **25,** 89–99 (2011).
36. Sonobe, S. *et al.* Proliferation of the hyperthermophilic archaeon *Pyrobaculum islandicum* by cell fission. *Extremophiles* **14,** 403–407 (2010).
37. Kieser, T., Bibb, M. J., Buttner, M. J., Chater, K. F. & Hopwood, D. A. *Practical Streptomyces genetics* (John Innes Foundation, 2000).
38. Novella, I. S., Barbes, C. & Sanchez, J. Sporulation of *Streptomyces antibioticus* ETH 7451 in submerged culture. *Can. J. Microbiol.* **38,** 769–773 (1992).
39. Livak, K. J. & Schmittgen, T. D. Analysis of relative gene expression data using real time quantitative PCR and the 2(-Delta Delta C(T)) Method. *Methods* **25,** 402–408 (2001).
40. Manteca, A., Sanchez, J., Jung, H. R., Schwämmle, V. & Jensen, O. N. Quantitative proteomics analysis of *Streptomyces coelicolor* development demonstrates that onset of secondary metabolism coincides with hypha differentiation. *Mol. Cell. Proteomics* **9,** 1423–1436 (2010).
41. Glatter, T. *et al.* Large-scale quantitative assessment of different in-solution protein digestion protocols reveals superior cleavage efficiency of tandem Lys-C/trypsin proteolysis over trypsin digestion. *J. Proteome Res.* **11,** 5145–5156 (2012).
42. Polpitiya, A. D. *et al.* DAnTE: a statistical tool for quantitative analysis of -omics data. *Bioinformatics* **24,** 1556–1558 (2008).

43. Ritchie, M. E. *et al.* Limma powers differential expression analyses for RNA-sequencing and microarray studies. *Nucleic Acids Res.* **43,** e47 (2015).
44. Haugland, R. P. *The Molecular Probes Handbook: a Guide to Fluorescent Probes and Labeling Technologies*. Ch. 15, 11th Edn. 651–729 (2010).
45. Frias, A., Manresa, A., de Oliveira, E., Lopez-Iglesias, C. & Mercadé, E. Membrane vesicles: a common feature in the extracellular matter of coldadapted Antarctic bacteria. *Microb. Ecol.* **59,** 476–486 (2010).

Acknowledgements

We thank the European Research Council (ERC Starting Grant; Strp-differentiation 280304), and the Spanish 'Ministerio de Economía y Competitividad' (MINECO; BIO2015-65709-R) for financial support. Support for R.K. from the European Union was obtained through the H2020 Programme grant iNEXT (grant No. 653706). N.G.Q. was funded by a Severo Ochoa fellowship (FICYT, Consejería de Educación y Ciencia, Spain). We thank Joseph R McCormick and Stuart Cantlay (Duquesne University) for providing the *ftsZ* mutant HU133; Michael S. VanNieuwenhze (Indiana University) for providing a sample of HADA; Sébastien Rigali (University of Liège) and Katherine Celler (Leiden University) for stimulating discussions; Ermelinda Tinetti (Invitrogen) for providing a sample of YOPRO-1; Ana Salas Bustamante, Angel Martinez Nistal, Marta Alonso Guervos and Tania Iglesias (Servicios Científico-Técnicos de la Universidad de Oviedo) for their support with flow cytometry, confocal microscopy and statistics; and Beatriz Gutierrez Magan (Universidad de Oviedo, Dpto. Biología Funcional, Área de Microbiología) for her laboratory assistance.

Author contributions

P.Y. and B.R. performed confocal microscopy and flow cytometry analysis. M.T.L.-G., N.G.Q. and P.Y. performed qRT–PCR analyses. J.W., P.Y. and G.P.v.W performed confocal microscopy time-lapse analyses. P.Y., B.R., M.T.L.G. and N.G.Q. performed the statistical analyses. J.W., R.I.K and A.J.K. performed cryo-electron microscopy. B.R., P.V.S., A.R.-W. and O.N.J. performed TMT proteomics. A.M. and P.Y. designed and supervised the study. A.M., P.Y. and G.P.v.W. wrote the manuscript.

Additional information

Supplementary Information accompanies this paper at http://www.nature.com/naturecommunications

Competing financial interests: The authors declare no competing financial interests.

Reprints and permission information is available online at http://npg.nature.com/reprintsandpermissions/

How to cite this article: Yagüe, P. *et al.* Subcompartmentalization by cross-membranes during early growth of Streptomyces hyphae. *Nat. Commun.* 7:12467 doi: 10.1038/ncomms12467 (2016).

This work is licensed under a Creative Commons Attribution 4.0 International License. The images or other third party material in this article are included in the article's Creative Commons license, unless indicated otherwise in the credit line; if the material is not included under the Creative Commons license, users will need to obtain permission from the license holder to reproduce the material. To view a copy of this license, visit http://creativecommons.org/licenses/by/4.0/

© The Author(s) 2016

CAPÍTULO 4

Análisis de la procesos de desarrollo diferención y producción antibiótico en fermentación industriales escala piloto (biorreactores de 2L)

Tal y como se ha ido describiendo en los capítulos anteriores, la diferenciación que tiene lugar durante el ciclo de desarrollo de *Streptomyces* es un tema muy estudiado y se relaciona directamente con la producción de metabolitos secundarios que sólo se activa en determinadas fases del ciclo. Sin embargo, en la producción a nivel industrial, en biorreactores, estos procesos de diferenciación son, en general, ignorados, y las fermentaciones se optimizan de forma empírica. De hecho, los parámetros más importantes en la industria para optimizar la producción consisten en factores como la composición de los medios de cultivo, optimización de cepas mediante mutagénesis y parámetros biofísicos como el pH, la concentración de oxígeno o la agitación, y muy pocas veces se hace un análisis del estado de desarrollo de los cultivos.

En este trabajo se analizó la relación entre la diferenciación y la producción de antibióticos en biorreactores a escala piloto en la cepa modelo *S. coelicolor*. El objetivo fue establecer un modelo general que incluya la diferenciación a la hora de optimizar la producción de metabolitos secundarios en fermentaciones industriales de *Streptomyces*, y que a su vez permita interpretar como las modificaciones clásicas en los parámetros físico-químicos afectan a la diferenciación del MII productor.

El objetivo de este capítulo se aborda en una publicación:

Manuscrito 4:

Rioseras B, López-García MT, Yagüe P, Sánchez J, Manteca A. 2014. "Mycelium differentiation and development of *Streptomyces coelicolor* in lab-scale bioreactors: Programmed cell death, differentiation, and lysis are closely linked to undecylprodigiosin and actinorhodin production". Bioresour Technol. 151:191-198.

Bioresource Technology 151 (2014) 191–198

Contents lists available at ScienceDirect

Bioresource Technology

journal homepage: www.elsevier.com/locate/biortech

Mycelium differentiation and development of *Streptomyces coelicolor* in lab-scale bioreactors: Programmed cell death, differentiation, and lysis are closely linked to undecylprodigiosin and actinorhodin production

Beatriz Rioseras, María Teresa López-García, Paula Yagüe, Jesús Sánchez, Ángel Manteca *

Área de Microbiología, Departamento de Biología Funcional e IUOPA, Facultad de Medicina, Universidad de Oviedo, 33006 Oviedo, Spain

HIGHLIGHTS

- Differentiation in bioreactors is comparable to solid sporulating cultures.
- Differentiation is linked to antibiotic production.
- Differentiation is one of the keys to interpreting fermentation parameters.
- General consensus: differentiation of the antibiotic-producing mycelium (MII).
- Antifoams can prevent massive pellet fragmentation/lysis.

ARTICLE INFO

Article history:
Received 26 August 2013
Received in revised form 18 October 2013
Accepted 21 October 2013
Available online 30 October 2013

Keywords:
Streptomyces
Bioreactor
Differentiation
Antibiotics
Programmed cell death

ABSTRACT

Streptomycetes are mycelium-forming bacteria that produce two thirds of clinically relevant secondary metabolites. Secondary metabolite production is activated at specific developmental stages of *Streptomyces* life cycle. Despite this, *Streptomyces* differentiation in industrial bioreactors tends to be underestimated and the most important parameters managed are only indirectly related to differentiation: modifications to the culture media, optimization of productive strains by random or directed mutagenesis, analysis of biophysical parameters, etc. In this work the relationship between differentiation and antibiotic production in lab-scale bioreactors was defined. *Streptomyces coelicolor* was used as a model strain. Morphological differentiation was comparable to that occurring during pre-sporulation stages in solid cultures: an initial compartmentalized mycelium suffers a programmed cell death, and remaining viable segments then differentiate to a second multinucleated antibiotic-producing mycelium. Differentiation was demonstrated to be one of the keys to interpreting biophysical fermentation parameters and to rationalizing the optimization of secondary metabolite production in bioreactors.

Crown Copyright © 2013 Published by Elsevier Ltd. All rights reserved.

1. Introduction

Streptomycetes are gram-positive, environmental soil bacteria that play important roles in the mineralization of organic matter. *Streptomyces* is extremely important in biotechnology, given that approximately two thirds of all clinical antibiotics and several other bioactive compounds are synthesized by members of this genus (Ruiz et al., 2010).

Streptomycetes are mycelial microorganisms with complex developmental cycles that include programmed cell death (PCD) and sporulation (reviewed in Claessen et al. (2006) and Yagüe et al. (2013)). In solid sporulating cultures, a compartmentalized mycelium (MI) initiates development. MI compartments are separated by septa formed by membranes which generally do not display thick cell walls (reviewed in Yagüe et al. (2013)). A fraction of MI cells undergo a highly ordered programmed cell death (PCD) (Yagüe et al., 2013), and remaining viable cells differentiate to a multinucleated mycelium that has only sporadic septa (MII). MII gradually begins to express the chaplin and rodlin proteins that assemble into the rodlet layer that, in turn, provides the surface hydrophobicity necessary to grow into the air (aerial mycelium) (reviewed in Claessen et al. (2006)). At the end of the cycle, hypha septation and sporulation take place. MI fulfills the vegetative role in *Streptomyces* and MII constitutes the reproductive stage that is destined to sporulate and also produces secondary metabolites (Yagüe et al., 2013). In previous works, it was reported that differentiation in non-sporulating liquid cultures (laboratory

Abbreviations: PCD, programmed cell death; MI, first compartmentalized mycelium; MII, second multinucleated mycelium; PI, propidium iodide; DOT, dissolved oxygen tension; OTR, oxygen transfer rates; OUR, oxygen uptake rate; PMT, photomultiplier tube.

* Corresponding author. Tel.: +34 985103555.
E-mail address: mantecaangel@uniovi.es (Á. Manteca).

0960-8524/$ - see front matter Crown Copyright © 2013 Published by Elsevier Ltd. All rights reserved.
http://dx.doi.org/10.1016/j.biortech.2013.10.068

flasks) was similar to that occurring during the pre-sporulation stages in solid cultures (reviewed in Yagüe et al. (2013)): an initial compartmentalized mycelium (MI) undergoes PCD and the remaining viable segments of this mycelium differentiate to a multinucleated mycelium (MII), i.e. the antibiotic-producing mycelium (Yagüe et al., 2013).

Most processes for secondary metabolite production are performed in bioreactors. Nevertheless, *Streptomyces* differentiation under these conditions has barely been studied, mainly due to the fact that most *Streptomyces* strains do not sporulate under these conditions. *Streptomyces* fermentation analysis and optimization has mainly been empirical and focused on the analysis of biophysical parameters, such as mycelial grouping (pellets, clumps), media composition, oxygenation, pH, agitation, temperature and, of course, levels of secondary metabolite production. Several studies have tested the optimal composition of culture media (Wentzel et al., 2012), analyzing the kind of hyphae grouping that is best suited for secondary metabolite production (dispersed hyphae vs. clumps or pellets) (van Veluw et al., 2012; van Wezel et al., 2006), analyzing the effects of bioreactor hydrodynamics on the physiology of *Streptomyces* (reviewed in Olmos et al. (2013)), or optimizing productive strains by random or directed mutagenesis (van Wezel et al., 2006). However, the complex development of *Streptomyces* under these conditions has not been fully understood and, as a direct consequence, there is no general consensus as to how morphology and other biophysical parameters correlate with secondary metabolite production. Fermentation parameters need to be optimized empirically for each strain and compound. For example, pellet and clump formation has been described as essential for obtaining good production of retamycin or nikkomycin (Pamboukian and Facciotti, 2004), but in the case of virginiamycin, there is no relationship between morphology and secondary metabolite production (Yang et al., 1996); high dissolved oxygen tensions (DOT) have been reported as necessary for the production of vancomycin (Dunstan et al., 2000), but not for the production of erythromycin (Clark et al., 1995), just to name a few examples.

The main objective of this work is to extend understanding of *Streptomyces* differentiation to lab-scale bioreactors, defining the kind of differentiation present under these conditions, how differentiation, fermentation parameters and secondary metabolite production are correlated, and describing a general model applicable to improving secondary metabolite production in *Streptomyces* industrial fermentations. *Streptomyces coelicolor* is one of the best-characterized *Streptomyces* strains (Chater, 2001). It produces various secondary metabolites, including two well-characterized antibiotics: undecylprodigiosin and actinorhodin. In order to facilitate comparisons with differentiation and development in bioreactors and other developmental conditions (solid cultures and laboratory flasks), *S. coelicolor* was used in this work as a model strain.

2. Methods

2.1. Strains, media, and culture conditions

S. coelicolor M145 was the strain used in this work. Cultures were performed in R5A sucrose-free liquid media (Fernandez et al., 1998). This culture medium contains MOPS buffer in sufficient concentration (100 mM) to maintain pH stable during cultivations. Laboratory flasks of 500 ml were filled with 100 ml of culture medium and incubated at 200 rpm and 30 °C. Bioreactor cultivations were performed in a 2-L bioreactor (Bio-Flo 110, New Brunswick Scientific, NJ, USA) equipped with a pH meter (Mettler Toledo, Switzerland), a polarographic dissolved oxygen electrode (InPro 6830, Mettler Toledo, Switzerland), and rushton impellers. As described above, the effect of pitched blade impellers in fermentations was also tested (data not shown). An initial working volume of 1.3 L at 30 °C and aeration of 1 L/min were used. Dissolved oxygen tension was set to a minimum of 3.8 mg/L (50% saturation), using an agitation interval of between 300 and 800 rpm, and pH was set at 6.8 using a computer-controlled peristaltic pump via automatic addition of 2 M KOH and 1 M HCl.

Flasks and bioreactors were inoculated directly with freshly prepared spores at 1×10^7 ("dense cultures") or 1×10^5 ("diluted cultures") spores/ml. Where indicated, culture medium was supplemented with antifoam (Biospumex 153K, BASF) to a final concentration of 1%. The effect of the antifoam in preventing early massive fragmentation/lysis was not so evident at lower concentrations (data not shown). More than 5 biological replicates were performed for each culture, and monitored morphologically and biochemically. However, extensive quantitative measurements were performed in only two of these biological replicates, and the quantitative data presented in the figures of this work correspond to the average ± SD of these two independent fermentations (biological replicates).

2.2. S. coelicolor repeated batch cultivations

"Dense cultures" (10^7 spores/ml), growing in R5A sucrose-free medium amended with antifoam (1% of Biospumex 153K, BASF), and using the growth parameters indicated above were grown in the bioreactor for 66 h. After that time-point, the full bioreactor contents were extracted into a 2-L sterile bottle using a peristaltic pump connected to the inoculation port. Mycelial pellets were allowed to sediment in a static state for 5 min, after which supernatant was removed under sterile conditions. The volume of medium extracted was replaced by the same volume of fresh, sterile, R5A medium amended with antifoam, and the whole culture was reintroduced into the bioreactor using again a peristaltic pump connected to the inoculation port.

2.3. Determination of the oxygen uptake rate (OUR) and oxygen transfer rate (OTR)

OUR was obtained from the slope of the plot of dissolved oxygen concentration over time following a momentary interruption of the air supply to the bioreactor. OTR was estimated according to the slope of dissolved oxygen recovery after aeration (fixed value of 1 L/min) and agitation (interval of between 300 and 800 rpm) was restored to the values present at the time at which the air supply was interrupted. OUR and OTR values were only estimated at developmental time points at which DOT values were less than 7 mg/L (90% saturation).

2.4. Streptomyces sampling throughout the differentiation cycle

Samples of *S. coelicolor* obtained from liquid cultures were centrifuged (7740*g*, 10 min at 4 °C). Supernatants of the culture medium were used to estimate extracellular proteins. Cellular extracts were obtained as follows: the mycelium pellets were resuspended in a known volume of buffer A (Tris–HCl 20 mM, pH 8, EDTA 1 mM, β-mercaptoethanol 7 mM, and complete EDTA-free Protease Inhibitor Cocktail Tablets from Roche) and ruptured using Fast-Prep (MP™ Biomedicals) with ⩽106 μm beads (Sigma, G8893500G) and three 20-s force 6.5 cycles, with 1 min on ice between each run. Finally, samples were centrifuged at 7740*g* in an Eppendorf microcentrifuge for 15 min at 4 °C; the resulting supernatant fraction was used as the cellular fraction.

2.5. Protein quantification

Determination of protein concentrations was carried out with the Bradford assay (Biorad) and a bovine serum albumin standard (Sigma). Protein measured in the supernatants of culture medium corresponded to extracellular protein; protein measured in the cellular extracts corresponded to intracellular protein; and the sum of both, corresponded to total protein.

2.6. Antibiotic quantification

Undecylprodigiosin and actinorhodin were quantified spectrophotometrically according to Tsao et al. (1985) and Bystrykh et al. (1996). In order to measure the total amount of actinorhodin (intracellular and extracellular), cells were ruptured in their culture medium by adding KOH 0.1 N. Cellular debris was discarded by centrifugation, and actinorhodin was quantified spectrophotometrically with a UV/visible spectrophotometer (Shimadzu, Model UV-1240), applying the linear Beer–Lambert relationship to estimate concentration (ε_{640} = 25,320). In the case of cultures with antifoam, acthinorhodin spectrophotometric measurements were performed at 4 °C, in order to prevent interference with turbidity due to the antifoam. Undecylprodigiosin was measured after vacuum drying the culture (including the mycelium and culture medium) followed by extraction with methanol, acidification with HCl (to 0.5 M), and spectrophotometric assay at 530 nm, again using the Beer–Lambert relationship to estimate concentration (ε_{530} = 100,500). In all cases, for the high concentration solutions, dilutions were performed to conduct the analysis in the linear Beer–Lambert region.

2.7. Viability staining

Culture samples were obtained and processed for microscopy at different incubation time points, as previously described (Manteca et al., 2008). Cells were stained with a cell-impermeant nucleic acid stain (propidium iodide, PI) in order to detect the dying cell population and with SYTO 9 green fluorescent nucleic acid stain (LIVE/DEAD Bac-Light Bacterial Viability Kit, Invitrogen, L-13152) to detect viable cells. The SYTO 9 green fluorescent stain labels all the cells, i.e. those with intact membranes, as well as those with damaged ones. In contrast, PI penetrates only bacteria with damaged membranes, decreasing SYTO 9 stain fluorescence when both dyes are present. Thus, in the presence of both stains, bacteria with intact cell membranes appear to fluoresce green, whereas bacteria with damaged membranes appear red. After leaving them for at least 10 min in the dark, the samples were examined under a Leica TCS-SP2-AOBS confocal laser-scanning microscope at a wavelength of either 488 nm or 568 nm excitation and 530 nm (green) or 630 nm (red) emission, respectively (optical sections about 0.2 μm). Images were mixed using Leica Confocal Software. In some cases, samples were also examined in differential interference contrast mode, available with the same equipment.

S. coelicolor unstained samples were used as controls to determine the minimum photomultiplier tube (PMT) gain necessary to detect autofluorescence in the confocal microscope. Green autofluorescence (Willemse and van Wezel, 2009) can interfere with green fluorescent fluorochromes as occurs, for instance, with GFP (Manteca et al., 2008; Willemse and van Wezel, 2009), and they can potentially interfere with SYTO9 green stain. However, in practice, there is no interference because the intensity of green autofluorescence is negligible when compared to the SYTO9 green fluorescence. Tenconi et al. (2013) have recently demonstrated the existence of red autofluorescence associated with undecylprodigiosin that displays an excitation-emission spectrum similar to PI. Under the experimental conditions used in this work, red autofluorescence was significantly less than PI fluorescence and the minimum PMT gain necessary to observe it was 860 V (using the 63× objective), 60% more than the PMT gain used to observe PI fluorescence (535 V under the 63× objective) (data not shown). Despite this, red autofluorescence was not negligible, and some of the red fluorescent background detected at later time points in the centers of mycelial pellets may be derived from undecylprodigiosin.

The antifoam used had green autofluorescence, however its intensity was very low in comparison with the SYTO9 green fluorescence. In addition, antifoam could be not confused with stained hyphae, because it was completely amorphous.

More than 30 images were analyzed for each developmental time point in a minimum of three independent cultures. The percentage of sporulation and MI compartmentalized hyphae were estimated by counting 200 hyphae, from different pictures, and different biological replicates, visualized independently in the same focal plane.

2.8. Nuclease activity gel analysis (zymograms)

Nucleases were separated in a 12% gel by SDS–PAGE containing 10 μg/ml of denatured calf thymus DNA (Sigma); 8.5 μg of protein were used per well. When necessary, protein samples were concentrated by filtration using Vivaspin 20 (10,000 molecular weight cutoff, Sartorius). After electrophoresis, the proteins were renatured by repeatedly washing the gel with the renaturation buffer (Tris–HCl 25 mM, pH 8.8, EDTA 1 mM, β-mercaptoethanol 7 mM) for 2 h at 4 °C. Nuclease activity was visualized by incubating the gels for 20 min at 37 °C in 20 mM Tris–HCl (pH 8.0), 7 mM 2-mercaptoethanol, 10 mM $MgCl_2$, 5 mM $CaCl_2$ and 10% DMSO buffer, as reported elsewhere (Nicieza et al., 1999), followed by staining with ethidium bromide and analysis under UV light. Micrococcal nuclease (16.7 kDa) and bovine pancreatic DNase I (31 kDa) (Amersham Pharmacia Biotech) were included as positive controls. The reproducibility of the data shown was corroborated by at least three independent cultures and nuclease analysis at various developmental time points.

3. Results and discussion

3.1. Differentiation of S. coelicolor M145 in 2 L-bioreactors

In order to facilitate comparison of *Streptomyces* differentiation in bioreactors with differentiation previously reported in laboratory flasks, a workflow similar to that used in flask cultures (Manteca et al., 2008) was utilized: R5A culture medium (without antifoam) were inoculated with either10^7 spores/ml (“dense cultures”) (Fig. 1 and Supplementary Fig. S1) or 10^5 spores/ml (“diluted cultures”) (Supplementary Figs. S2 and S3). Despite the fact that some foam was formed in the bioreactor, it was not excessive, and cultures were initially performed without defoamers, in order to facilitate direct comparison with differentiation previously described in flask cultures (Manteca et al., 2008). Morphological differentiation was analyzed by means of confocal microscopy on cultures stained with the vital stains SYTO9 and propidium iodide (see Section 2 for details). At early time points, 100% of the hyphae presented the regular discontinuities and gaps (Supplementary Fig. S1E) previously described for MI hyphae (Manteca et al., 2008). MI differentiated into a second multinucleated mycelium (MII) that had only sporadic gaps (compare MI hyphae from Supplementary Fig. S1E with MII hyphae from Supplementary Fig. S1F). There was also a transition phase in which some segments of the MI started to grow in the form of hyphae with more widely spaced septa (MII) while other parts of the hyphae

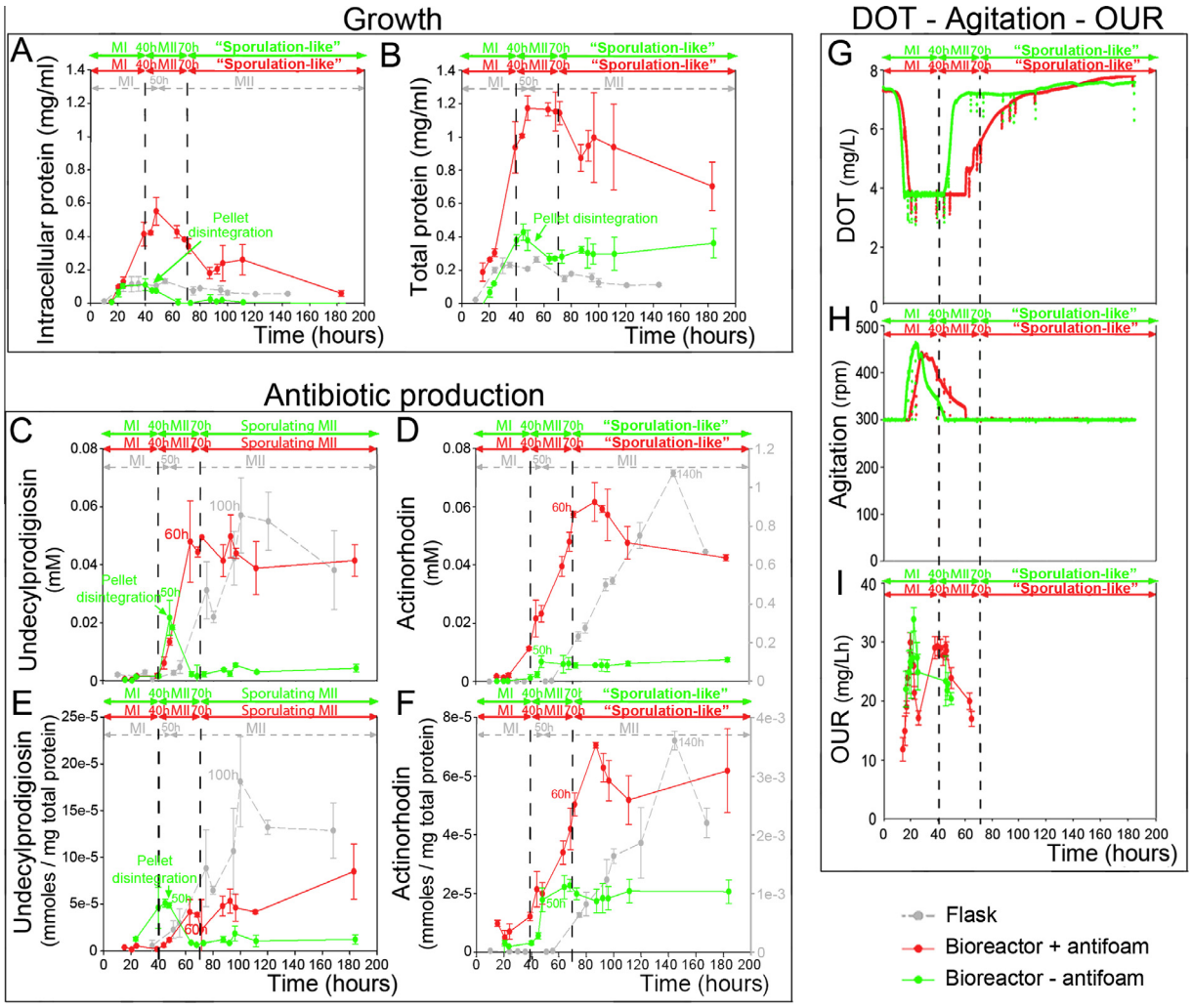

Fig. 1. Time-course of fermentation parameters. The data correspond to "dense cultures" (10^7 spores/ml) of *Streptomyces coelicolor* M145. Green lines, 2-L bioreactors, R5A without antifoam; red lines, 2-L bioreactors, R5A with antifoam; gray lines, laboratory flasks, R5A without antifoam. (A) and (B) Growth curves (intracellular protein and total protein). (C)–(F) Antibiotic production (undecylprodigiosin and actinorhodin). Actinorhodin levels in the laboratory flasks in (D) and (F) have their own scales on the right. Time points at which maximum antibiotic productions was reached are indicated. (G)–(I) DOT, Agitation and OUR. Values are the average ± SD from two biological replicates.

remained in the MI stage (data not shown). Cell death started in the centers of MI mycelial pellets (propidium iodide staining) (Supplementary Fig. S1A) and exhibited the hallmarks previously reported for *Streptomyces* PCD (reviewed in Yagüe et al. (2013)), including the activation of non-sequence specific nucleases involved in chromosomal DNA degradation (Supplementary Fig. S4A).

One of the most important differences observed in the bioreactor with respect to laboratory flasks for the *Streptomyces* strain and culture conditions used in this work, was the existence of massive fragmentation and disintegration of mycelial pellets at around 50 h of fermentation. This massive disintegration was observed microscopically, in the irregular shape of the pellets (Supplementary Fig. S1B) or the fissures crossing them internally (Supplementary Fig. S1C), and macroscopically, in the form of the apparent clarification of the culture medium (notice that bioreactor probes are clearly visible in the bioreactor vessel) (Supplementary Fig. S1L and M). This pellet disintegration correlated with a sudden fall in intracellular protein levels (Fig. 1A), which decreased from 0.1 mg/ml prior to the massive pellet disintegration to 0.0002 mg/ml after that. The few pellets that did not lose their integrity continued to grow in diameter (up to 530–600 μm in the "dense cultures") (Supplementary Fig. S1D). Most of the biomass in these pellets corresponded to dying cells (red staining) (Supplementary Fig. S1D) and, consequently, the number of remaining viable hyphae (green staining) in the bioreactor following massive pellet disintegration was extremely low. This kind of mycelial disintegration has been previously described as "massive lysis" in several *Streptomyces* fermentations, such as *Streptomyces clavuligerus* (reducing mycelium by more than 30%) (Roubos et al., 2001), *Streptomyces* spp. (Techapun et al., 2003), *Streptomyces albulus* (Shih and Shen, 2006), or *S. coelicolor* (Ozergin-Ulgen and Mavituna, 1993), to name just a few examples. This "massive lysis" differs from the "fragmentation of the mycelial clumps" described in some cases (van Wezel et al., 2006), which basically consists of the fragmentation of large clumps into small clumps, but without the early massive hyphal lysis reported in this work as well as others (Ozergin-Ulgen and Mavituna, 1993; Roubos et al., 2001; Shih and Shen, 2006; Techapun et al., 2003). The reason why this phenomenon occurred in some streptomycetes and not in others remains unknown. In *S. coelicolor* growing under the growth conditions used in this work, true lysis started in hyphae located at the centers of the pellets (beginning at times as early as 15 h) (Supplementary Fig. S1A), long before massive fragmentation took place (around 50 h) (Supplementary Fig. S1B and C). This massive pellet disintegration did not occur in laboratory flasks

(Manteca et al., 2008), where it was observed neither macroscopically nor microscopically (data not shown), as reflected by the absence of the dramatic decrease in the intracellular protein described above in the bioreactor cultures (Fig. 1A). Hence, it seems that massive pellet disintegration depends on the hydrodynamics of the bioreactor combined with the tendency of *S. coelicolor* to form large pellets under the culture conditions used in this work.

Another important difference between bioreactor- and laboratory flask-cultured samples was the existence of a sporulation-like process, beginning at around 70 h, and affecting some 5% of hyphae that remained viable at these time points (see quantification criteria in Section 2). Two of the most important features of sporulation, division and separation of nucleoids (Supplementary Fig. S1G), and the physical strangulation of hypha forming chains of individual round segments (Supplementary Fig. S1H), were observed. Further work will be necessary to characterize if these round segments present the resistance properties characterizing *Streptomyces* spores formed in solid cultures (Lee and Rho, 1993).

Antibiotic production was accelerated in the bioreactor, peaking at 100–140 h in laboratory flasks vs. 50 h in the bioreactor (Fig. 1C and D). MII differentiation was slightly accelerated, from 50 h in laboratory flasks (Manteca et al., 2008) to around 40 h in the bioreactor (Supplementary Fig. S1 and data not shown). Antibiotic biosynthesis was halted after pellet disintegration, with maximum undecylprodigiosin production levels slightly lower in the bioreactor with respect to the laboratory flasks (0.02 mM vs. 0.06 mM observed in flasks) (Fig. 1C) and dramatically lower in the case of actinorhodin (0.007 mM vs. 1 mM observed in flasks) (Fig. 1D). These results match previous works reporting that undecylprodigiosin and actinorhodin are synthesized differentially in *S. coelicolor* fermentations (Sevcikova and Kormanec, 2004) and illustrates the important and well-known issue that, in addition to hyphal differentiation, there are specific regulatory mechanisms for different secondary metabolites.

Biophysical fermentation parameters, such as dissolved oxygen tension (DOT), agitation, and oxygen uptake rates (OUR), correlated well with differentiation (Fig. 1G–I): DOT fell from saturation to a fixed level (50% saturation), probably due to hyphal growth and respiration (Fig. 1G); there was a concomitant increase in agitation to maintain oxygen levels at the fixed level (Fig. 1H); once pellet disintegration started (see above), biological oxygen consumption and agitation decreased gradually, and dissolved oxygen levels increased suddenly to saturation. OUR values peaked at 20 h (MI stage) (Fig. 1I) and fell during the PCD of the MI; they also did not recover during the MII stage, probably due to early massive pellet disintegration/lysis described above. OUR values were consistently lower than oxygen transfer rates (OTR) (data not shown), indicating that oxygen did not limit growth at any time. Interestingly, *Streptomyces coelicolor* OUR values measured in this work were quite low, with peak values of 30 mg/L h (Fig. 1I). This might be a direct consequence of the unusual development of *S. coelicolor*, in which most of the biomass in the mycelial pellets is dying and therefore does not consume oxygen. This constitutes an elegant example of the importance of understanding *Streptomyces* differentiation, so as to be able to interpret classical biophysical fermentation parameters in the model strain *S. coelicolor* and conceivably in other industrial relevant streptomycetes, which is one of the most important conclusions of this work. Information concerning oxygen uptake kinetics of *Streptomyces* cultures is scarce despite their industrial importance. OUR values vary widely between strains, from 2.88 mg O_2 g $cell^{-1}$ h^{-1} in *S. lividans* (Magnolo et al., 1991) to 320 mg O_2 g $cell^{-1}$ h^{-1} in *S. clavuligerus* (Yegneswaran et al., 1991). The meaning of these differences is difficult to interpret due to the absence of any indication as to mycelium differentiation/PCD in most of these works. Ozergin-Ulgen and Mavituna (1998) described maximum OUR values for *S. coelicolor* of 192 mg/L h, 6.4-fold higher than the maximum OUR detected in this work for the same strain. This might be due to important differences in the bioreactor vessel used in Ozergin-Ulgen and Mavituna work (1998), which had large baffles instead of the smooth vessels used in this work. Baffles are in fact routinely used in laboratory flask cultures to prevent pellet formation in *S. coelicolor* (Kieser et al., 2000), and a dispersal growth could prevent cell death and increase OUR. An analysis of hyphae differentiation, development and PCD would be essential to address these differences in OURs between different *Streptomyces* strains and culture conditions.

Inoculation density is one of the well-known fermentation parameters that is usually conducive to modifications in growth and production. In order to test how this parameter would affect differentiation in the bioreactors, a 100-fold dilution, 10^5 spores/ml (“diluted cultures”), was used. The same kind of differentiation described above for “dense” culture, was also observed in “diluted” cultures (Supplementary Figs. S2 and S3): MI differentiated to MII (Supplementary Fig. S2) after a PCD that activated the non-sequence specific nucleases (Supplementary Fig. S4B); there was an early massive lysis of pellets (Supplementary Fig. S2), and sporulation-like processes were also observed (Supplementary Fig. S2) affecting approximately 5% of the hyphae. Massive pellet disintegration occurred at similar developmental time points in “dense” and “diluted” cultures (50 h, when the pellet diameter was 500 μm), but the biomass (number of pellets) was much lower in “diluted” compared to “dense” cultures: 0.016 mg/ml of intracellular protein in “diluted” (Supplementary Fig. S3A) vs. 0.07 mg/ml in “dense” cultures (Fig. 1A). Antibiotic production, DOT, agitation, and OUR also correlated well with differentiation (Supplementary Fig. S3G–I).

3.2. Differentiation of *S. coelicolor* M145 in 2-L bioreactors supplemented with antifoam

As commented above, the onset of antibiotic production in the bioreactor was more rapid than in laboratory flasks (Manteca et al., 2008), but the final levels of production were very low. In order to improve production in the bioreactor, growing conditions were modified to try to prevent the early massive lysis, so growth would more to resemble the development observed in flasks. The most obvious difference between bioreactors and laboratory flasks is the impellers used for agitation in the case of the bioreactor, so the first experimental approach to trying to prevent lysis was to reduce agitation to minimum levels (50 rpm); however, the same extension of pellet disintegration was observed (data not shown). Similar results were observed at different agitation rates (50, 100, 200 or 300 rpm) (data not shown). Second, Rushton impellers were replaced by a gentler impeller (pitched blade impellers), but similar results were again obtained (data not shown). Finally, the culture medium’s rheology was modified reducing surface tension by means of an antifoam agent (Biospumex 153K, BASF), at a concentration of 1%. Under these conditions, massive fragmentation of the pellets was avoided, as observed under the confocal microscope (compare Supplementary Fig. S1B and C with Supplementary Fig. S5B, noting the absence of fissures in the pellets) and macroscopically by the high turbidity of the cultures (compare Supplementary Fig. S5K and L with Supplementary Fig. S1L and M). The change was also reflected in the high levels of intracellular protein, which reached a maximum of 0.6 mg/ml (Fig. 1A) vs. the 0.1 mg/ml observed in cultures without antifoam (Fig. 1A). This effect of preventing early fragmentation/lysis was only observed at relatively high concentrations of antifoam (1%, see Section 2 for details). The reason why antifoam prevents pellet disintegration is as yet unknown; however, the antifoam tended to coat the mycelial pellets (as can observed by its own autofluorescence in

Supplementary Fig. S5C) and the hydrophobic forces generated may have prevented this phenomenon. Antifoams are often used with *S. coelicolor* (Wentzel et al., 2012) as well as other *Streptomyces* fermentations to prevent foam formation, or even, in some cases to be used as carbon sources (Perlman and Wagman, 1952). They are usually added automatically in small amounts when foam is detected by a specific probe, and in some cases, they are added directly to the culture medium at concentrations up to 0.1% (Wentzel et al., 2012). However, to the best of our knowledge, this is the first time that early pellet fragmentation/lysis has been demonstrated to be prevented by adding antifoam to the culture media at relatively high concentrations, a fact that might be useful for preventing lysis in other industrial streptomycetes.

Under the conditions used in this work, antifoam led to a moderate increase in undecylprodigiosin production (0.05 mM vs. 0.02 mM in the case of cultures without antifoam) (Fig. 1C), but it was also slightly delayed when production was referenced to cellular protein (Fig. 1E). This level of production was comparable to the production observed in laboratory flasks (0.05 mM) (Fig. 1C). Actinorhodin production was also increased with respect to cultures without antifoam (0.06 mM in cultures with antifoam vs. 0.006 mM in cultures without antifoam), although it was far from the production levels obtained in laboratory flasks (1 mM) (Fig. 1D). Similar to the arrest in cellular metabolism associated with sporulation in solid sporulating cultures (Chater and Horinouchi, 2003), inhibition of actinorhodin production might be a consequence of a change in hyphae metabolism/differentiation, affecting most of the hyphae, and culminating in the sporulation-like processes which continued to affect some 5% of the hyphae in the case of "dense cultures" amended with antifoam (Supplementary Fig. S5F and G).

Biophysical fermentation parameters also correlated well with differentiation in cultures with antifoam (Fig. 1G–I): DOT fell from saturation (100%) to the set level (50% saturation) (Fig. 2G), leading to increased agitation (Fig. 1H); the absence of pellet disintegration might prolong the oxygen consumption phase, generating the two peaks of OUR separated by a stage of low oxygen consumption (Fig. 1I). The latter may reflect a transient arrest in metabolism (oxygen consumption) preceding MII differentiation similar to that previously reported in laboratory flasks (reviewed in Yagüe et al. (2013)). These two maxima in OUR were very unusual, and are another nice illustration of the necessity of understanding *Streptomyces* differentiation in order to interpret fermentation parameters. As in the case of fermentations without antifoam, oxygen levels did not limit growth; OUR levels were consistently lower than OTR values at any given point in time (data not shown).

Antifoam also prevented pellet disintegration in the "diluted" cultures (Supplementary Figs S3 and S6). Interestingly, the sporulation-like processes observed in "dense" cultures amended with antifoam were not observed in the "diluted" cultures (Supplementary Fig. S6F). Sporulation in *S. coelicolor* liquid cultures is very unusual and to the best of our knowledge, has only been reported once before in laboratory flasks suffering nutritional downshifts (Daza et al., 1989). The differentiation signals activating sporulation in the bioreactors remain unknown. However, if it is considered that sporulation is triggered by environmental/biological stresses (Chater, 2001), the high growth rates achieved in the bioreactors together with pellet disintegration might approach the development occurring in stressed solid sporulating cultures. In the absence of pellet disintegration, putative differentiation diffusible signals (Chater et al., 2010; Horinouchi and Beppu, 1992) generated by stressed cells suffering PCD (Yagüe et al., 2013) would be hidden in the centers of the pellets.

The highest levels of antibiotic production were reached in the "diluted cultures" amended with antifoam. The maximum production levels were around 0.2 mM in the "diluted" cultures

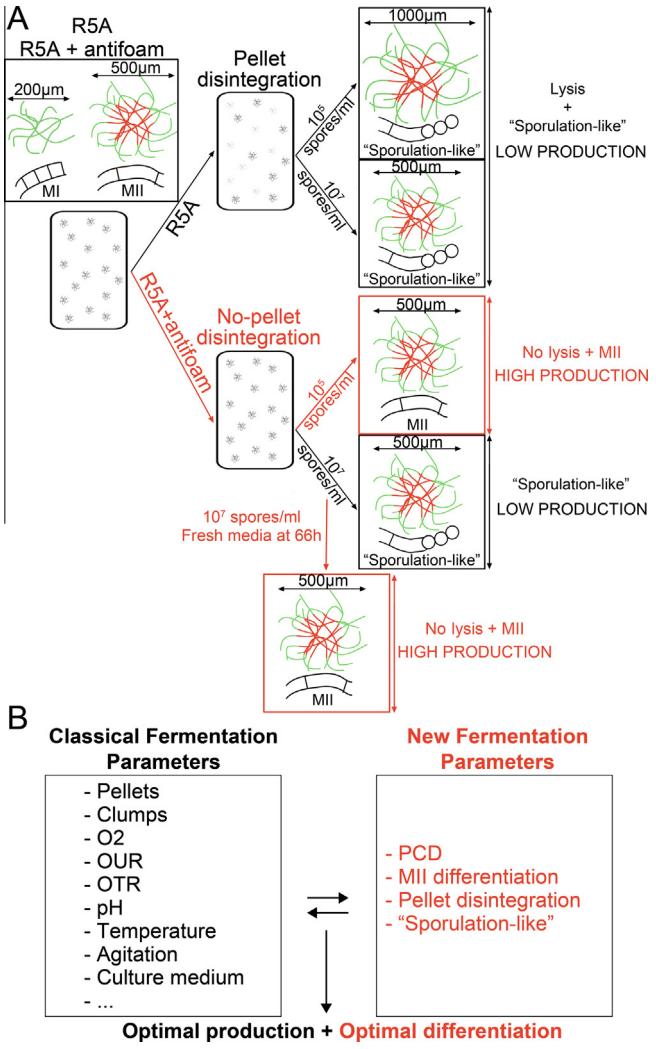

Fig. 2. Scheme illustrating *S. coelicolor* differentiation in bioreactors. (A) *S. coelicolor* differentiation growing in R5A sucrose-free medium with and without antifoam, at two spore inoculations (10^5 and 10^7 spores/ml). Red corresponds to dying hyphae (PI staining) and green to viable hyphae (SYTO9 staining). The optimal fermentation workflow is highlighted in red. (B) Comparison between classic (black letters) and new (red letters) fermentation parameters established in this work. See text for details.

(Supplementary Fig. S3C and D) vs. 0.05 mM obtained in the "dense" cultures with antifoam (Fig. 1C and D) for both, undecylprodigiosin and actinorhodin. By contrast, growth in the "diluted" cultures, measured as total protein/ml, was half that in the "dense" cultures (compare Fig. 1B and Supplementary Fig. S3B). As a consequence, the sporulation-like processes observed in some 5% of the hyphae in the cultures without antifoam and in the "dense" cultures with antifoam correlate with a block in the production of secondary metabolites in the whole mycelium. This is another example of how growth/biomass production is not sufficient to guarantee secondary metabolite production in *Streptomyces*.

3.3. Optimization of MII differentiation and antibiotic production in S. coelicolor fermentations: repeated batch cultivations

As outlined in Fig. 2A, the highest levels of antibiotic production were reached by preventing pellet disintegration (using antifoams), blocking sporulation-like processes (using low inocula; i.e. slow growth rates), and prolonging the antibiotic-producing phase (MII). In spite of that, antibiotic production was faster in the "dense

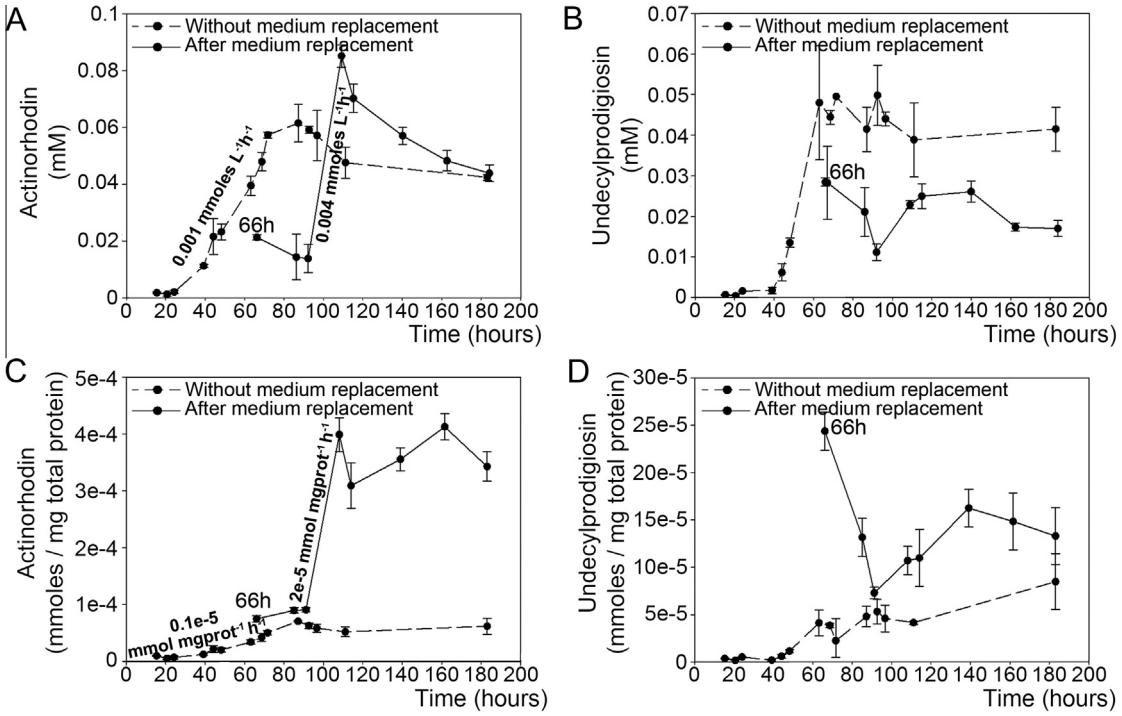

Fig. 3. Time-course of antibiotic production in *Streptomyces coelicolor* repeated batch fermentations. (A) Undecylprodigiosin (mM). (B) Actinorhodin (mM). (C) Undecylprodigiosin (mmol/mg total protein). (D) Actinorhodin (mmol/mg total protein). Rates of actinorhodin production (slopes) are indicated in the graphs. Antibiotic concentration values are the average ± SD from two biological replicates. See text for details.

cultures" (maximum undecylprodigiosin levels at 60 h) (Fig. 1C) than in the "diluted cultures" (maximum undecylprodigiosin levels at 80 h) (Supplementary Fig. S3C). The possibility of combining the rate of antibiotic production reached in the "dense cultures" with the high yields obtained in the "diluted cultures" was tested. To do so, the possibility of repressing the sporulation-like processes observed in "dense cultures" was explored, by replacing culture medium with fresh medium once undecylprodigiosin reached maximum levels (66 h) (Fig. 1C) but prior to sporulation. Under these conditions, there was no significant increase in mycelial biomass (measured as either total or intracellular protein/ml; data not shown). The mycelium remained at the MII stage (Supplementary Fig. S7) and there was not sporulation (Supplementary Fig. S7). After an unsurprising delay of approximately 20 h, there was very rapid production of actinorhodin (0.004 mmol/L h, 4-fold faster than in the original culture) (Fig. 3A). In the case of undecylprodigiosin, there was also a delay of 20 h prior to production, but in this case, production was very weak (Fig. 3B), which once again demonstrates that in addition to differentiation there are specific regulators for different secondary metabolites. Moreover, the production of both antibiotics normalized by total protein was consistently higher in the repeated batch cultivation than in the original cultures (Fig. 3C and D). This kind of experimental workflow opens up the possibility of maintaining the mycelium in the productive stage (MII) indefinitely, replacing culture medium periodically after MII differentiation and once antibiotic production has already peaked.

3.4. Future perspectives

Different streptomycetes show different behaviors in liquid cultures: some species form large pellets, such as *S. coelicolor*, others growth more dispersed, as for instance *S. clavuligerus* (Roubos et al., 2001), while still others such as *Streptomyces griseus* sporulate (Kendrick and Ensign, 1983), etc. As a consequence, the effect of fermentation parameter modifications in different species cannot be easily predicted. The workflow proposed here for *S. coelicolor* (optimization of antibiotic-producing mycelium differentiation, prevention of sporulation) might be applied to rationalizing the biological effects of classical biophysical fermentation parameters, and to facilitating the optimization of secondary metabolite production in industrial streptomycetes. In addition, preventing early massive pellet fragmentation/lysis by adding antifoam directly to the culture medium at relatively high concentrations is novel, and may be useful for preventing lysis in other industrial streptomycetes.

4. Conclusions

The most important conclusions reached in this work, were: first, the existence of a progressive morphological differentiation in *S. coelicolor* growing in lab-scale bioreactors (PCD, MII differentiation, pellet disintegration, and a kind of sporulation) comparable to that occurring in solid cultures; second, it was demonstrated that this differentiation is one of the keys to interpreting typical fermentation parameters (growth, antibiotic production, dissolved oxygen tension, agitation and oxygen uptake rates) (outlined in Fig. 2B); third, a general consensus to improve secondary metabolite production in *S. coelicolor* was proposed: optimization of the differentiation of the antibiotic-producing mycelium (MII).

Acknowledgements

We wish to thank the European Research Council (ERC Starting Grant; Strp-differentiation 280304) for economic support; Dr. J.L. Gallego (Universidad de Oviedo, Área de Prospección e Investigación Minera) for providing the Bioreactor; Prof. L.A. Garcia and Dr. S. Alonso (Universidad de Oviedo, Dpto. Ingeniería Química) for helping with bioreactor management; A. Wentzel (Department of Biotechnology, SINTEF Materials and Chemistry,

Norway) for discussions about antifoams, Beatriz Gutierrez Magan (Universidad de Oviedo, Dpto. Biología Funcional, Área de Microbiología) for laboratory assistance, and Proof-Reading-Service.com for proofreading the text.

Appendix A. Supplementary data

Supplementary data associated with this article can be found, in the online version, at http://dx.doi.org/10.1016/j.biortech.2013.10.068.

References

Bystrykh, L.V., Fernandez-Moreno, M.A., Herrema, J.K., Malpartida, F., Hopwood, D.A., Dijkhuizen, L., 1996. Production of actinorhodin-related "blue pigments" by *Streptomyces coelicolor* A3(2). J. Bacteriol. 178, 2238–2244.

Chater, K.F., 2001. Regulation of sporulation in *Streptomyces coelicolor* A3(2), a checkpoint multiplex? Curr. Opin. Microbiol. 4, 667–673.

Chater, K.F., Horinouchi, S., 2003. Signalling early developmental events in two highly diverged *Streptomyces* species. Mol. Microbiol. 48, 9–15.

Chater, K.F., Biró, S., Lee, K.J., Palmer, T., Schrempf, H., 2010. The complex extracellular biology of *Streptomyces*. FEMS Microbiol. Rev. 34, 171–198.

Claessen, D., de Jong, W., Dijkhuizen, L., Wösten, H.A., 2006. Regulation of *Streptomyces* development, reach for the sky! Trends Microbiol. 14, 313–319.

Clark, G.J., Langley, D., Bushell, M.E., 1995. Oxygen limitation can induce microbial secondary metabolite formation, investigations with miniature electrodes in shaker and bioreactor culture. Microbiology 141, 663–669.

Daza, A., Martín, J.F., Dominguez, A., Gil, J.A., 1989. Sporulation of several species of *Streptomyces* in submerged cultures after nutritional downshift. J. Gen. Microbiol. 135, 2483–2491.

Dunstan, G.H., Avignone-Rossa, C., Langley, D., Bushell, M.E., 2000. The vancomycin biosynthetic pathway is induced in oxygen-limited *Amycolatopsis orientalis* (ATCC 19795) cultures that do not produce antibiotic. Enzyme Microb. Technol. 27, 502–510.

Fernandez, E., Weissbach, U., Sanchez-Reillo, C., Braña, A.F., Mendez, C., Rohr, J., Salas, J.A., 1998. Identification of two genes from *Streptomyces argillaceus* encoding glycosyltransferases involved in transfer of a disaccharide during biosynthesis of the antitumor drug mithramycin. J. Bacteriol. 180, 4929–4937.

Horinouchi, S., Beppu, T., 1992. Autoregulatory factors and communication in actinomycetes. Annu. Rev. Microbiol. 46, 377–398.

Kendrick, K.E., Ensign, J.C., 1983. Sporulation of *Streptomyces griseus* in submerged culture. J. Bacteriol. 155, 357–366.

Kieser, T., Bibb, M.J., Buttner, M.J., Chater, K.F., Hopwood, D.A., 2000. Practical *Streptomyces* Genetics. John Innes Foundation, Norwich.

Lee, K.J., Rho, Y.T., 1993. Characteristics of spores formed by surface and submerged cultures of *Streptomyces albidoflavus* SMF301. J. Gen. Microbiol. 139, 3131–3137.

Magnolo, S.K., Leenutaphong, D.L., DeModena, J.A., Curtin, J.E., Bailey, J.E., Galazzo, J.L., Hughes, D.E., 1991. Actinorhodin production by *Streptomyces coelicolor* and growth of *Streptomyces lividans* are improved by the expression of a bacterial haemoglobin. Biotechnology (NY) 9, 473–476.

Manteca, A., Alvarez, R., Salazar, N., Yagüe, P., Sánchez, J., 2008. Mycelium differentiation and antibiotic production in submerged cultures of *Streptomyces coelicolor*. Appl. Environ. Microbiol. 74, 3877–3886.

Nicieza, R.G., Huergo, J., Connolly, B.A., Sánchez, J., 1999. Purification, characterization, and role of nucleases and serine proteases in *Streptomyces* differentiation: analogies with the biochemical processes described in late steps of eukaryotic apoptosis. J. Biol. Chem. 274, 20366–20375.

Olmos, E., Mehmood, N., Haj Husein, L., Goergen, J.L., Fick, M., Delaunay, S., 2013. Effects of bioreactor hydrodynamics on the physiology of *Streptomyces*. Bioprocess Biosyst. Eng. 36, 259–272.

Ozergin-Ulgen, K., Mavituna, F., 1993. Actinorhodin production by *Streptomyces coelicolor* A3(2): kinetic parameters related to growth, substrate uptake and production. Appl. Microbiol. Biotechnol. 40, 457–462.

Ozergin-Ulgen, K., Mavituna, F., 1998. Oxygen transfer and uptake in *Streptomyces coelicolor* A3(2) culture in a batch bioreactor. J. Chem. Technol. Biotechnol. 73, 243–250.

Pamboukian, C.R.D., Facciotti, M.C.R., 2004. Production of the antitumoral retamycin during continuous fermentations of *Streptomyces olindensis*. Process Biochem. 39, 2249–2255.

Perlman, D., Wagman, G.H., 1952. Studies on the utilization of lipids by *Streptomyces griseus*. J. Bacteriol. 63, 253–262.

Roubos, J.A., Krabben, P., Luiten, R.G., Verbruggen, H.B., Heijnen, J.J., 2001. A quantitative approach to characterizing cell lysis caused by mechanical agitation of *Streptomyces clavuligerus*. Biotechnol. Prog. 17, 336–347.

Ruiz, B., Chávez, A., Forero, A., García-Huante, Y., Romero, A., Sánchez, M., Rocha, D., Sánchez, B., Rodríguez-Sanoja, R., Sánchez, S., Langley, E., 2010. Production of microbial secondary metabolites, regulation by the carbon source. Crit. Rev. Microbiol. 36, 146–167.

Sevcikova, B., Kormanec, J., 2004. Differential production of two antibiotics of *Streptomyces coelicolor* A3(2), actinorhodin and undecylprodigiosin, upon salt stress conditions. Arch. Microbiol. 181, 384–389.

Shih, I.L., Shen, M.H., 2006. Optimization of cell growth and poly(ε-lysine) production in batch and fed-batch cultures by *Streptomyces albulus* IFO 14147. Process Biochem. 41, 1644–1649.

Techapun, C., Poosaran, N., Watanabe, M., Sasaki, K., 2003. Optimization of aeration and agitation rates to improve cellulase-free xylanase production by thermotolerant *Streptomyces* sp Ab106 and repeated fed-batch cultivation using agricultural waste. J. Biosci. Bioeng. 95, 298–301.

Tenconi, E., Guichard, P., Motte, P., Matagne, A., Rigali, S., 2013. Use of red autofluorescence for monitoring prodiginine biosynthesis. J. Microbiol. Methods 93, 138–143.

Tsao, S.W., Rudd, B.A., He, X.G., Chang, C.J., Floss, H.G., 1985. Identification of a red pigment from *Streptomyces coelicolor* A3(2) as a mixture of prodigiosin derivatives. J. Antibiot. (Tokyo) 38, 128–131.

van Veluw, G.J., Petrus, M.L., Gubbens, J., de Graaf, R., de Jong, I.P., van Wezel, G.P., Wösten, H.A., Claessen, D., 2012. Analysis of two distinct mycelial populations in liquid-grown *Streptomyces* cultures using a flow cytometry-based proteomics approach. Appl. Microbiol. Biotechnol. 96, 1301–1312.

van Wezel, G.P., Krabben, P., Traag, B.A., Keijser, B.J., Kerste, R., Vijgenboom, E., Heijnen, J.J., Kraal, B., 2006. Unlocking *Streptomyces* spp. for use as sustainable industrial production platforms by morphological engineering. Appl. Environ. Microbiol. 72, 5283–5288.

Wentzel, A., Bruheim, P., Øverby, A., Jakobsen, Ø.M., Sletta, H., Omara, W.A., Hodgson, D.A., Ellingsen, T.E., 2012. Optimized submerged batch fermentation strategy for systems scale studies of metabolic switching in *Streptomyces coelicolor* A3(2). BMC Syst. Biol. 6, 59.

Willemse, J., van Wezel, G.P., 2009. Imaging of *Streptomyces coelicolor* A3(2) with reduced autofluorescence reveals a novel stage of FtsZ localization. PLoS ONE 4, e4242.

Yagüe, P., López-García, M.T., Rioseras, B., Sánchez, J., Manteca, A., 2013. Pre-sporulation stages of *Streptomyces* differentiation, state-of-the-art and future perspectives. FEMS Microbiol. Lett. 342, 79–88.

Yang, Y.K., Morikawa, M., Shimizu, H., Shioya, S., Suga, K.I., Nihira, T., Yamada, Y., 1996. Image analysis of mycelial morphology in virginiamycin production by batch culture of *Streptomyces virginiae*. J. Ferm. Bioeng. 81, 7–12.

Yegneswaran, P.K., Gray, M.R., Thompson, B.G., 1991. Experimental simulation of dissolved oxygen fluctuations in large fermentors: effect on *Streptomyces clavuligerus*. Biotechnol. Bioeng. 38, 1203–1209.

DISCUSIÓN

Tal y como se ha ido exponiendo a lo largo de la tesis, el ciclo de vida tradicional de *Streptomyces* se centraba en las fases de micelio sustrato, aéreo y esporulación, por lo que éstas son las fases mejor caracterizadas. Por el contrario, las fases tempranas del desarrollo no contempladas en el ciclo tradicional (MI, transición MI-MII) han sido muy poco estudiadas. En esta tesis se ha contribuido a la caracterización de estas fases menos conocidas que resultan clave para comprender la diferenciación que desencadena el desarrollo del MII productor de metabolitos secundarios y, por lo tanto, su estudio es también interesante desde el punto de vista industrial.

1. Diferencias entre los proteomas y fosfoproteomas del MI y MII

Uno de los objetivos de esta tesis consistió en analizar las diferencias entre las distintas fases del desarrollo (principalente entre MI y MII) mediante técnicas de proteómica y fosfoproteómica cuantitativa. Los resultados obtenidos nos permiten tener una visión global de lo que ocurre, a nivel de proteínas, durante el desarrollo; especialmente en la transición MI-MII. Este estudio además aportó importantes avances metodológicos en el campo de la fosfoproteómica en bacterias.

En cuanto a la proteómica, este trabajo supone un récord en la cantidad de proteínas cuantificadas (44,3% del proteoma de *S. coelicolor*) superando los trabajos de proteómica cuantitativa en *Streptomyces* existentes hasta el momento en los que se cuantificó el 8% (Manteca et al., 2010a; Manteca et al., 2010b) y el 25% del proteoma (Gubbens et al., 2012). Se observó que las mayores diferencias en el proteoma se encuentran entre las fases de MI y MII lo cual confirmó los resultados obtenidos en trabajos previos (Manteca et al., 2010a; Manteca et al., 2010b). Las proteínas que aparecen al alza en las fases de MI son principalmente proteínas involucradas en el

metabolismo primario y síntesis proteica; mientras que las proteínas detectadas al alza en el MII son proteínas relacionadas con la síntesis de metabolitos secundarios y cubiertas hidrofóbicas. Esto demuestra que el MI es la fase vegetativa mientras que el MII es el micelio diferenciado y productor de metabolitos secundarios.

La abundancia de proteínas clave del desarrollo concuerda con lo esperado. Por ejemplo, las proteínas implicadas en la formación de las cubiertas hidrofóbicas del micelio aéreo están reguladas al alza en las fases de micelio aéreo, las proteínas implicadas en la esporulación lo están en la fase de esporulación; o las proteínas implicadas en la síntesis de metabolitos secundarios están reguladas al alza durante las fases de MII. Esta parte de los resultados sirve para validar los datos obtenidos ya que nos indica que estos tienen sentido biológico. No obstante, la parte más interesante de nuestros resultados son las proteínas no caracterizadas, algunas de las cuales tienen homologías con proteínas reguladoras y que constituyen una base de datos muy prometedora de posbibles reguladores del desarrollo y diferenciación a explorar en futuros experimentos. Algunos de estos reguladores podrían estar implicados en la activación del metabolismo secundario en el MII. Como se adelantaba en la introducción, existen multitud de antibióticos cuyas rutas biosinteticas son conocidas, pero sin embargo no se ha conseguido activar su producción. La activación de estas rutas crípticas, así como la optimización de la producción de metabolitos ya conocidos se puede llevar a cabo a través de diferentes estrategias (véase introducción, apartado 4). Entender las rutas biomoleculares que controlan la activación del metabolismo secundario en el MII, puede ser una de las claves para su activación.

También se han detectado 47 proteínas involucradas en procesos de división celular con diferentes abundancias en las fases de MI y MII y

hemos observado que el 66% de estas proteínas, como es el caso de FtsZ (véase más abajo, apartado "2. División celular"), tienen una abundancia mayor en fases de MI que en fases de esporulación. Esto sugiere un posible papel de estas proteínas en la división celular y compartimentalización del MI. Caracterizar la función biológica de estas proteínas será un objetivo interesante de cara al futuro, que nos permitiría conocer más acerca de la regulación de la compartimentalización del MI, por el momento desconocida.

Existe una buena correlación (mayor del 85%) entre los datos de proteómica de esta tesis y los datos de transcriptómica obtenidos en trabajos anteriores por nuestro grupo de investigación usando las mismas condiciones de cultivo (Yague et al., 2013b). Es decir, con pocas excepciones genes y proteínas siguen la misma tendencia en las diferentes fases del desarrollo analizadas. Proteínas y ARNm son moléculas diferentes y no tienen por qué tener una buena correlación debido a diversos factores como la estabilidad o la degradación que es diferente para ambas moléculas, lo que constituye algunos de los principales mecanismos de regulación genética (de Sousa Abreu et al., 2009). Sin embargo, en este caso, la buena correlación se debe a que las diferencias entre las fases que estamos comparando (MI y MII) son mucho más grandes que la variabilidad debida a las diferentes tasas de renovación de transcritos/proteínas o la variabilidad de las metodologías empleadas (proteómica y transcriptómica).

Los experimentos de fosfoproteómica que se llevaron a cabo en esta tesis, supusieron un verdadero reto ya que como vimos en la introducción, la fosforilación en procariotas es muy escasa lo que hace necesaria una buena optimización de las técnicas de enriquecimiento. La mayor parte de trabajos de fosfoproteómica utilizan la técnica de

fosfoenriquecimiento de TiO2. Sin embargo, en procariotas, esta técnica es poco eficiente. En un trabajo previo de nuestro grupo, se optimizó esta técnica combinándola con un pre-enriquecimiento mediante CPP, lo cual aumentó considerablemente la cantidad de fosfopéptidos identificados (Manteca et al., 2011). Esto es debido a la existencia de un umbral en la proporción de fosfopéptidos por debajo del cual el TiO2 fracasa en el fosfoenriquecimiento de la muestra. Mediante la realización de un preenriquecimiento con CPP, se consigue que la proporción de fosfopéptidos en la muestra aumente lo suficiente para que el TiO2 sea más eficiente (figura 20). En esta tesis doctoral se empleó CPP-TiO2 como técnica de enriquecimiento en fosfopéptidos, combinado con marcaje de masa isobárico (TMT) para la realización de la cuantificación de las variaciones en la abundancia de los fosfopéptidos durante el desarrollo. Los resultados de esta tesis constituyen el primer estudio de fosforproteómica en bacterias en el que se demuestra que la fosforilación en Ser/Thr/Tyr se correlaciona con la diferenciación, siendo las fases de MII y esporulación aquellas en las que la fosforilación es mucho más abundante. No obstante, la cantidad de fosfopéptidos que se llegaron a identificar en este estudio fue menor que en el trabajo anterior realizado por nuestro grupo de investigación, en el que no se realizó ningún marcaje (Manteca et al., 2011) (véase introducción, tabla 3). El TMT, como el resto de técnicas de cuantificación mediante marcaje de masa isobárico, conlleva la mezcla de las diferentes fases del desarrollo analizadas en una misma muestra, lo que minimiza la variación experimental, y maximiza la reproducibilidad de los datos cuantitativos. Sin embargo, en casos como el nuestro, en los que existe mucha diferencia en la cantidad de proteínas fosforiladas entre las diferentes fases analizadas (MI, MII), la mezcla de las muestras puede hacer que el nivel de fosforilación global disminuya por debajo del umbral necesario para que el TiO2 sea eficaz (figura 20). Esto

explicaría que en este trabajo, la cantidad final de fosfopéptidos cuantificados, sea menor que en el trabajos realizados anteriormente mediante "*label free*" (Manteca et al., 2011). Como consecuencia, se puede concluir que para realizar estudios de fosfoproteómica en bacterias, se debe ponderar si interesa más la identificación de gran cantidad de fosfopéptidos, aunque la cuantificación no sea muy fiable (técnica *"label-free"*), o si por el contrario se prefiere una cuantificación mucho más precisa pero con un rango dinámico menor (técnicas basadas en marcaje).

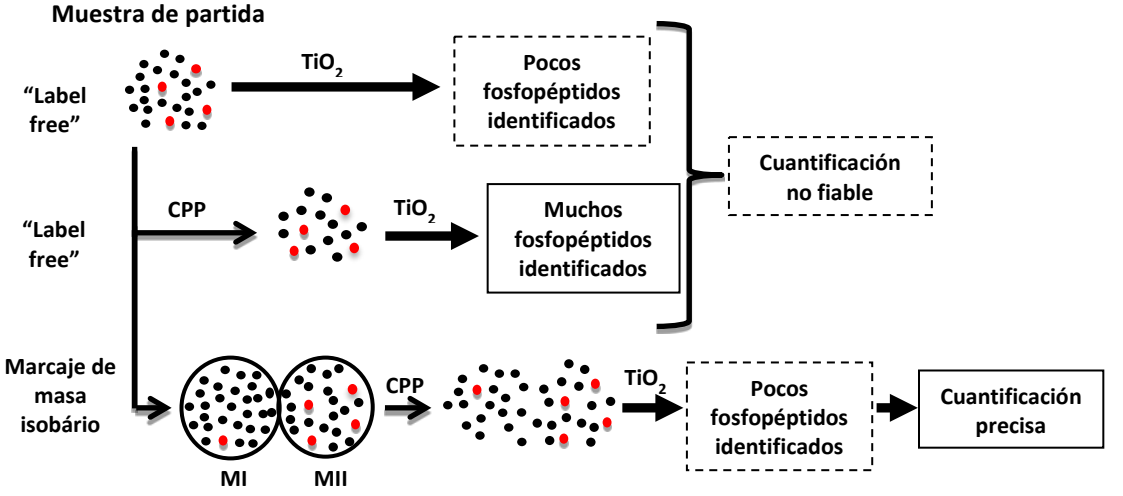

Fig 20. Técnicas de fosfoproteómica cuantitativa. La muestra de partida contiene mezcla de péptidos (bolas negras) y fosfopéptidos en menor proporción (bolas rojas). Ventaja de realizar un preenriquecimiento con CPP: más cantidad de fosfopéptidos identificados. Ventajas y limitaciones de las técnicas "*label free"* (buena identificación, mala cuantificación) frente a técnicas con marcaje isobárico (mala identificación, buena cuantificación).

Como vimos en los resultados de esta tesis (véase resultados de manuscrito 1), existe un aumento de la fosforilación en residuos de Ser/Thr/Tyr que acompaña la diferenciación y esporulación. Esto demuestra, tal y como se había sugerido en trabajos anteriores (Manteca et al., 2011), que la fosforilación de Ser/Thr/Tyr tiene un importante papel en la regulación de la esporulación. Este es un campo aún por explorar y su

estudio resultaría interesante para comprender la diferenciación del MII. Entre las proteínas diferencialmente fosforiladas hay proteínas muy reguladoras muy interesantes, cuya fosforilación puede modular su función. Por ejemplo, FtsZ está fosforilada en un residuo de serina, y esta fosforilación es significativamente mayor en la fase de esporulación que en fase de MI. Esto indica un posible papel de la fosforilación de FtsZ en la regulación de la división celular, algo desconocido hasta el momento y su estudio sería de gran interés.

2. Modificaciones de la pared celular durante las fases de esporulación y germinación.

El segundo objetivo de esta tesis incluye el estudio de las modificaciones de la pared celular que tienen lugar durante la esporulación y la germinación. SCO4439, uno de los genes que fue identificado como diferencialmente expresado durante el desarrollo, y la proteína que codifica como diferencialmente fosforilada (en este y otros trabajos: (Manteca et al., 2011;Yague et al., 2013b)), fue mutado. SCO4439 codifica para una carboxipeptidasa, cuya caracterización ha permitido avanzar en el conocimiento de los procesos de germinación. Como se adelantaba en la introducción, esta proteína es una PBP que no pertenece a la familia SEDS y a diferencia de estas, es dispensable para la supervivencia de la bacteria. Sin embargo, su mutación resultó en alteraciones importantes: un gran hinchamiento de las esporas durante la germinación, mayor cantidad de enlaces "*crosslinking"* en el peptidoglicano de las esporas, aumento de la resistencia de las esporas a determinadas condiciones adversas como el ácido o el calor, y menor resistencia a antibióticos glucopéptidos. El trabajo realizado ha llevado a proponer un modelo biomolecular que permite relacionar la actividad carboxipeptidasa de esta proteína con los fenotipos observados tras su mutación (figura 21). En el caso del mutante, la

ausencia de la actividad carboxipeptidasa hace que haya muchas más cadenas laterales de peptidoglicano intactas (pentapéptidos), que son el sustrato de las transpeptidasas. Como consecuencia de esto, hay muchos más enlaces "*crosslinking"* entre las cadenas del peptidoglicano lo que hace que las paredes de las esporas sean más resistentes al ácido y al calor y puedan soportar el hinchamiento característico de las fases iniciales de la germinación durante mucho más tiempo que la cepa silvestre. Esto se traduce en la observación de esas esporas tan grandes en tiempos tempranos tras la germinación.

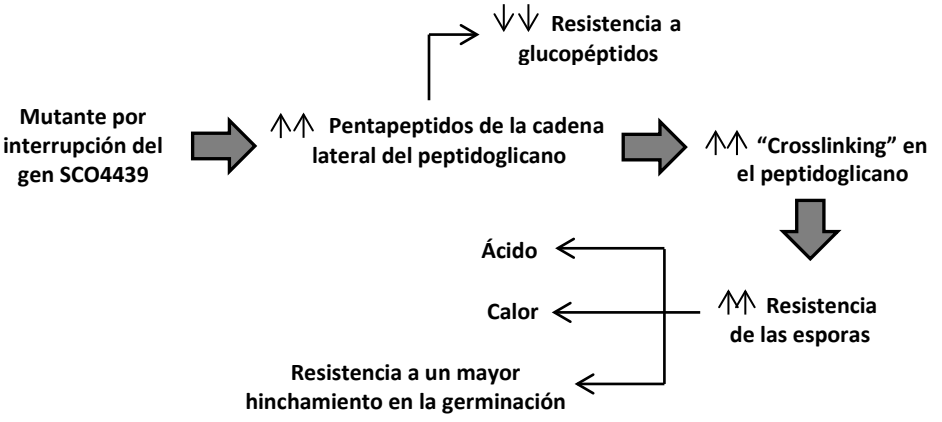

Fig. 21. Modelo biomolecular que relaciona la actividad de la carboxipeptidasa SCO4439 con los fenotipos que resultan de su mutación.

Además, la caracterización de esta proteína nos ha permitido predecir la existencia de una nueva fase de germinación cuya existencia ha sido demostrada por experimentos de *"time-lapse*" realizados en las cepas silvestre y mutante. Esta nueva fase tiene lugar tras las etapas de oscurecimiento e hinchamiento conocidas tradicionalmente y coincide con la fase de emergencia del tubo germinativo (véase introducción, apartado 3.1). Esta etapa consiste en el deshinchamiento de las esporas una vez que tiene lugar la ruptura de su pared celular por no poder resistir el creciente hinchamiento. Se ha observado que en la cepa silvestre de *S. coelicolor* la

emergencia del tubo germinativo coincide con la ruptura de la pared celular y con el fin del hinchamiento de la espora que permanece viable tras el deshinchamiento. Por el contrario, en la cepa mutante el hinchamiento de la espora continúa tras la emergencia del tubo germinativo alcanzando gran tamaño, hasta que comienza el deshinchamiento repentino, debido a la ruptura de la pared celular, y la célula pierde su viabilidad (figura 22).

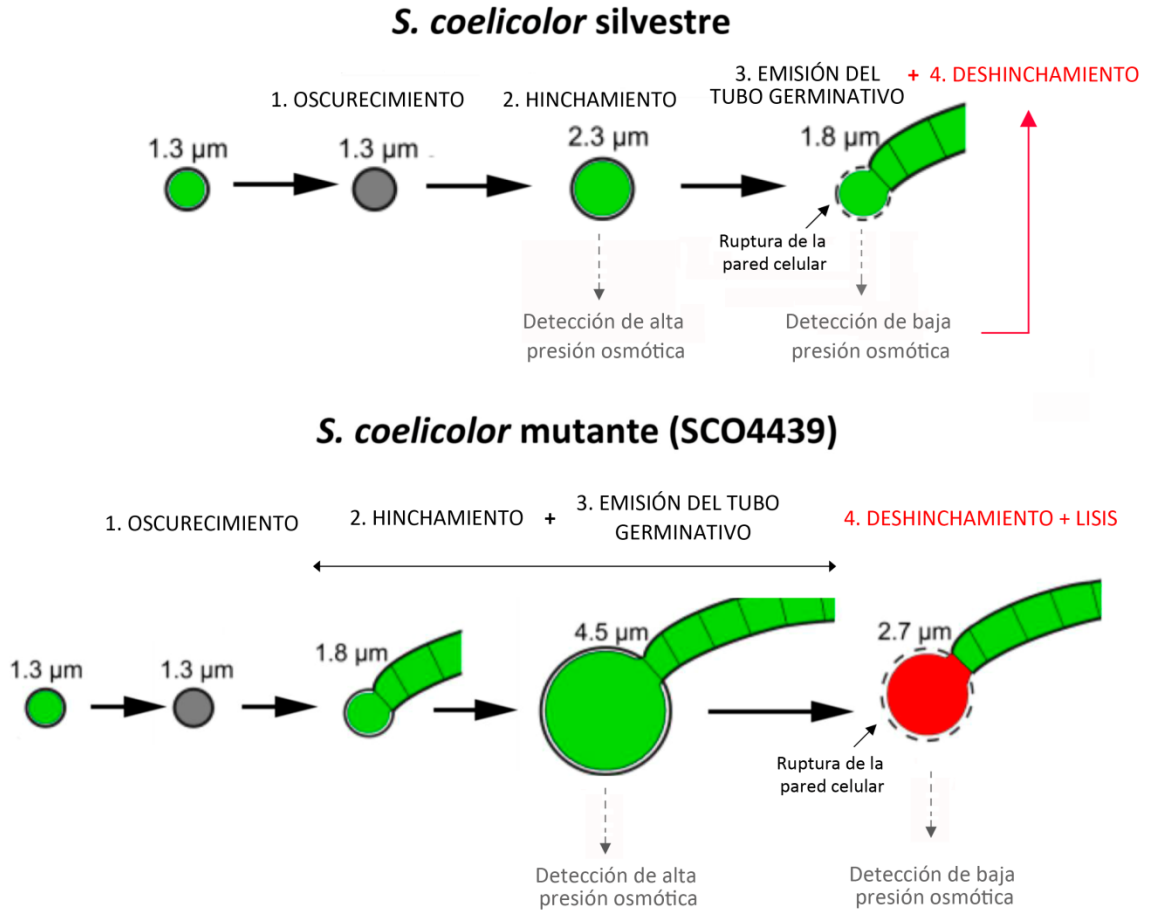

Fig 22. Esquema de la germinación de *Streptomyces coelicolor* (silvestre y mutante del gen SCO4439). Hifa de color verde representa tinción con SYTO9 (células vivas), hifa en rojo tinción con IP (células muertas). La nueva fase de germinación (deshinchamiento de las esporas) aparece en rojo. En gris está el mecanismo de regulación propuesto: la espora comenzaría a deshincharse cuando detecta baja presión osmótica.

Estos resultados sugieren la existencia de un mecanismo de control de la fase de hinchamiento desconcido hasta la fecha. De algún modo, la espora activa los sistemas de captación de agua, que activan el hinchamiento de la espora y el aumento de la presión intracelular, que posiblemente faciliten la emisión del tubo germinativo. Una vez se emite el tubo germinativo, la pared celular ya no resiste más la presión, y se rompe, disminuyéndose la presión celular, y desactivándose los hipotéticos sistemas de captación de agua/hinchamiento. En el mutante, la pared celular es más resistente debido a la mayor cantidad de enlaces "*crosslinking"*, y soporta mayores presiones, lo que de algún modo retroalimenta la captación de agua e hinchamiento tras la emisión del tubo germinativo. Una vez que la pared celular no resiste más el hinchamiento y se rompe, la espora original pierde su viabilidad, quizá debido a que el gran tamaño que ha adquirido haga que no pueda mantener la turgencia celular sin la cubierta de la espora original (figura 22). Hará falta más trabajo para llegar a comprender los mecanismos osmóticos que controlan estas fases de hinchaminento y emergencia del tubo germinativo, que hasta la fecha permanecen prácticamente desconocidos. No obstante, el mutante en el gen SCO4439 demuestra que estos mecanismos osmóticos existen. Estos resultados sobre la germinación de *Streptomyces* se correlacionan con las observaciones realizadas en otras especies como es el caso de *Bacillus,* donde se ha descrito que existe una relación entre la proporción de enlaces "*crosslinking"* en la pared de las esporas, la hidratación de las mismas y la velocidad de germinación (Meador-Parton & Popham, 2000).

El hecho de que el hinchamiento de las esporas tenga lugar para facilitar la emergencia del tubo germinativo ya había sido descrito por Hardisson et al. (1978) cuando se caracterizaron las tres fases conocidas de la germinación (oscurecimiento, hinchamiento, emergencia del tubo germinativo). Desde entonces, poco es lo que se ha descubierto acerca de

cómo tiene lugar esta regulación. Recientemente se hicieron dos avances importantes. El primero fue la observación de que en estas fases de germinación existe un aumento de expresión de determinados factores sigma relacionados con respuesta a estrés. Por ejemplo, el factor SigE que está involucrado en la reconstrucción de la pared tras la actuación de las hidrolasas, o el factor SigH que se activa en la fases de hinchamiento como respuesta al estrés osmótico que se produce debido a la entrada masiva de agua en la célula (Bobek et al., 2014). El segundo, aún más reciente describe que los factores que promueven la resucitación (Rpf) participan en la remodelación del peptidoglicano que tiene lugar durante esta fase de germinación (Sexton et al., 2015). Existen otras muchas proteínas involucradas en esta remodelación de la pared en esta fase, entre las que se encontraría la proteína SCO4439 que junto con otras PBPs actuaría para mantener una adecuada proporción de enlaces "*crosslinking"* en el peptidoglicano. En la naturaleza esta adecuada proporción de enlaces "*crosslinking"* sería necesaria para regular el equilibrio entre la resistencia de las esporas y la germinación.

Por otra parte, los pentapéptidos de cadenas laterales del peptidoglicano, cuya presencia aumenta en el mutante SCO4439, son la diana de los antbióticos glucopéptidos (véase introducción, capítulo 5.3), lo que explica que el mutante tenga menos resistencia a este tipo de antibióticos (figura 21). Esto se observó con los dos antibióticos probados: vancomicina y teicoplanina. *S. coelicolor* es resistente natural a vancomicina, pero no a teicoplanina, debido a que contiene los genes de resistencia vanRSJKHAX que son inducidos por vancomicina pero no por teicoplanina. En esta tesis hemos visto que la carbxipeptidasa SCO4439 colaboraría indirectamente con estas proteínas codificadas por el *cluster* de genes *van* en su misión de disminuir la cantidad de pentapéptidos con D-Ala D-Ala terminal disponibles, disminuyendo con ello la acción de los

antibióticos glucopéptidos. En trabajos recientes se ha demostrado la existencia de otras carboxipeptidasas (tipo VanY) que contribuyen a la resistencia a glucopéptidos en actinomycetes productores de estos antibióticos y actúan eliminando la D-Ala terminal de los precursores del pentapéptido del peptidoglicano (Binda et al., 2012; Schaberle et al., 2011). Resulta muy interesante que estas carboxipeptidasas tienen grandes homologías con la proteína SCO4439. Conocer el papel biológico de estas y otras proteínas involucradas en la resistencia antimicrobiana, es importante para comprender la evolución de estas resistencias en la naturaleza.

En cuanto a la estructura, la proteína SCO4439 es muy peculiar, ya que es la primera PBP conocida en la que aparte del dominio carboxipeptidasa que se localiza en el extremo carboxilo y cuyas funciones se han descrito más arriba, tiene un posible regulador transcripcional en su extremo amino de función desconocida pero cuya presencia sabemos que es totalmente dispensable para la actividad del dominio carboxipeptidasa. Además, contiene un dominio transmembrana localizado en el medio de la proteína, separando el dominio regulador que se situaría hacia el citosol, del dominio carboxipeptidasa que estaría en el espacio periplásmico. Esto es también inusual ya que normalmente las PBPs conocidas están ancladas a la membrana en su extremo amino y se proyectan hacia el espacio periplásmico donde ejercen su actividad. En los experimentos de fosfoproteómica realizados en esta tesis, se detectó fosforilación en un residuo de treonina situado en el dominio regulador de la proteína SCO4439. Además, se vio que esta fosforilación aumenta de forma significativa en fases de MII temprano y esporulante respecto a las fases de MI. Resultaría muy interesante estudiar la función de este dominio regulador y al igual que lo que ocurría en el mutante FtsZ, sería también interesante ver cómo le afecta esta regulación por fosforilación.

3. División celular y compartimentalización del MI

El tercer objetivo de esta tesis doctoral, incluye el estudio de los procesos de compartimentalización y división celular durante la fase de MI. En el contexto del ciclo tradicional los únicos procesos de división celular que se estudiaban eran los específicos del micelio sustrato y aéreo (formación de tabiques esporádicos en las hifas) y los que tienen lugar durante la esporulación. Estos procesos de división celular y su regulación están relativamente bien caracterizados en la literatura, sobre todo los que tienen lugar durante la esporulación, que en el contexto del ciclo de desarrollo tradicional se consideraba la única fase de formación de células unigenómicas (Flardh, 2003). En esta tesis hemos descubierto la existencia de un nuevo tipo de división celular en las hifas de MI basado en la formación de tabiques de membrana (sin pared) a diferencia de los tabiques conocidos hasta el momento, formados por membrana y pared celular. Celler et al., (2016) también descubieron, de forma independiente a nosotros, la existencia de estos tabiques de membrana sin pared celular. La detección de estas membranas sin pared ha pasado inadvertida hasta ahora, debido a la dificultad metodológica de su visualización en el denso citoplasma de las hifas de Streptomyces. Las técnicas empleadas para la observación directa de las membranas (microscopía electrónica y tinción con colorantes fluorescentes lipofílicos, FM4-64), generan tinciones heterogéneas, que no permiten observar todas las membranas celulares, ni siquiera la membrana extracelular pudo ser observada en el 100% de las hifas analizadas (véase resultados de manuscrito 2). A pesar de estas limitaciones metodológicas, en esta tesis hemos sido capaces de determinar la frecuencia de tabicación del MI, gracias al uso de diversas tinciones fluorescentes: colorantes fluorescentes de viabilidad, tinciones de membrana y de pared, formación de “Z-ladders” observados mediante la fusión de FtsZ con eGFP (esquemetizado en la figura 23). El primer

indicio que nos hizo sospechar la existencia de estas membranas, fue la observación de que durante la MCP del MI, dentro de la misma hifa existen compartimentos con diferente permeabilidad a determinados colorantes vitales (IP, YOPRO-1); lo cual indica la existencia de una barrera separando estos compartimentos con las propiedades de permeabilidad de una membrana. Se cuantificó que estas barreras de permeabilidad se disponen siguiendo un patrón con una separación media de 1µm en las hifas de MI. En esta tesis también se ha demostrado la existencia de anillos Z formados por la acumulación de la proteína FtsZ en las fases de MI con una separación de 1 µm ("Z-ladders"). Combinando diferentes tinciones, se demostró que al menos alguno de los anillos Z observados colocalizan con membranas sin pared (nuevos tabiques), y otros con membranas con pared (tabiques normales con membrna y peptidoglicano); algunos también colocalizan con las barreras de permeabilidad separando segmentos celulares permeables al IP de segmentos impermeables. Tomando en consideración todos los resultados, está claro que, aunque no hemos encontrado una metodología que nos permita observar todas las membranas presentes en el MI, el hecho de que las barreras de permeabilidad observadas colocalicen con membranas y anillos Z, demuestra que estas barreras de permeabilidad son membranas (figura 23). Además, en las fases de MII multinucleado, las barreras de permeabilidad y los anillos Z son esporádicos, demostrando que la frecuencia de separación de 1 µm es algo específico de la fase de MI. Los tabiques de membrana sin pared, no se observaron en el MII, aunque no se puede excluir que existan con una frecuencia baja. Para terminar, sólo la fase de MI es capaz de formar protoplastos en cantidades elevadas, lo que de nuevo demuestra que el MI está altamente compartimentalizado. En resumen, todos los resultados que hemos obtenido indican que el MI está

compartimentalizado por tabiques de membrana que separan segmentos celulares de 1 µm de longitud (figura 23).

Además de las membranas sin pared que separan segmentos celulares, tanto nosotros, como Celler et al., (2016), detectamos, de forma independiente, y de nuevo en las fases de MI, la existencia de un segundo tipo de membrana que consiste en membranas internas en forma de vesículas, independientes de la membrana extracelular. Este tipo de estructuras ya fue descrito con anterioridad por (Glauert & Hopwood, 1959). Celler et al., (2016) describieron que las zonas de la hifa en las que se forman estas versículas son zonas libres de ADN, ya que no se tiñen con colorantes fluorescentes que tiñen ADN, y propusieron que esas vesículas podrían estar actuando como protección de los nucleoides durante la formación de los septos, favoreciendo así la correcta segregación de los cromosomas durante el proceso de división. Sin embargo, otra hipótesis propuesta por nuestro grupo de investigación, es que esas vesículas pueden ser consecuencia del desmantelamiento que tiene lugar en las células muertas, y se formarían durante las últimas fases de MCP no tiñéndose estos segmentos con los colorantes de ADN, porque el ADN en esa fase estaría completamente degradado por la acción de las nucleasas activadas durante la MCP. Más trabajo es necesario para determinar cuál de las hipótesis (si alguna) es correcta.

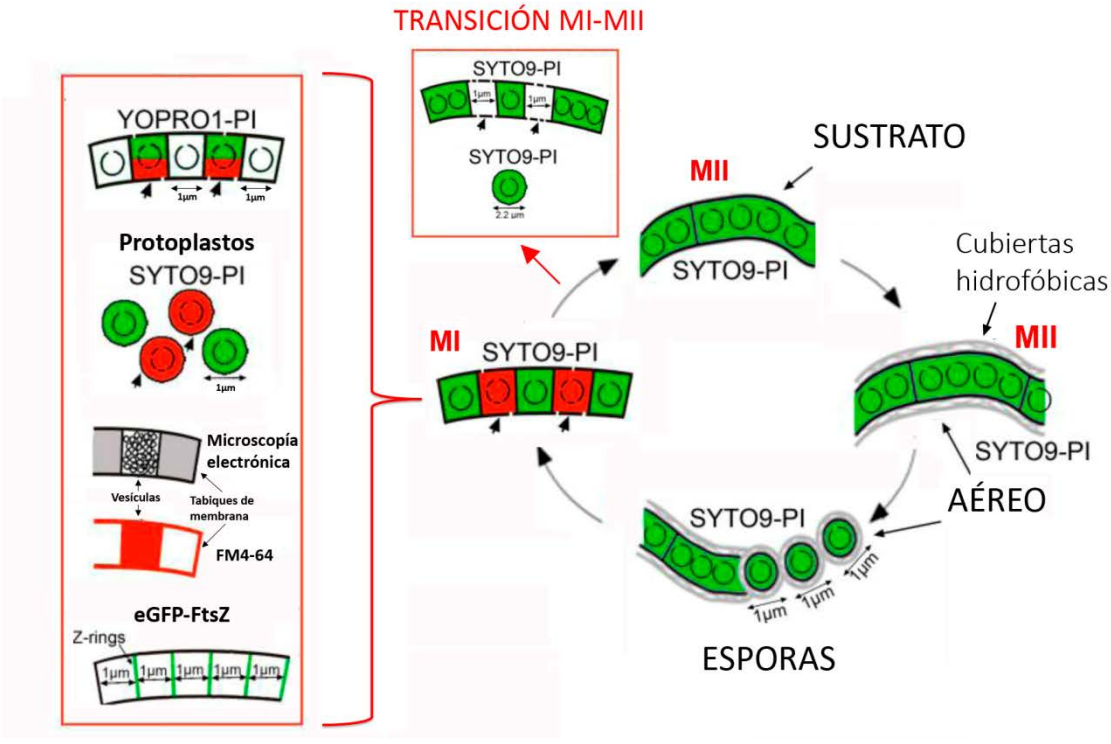

Fig 23. Ciclo de desarrollo de *Streptomyces*. Se muestran los resultados obtenidos por diferentes técnicas que prueban la existencia de los tabiques de membrana del MI. En rojo: células muertas (teñidas con IP). En verde: células vivas (teñidas con SYTO9 o YOPRO-1). Círculos abiertos dentro de los compartimentos: ADN cromosómico intacto. Círculos fragmentados: ADN degradado. Discontinuidades de las membranas: cambios en la permeabilidad en células que están sufriendo procesos de MCP; las puntas de flecha señalan estas células. La tinción de membranas con el colorante FM4-64 se muestra en rojo.

FtsZ es la proteína clave en la división celular bacteriana, y también en la de *Streptomyces*, (véase introducción, capítulo 3.4). El gen ftsZ codifica para una proteína homóloga a la tubulina y es un gen esencial en todas las bacterias salvo en *Streptomyces* (McCormick et al., 1994). Hasta ahora, el por qué la cepa mutante FtsZ de *Streptomyces* era viable, era un gran misterio que desconcertaba a la comunidad científica. En esta tesis se ha demostrado que el mutante FtsZ está completamente tabicado por tabiques de membrana sin pared, con una separación media de 1 µm, lo

que explica por qué este mutante es viable, y sus hifas resisten la fragmentación. La presencia de tabiques de membrana en el mutante FtsZ demuestra que FtsZ no es esencial para su formación. No obstante, tal como se comentó más arriba, FtsZ participa en la formación de estos tabiques, ya que durante la fase de MI se forman "Z ladders", y el gen FtsZ, de hecho se transcribe más durante las fases de MI que durante las fases de MII o esporulación (Yague et al., 2013b). Hará falta más trabajo para entender la regulación de la división del MI, así como del papel de FtsZ en la misma. Un estudio que podría ser interesante realizar de cara al futuro, sería analizar las diferencias, si existen, entre los tabiques de membrana formados en presencia y ausencia de FtsZ.

La existencia de tabiques de membrana en el MI, hace que las hifas sean más resistentes frente a condiciones adversas ya que si una parte de la hifa se daña, el resto de compartimentos pueden permanecer viables. Además esta subcompartimentalización proporciona un nivel adicional de organización que apoya el estilo de vida multicelular de estas bacterias. Será necesario más trabajo para llegar a conocer la función biológica de este tipo de división, pero nuestros resultados acaban con el dogma de que las hifas vegetativas de *Streptomyces* son multinucleadas y sólo tienen tabiques esporádicos.

Como hemos visto, el estudio de los procesos de división celular, y la remodelación de la pared celular, es clave para comprender muchos aspectos del desarrollo de *Streptomyces* y por ello, gran parte de esta tesis doctoral se ha centrado en caracterizar determinadas proteínas o eventos que ocurren dentro del contexto de la división celular. Desde el punto de vista de la aplicabilidad, el estudio de todas estas proteínas involucradas en la división celular puede resultará interesante por ejemplo en la búsqueda de nuevas dianas terapéuticas.

4. Diferenciación y desarrollo en biorreactores a escala piloto

El cuarto objetivo fue analizar los procesos de desarrollo, diferenciación y producción de antibiótico en fermentaciones industriales a escala piloto. Se analizó el ciclo de desarrollo de *S. coelicolor*, en cultivo líquido, en biorreactores de 2L, y se probaron dos tipos de inóculos: "denso" (10^7 esporas/ml) y "diluido" (10^5 esporas/ml) (figura 24). El ciclo de vida en biorreactor, fue similar al descrito en matraz (Manteca et al., 2008), con el desarrollo de un MI que crece formando pellets, y que tras la MCP que ocurre en el centro de los pellets, se diferencia a MII productor. Sin embargo, se observaron dos grandes diferencias en los cultivos llevados a cabo en biorreactor frente a lo que ocurría en matraz. La primera, es que en el biorreactor se observó una lisis masiva de los pellets; esto ocurría con ambos tipos de inóculo, una vez que se había activado la producción de antibióticos. Aunque esta lisis ya ha sido descrita anteriormente en fermentaciones de *Streptomyces* (Roubos et al., 2001; Techapun et al., 2003), el motivo sigue siendo desconocido. En este caso, podría deberse a las características hidrodinámicas del biorreactor. La segunda gran diferencia es que en el biorreactor, algunas de las hifas que permanecen viables tras la lisis masiva de los pellets, sufren procesos de esporulación. La esporulación de *S. coelicolor* en cultivo líquido es muy inusual y solo se ha descrito antes en condiciones en las que hay déficit nutricional (Daza et al., 1989). Aunque se desconocen las señales que activan la esporulación en el biorreactor, sí se sabe que en medio sólido la esporulación se desencadena en situaciones de estrés (Chater, 2001). Las altas tasas de crecimiento que se alcanzan en el biorreactor unido a la desintegración masiva de los pellets, puede estar generando una situación de estrés similar a la que tenía lugar en medio sólido, que hace que se liberen señales difusibles que inducen la esporulación (Chater et al., 2010; Horinouchi & Beppu, 1992).

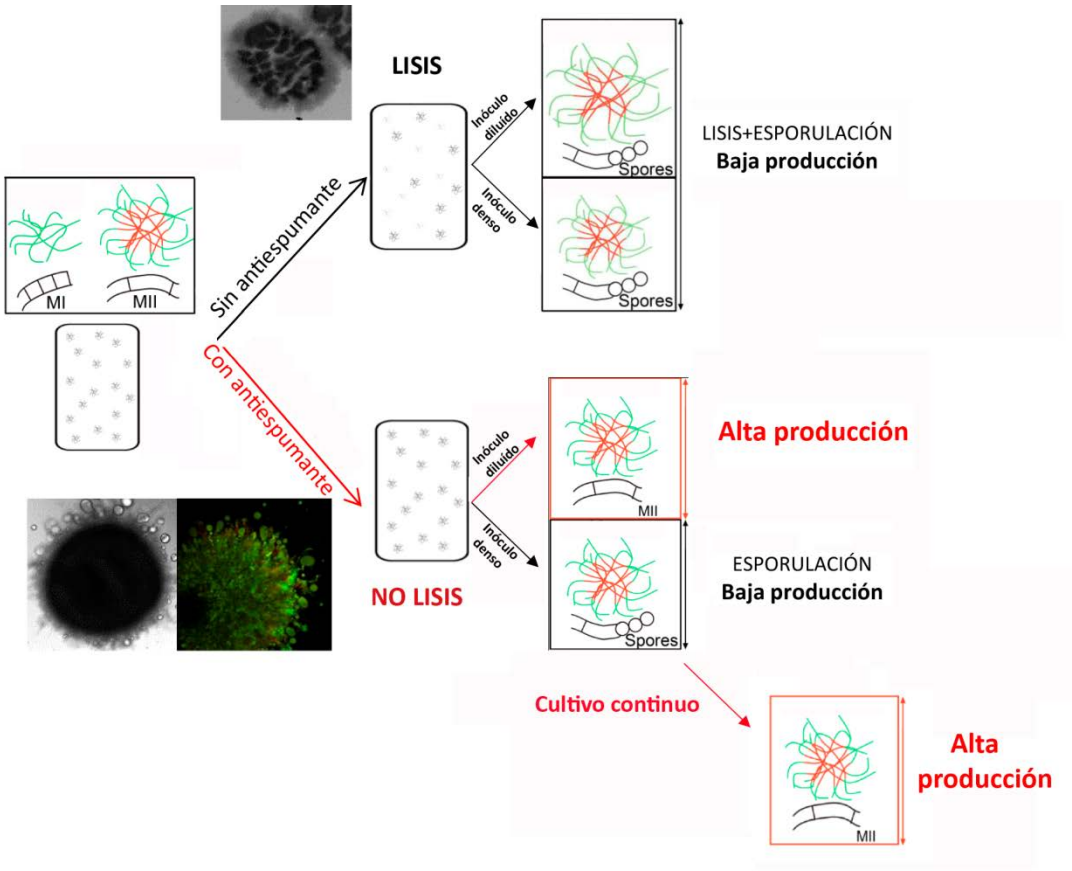

Fig 24. Esquema de la diferenciación de *S. coelicolor* creciendo en biorreactor de 2L, en medio sin antiespumante (en negro, parte superior) y con antiespumante (en rojo, parte inferior) con inóculo denso y diluído. Las condiciones que reportan una mayor producción se marcan en rojo. En el esquema de los pellets en verde se representa las hifas teñidas con SYTO9 (células vivas) y en rojo las hifas teñidas con IP (células muertas). Imagen a microscopía de contraste de fases y confocal (colorantes vitales SYTO9/IP) de los pellets de *Streptomyces* sin y con antiespumante.

Tanto la lisis (disminuye la cantidad de MII productor viable) como la esporulación (inactiva el metabolismo) son dos procesos que disminuyen la producción; haciendo que esta sea muy baja, mucho menor que en matraz. Se consiguió evitar la lisis masiva mediante la adición de antiespumante al medio (figura 24). Aunque se desconoce el motivo, sí se ha observado que el antiespumante tiende a recubrir los pellets de micelio de forma que

podría estar actuando de capa protectora evitando su fragmentación. Los antiespumantes se usan en los biorreactores de forma rutinaria para prevenir la formación de espuma. Normalemente se añaden en pequeñas cantidades de forma automática una vez que una sonda detecta la formación de espuma. En nuestro conocimiento, esta es la primera vez que se ha descrito que añadir concentraciones relativamente elevadas de antiespumante al medio de cultivo, desde el comienzo del cultivo, puede prevenir la lisis de los pellets, que en algunos casos supone el principal problema de las fermentaciones.

El bloqueo de la lisis masiva mediante la adición de antiespumante, consiguió aumentar la producción en cultivos realizados con inóculos diluidos. Sin embargo, en cultivos que parten de inóculos densos, la producción sigue siendo baja debido a que aunque se consigue prevenir la lisis, las hifas terminan esporulando. Puede que la alta densidad de células que existe en esta condición hace que se sigan liberando las señales que induzcan la esporulación. Desde el punto de vista industrial, donde el tiempo es una de las principales limitaciones, la optimización de estos cultivos realizados con inóculos densos resultaría muy interesante ya que en ellos se alcanza antes el pico de producción. Para llevar a cabo esta optimización se intentó solucionar el problema de la esporulación mediante el diseño de un sistema continuo que consistió en cambiar el medio de cultivo del biorreactor por medio fresco en el punto donde se alcanza la máxima producción, pero antes de que se desencadene la esporulación. Con esto se consiguió eliminar las señales difusibles del medio responsables de desencadenar la esporulación y como consecuencia, y se logró mantener la fase productora de MII indefinidamente dando como resultado altos niveles de producción (figura 24).

Como se adelantaba más arriba, los parámetros clásicos utilizados para optimizar la producción a nivel industrial consisten en: composición del medio de cultivo, morfología del micelio, optimización de cepas por mutagénesis o parámetros biofísicos como: pH, agitación, temperatura, O_2, etc. (figura 25). Muchos de estos parámetros generan desacuerdos a la hora de llegar a un consenso de qué condiciones deben usarse para optimizar la producción. Por ejemplo varios autores han analizado las diferentes formas de agrupación de las hifas de *Streptomyces* en cultivo líquido: crecimiento disperso de las hifas, crecimiento en forma de *clumps* o *pellets*; y no ha habido un acuerdo de cuál es la más favorable para la producción de metabolitos secundarios ya que se ha visto que varía en función de las condiciones de cultivo y la cepa utilizada (van Veluw et al., 2012; van Wezel et al., 2006). En esta tesis doctoral se ha llegado a la conclusión de que lo realmente importante para optimizar la producción en *Streptomyces* es favorecer la diferenciación del MI a MII y mantener esta fase de MII productor. Además, se han descrito por primera vez nuevos parámetros como la MCP, la diferenciación, la lisis o la esporulación que son fundamentales para comprender y mejorar la producción de metabolitos secundarios en *Streptomyces* (figura 25).

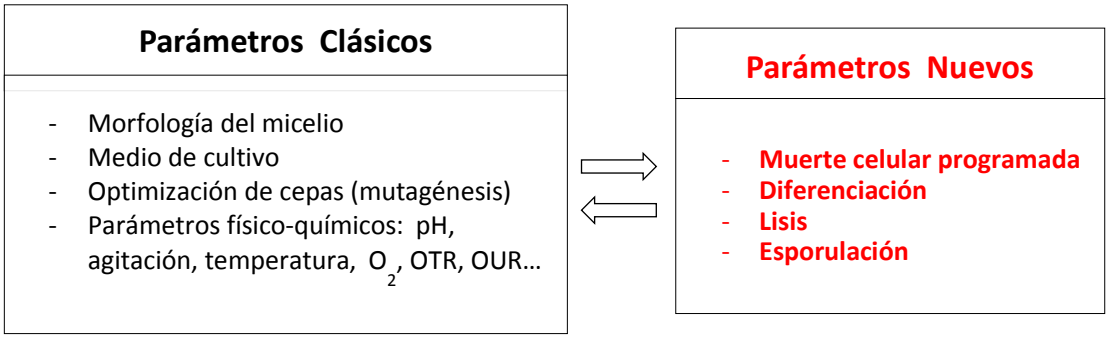

Fig 25. Parámetros clásicos (en negro) y nuevos parámetros propuestos en esta tesis (en rojo) para optimizar la producción en cultivos de *Streptomyces* a nivel industrial.

CONCLUSIONES/ CONCLUSIONS

1. Los experimentos de proteómica realizados han permitido la cuantificación del 44,3% del proteoma de *S. coelicor,* lo que constituye un récord en proteómica cuantitativa de *Streptomyces*.

2. Los experimentos de proteómica cuantitativa realizados a lo largo del desarrollo revelan que las mayores diferencias se encuentran entre las fases de MI y MII. El proteoma del MI está enriquecido en proteínas del metabolismo primario, mientras que el del MII lo está en proteínas del metabolismo secundario.

3. Muchas de las proteínas relacionadas con la división celular se han detectado al alza en las fases de MI, lo que indica un posible papel de estas proteínas en el nuevo tipo de división celular que tiene lugar en esta fase. Entre estas proteínas se encuentra la conocida proteína de división celular FtsZ.

4. Existe una buena correlación entre los datos de proteómica obtenidos en este trabajo y los datos de transcriptómica de trabajos anteriores, lo que indica que las diferencias entre las fases que estamos comparando (MI y MII), son mucho más grandes que la variabilidad generada por el trunover específico de transcritos/proteínas, o la variabilidad metodológica intrínseca a las técnicas de proteómica/transcriptómica.

5. En los experimentos de fosfoproteómica cuantitativa, la cuantificación mediante marcaje de masa isobárico, reporta menor cantidad de fosfopéptidos identificados, pero una cuantificación más precisa que la cuantificación libre de marcaje.

6. Existe un aumento de la fosforilación en residuos de Ser/Thr/Tyr que acompaña la diferenciación de *Streptomyces* (MII y esporulación), lo que indica un papel de la fosforilación en la regulación de la diferenciación.

7. Se ha creado una base de datos con las proteínas y fosfopéptidos que muestran diferente abundancia durante el desarrollo. Gran parte de las proteínas y fosforilaciones detectadas tienen, por el momento, función desconocida, y son potenciales reguladores y efectores de diferenciación y activación del metabolismo secundario a estudiar en el futuro.

8. Se ha demostrado que la carboxipeptidasa SCO4439 está involucrada en la remodelación del peptidoglicano en las esporas, actuando junto con otras PBPs durante las fases de germinación para mantener una adecuada proporción de enlaces "*crosslinking"*, la cual controla el equilibrio entre resistencia de las esporas y capacidad de germinación.

9. La caracterización de la carboxipeptidasa SCO4439 ha permitido descubrir una nueva fase de la germinación que tiene lugar tras las conocidas etapas de oscurecimiento e hinchamiento y que consiste en el deshinchamiento de las esporas una vez que se produce la ruptura de su pared celular por no poder soportar más el hinchamiento.

10. La caracterización de la carboxipeptidasa SCO4439 ha permitido observar que esta proteína colabora indirectamente con las proteínas codificadas por el *cluster* de genes *van* en su misión de disminuir la cantidad de pentapéptidos del peptidoglicano con D-Ala D-Ala terminal disponibles, que es la diana de los antibióticos glucopéptidos como

vancomicina y teicoplanina, aumentando con ello la resistencia a estos antibióticos.

11. Los resultados obtenidos a lo largo de esta tesis doctoral demuestran que en la fase de MI existen dos tipos de tabiques: unos formados solo por membrana que se disponen con una separación media de 1 µm a lo largo de la hifa, y otros formados por membrana y pared celular de frecuencia mucho menor.

12. La proteína FtsZ participa en el nuevo tipo de división celular que tiene lugar en fases de MI y que consiste en formación de tabiques de membrana, sin pared. Sin embargo, esta proteína no es esencial para este tipo de división.

13. En los cultivos líquidos de *S. coelicolor* realizados en biorreactores (escala piloto) se ha visto que existe una diferenciación morfológica (con procesos de MCP, diferenciación de MII, desintegración de los pellets y esporulación) comparable a lo que ocurre en cultivos sólidos.

14. Se ha demostrado que la diferenciación es una de las claves para interpretar los parámetros clásicos utilizados en la optimización de las fermentaciones industriales (agitación, pH, temperatura, etc.). Se han definido nuevos parámetros como la MCP, la diferenciación, la lisis o la esporulación que son fundamentales para comprender y mejorar la producción de metabolitos secundarios en *Streptomyces.*

1. The 43% of *S.coelicolor* proteome was quantified. This is record in *Streptomyces* qantitative proteomics.

2. The quantitative proteomic experiments show that the biggest differences are between the MI and MII stages. The MI proteome contains a lot of proteins from the primary metabolism while the MII have more proteins from the secondary metabolism.

3. Many of the proteins related to cellular division processes have been detected up-regulated at MI stage showing a possible role of these proteins in the novel mechanism of cell division established in this phase. The very known division protein FtsZ is one of these proteins.

4. There is a good correlation between the proteomic data from this work and the transcriptomic data from previous papers. This suggest that the phases we are comparing (MI and MII) are too much different than the variability produced by the transcript/proteomic trunover, or the methodological variability of proteomic / transcriptomic techniques.

5. The isobaric labeling quantification reports less amount of phosphopeptides identifications but a better quantification than the label free quantification.

6. There is a drmatic increase in Ser/Thr/Tyr protein phosphorylation accompany *Streptomyces* differentiation (MII and sporulation). This result demonstrates an important role of Ser/Thr/Tyr phosphorylation in the regulation of differentiation.

7. A database with the proteins and phosphopeptides that show different abundances during the development has been created. Many of the proteins and phosphorylated peptides detected have, for the moment, unknown function so they are potential regulators and effectors of differentiation and activation of secondary metabolism and it would be interesting to study them in the future.

8. It has been demonstrated that the SCO4439 carboxypeptidase is involved in spore peptidoglycan remodelling acting together with other PBPs during the germination phases to maintain an adequate crosslinking ratio, which controls the balance between spore resistance and germination capacity.

9. The SCO4439 carboxypeptidase characterization has allowed us to discover a new phase of the germination that takes place after the known stages: darkening and swelling. It consists in the spores deswelling once their cell wall has broken due to it was not able to resist the swelling longer.

10. The SCO4439 carboxypeptidase characterization has allowed us to observe that this protein indirectly collaborates with the proteins encoded by the gene cluster *van* in their role to decrease the amount of pentapeptides with available D-Ala D-Ala in the peptidoglycan, which is the target of glycopeptide antibiotics such as vancomycin and teicoplanin resulting in an increasing of these antibiotics resistance.

11. The results obtained in this work demonstrate that in the MI phase there are two different types of compartimentalizations: ones based on cross-membranes with a high-frequency distribution (mean

separation of 1 µm along the hypha) and others formed by membrane and cell wall distributed with a much lower frequency.

12. The FtsZ protein is involved in the novel mechanism of cell division that take place in MI phase consisting in the cross-membranes formation without cell wall. However this protein is not essential for this kind of cell division.

13. In liquid cultures of *S. coelicolor* carried out in bioreactors (pilot scale) a morphological differentiation has been observed (with programmed cell death processes, MII differentiation, pellets disintegration and sporulation) comparable to what happens in solid cultures.

14. It has been demonstrated that the differentiation is a key factor to understand the classical parameters used in the optimization of industrial fermentations (agitation, pH, temperature, etc.). New parameters such as programmed cell death, differentiation, lysis or sporulation have been defined that result essential for understanding and improving the production of secondary metabolites in *Streptomyces.*

REFERENCIAS

Aivaliotis, M., Macek, B., Gnad, F., Reichelt, P., Mann, M., Oesterhelt, D. 2009. Ser/Thr/Tyr protein phosphorylation in the archaeon Halobacterium salinarum--a representative of the third domain of life. *PLoS One*, **4**(3), e4777.

Akanuma, G., Ueki, M., Ishizuka, M., Ohnishi, Y., Horinouchi, S. 2011. Control of aerial mycelium formation by the BldK oligopeptide ABC transporter in Streptomyces griseus. *FEMS Microbiol Lett*, **315**(1), 54-62.

Allahverdiyev, A.M., Bagirova, M., Abamor, E.S., Ates, S.C., Koc, R.C., Miraloglu, M., Elcicek, S., Yaman, S., Unal, G. 2013. The use of platensimycin and platencin to fight antibiotic resistance. *Infection and drug resistance*, **6**, 99-114.

Anderson, T.B., Brian, P., Champness, W.C. 2001. Genetic and transcriptional analysis of absA, an antibiotic gene cluster-linked two-component system that regulates multiple antibiotics in Streptomyces coelicolor. *Mol Microbiol*, **39**(3), 553-66.

Bai, X., Ji, Z. 2012. Phosphoproteomic investigation of a solvent producing bacterium Clostridium acetobutylicum. *Appl Microbiol Biotechnol*, **95**(1), 201-11.

Basell, K., Otto, A., Junker, S., Zuhlke, D., Rappen, G.M., Schmidt, S., Hentschker, C., Macek, B., Ohlsen, K., Hecker, M., Becher, D. 2014. The phosphoproteome and its physiological dynamics in Staphylococcus aureus. *Int J Med Microbiol*, **304**(2), 121-32.

Bentley, S.D., Chater, K.F., Cerdeno-Tarraga, A.M., Challis, G.L., Thomson, N.R., James, K.D., Harris, D.E., Quail, M.A., Kieser, H., Harper, D., Bateman, A., Brown, S., Chandra, G., Chen, C.W., Collins, M., Cronin, A., Fraser, A., Goble, A., Hidalgo, J., Hornsby, T., Howarth, S., Huang, C.H., Kieser, T., Larke, L., Murphy, L., Oliver, K., O'Neil, S., Rabbinowitsch, E., Rajandream, M.A., Rutherford, K., Rutter, S., Seeger, K., Saunders, D., Sharp, S., Squares, R., Squares, S., Taylor, K., Warren, T., Wietzorrek, A., Woodward, J., Barrell, B.G., Parkhill, J., Hopwood, D.A. 2002. Complete genome sequence of the model actinomycete Streptomyces coelicolor A3(2). *Nature*, **417**(6885), 141-7.

Bibb, M.J., Molle, V., Buttner, M.J. 2000. sigma(BldN), an extracytoplasmic function RNA polymerase sigma factor required for aerial mycelium formation in Streptomyces coelicolor A3(2). *J Bacteriol*, **182**(16), 4606-16.

Bignell, D.R., Warawa, J.L., Strap, J.L., Chater, K.F., Leskiw, B.K. 2000. Study of the bldG locus suggests that an anti-anti-sigma factor and an anti-sigma factor may be involved in Streptomyces coelicolor antibiotic production and sporulation. *Microbiology*, **146 (Pt 9)**, 2161-73.

Binda, E., Marcone, G.L., Pollegioni, L., Marinelli, F. 2012. Characterization of VanYn, a novel D,D-peptidase/D,D-carboxypeptidase involved in glycopeptide antibiotic resistance in Nonomuraea sp. ATCC 39727. *FEBS J*, **279**(17), 3203-13.

Bobek, J., Strakova, E., Zikova, A., Vohradsky, J. 2014. Changes in activity of metabolic and regulatory pathways during germination of S. coelicolor. *BMC Genomics*, **15**, 1173.

Bos, J., Yakhnina, A.A., Gitai, Z. 2012. BapE DNA endonuclease induces an apoptotic-like response to DNA damage in Caulobacter. *Proc Natl Acad Sci U S A*, **109**(44), 18096-101.

Buchanan, R.E. 1916. Studies in the Nomenclature and Classification of Bacteria: The Problem of Bacterial Nomenclature. *J Bacteriol*, **1**(6), 591-6.

Burger, A., Sichler, K., Kelemen, G., Buttner, M., Wohlleben, W. 2000. Identification and characterization of the mre gene region of Streptomyces coelicolor A3(2). *Mol Gen Genet*, **263**(6), 1053-60.

Cal, S., Nicieza, R.G., Connolly, B.A., Sanchez, J. 1996. Interaction of the periplasmic dG-selective Streptomyces antibioticus nuclease with oligodeoxynucleotide substrates. *Biochemistry*, **35**(33), 10828-36.

Celler, K., Koning, R.I., Willemse, J., Koster, A.J., van Wezel, G.P. 2016. Cross-membranes orchestrate compartmentalization and morphogenesis in Streptomyces. *Nat Commun*, **7**, ncomms11836.

Claessen, D., de Jong, W., Dijkhuizen, L., Wosten, H.A. 2006. Regulation of Streptomyces development: reach for the sky! *Trends Microbiol*, **14**(7), 313-9.

Claessen, D., Rink, R., de Jong, W., Siebring, J., de Vreugd, P., Boersma, F.G., Dijkhuizen, L., Wosten, H.A. 2003. A novel class of secreted hydrophobic proteins is involved in aerial hyphae formation in Streptomyces coelicolor by forming amyloid-like fibrils. *Genes Dev*, **17**(14), 1714-26.

Coates, A.R., Halls, G., Hu, Y. 2011. Novel classes of antibiotics or more of the same? *Br J Pharmacol*, **163**(1), 184-94.

Cohn, F. 1875. Untersuchungen über Bakterien. [Investigations on bacteria].II. *Beiträge zur Biologie der Pflanzen*, **1**, 141-204.

Chahrour, O., Cobice, D., Malone, J. 2015. Stable isotope labelling methods in mass spectrometry-based quantitative proteomics. *J Pharm Biomed Anal*, **113**, 2-20.

Chakraburtty, R., White, J., Takano, E., Bibb, M. 1996. Cloning, characterization and disruption of a (p)ppGpp synthetase gene (relA) of Streptomyces coelicolor A3(2). *Mol Microbiol*, **19**(2), 357-368.

Challis, G.L., Hopwood, D.A. 2003. Synergy and contingency as driving forces for the evolution of multiple secondary metabolite production by Streptomyces species. *Proc Natl Acad Sci U S A*, **100 Suppl 2**, 14555-61.

Champness, W.C. 1988. New loci required for Streptomyces coelicolor morphological and physiological differentiation. *J Bacteriol*, **170**(3), 1168-74.

Chang, S., Sievert, D.M., Hageman, J.C., Boulton, M.L., Tenover, F.C., Downes, F.P., Shah, S., Rudrik, J.T., Pupp, G.R., Brown, W.J., Cardo, D., Fridkin,

S.K., Vancomycin-Resistant Staphylococcus aureus Investigative, T. 2003. Infection with vancomycin-resistant Staphylococcus aureus containing the vanA resistance gene. *N Engl J Med*, **348**(14), 1342-7.

Chater, K.F. 1984. Morphological and Physiological Differentiation in Streptomyces *Cold Spring Harbor Laboratory Press*, 89-115.

Chater, K.F. 2001. Regulation of sporulation in Streptomyces coelicolor A3(2): a checkpoint multiplex? *Curr Opin Microbiol*, **4**(6), 667-73.

Chater, K.F., Biro, S., Lee, K.J., Palmer, T., Schrempf, H. 2010. The complex extracellular biology of Streptomyces. *FEMS Microbiol Rev*, **34**(2), 171-98.

Chatterjee, I., Neumayer, D., Herrmann, M. 2010. Senescence of staphylococci: using functional genomics to unravel the roles of ClpC ATPase during late stationary phase. *Int J Med Microbiol*, **300**(2-3), 130-6.

Davis, N.K., Chater, K.F. 1990. Spore colour in Streptomyces coelicolor A3(2) involves the developmentally regulated synthesis of a compound biosynthetically related to polyketide antibiotics. *Mol Microbiol*, **4**(10), 1679-91.

Davis, N.K., Chater, K.F. 1992. The Streptomyces coelicolor whiB gene encodes a small transcription factor-like protein dispensable for growth but essential for sporulation. *Mol Gen Genet*, **232**(3), 351-8.

Daza, A., Martin, J.F., Dominguez, A., Gil, J.A. 1989. Sporulation of several species of Streptomyces in submerged cultures after nutritional downshift. *J Gen Microbiol*, **135**(9), 2483-91.

de Jong, W., Manteca, A., Sanchez, J., Bucca, G., Smith, C.P., Dijkhuizen, L., Claessen, D., Wosten, H.A. 2009. NepA is a structural cell wall protein involved in maintenance of spore dormancy in Streptomyces coelicolor. *Mol Microbiol*, **71**(6), 1591-603.

de Sousa Abreu, R., Penalva, L.O., Marcotte, E.M., Vogel, C. 2009. Global signatures of protein and mRNA expression levels. *Mol Biosyst*, **5**(12), 1512-26.

Elliot, M., Damji, F., Passantino, R., Chater, K., Leskiw, B. 1998. The bldD gene of Streptomyces coelicolor A3(2): a regulatory gene involved in morphogenesis and antibiotic production. *J Bacteriol*, **180**(6), 1549-55.

Engelberg-Kulka, H., Amitai, S., Kolodkin-Gal, I., Hazan, R. 2006. Bacterial programmed cell death and multicellular behavior in bacteria. *PLoS Genet*, **2**(10), e135.

Facey, P.D., Hitchings, M.D., Saavedra-Garcia, P., Fernandez-Martinez, L., Dyson, P.J., Del Sol, R. 2009. Streptomyces coelicolor Dps-like proteins: differential dual roles in response to stress during vegetative growth and in nucleoid condensation during reproductive cell division. *Mol Microbiol*, **73**(6), 1186-202.

Feitelson, J.S., Malpartida, F., Hopwood, D.A. 1985. Genetic and biochemical characterization of the red gene cluster of Streptomyces coelicolor A3(2). *J Gen Microbiol*, **131**(9), 2431-41.

Fischbach, M.A., Walsh, C.T. 2009. Antibiotics for emerging pathogens. *Science*, **325**(5944), 1089-93.

Fishov, I., Woldringh, C.L. 1999. Visualization of membrane domains in Escherichia coli. *Mol Microbiol*, **32**(6), 1166-72.

Flardh, K. 2003. Growth polarity and cell division in Streptomyces. *Curr Opin Microbiol*, **6**(6), 564-71.

Flardh, K., Buttner, M.J. 2009. Streptomyces morphogenetics: dissecting differentiation in a filamentous bacterium. *Nat Rev Microbiol*, **7**(1), 36-49.

Ge, R., Sun, X., Xiao, C., Yin, X., Shan, W., Chen, Z., He, Q.Y. 2011. Phosphoproteome analysis of the pathogenic bacterium Helicobacter pylori reveals over-representation of tyrosine phosphorylation and multiply phosphorylated proteins. *Proteomics*, **11**(8), 1449-61.

Genilloud, O. 2014. The re-emerging role of microbial natural products in antibiotic discovery. *Antonie Van Leeuwenhoek*, **106**(1), 173-88.

Ghosh, A.S., Chowdhury, C., Nelson, D.E. 2008. Physiological functions of D-alanine carboxypeptidases in Escherichia coli. *Trends Microbiol*, **16**(7), 309-17.

Glauert, A.M., Hopwood, D.A. 1959. A membranous component of the cytoplasm in Streptomyces coelicolor. *J Biophys Biochem Cytol*, **6**, 515-6.

Gram, C. 1884. The differential staining of Schizomycetes in tissue sections and in dried preparations. *Fortschritte der Medizin*, **2**, 185-9

Gramajo, H.C., Takano, E., Bibb, M.J. 1993. Stationary-phase production of the antibiotic actinorhodin in Streptomyces coelicolor A3(2) is transcriptionally regulated. *Mol Microbiol*, **7**(6), 837-45.

Grund, A.D., Ensign, J.C. 1985. Properties of the germination inhibitor of Streptomyces viridochromogenes spores. *J Gen Microbiol*, **131**(4), 833-47.

Gubbens, J., Janus, M., Florea, B.I., Overkleeft, H.S., van Wezel, G.P. 2012. Identification of glucose kinase-dependent and -independent pathways for carbon control of primary metabolism, development and antibiotic production in Streptomyces coelicolor by quantitative proteomics. *Mol Microbiol*, **86**(6), 1490-507.

Guijarro, J.A., Suarez, J.E., Salas, J.A., Hardisson, C. 1983. Pattern of protein degradation during germination of Streptomyces antibioticus spores. *Can J Microbiol*, **29**(6), 637-43.

Guiral, S., Mitchell, T.J., Martin, B., Claverys, J.P. 2005. Competence-programmed predation of noncompetent cells in the human pathogen Streptococcus pneumoniae: genetic requirements. *Proc Natl Acad Sci U S A*, **102**(24), 8710-5.

Hackl, S., Bechthold, A. 2015. The Gene bldA, a regulator of morphological differentiation and antibiotic production in streptomyces. *Arch Pharm (Weinheim)*, **348**(7), 455-62.

Hagedorn, C. 1976. Influences of soil acidity on Streptomyces populations inhabiting forest soils. *Appl Environ Microbiol*, **32**(3), 368-75.

Hair, P.I., Keam, S.J. 2007. Daptomycin: a review of its use in the management of complicated skin and soft-tissue infections and Staphylococcus aureus bacteraemia. *Drugs*, **67**(10), 1483-512.

Haiser, H.J., Yousef, M.R., Elliot, M.A. 2009. Cell wall hydrolases affect germination, vegetative growth, and sporulation in Streptomyces coelicolor. *J Bacteriol*, **191**(21), 6501-12.

Hardisson, C., Manzanal, M.B., Salas, J.A., Suarez, J.E. 1978. Fine structure, physiology and biochemistry of arthrospore germination in Streptomyces antibioticus. *J Gen Microbiol*, **105**(2), 203-14.

Heichlinger, A., Ammelburg, M., Kleinschnitz, E.M., Latus, A., Maldener, I., Flardh, K., Wohlleben, W., Muth, G. 2011. The MreB-like protein Mbl of Streptomyces coelicolor A3(2) depends on MreB for proper localization and contributes to spore wall synthesis. *J Bacteriol*, **193**(7), 1533-42.

Hesketh, A., Bucca, G., Laing, E., Flett, F., Hotchkiss, G., Smith, C.P., Chater, K.F. 2007. New pleiotropic effects of eliminating a rare tRNA from Streptomyces coelicolor, revealed by combined proteomic and transcriptomic analysis of liquid cultures. *BMC Genomics*, **8**, 261.

Hochman, A. 1997. Programmed cell death in prokaryotes. *Crit Rev Microbiol*, **23**(3), 207-14.

Hodgson, D.A. 2000. Primary metabolism and its control in streptomycetes: a most unusual group of bacteria. *Adv Microb Physiol*, **42**, 47-238.

Hong, H.J., Hutchings, M.I., Buttner, M.J., Biotechnology, Biological Sciences Research Council, U.K. 2008. Vancomycin resistance VanS/VanR two-component systems. *Adv Exp Med Biol*, **631**, 200-13.

Hong, H.J., Hutchings, M.I., Hill, L.M., Buttner, M.J. 2005. The role of the novel Fem protein VanK in vancomycin resistance in Streptomyces coelicolor. *J Biol Chem*, **280**(13), 13055-61.

Hong, H.J., Hutchings, M.I., Neu, J.M., Wright, G.D., Paget, M.S., Buttner, M.J. 2004. Characterization of an inducible vancomycin resistance system in Streptomyces coelicolor reveals a novel gene (vanK) required for drug resistance. *Mol Microbiol*, **52**(4), 1107-21.

Hopwood, D.A. 2007. *Streptomyces in nature and medicine: the antibiotic markers.*

Horinouchi, S., Beppu, T. 1992. Autoregulatory factors and communication in actinomycetes. *Annu Rev Microbiol*, **46**, 377-98.

Horinouchi, S., Hara, O., Beppu, T. 1983. Cloning of a pleiotropic gene that positively controls biosynthesis of A-factor, actinorhodin, and prodigiosin in Streptomyces coelicolor A3(2) and Streptomyces lividans. *J Bacteriol*, **155**(3), 1238-48.

Hu, C.W., Lin, M.H., Huang, H.C., Ku, W.C., Yi, T.H., Tsai, C.F., Chen, Y.J., Sugiyama, N., Ishihama, Y., Juan, H.F., Wu, S.H. 2012. Phosphoproteomic analysis of Rhodopseudomonas palustris reveals

the role of pyruvate phosphate dikinase phosphorylation in lipid production. *J Proteome Res*, **11**(11), 5362-75.

Hugonnet, J.E., Haddache, N., Veckerle, C., Dubost, L., Marie, A., Shikura, N., Mainardi, J.L., Rice, L.B., Arthur, M. 2014. Peptidoglycan cross-linking in glycopeptide-resistant Actinomycetales. *Antimicrob Agents Chemother*, **58**(3), 1749-56.

Hunt, A.C., Servin-Gonzalez, L., Kelemen, G.H., Buttner, M.J. 2005. The bldC developmental locus of Streptomyces coelicolor encodes a member of a family of small DNA-binding proteins related to the DNA-binding domains of the MerR family. *J Bacteriol*, **187**(2), 716-28.

Jakimowicz, D., van Wezel, G.P. 2012. Cell division and DNA segregation in Streptomyces: how to build a septum in the middle of nowhere? *Mol Microbiol*, **85**(3), 393-404.

Jayapal, K.P., Philp, R.J., Kok, Y.J., Yap, M.G., Sherman, D.H., Griffin, T.J., Hu, W.S. 2008. Uncovering genes with divergent mRNA-protein dynamics in Streptomyces coelicolor. *PLoS One*, **3**(5), e2097.

Kawamoto, S., Watanabe, H., Hesketh, A., Ensign, J.C., Ochi, K. 1997. Expression analysis of the ssgA gene product, associated with sporulation and cell division in Streptomyces griseus. *Microbiology*, **143 (Pt 4)**, 1077-86.

Kelemen, G.H., Plaskitt, K.A., Lewis, C.G., Findlay, K.C., Buttner, M.J. 1995. Deletion of DNA lying close to the glkA locus induces ectopic sporulation in Streptomyces coelicolor A3(2). *Mol Microbiol*, **17**(2), 221-30.

Kieser, T., Bibb, M.J., Chater, K.F., Hopwood, D.A. 2000. *Practical Streptomyces genetics*. The John Innes Foundation, Norwich, UK.

Kim, D.W., Chater, K.F., Lee, K.J., Hesketh, A. 2005. Effects of growth phase and the developmentally significant bldA-specified tRNA on the membrane-associated proteome of Streptomyces coelicolor. *Microbiology*, **151**(Pt 8), 2707-20.

Kim, H.J., Calcutt, M.J., Schmidt, F.J., Chater, K.F. 2000. Partitioning of the linear chromosome during sporulation of Streptomyces coelicolor A3(2) involves an oriC-linked parAB locus. *J Bacteriol*, **182**(5), 1313-20.

Koonin, E.V., Aravind, L. 2002. Origin and evolution of eukaryotic apoptosis: the bacterial connection. *Cell Death Differ*, **9**(4), 394-404.

Kormanec, J., Sevcikova, B. 2002. The stress-response sigma factor sigma(H) controls the expression of ssgB, a homologue of the sporulation-specific cell division gene ssgA, in Streptomyces coelicolor A3(2). *Mol Genet Genomics*, **267**(4), 536-43.

Lai, C., Xu, J., Tozawa, Y., Okamoto-Hosoya, Y., Yao, X., Ochi, K. 2002. Genetic and physiological characterization of rpoB mutations that activate antibiotic production in Streptomyces lividans. *Microbiology*, **148**(Pt 11), 3365-73.

Lee, H.N., Huang, J., Im, J.H., Kim, S.H., Noh, J.H., Cohen, S.N., Kim, E.S. 2010. Putative TetR family transcriptional regulator SCO1712 encodes an

antibiotic downregulator in Streptomyces coelicolor. *Appl Environ Microbiol*, **76**(9), 3039-43.

Licona-Cassani, C., Lim, S., Marcellin, E., Nielsen, L.K. 2014. Temporal dynamics of the Saccharopolyspora erythraea phosphoproteome. *Mol Cell Proteomics*, **13**(5), 1219-30.

Lim, S., Marcellin, E., Jacob, S., Nielsen, L.K. 2015. Global dynamics of Escherichia coli phosphoproteome in central carbon metabolism under changing culture conditions. *J Proteomics*, **126**, 24-33.

Lin, M.H., Hsu, T.L., Lin, S.Y., Pan, Y.J., Jan, J.T., Wang, J.T., Khoo, K.H., Wu, S.H. 2009. Phosphoproteomics of Klebsiella pneumoniae NTUH-K2044 reveals a tight link between tyrosine phosphorylation and virulence. *Mol Cell Proteomics*, **8**(12), 2613-23.

Ling, L.L., Schneider, T., Peoples, A.J., Spoering, A.L., Engels, I., Conlon, B.P., Mueller, A., Schaberle, T.F., Hughes, D.E., Epstein, S., Jones, M., Lazarides, L., Steadman, V.A., Cohen, D.R., Felix, C.R., Fetterman, K.A., Millett, W.P., Nitti, A.G., Zullo, A.M., Chen, C., Lewis, K. 2015. A new antibiotic kills pathogens without detectable resistance. *Nature*, **517**(7535), 455-9.

Liu, G., Chater, K.F., Chandra, G., Niu, G., Tan, H. 2013. Molecular regulation of antibiotic biosynthesis in streptomyces. *Microbiol Mol Biol Rev*, **77**(1), 112-43.

Lu, Y., He, J., Zhu, H., Yu, Z., Wang, R., Chen, Y., Dang, F., Zhang, W., Yang, S., Jiang, W. 2011. An orphan histidine kinase, OhkA, regulates both secondary metabolism and morphological differentiation in Streptomyces coelicolor. *J Bacteriol*, **193**(12), 3020-32.

Macek, B., Gnad, F., Soufi, B., Kumar, C., Olsen, J.V., Mijakovic, I., Mann, M. 2008. Phosphoproteome analysis of E. coli reveals evolutionary conservation of bacterial Ser/Thr/Tyr phosphorylation. *Mol Cell Proteomics*, **7**(2), 299-307.

Macek, B., Mijakovic, I., Olsen, J.V., Gnad, F., Kumar, C., Jensen, P.R., Mann, M. 2007. The serine/threonine/tyrosine phosphoproteome of the model bacterium Bacillus subtilis. *Mol Cell Proteomics*, **6**(4), 697-707.

Manteca, A., Alvarez, R., Salazar, N., Yague, P., Sanchez, J. 2008. Mycelium differentiation and antibiotic production in submerged cultures of Streptomyces coelicolor. *Appl Environ Microbiol*, **74**(12), 3877-86.

Manteca, A., Claessen, D., Lopez-Iglesias, C., Sanchez, J. 2007. Aerial hyphae in surface cultures of Streptomyces lividans and Streptomyces coelicolor originate from viable segments surviving an early programmed cell death event. *FEMS Microbiol Lett*, **274**(1), 118-25.

Manteca, A., Fernandez, M., Sanchez, J. 2006. Cytological and biochemical evidence for an early cell dismantling event in surface cultures of Streptomyces antibioticus. *Res Microbiol*, **157**(2), 143-52.

Manteca, A., Fernandez, M., Sanchez, J. 2005a. A death round affecting a young compartmentalized mycelium precedes aerial mycelium

dismantling in confluent surface cultures of Streptomyces antibioticus. *Microbiology*, **151**(Pt 11), 3689-97.

Manteca, A., Fernandez, M., Sanchez, J. 2005b. Mycelium development in Streptomyces antibioticus ATCC11891 occurs in an orderly pattern which determines multiphase growth curves. *BMC Microbiol*, **5**, 51.

Manteca, A., Jung, H.R., Schwammle, V., Jensen, O.N., Sanchez, J. 2010a. Quantitative proteome analysis of Streptomyces coelicolor Nonsporulating liquid cultures demonstrates a complex differentiation process comparable to that occurring in sporulating solid cultures. *J Proteome Res*, **9**(9), 4801-11.

Manteca, A., Sanchez, J. 2009. Streptomyces development in colonies and soils. *Appl Environ Microbiol*, **75**(9), 2920-4.

Manteca, A., Sanchez, J., Jung, H.R., Schwammle, V., Jensen, O.N. 2010b. Quantitative proteomics analysis of Streptomyces coelicolor development demonstrates that onset of secondary metabolism coincides with hypha differentiation. *Mol Cell Proteomics*, **9**(7), 1423-36.

Manteca, A., Ye, J., Sanchez, J., Jensen, O.N. 2011. Phosphoproteome analysis of Streptomyces development reveals extensive protein phosphorylation accompanying bacterial differentiation. *J Proteome Res*, **10**(12), 5481-92.

Marmann, A., Aly, A.H., Lin, W., Wang, B., Proksch, P. 2014. Co-cultivation--a powerful emerging tool for enhancing the chemical diversity of microorganisms. *Mar Drugs*, **12**(2), 1043-65.

McCormick, J.R., Flardh, K. 2012. Signals and regulators that govern Streptomyces development. *FEMS Microbiol Rev*, **36**(1), 206-31.

McCormick, J.R., Su, E.P., Driks, A., Losick, R. 1994. Growth and viability of Streptomyces coelicolor mutant for the cell division gene ftsZ. *Mol Microbiol*, **14**(2), 243-54.

Meador-Parton, J., Popham, D.L. 2000. Structural analysis of Bacillus subtilis spore peptidoglycan during sporulation. *J Bacteriol*, **182**(16), 4491-9.

Meeske, A.J., Riley, E.P., Robins, W.P., Uehara, T., Mekalanos, J.J., Kahne, D., Walker, S., Kruse, A.C., Bernhardt, T.G., Rudner, D.Z. 2016. SEDS proteins are a widespread family of bacterial cell wall polymerases. *Nature*, **537**(7622), 634-638.

Mendez, C., Chater, K.F. 1987. Cloning of whiG, a gene critical for sporulation of Streptomyces coelicolor A3(2). *J Bacteriol*, **169**(12), 5715-20.

Miguelez, E.M., Hardisson, C., Manzanal, M.B. 1999. Hyphal death during colony development in Streptomyces antibioticus: morphological evidence for the existence of a process of cell deletion in a multicellular prokaryote. *J Cell Biol*, **145**(3), 515-25.

Mikulik, K., Khanh-Hoang, Q., Halada, P., Bezouskova, S., Benada, O., Behal, V. 1999. Expression of the Csp protein family upon cold shock and production of tetracycline in Streptomyces aureofaciens. *Biochem Biophys Res Commun*, **265**(2), 305-10.

Misra, S.K., Milohanic, E., Ake, F., Mijakovic, I., Deutscher, J., Monnet, V., Henry, C. 2011. Analysis of the serine/threonine/tyrosine phosphoproteome of the pathogenic bacterium Listeria monocytogenes reveals phosphorylated proteins related to virulence. *Proteomics*, **11**(21), 4155-65.

Misra, S.K., Moussan Desiree Ake, F., Wu, Z., Milohanic, E., Cao, T.N., Cossart, P., Deutscher, J., Monnet, V., Archambaud, C., Henry, C. 2014. Quantitative proteome analyses identify PrfA-responsive proteins and phosphoproteins in Listeria monocytogenes. *J Proteome Res*, **13**(12), 6046-57.

Mistry, B.V., Del Sol, R., Wright, C., Findlay, K., Dyson, P. 2008. FtsW is a dispensable cell division protein required for Z-ring stabilization during sporulation septation in Streptomyces coelicolor. *J Bacteriol*, **190**(16), 5555-66.

Molle, V., Buttner, M.J. 2000. Different alleles of the response regulator gene bldM arrest Streptomyces coelicolor development at distinct stages. *Mol Microbiol*, **36**(6), 1265-78.

Murray, L., Hentges, F., Hill, J., Karpf, J., Mistry, B., Kreutz, M., Woodall, P., Moss, T., Goodacre, T., Cleft, L., Palate Study, T. 2008. The effect of cleft lip and palate, and the timing of lip repair on mother-infant interactions and infant development. *J Child Psychol Psychiatry*, **49**(2), 115-23.

Nemmara, V.V., Dzhekieva, L., Sarkar, K.S., Adediran, S.A., Duez, C., Nicholas, R.A., Pratt, R.F. 2011. Substrate specificity of low-molecular mass bacterial DD-peptidases. *Biochemistry*, **50**(46), 10091-101.

Nicieza, R.G., Huergo, J., Connolly, B.A., Sanchez, J. 1999. Purification, characterization, and role of nucleases and serine proteases in Streptomyces differentiation. Analogies with the biochemical processes described in late steps of eukaryotic apoptosis. *J Biol Chem*, **274**(29), 20366-75.

Ning, S.B., Guo, H.L., Wang, L., Song, Y.C. 2002. Salt stress induces programmed cell death in prokaryotic organism Anabaena. *J Appl Microbiol*, **93**(1), 15-28.

Noens, E.E., Mersinias, V., Willemse, J., Traag, B.A., Laing, E., Chater, K.F., Smith, C.P., Koerten, H.K., van Wezel, G.P. 2007. Loss of the controlled localization of growth stage-specific cell-wall synthesis pleiotropically affects developmental gene expression in an ssgA mutant of Streptomyces coelicolor. *Mol Microbiol*, **64**(5), 1244-59.

Novotna, G., Hill, C., Vincent, K., Liu, C., Hong, H.J. 2012. A novel membrane protein, VanJ, conferring resistance to teicoplanin. *Antimicrob Agents Chemother*, **56**(4), 1784-96.

Ochi, K. 1990. Streptomyces relC mutants with an altered ribosomal protein ST-L11 and genetic analysis of a Streptomyces griseus relC mutant. *J Bacteriol*, **172**(7), 4008-16.

Ogawa, N., Kuroda, K., Ogawara, S., Miyake, N., Machida, K. 2014. [Psychophysiological effects of hand massage in geriatric facility residents]. *Nihon Eiseigaku Zasshi*, **69**(1), 24-30.

Ogawara, H. 2015. Penicillin-binding proteins in Actinobacteria. *J Antibiot (Tokyo)*, **68**(4), 223-45.

Onaka, H., Nakagawa, T., Horinouchi, S. 1998. Involvement of two A-factor receptor homologues in Streptomyces coelicolor A3(2) in the regulation of secondary metabolism and morphogenesis. *Mol Microbiol*, **28**(4), 743-53.

Ou, X., Zhang, B., Zhang, L., Zhao, G., Ding, X. 2009. Characterization of rrdA, a TetR family protein gene involved in the regulation of secondary metabolism in Streptomyces coelicolor. *Appl Environ Microbiol*, **75**(7), 2158-65.

Pamboukian, C.R., Facciotti, M.C. 2004. Production of antitumoral retamycin during fed-batch fermentations of Streptomyces olindensis. *Appl Biochem Biotechnol*, **112**(2), 111-22.

Park, U.M., Suh, J.W., Hong, S.K. 2000. Genetic Analysis of absR, a new abs locus of Streptomyces coelicolor. *J Microbiol Biotechnol* **10**, 169-175.

Parker, J.L., Jones, A.M., Serazetdinova, L., Saalbach, G., Bibb, M.J., Naldrett, M.J. 2010. Analysis of the phosphoproteome of the multicellular bacterium Streptomyces coelicolor A3(2) by protein/peptide fractionation, phosphopeptide enrichment and high-accuracy mass spectrometry. *Proteomics*, **10**(13), 2486-97.

Petersen, F., Zahner, H., Metzger, J.W., Freund, S., Hummel, R.P. 1993. Germicidin, an autoregulative germination inhibitor of Streptomyces viridochromogenes NRRL B-1551. *J Antibiot (Tokyo)*, **46**(7), 1126-38.

Pethe, K., Sequeira, P.C., Agarwalla, S., Rhee, K., Kuhen, K., Phong, W.Y., Patel, V., Beer, D., Walker, J.R., Duraiswamy, J., Jiricek, J., Keller, T.H., Chatterjee, A., Tan, M.P., Ujjini, M., Rao, S.P., Camacho, L., Bifani, P., Mak, P.A., Ma, I., Barnes, S.W., Chen, Z., Plouffe, D., Thayalan, P., Ng, S.H., Au, M., Lee, B.H., Tan, B.H., Ravindran, S., Nanjundappa, M., Lin, X., Goh, A., Lakshminarayana, S.B., Shoen, C., Cynamon, M., Kreiswirth, B., Dartois, V., Peters, E.C., Glynne, R., Brenner, S., Dick, T. 2010. A chemical genetic screen in Mycobacterium tuberculosis identifies carbon-source-dependent growth inhibitors devoid of in vivo efficacy. *Nat Commun*, **1**, 57.

Polpitiya, A.D., Qian, W.J., Jaitly, N., Petyuk, V.A., Adkins, J.N., Camp, D.G., 2nd, Anderson, G.A., Smith, R.D. 2008. DAnTE: a statistical tool for quantitative analysis of -omics data. *Bioinformatics*, **24**(13), 1556-8.

Pope, M.K., Green, B., Westpheling, J. 1998. The bldB gene encodes a small protein required for morphogenesis, antibiotic production, and catabolite control in Streptomyces coelicolor. *J Bacteriol*, **180**(6), 1556-62.

Prisic, S., Dankwa, S., Schwartz, D., Chou, M.F., Locasale, J.W., Kang, C.M., Bemis, G., Church, G.M., Steen, H., Husson, R.N. 2010. Extensive

phosphorylation with overlapping specificity by Mycobacterium tuberculosis serine/threonine protein kinases. *Proc Natl Acad Sci U S A*, **107**(16), 7521-6.

Rauniyar, N., Yates, J.R., 3rd. 2014. Isobaric labeling-based relative quantification in shotgun proteomics. *J Proteome Res*, **13**(12), 5293-309.

Ravichandran, A., Sugiyama, N., Tomita, M., Swarup, S., Ishihama, Y. 2009. Ser/Thr/Tyr phosphoproteome analysis of pathogenic and non-pathogenic Pseudomonas species. *Proteomics*, **9**(10), 2764-75.

Ravikumar, V., Shi, L., Krug, K., Derouiche, A., Jers, C., Cousin, C., Kobir, A., Mijakovic, I., Macek, B. 2014. Quantitative phosphoproteome analysis of Bacillus subtilis reveals novel substrates of the kinase PrkC and phosphatase PrpC. *Mol Cell Proteomics*, **13**(8), 1965-78.

Reynolds, P.E. 1989. Structure, biochemistry and mechanism of action of glycopeptide antibiotics. *Eur J Clin Microbiol Infect Dis*, **8**(11), 943-50.

Rigali, S., Titgemeyer, F., Barends, S., Mulder, S., Thomae, A.W., Hopwood, D.A., van Wezel, G.P. 2008. Feast or famine: the global regulator DasR links nutrient stress to antibiotic production by Streptomyces. *EMBO Rep*, **9**(7), 670-5.

Rodriguez-Garcia, A., Barreiro, C., Santos-Beneit, F., Sola-Landa, A., Martin, J.F. 2007. Genome-wide transcriptomic and proteomic analysis of the primary response to phosphate limitation in Streptomyces coelicolor M145 and in a DeltaphoP mutant. *Proteomics*, **7**(14), 2410-29.

Roubos, J.A., Krabben, P., Luiten, R.G., Verbruggen, H.B., Heijnen, J.J. 2001. A quantitative approach to characterizing cell lysis caused by mechanical agitation of Streptomyces clavuligerus. *Biotechnol Prog*, **17**(2), 336-47.

Ryan F. Seipke, M.K., Matthew I. Hutchings. 2012. Streptomyces as symbionts: an emerging and widespread theme? *FEMS Microbiology Reviews*, **36**(4), 862-876.

Ryding, N.J., Bibb, M.J., Molle, V., Findlay, K.C., Chater, K.F., Buttner, M.J. 1999. New sporulation loci in Streptomyces coelicolor A3(2). *J Bacteriol*, **181**(17), 5419-25.

Salas, J.A., Guijarro, J.A., Hardisson, C. 1983. High calcium content in Streptomyces spores and its release as an early event during spore germination. *J Bacteriol*, **155**(3), 1316-23.

Salerno, P., Larsson, J., Bucca, G., Laing, E., Smith, C.P., Flardh, K. 2009. One of the two genes encoding nucleoid-associated HU proteins in Streptomyces coelicolor is developmentally regulated and specifically involved in spore maturation. *J Bacteriol*, **191**(21), 6489-500.

Santos-Beneit, F., Martıín, J.F. 2013. Vancomycin resistance in Streptomyces coelicolor is phosphate-dependent but is not mediated by the PhoP regulator. *Journal of Global Antimicrobial Resistance*(1), 109-113.

Schaberle, T.F., Vollmer, W., Frasch, H.J., Huttel, S., Kulik, A., Rottgen, M., von Thaler, A.K., Wohlleben, W., Stegmann, E. 2011. Self-resistance and

cell wall composition in the glycopeptide producer Amycolatopsis balhimycina. *Antimicrob Agents Chemother*, **55**(9), 4283-9.

Schleifer, K.H., Kandler, O. 1972. Peptidoglycan types of bacterial cell walls and their taxonomic implications. *Bacteriol Rev*, **36**(4), 407-77.

Sevcikova, B., Kormanec, J. 2003. The ssgB gene, encoding a member of the regulon of stress-response sigma factor sigmaH, is essential for aerial mycelium septation in Streptomyces coelicolor A3(2). *Arch Microbiol*, **180**(5), 380-4.

Sexton, D.L., St-Onge, R.J., Haiser, H.J., Yousef, M.R., Brady, L., Gao, C., Leonard, J., Elliot, M.A. 2015. Resuscitation-promoting factors are cell wall-lytic enzymes with important roles in the germination and growth of Streptomyces coelicolor. *J Bacteriol*, **197**(5), 848-60.

Sharma, K., D'Souza, R.C., Tyanova, S., Schaab, C., Wisniewski, J.R., Cox, J., Mann, M. 2014. Ultradeep human phosphoproteome reveals a distinct regulatory nature of Tyr and Ser/Thr-based signaling. *Cell Rep*, **8**(5), 1583-94.

Silhavy, T.J., Kahne, D., Walker, S. 2010. The bacterial cell envelope. *Cold Spring Harb Perspect Biol*, **2**(5), a000414.

Simkhada, J.R., Cho, S.S., Park, S.J., Mander, P., Choi, Y.H., Lee, H.J., Yoo, J.C. 2010. An oxidant- and organic solvent-resistant alkaline metalloprotease from Streptomyces olivochromogenes. *Appl Biochem Biotechnol*, **162**(5), 1457-70.

Soares, N.C., Spat, P., Krug, K., Macek, B. 2013. Global dynamics of the Escherichia coli proteome and phosphoproteome during growth in minimal medium. *J Proteome Res*, **12**(6), 2611-21.

Soares, N.C., Spat, P., Mendez, J.A., Nakedi, K., Aranda, J., Bou, G. 2014. Ser/Thr/Tyr phosphoproteome characterization of Acinetobacter baumannii: comparison between a reference strain and a highly invasive multidrug-resistant clinical isolate. *J Proteomics*, **102**, 113-24.

Sogaard-Andersen, L., Yang, Z. 2008. Programmed cell death: role for MazF and MrpC in Myxococcus multicellular development. *Curr Biol*, **18**(8), R337-9.

Soufi, B., Gnad, F., Jensen, P.R., Petranovic, D., Mann, M., Mijakovic, I., Macek, B. 2008. The Ser/Thr/Tyr phosphoproteome of Lactococcus lactis IL1403 reveals multiply phosphorylated proteins. *Proteomics*, **8**(17), 3486-93.

Stocks, S.M., Thomas, C.R. 2001. Viability, strength, and fragmentation of Saccharopolyspora erythraea in submerged fermentation. *Biotechnol Bioeng*, **75**(6), 702-9.

Sun, J., Hesketh, A., Bibb, M. 2001. Functional analysis of relA and rshA, two relA/spoT homologues of Streptomyces coelicolor A3(2). *J Bacteriol*, **183**(11), 3488-98.

Sun, X., Ge, F., Xiao, C.L., Yin, X.F., Ge, R., Zhang, L.H., He, Q.Y. 2010. Phosphoproteomic analysis reveals the multiple roles of

phosphorylation in pathogenic bacterium Streptococcus pneumoniae. *J Proteome Res*, **9**(1), 275-82.

Susstrunk, U., Pidoux, J., Taubert, S., Ullmann, A., Thompson, C.J. 1998. Pleiotropic effects of cAMP on germination, antibiotic biosynthesis and morphological development in Streptomyces coelicolor. *Mol Microbiol*, **30**(1), 33-46.

Takahata, Y., Inoue, M., Kim, K., Iio, Y., Miyamoto, M., Masui, R., Ishihama, Y., Kuramitsu, S. 2012. Close proximity of phosphorylation sites to ligand in the phosphoproteome of the extreme thermophile Thermus thermophilus HB8. *Proteomics*, **12**(9), 1414-30.

Takano, E., Tao, M., Long, F., Bibb, M.J., Wang, L., Li, W., Buttner, M.J., Bibb, M.J., Deng, Z.X., Chater, K.F. 2003. A rare leucine codon in adpA is implicated in the morphological defect of bldA mutants of Streptomyces coelicolor. *Mol Microbiol*, **50**(2), 475-86.

Techapun, C., Poosaran, N., Watanabe, M., Sasaki, K. 2003. Optimization of aeration and agitation rates to improve cellulase-free xylanase production by thermotolerant Streptomyces sp. Ab106 and repeated fed-batch cultivation using agricultural waste. *J Biosci Bioeng*, **95**(3), 298-301.

Thingholm, T.E., Jensen, O.N. 2009. Enrichment and characterization of phosphopeptides by immobilized metal affinity chromatography (IMAC) and mass spectrometry. *Methods Mol Biol*, **527**, 47-56, xi.

Thingholm, T.E., Jorgensen, T.J., Jensen, O.N., Larsen, M.R. 2006. Highly selective enrichment of phosphorylated peptides using titanium dioxide. *Nat Protoc*, **1**(4), 1929-35.

Thompson, C.J., Fink, D., Nguyen, L.D. 2002. Principles of microbial alchemy: insights from the Streptomyces coelicolor genome sequence. *Genome Biol*, **3**(7), REVIEWS1020.

Uguru, G.C., Stephens, K.E., Stead, J.A., Towle, J.E., Baumberg, S., McDowall, K.J. 2005. Transcriptional activation of the pathway-specific regulator of the actinorhodin biosynthetic genes in Streptomyces coelicolor. *Mol Microbiol*, **58**(1), 131-50.

van Veluw, G.J., Petrus, M.L., Gubbens, J., de Graaf, R., de Jong, I.P., van Wezel, G.P., Wosten, H.A., Claessen, D. 2012. Analysis of two distinct mycelial populations in liquid-grown Streptomyces cultures using a flow cytometry-based proteomics approach. *Appl Microbiol Biotechnol*, **96**(5), 1301-12.

van Wezel, G.P., Krabben, P., Traag, B.A., Keijser, B.J., Kerste, R., Vijgenboom, E., Heijnen, J.J., Kraal, B. 2006. Unlocking Streptomyces spp. for use as sustainable industrial production platforms by morphological engineering. *Appl Environ Microbiol*, **72**(8), 5283-8.

van Wezel, G.P., **McDowall**, K.J. 2011. The regulation of the secondary metabolism of Streptomyces: new links and experimental advances. *Nat Prod Rep*, **28**(7), 1311-33.

Vida, T.A., Emr, S.D. 1995. A new vital stain for visualizing vacuolar membrane dynamics and endocytosis in yeast. *J Cell Biol*, **128**(5), 779-92.

W. Whitman, M. Goodfellow, P. Kämpfer, H. J. Busse, M. Trujillo, W. Ludwig, Suzuki, K.I. 2012. *Bergey's Manual of Systematic Bacteriology: Volume 5: The Actinobacteria. Part A.*, Springer Science & Business Media.

Waksman, S.A., Henrici, A.T. 1943. The Nomenclature and Classification of the Actinomycetes. *J Bacteriol*, **46**(4), 337-41.

Wang, C., Ge, H., Dong, H., Zhu, C., Li, Y., Zheng, J., Cen, P. 2007. A novel pair of two-component signal transduction system ecrE1/ecrE2 regulating antibiotic biosynthesis in Streptomyces coelicolor. *Biologia*, **62**(5), 511-516.

Wang, S.L., Fan, K.Q., Yang, X., Lin, Z.X., Xu, X.P., Yang, K.Q. 2008. CabC, an EF-hand calcium-binding protein, is involved in Ca2+-mediated regulation of spore germination and aerial hypha formation in Streptomyces coelicolor. *J Bacteriol*, **190**(11), 4061-8.

Wilkins, M. 2009. Proteomics data mining. *Expert Rev Proteomics*, **6**(6), 599-603.

Willemse, J., Borst, J.W., de Waal, E., Bisseling, T., van Wezel, G.P. 2011. Positive control of cell division: FtsZ is recruited by SsgB during sporulation of Streptomyces. *Genes Dev*, **25**(1), 89-99.

Willey, J., Schwedock, J., Losick, R. 1993. Multiple extracellular signals govern the production of a morphogenetic protein involved in aerial mycelium formation by Streptomyces coelicolor. *Genes Dev*, **7**(5), 895-903.

Williams, S.T. 1985. *Oligotrophy in soil: fact or fiction?* Academic press, London.

Wu, G., Zhi, W., Hu, Y., Liang, M., Yang, W. 2016. Comparative Proteomic Analysis of Streptomyces aureochromogenes Under Different Carbon Sources and Insights into Polyoxin Production. *Appl Biochem Biotechnol*, **180**(3), 491-503.

Xu, G., Wang, J., Wang, L., Tian, X., Yang, H., Fan, K., Yang, K., Tan, H. 2010. "Pseudo" gamma-butyrolactone receptors respond to antibiotic signals to coordinate antibiotic biosynthesis. *J Biol Chem*, **285**(35), 27440-8.

Yague, P., Lopez-Garcia, M.T., Rioseras, B., Sanchez, J., Manteca, A. 2012. New insights on the development of Streptomyces and their relationships with secondary metabolite production. *Curr Trends Microbiol*, **8**, 65-73.

Yague, P., Lopez-Garcia, M.T., Rioseras, B., Sanchez, J., Manteca, A. 2013a. Pre-sporulation stages of Streptomyces differentiation: state-of-the-art and future perspectives. *FEMS Microbiol Lett*, **342**(2), 79-88.

Yague, P., Rodriguez-Garcia, A., Lopez-Garcia, M.T., Martin, J.F., Rioseras, B., Sanchez, J., Manteca, A. 2013b. Transcriptomic analysis of Streptomyces coelicolor differentiation in solid sporulating cultures:

first compartmentalized and second multinucleated mycelia have different and distinctive transcriptomes. *PLoS One*, **8**(3), e60665.

Yague, P., Rodriguez-Garcia, A., Lopez-Garcia, M.T., Rioseras, B., Martin, J.F., Sanchez, J., Manteca, A. 2014. Transcriptomic analysis of liquid non-sporulating Streptomyces coelicolor cultures demonstrates the existence of a complex differentiation comparable to that occurring in solid sporulating cultures. *PLoS One*, **9**(1), e86296.

Zappia, G., Menendez, P., Monache, G.D., Misiti, D., Nevola, L., Botta, B. 2007. The contribution of oxazolidinone frame to the biological activity of pharmaceutical drugs and natural products. *Mini Rev Med Chem*, **7**(4), 389-409.

Zupan, J.R., Cameron, T.A., Anderson-Furgeson, J., Zambryski, P.C. 2013. Dynamic FtsA and FtsZ localization and outer membrane alterations during polar growth and cell division in Agrobacterium tumefaciens. *Proc Natl Acad Sci U S A*, **110**(22), 9060-5.

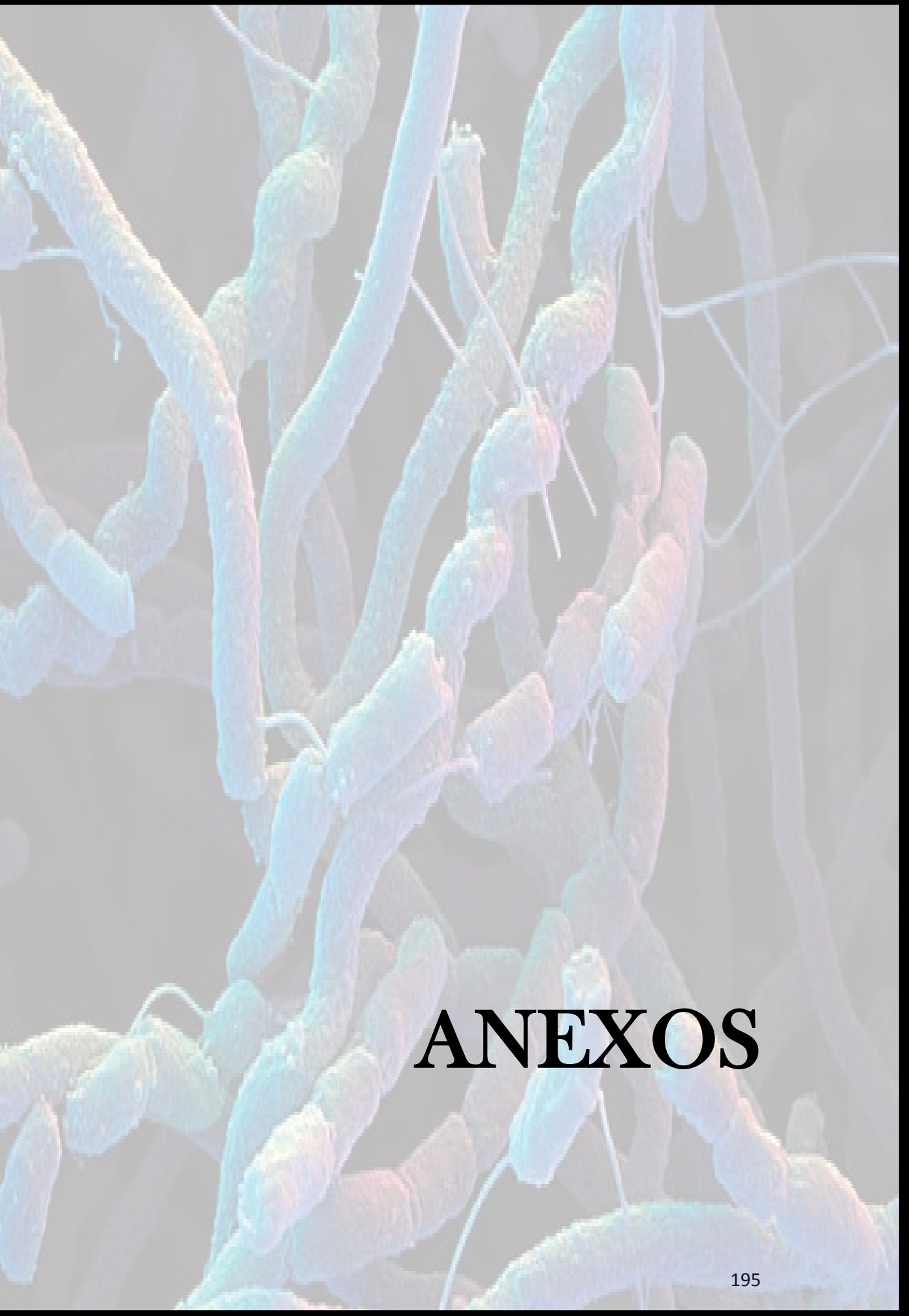

ANEXOS

ANEXO 1
Material Suplementario del Manuscrito 1

En este anexo se incluye el material suplementario del **manuscrito 1**:

Supplemental Fig. 1: *"Heat map"* con la abundancia de las proteínas cuantificadas.

Supplemental Fig. 2: *"Heat map"* con la abundancia de los fosfopéptidos cuantificados.

"Supplemental Table 1" y **"Supplemental Table 2"** corresponden a los datos de proteómica y fosfoproteómica cuantitativa y se encuentran en el formato digital de esta Tesis.

Supplemental Fig. 1: Protein abundance heat map of the non-phosphoproteins. Yellow less abundant; red more abundant

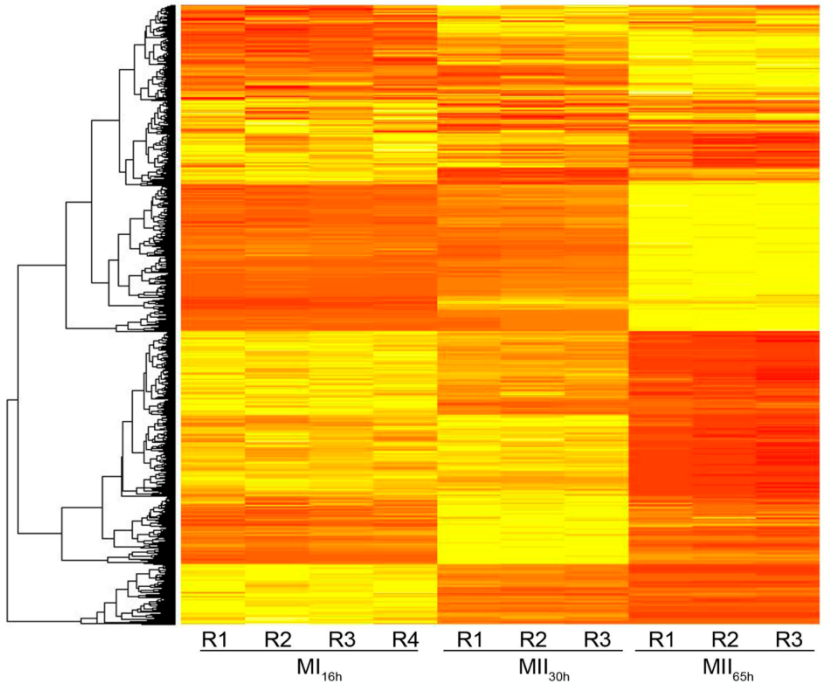

Supplemental Fig. 2: Phosphopeptide abundance heat map. Yellow more abundant; red, less abundant

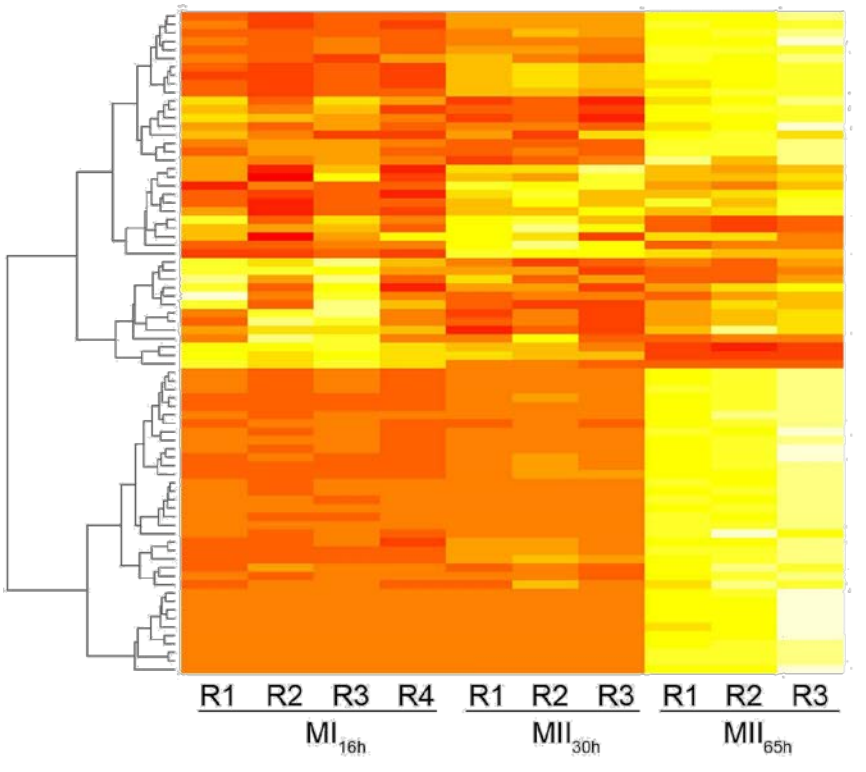

ANEXO 2
Material Suplementario del Manuscrito 2

En este anexo se incluye el material suplementario del **manuscrito 2**:

Supplementary Fig. S1. Imágenes usadas para cuantificar el diámetro de las esporas en *S. coelicolor* SCO4439::Tn5062 y SCO4439::Tn5062[pBRB3*].

Supplementary Fig. S2. Imágenes usadas para cuantificar el diámetro de las esporas en *S. coelicolor* [pMS82] y SCO4439::Tn5062[pBRB3].

"Supplementary Movie 1", "Supplementary Movie 2", "Supplementary Movie 3" y **"Supplementary Movie 4"** corresponden a los experimentos de *"time-lapse"* con microscopía confocal de la germinación de las esporas de las cepas *S. coelicolor* silvestre, *SCO4439::Tn5062, SCO4439::Tn5062* [pBRB3] y SCO4439::Tn5062[pBRB3*] respectivamente. Este material se encuentra en el formato digital de esta Tesis.

Fig. S1. MASTER IMAGES USED TO QUANTIFY SPORE DIAMETER

Streptomyces coelicolor 5-hours. Spore diameters measured are labelled by lines.

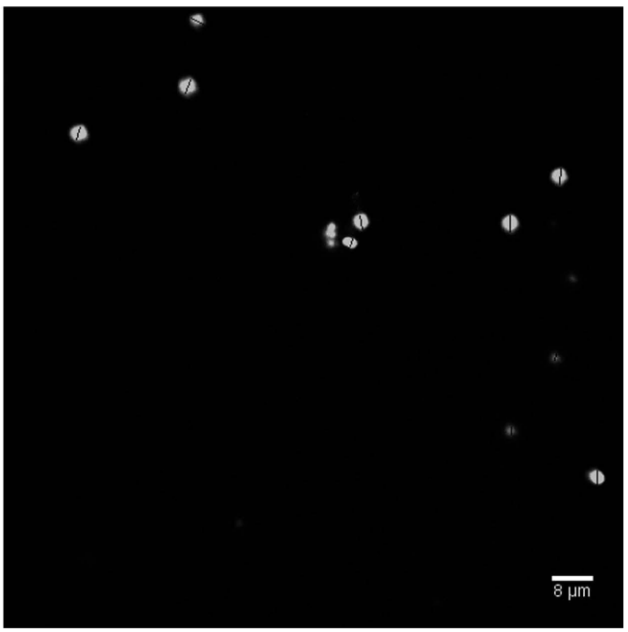

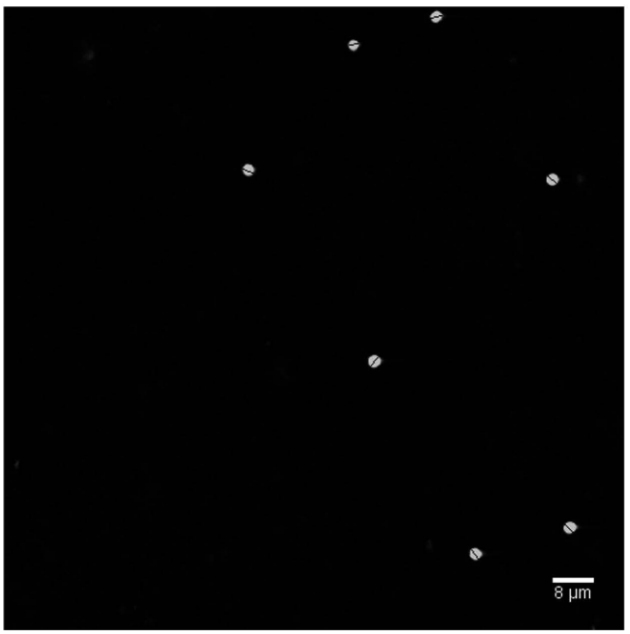

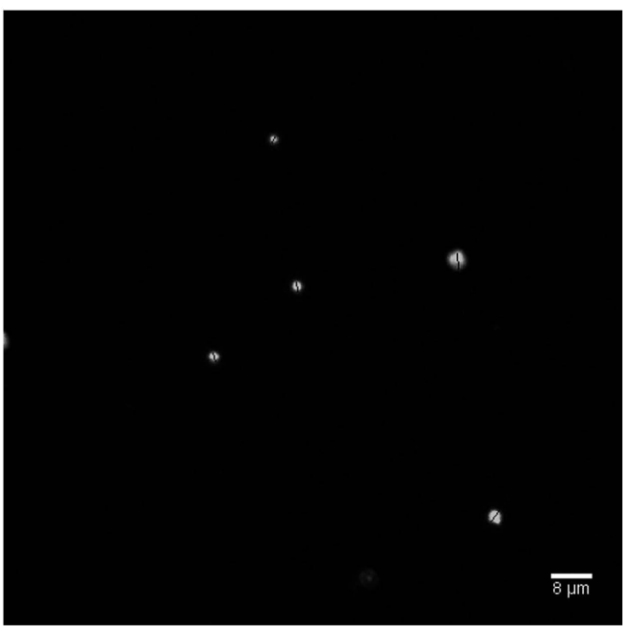

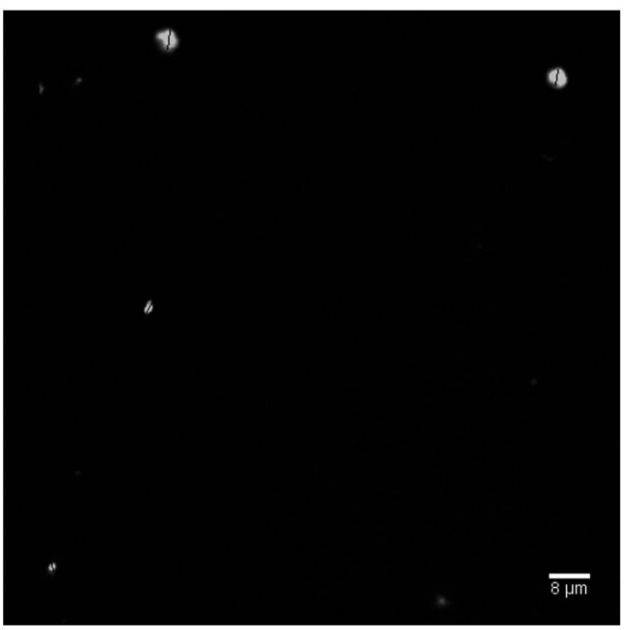

Fig. S1. MASTER IMAGES USED TO QUANTIFY SPORE DIAMETER

Streptomyces coelicolor 5-hours. Spore diameters measured are labelled by lines.

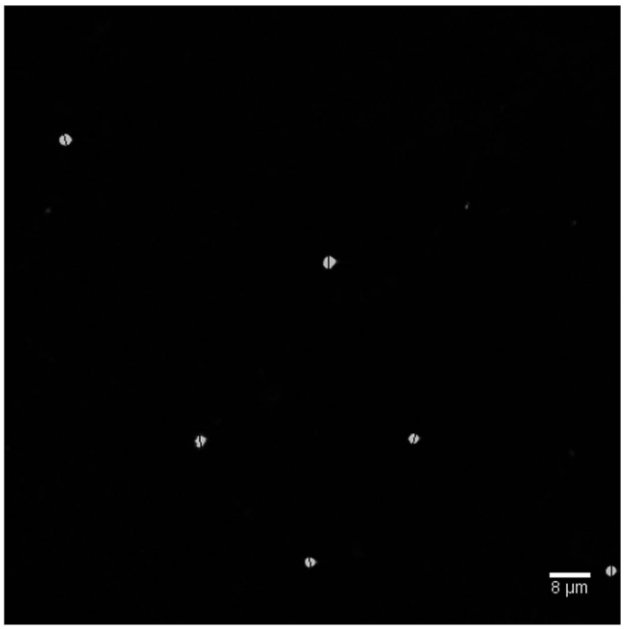

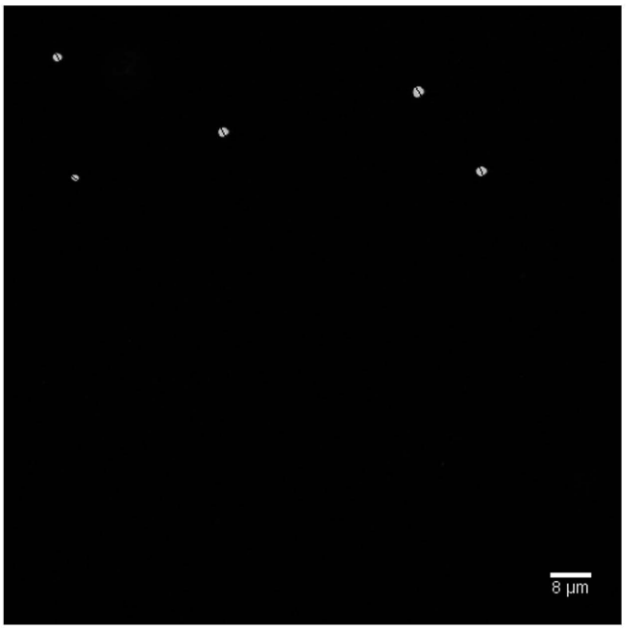

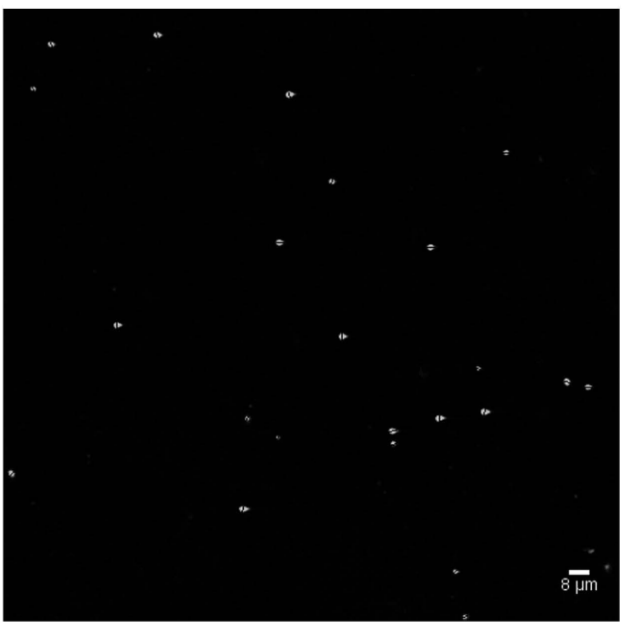

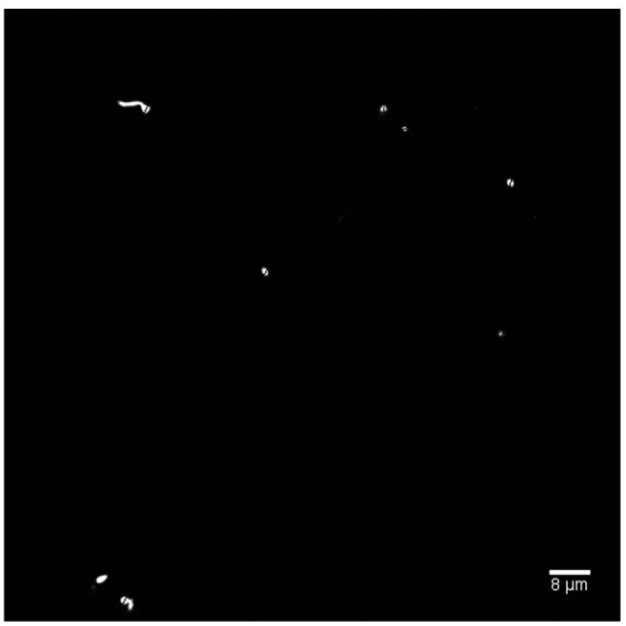

Fig. S1. MASTER IMAGES USED TO QUANTIFY SPORE DIAMETER

Streptomyces coelicolor 5-hours. Spore diameters measured are labelled by lines.

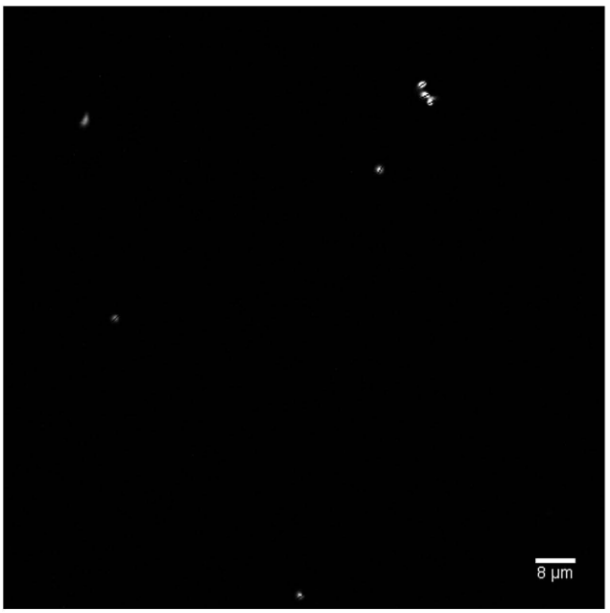

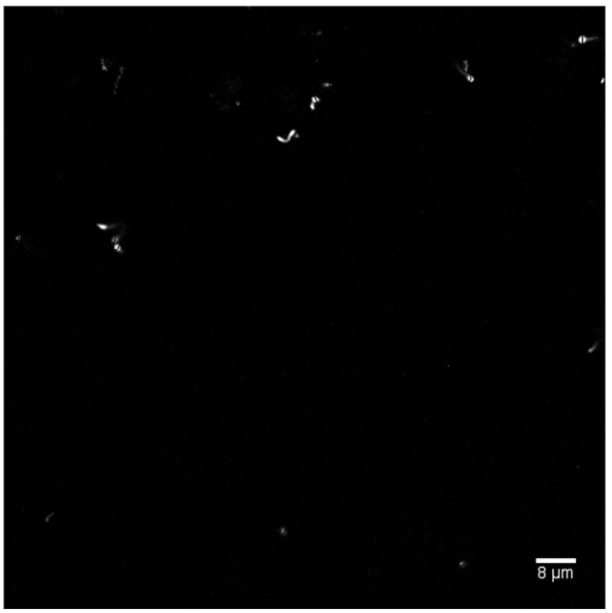

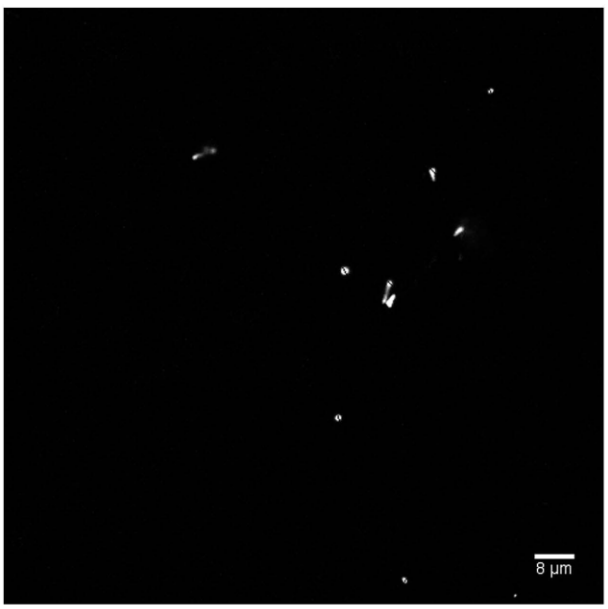

Fig. S1. MASTER IMAGES USED TO QUANTIFY SPORE DIAMETER

Streptomyces coelicolor wild type. 8-hours. Spore diameters measured are labelled by lines.

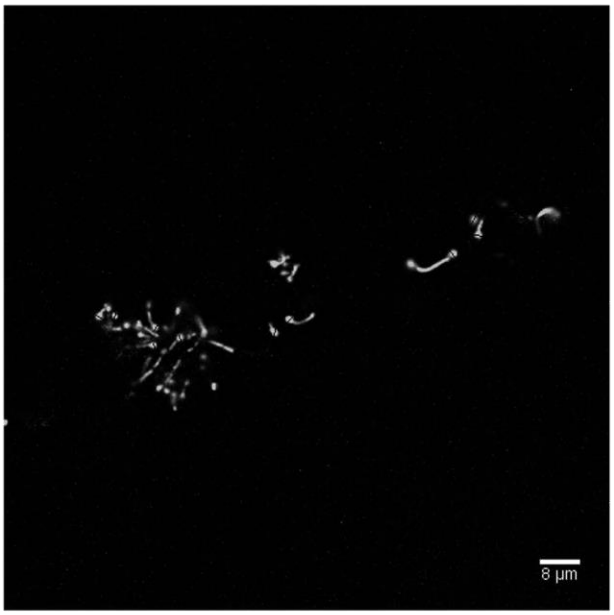

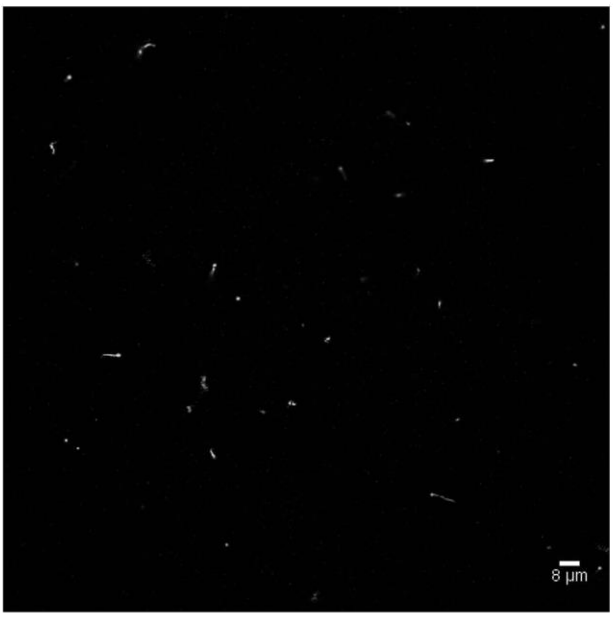

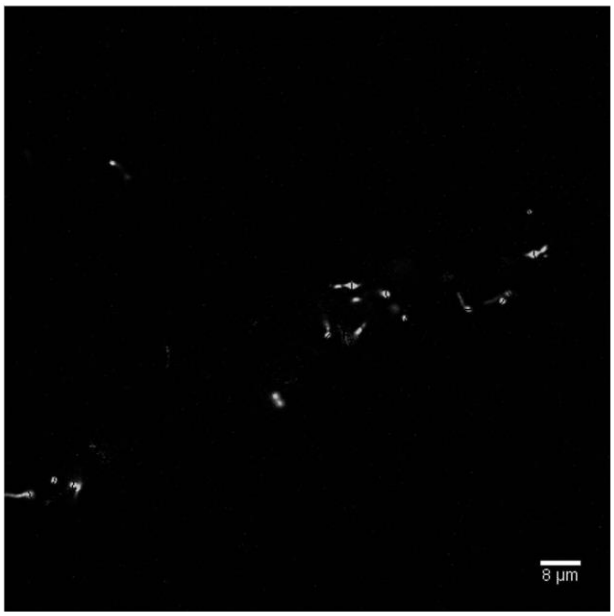

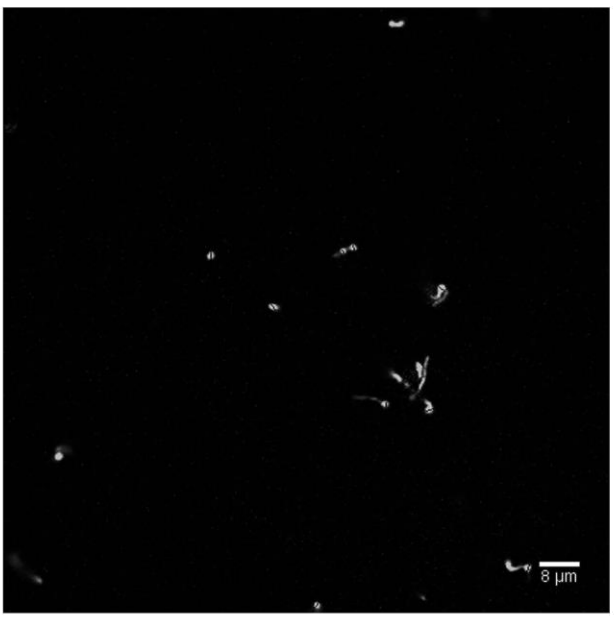

Fig. S1. MASTER IMAGES USED TO QUANTIFY SPORE DIAMETER

Streptomyces coelicolor wild type. 8-hours. Spore diameters measured are labelled by lines.

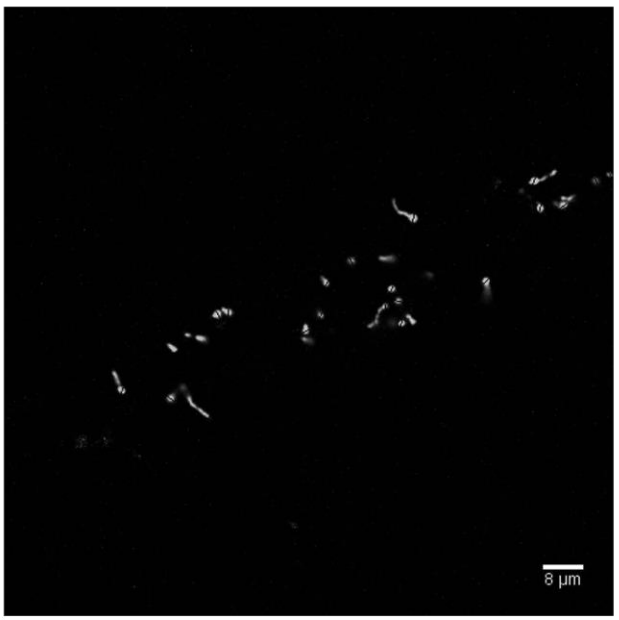

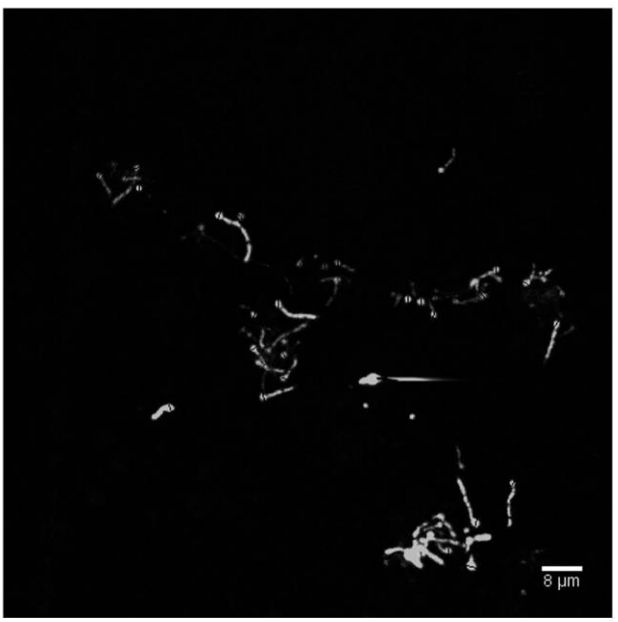

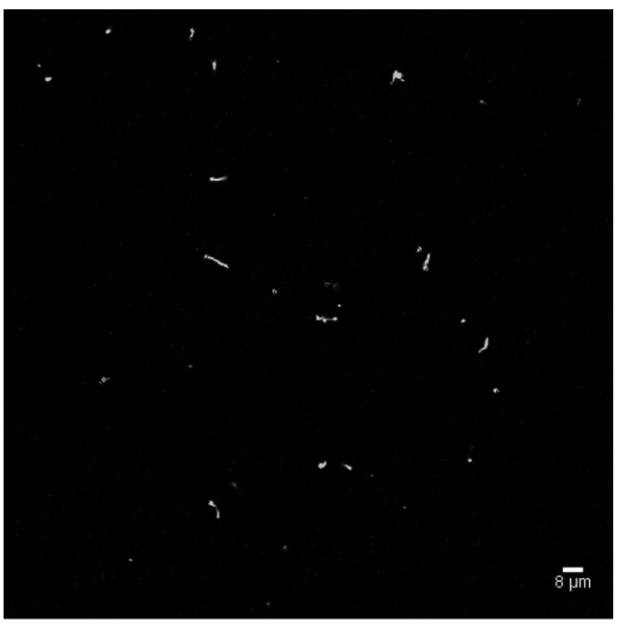

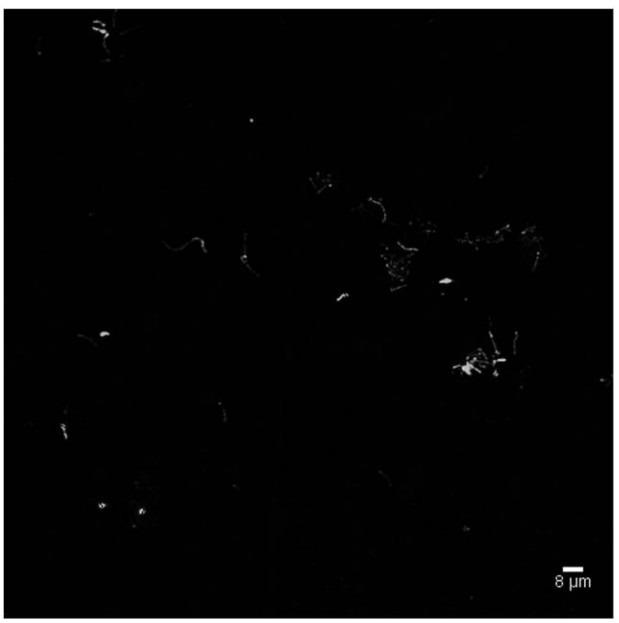

Fig. S1. MASTER IMAGES USED TO QUANTIFY SPORE DIAMETER

Streptomyces coelicolor wild type. 15-hours. Spore diameters measured are labelled by lines.

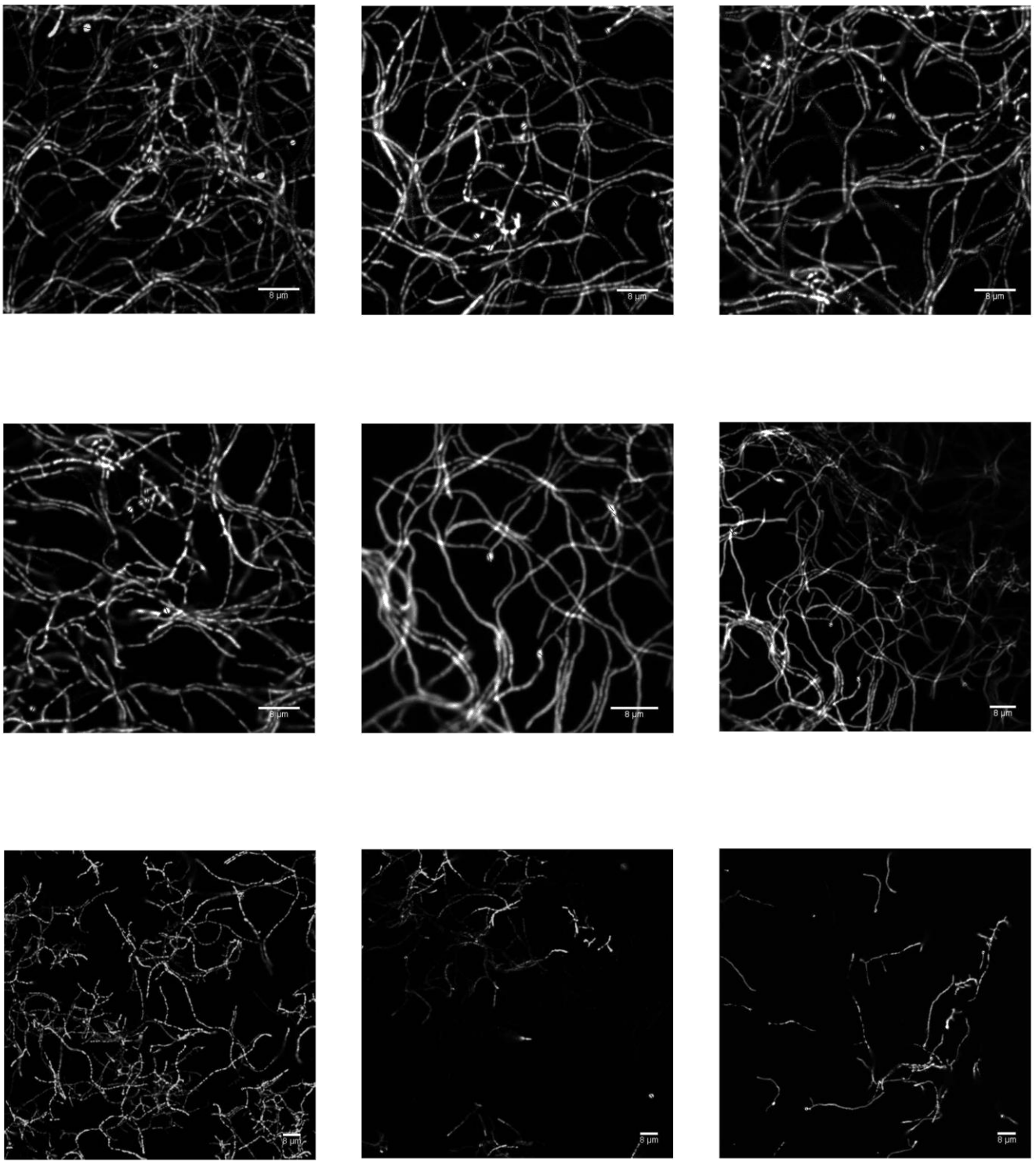

Fig. S1. MASTER IMAGES USED TO QUANTIFY SPORE DIAMETER

Streptomyces coelicolor wild type. 15-hours. Spore diameters measured are labelled by lines.

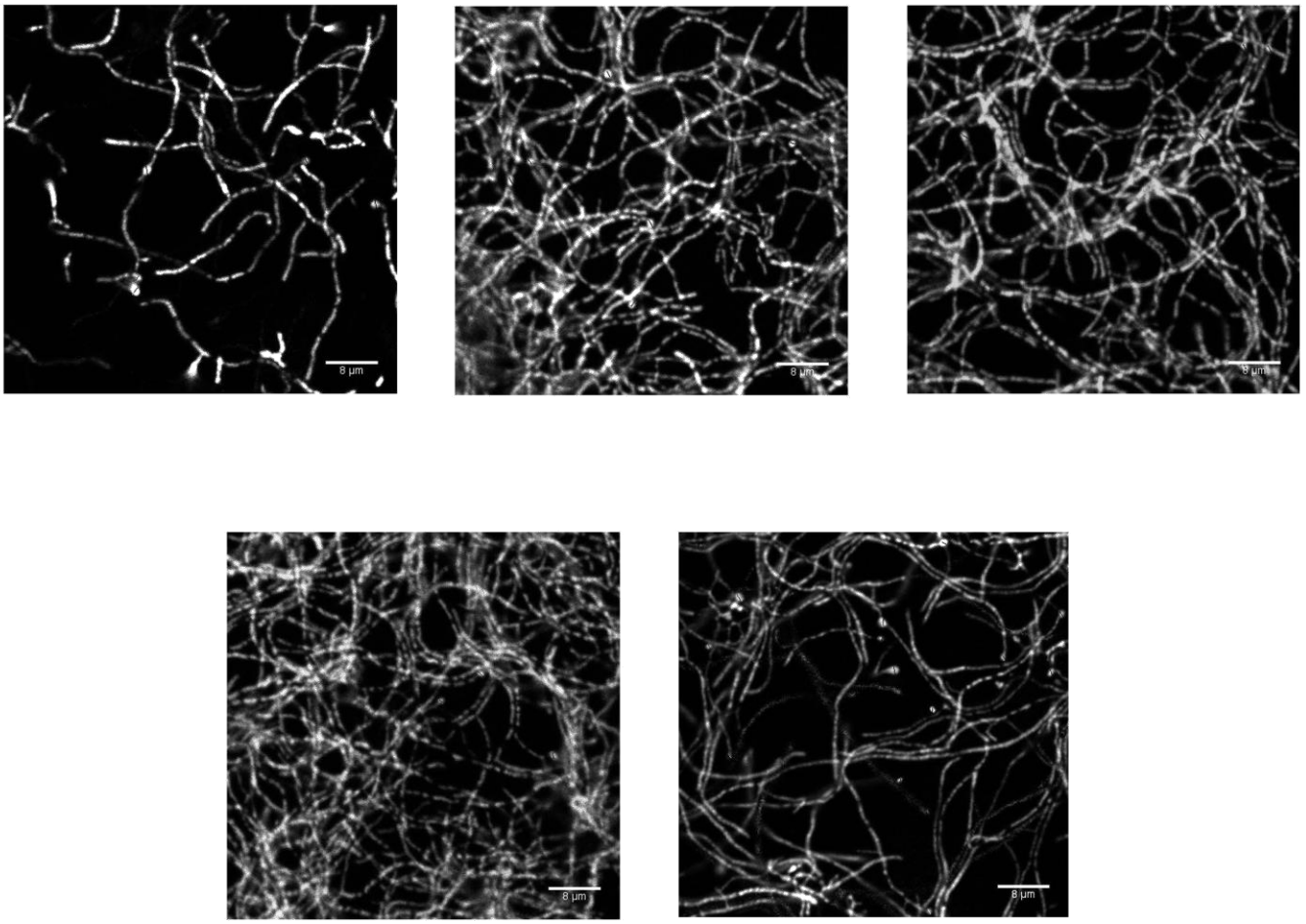

Fig. S1. MASTER IMAGES USED TO QUANTIFY SPORE DIAMETER

Streptomyces coelicolor::Tn5062 5-hours. Spore diameters measured are labelled by lines.

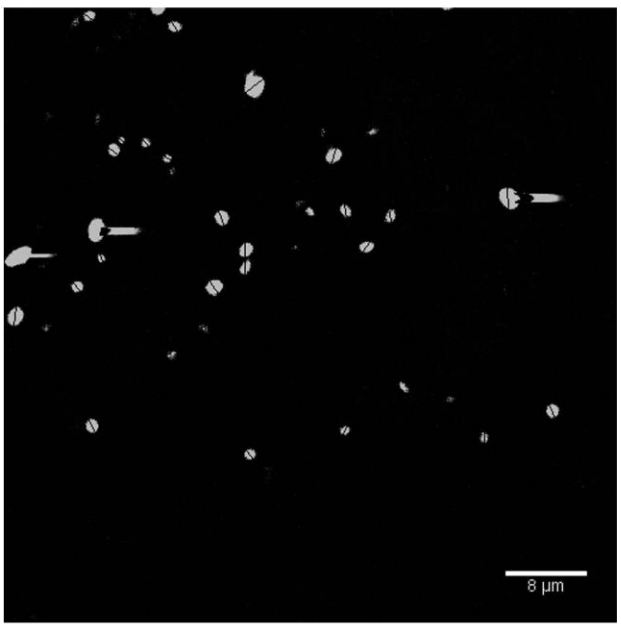

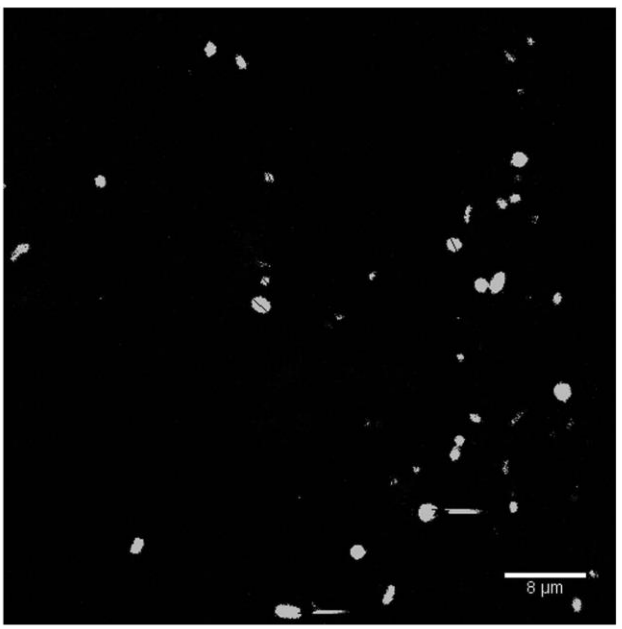

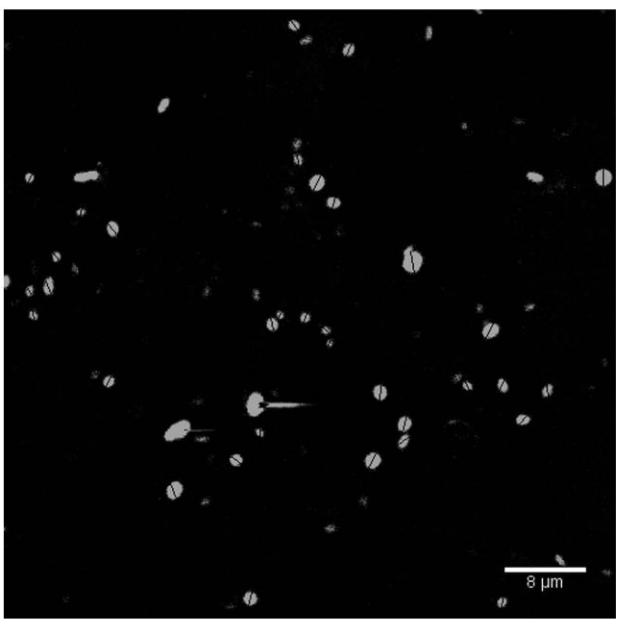

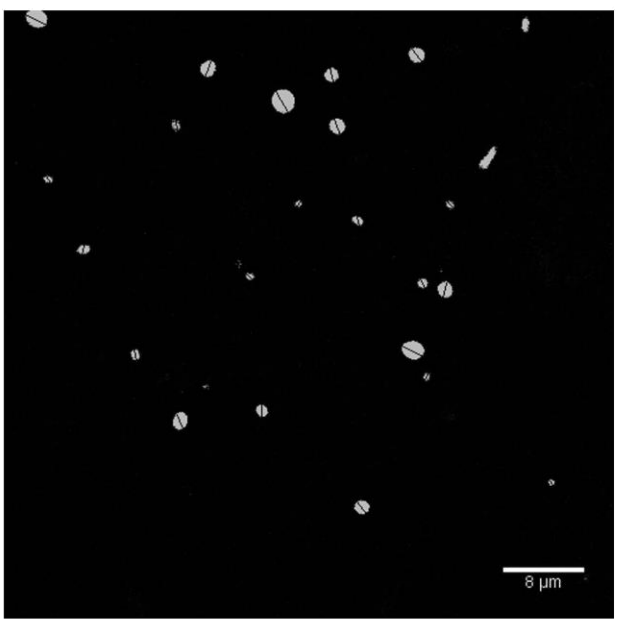

Fig. S1. MASTER IMAGES USED TO QUANTIFY SPORE DIAMETER

Streptomyces coelicolor::Tn5062 5-hours. Spore diameters measured are labelled by lines.

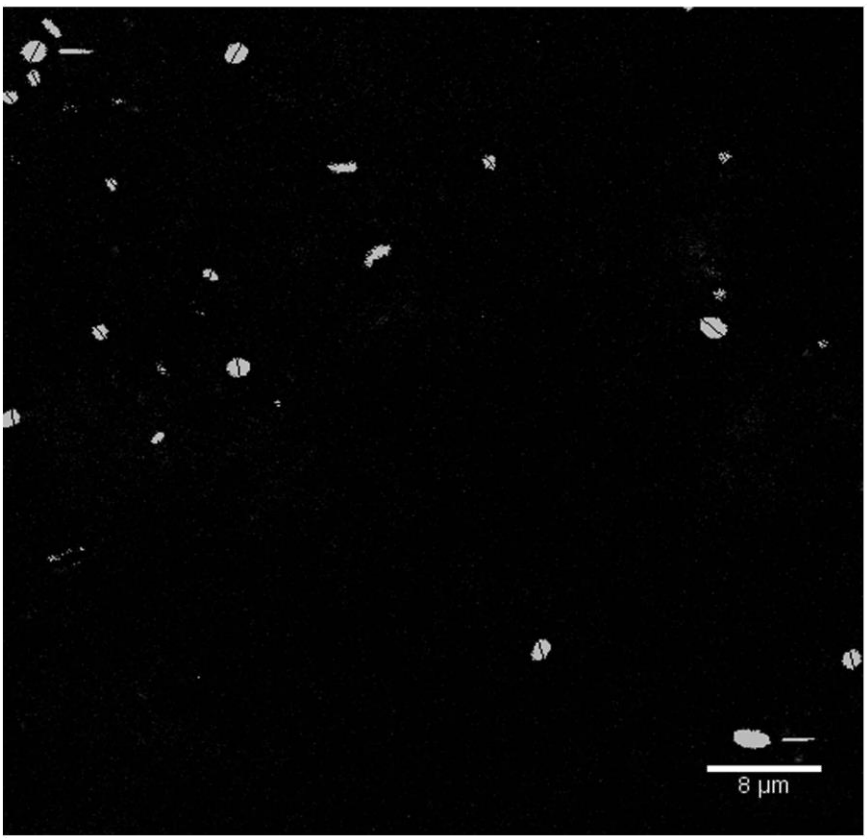

Fig. S1. MASTER IMAGES USED TO QUANTIFY SPORE DIAMETER

Streptomyces coelicolor::Tn5062 8-hours. Spore diameters measured are labelled by lines.

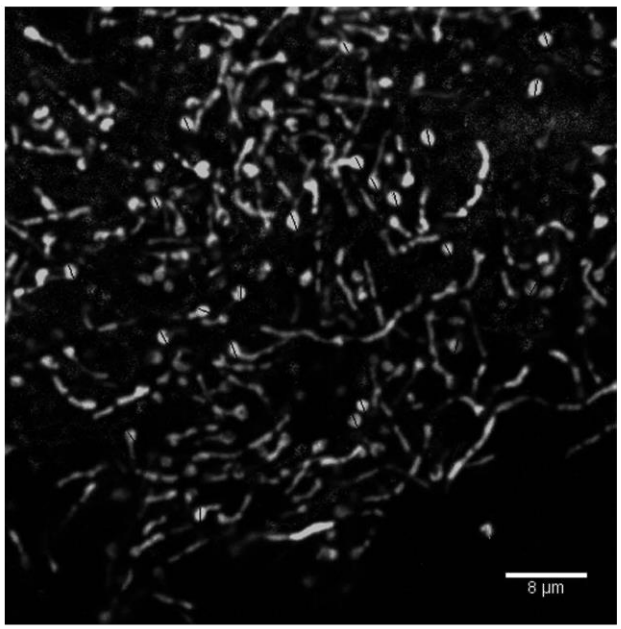

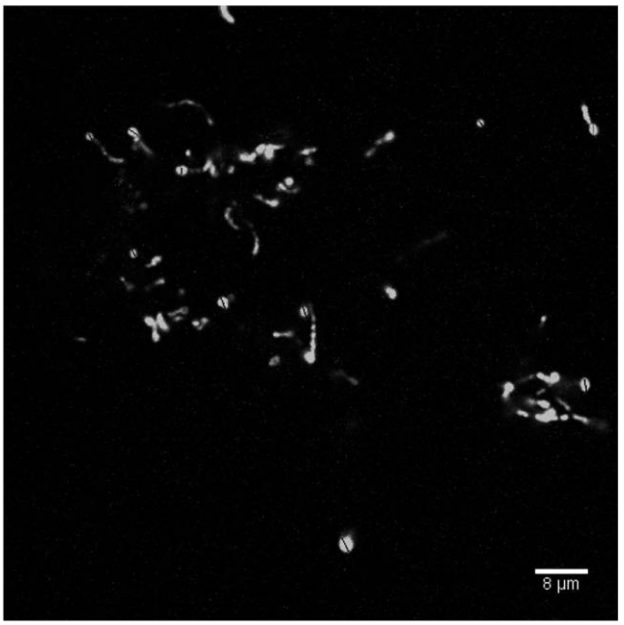

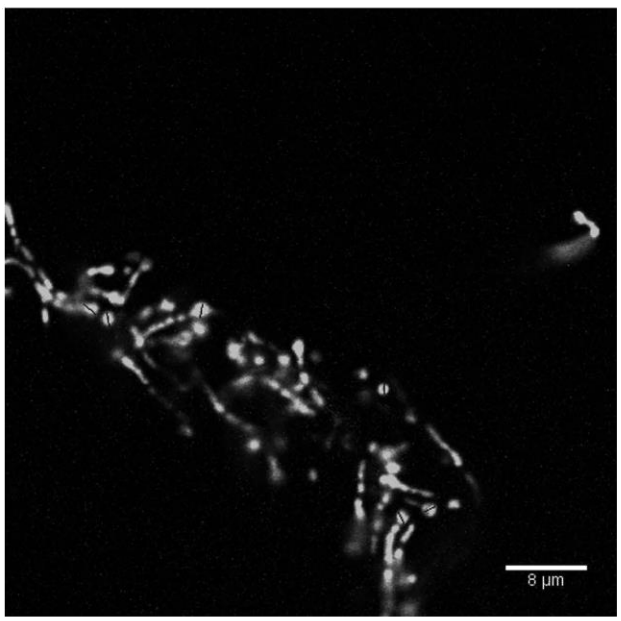

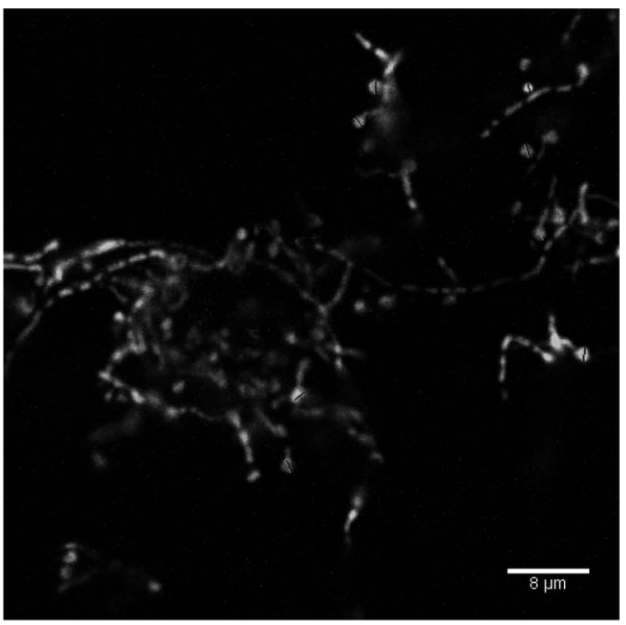

Fig. S1. MASTER IMAGES USED TO QUANTIFY SPORE DIAMETER

Streptomyces coelicolor::Tn5062 8-hours. Spore diameters measured are labelled by lines.

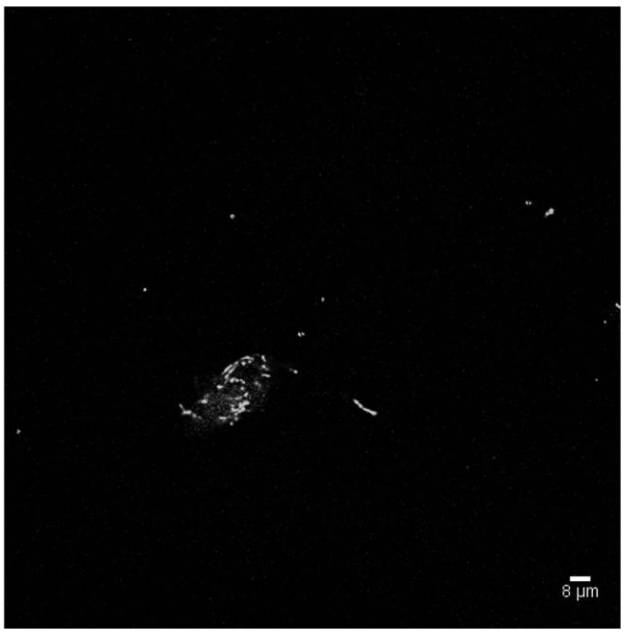

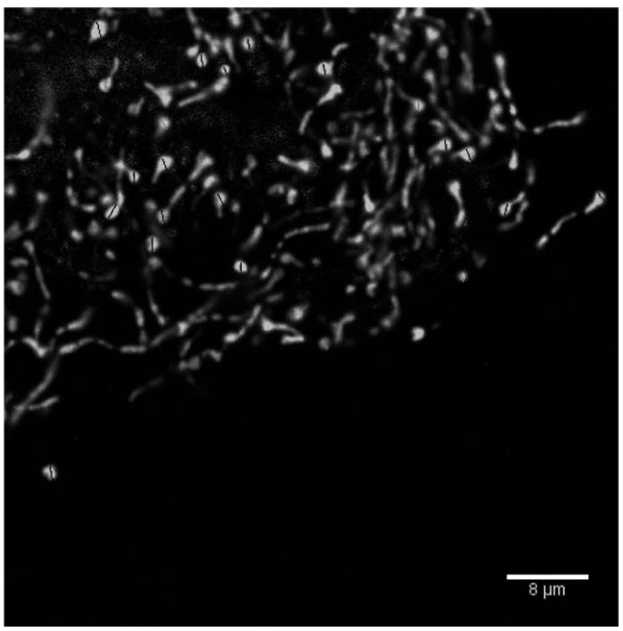

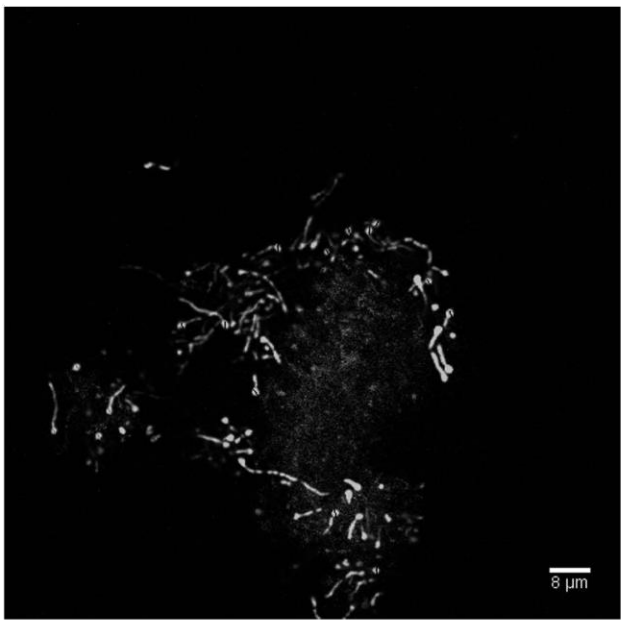

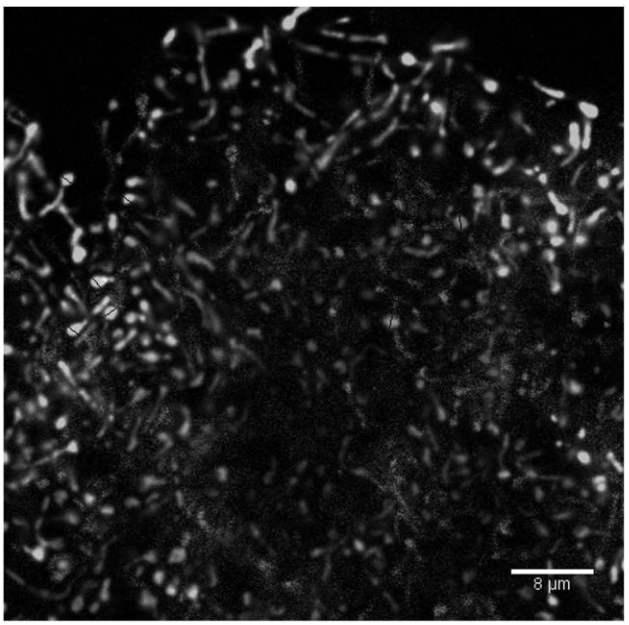

Fig. S1. MASTER IMAGES USED TO QUANTIFY SPORE DIAMETER

Streptomyces coelicolor SCO4439::Tn5062. 15-hours. Spore diameters measured are labelled by lines.

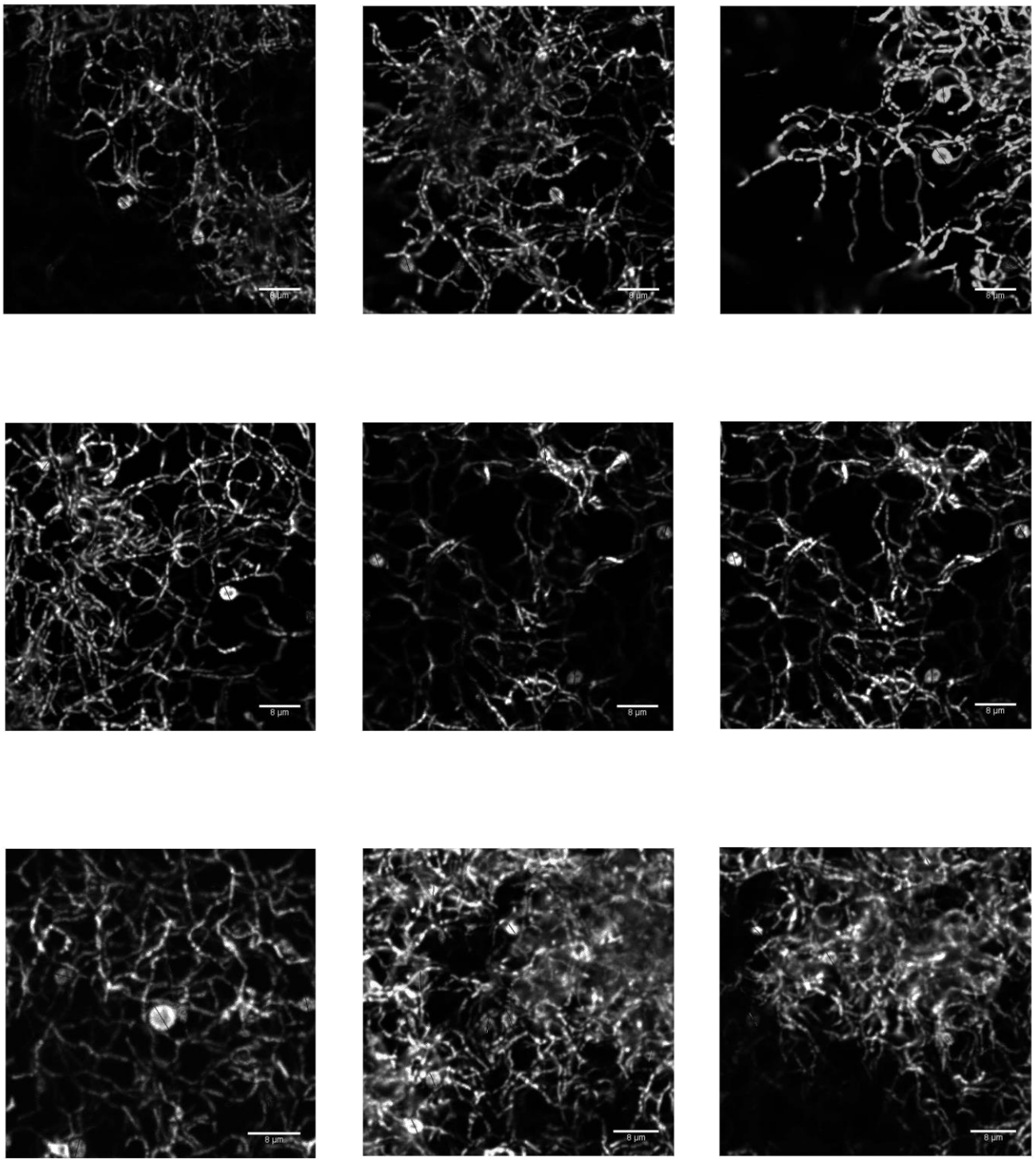

Fig. S1. MASTER IMAGES USED TO QUANTIFY SPORE DIAMETER

Streptomyces coelicolor SCO4439::Tn5062. 15-hours. Spore diameters measured are labelled by lines.

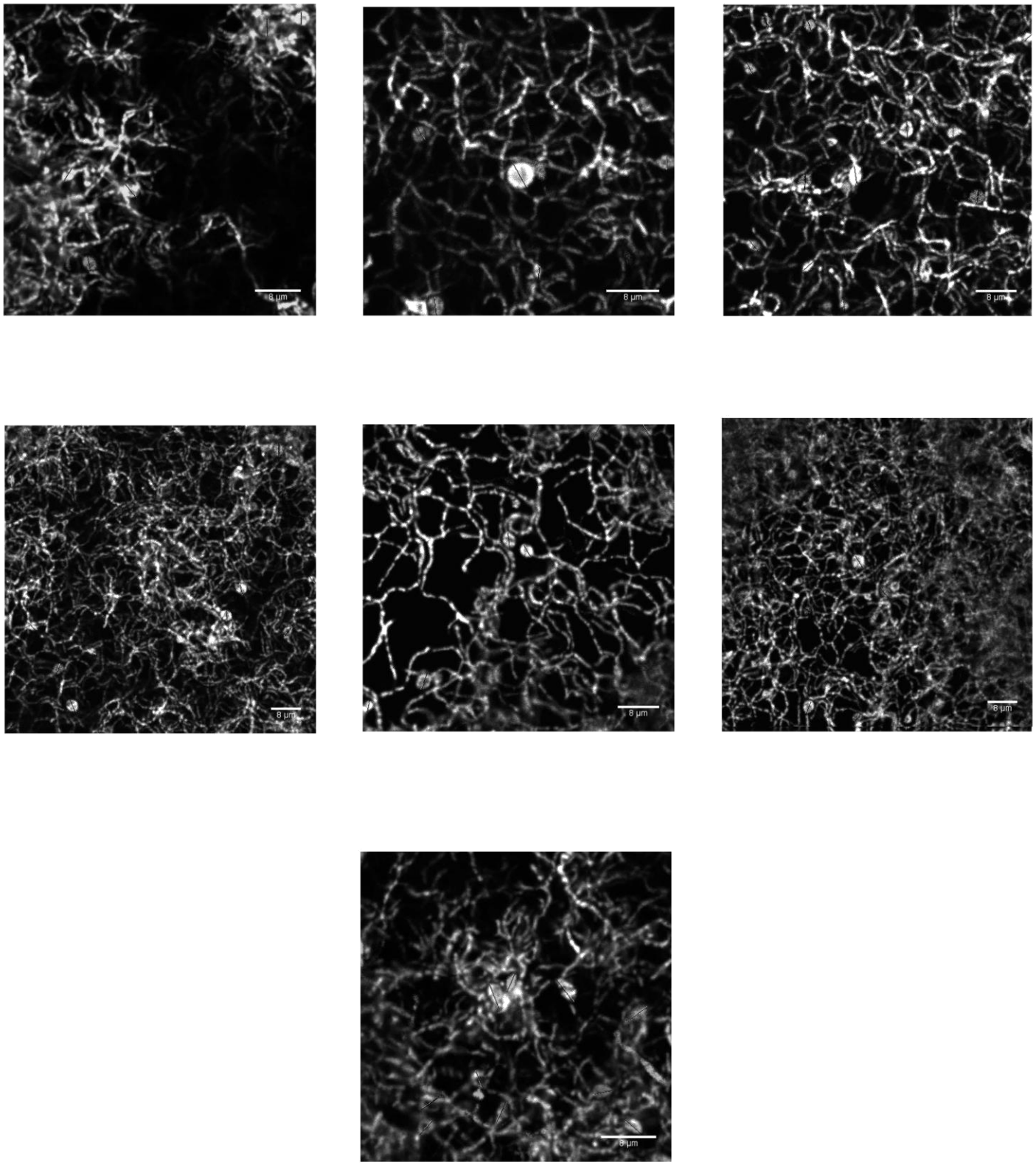

Fig. S1. MASTER IMAGES USED TO QUANTIFY SPORE DIAMETER

Streptomyces coelicolor::Tn5062[pBR3*] 5-hours. Spore diameters measured are labelled by lines.

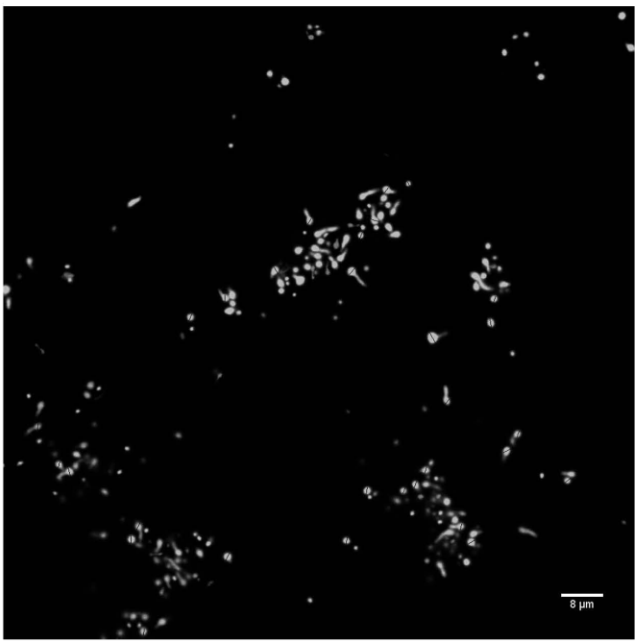

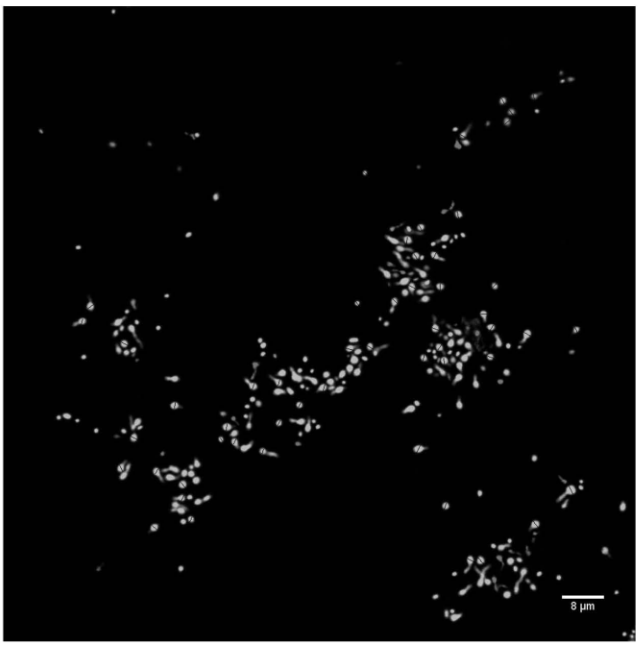

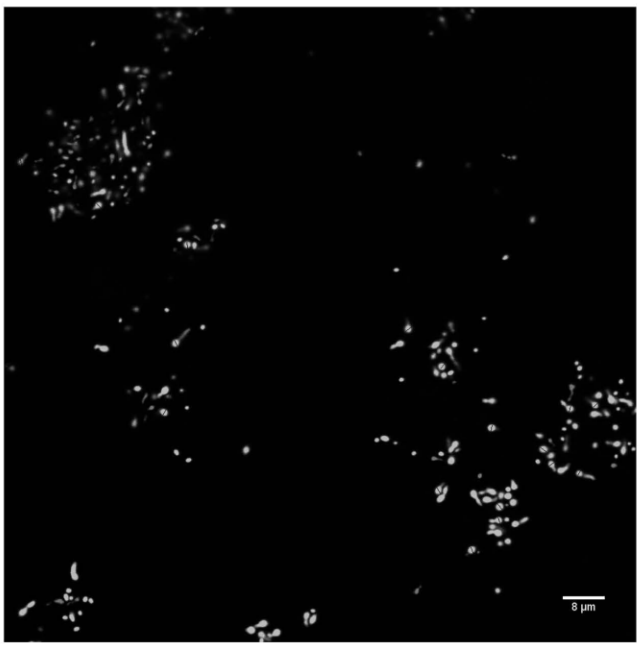

Fig. S1. MASTER IMAGES USED TO QUANTIFY SPORE DIAMETER

Streptomyces coelicolor::Tn5062[pBR3*] 8-hours. Spore diameters measured are labelled by lines.

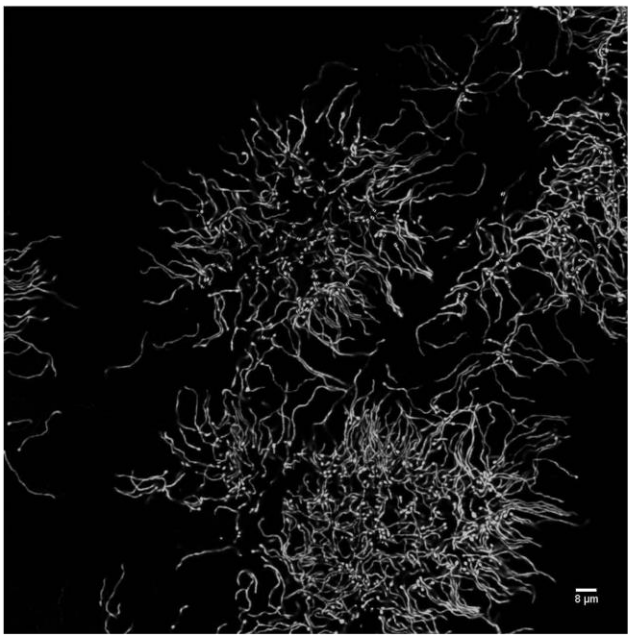

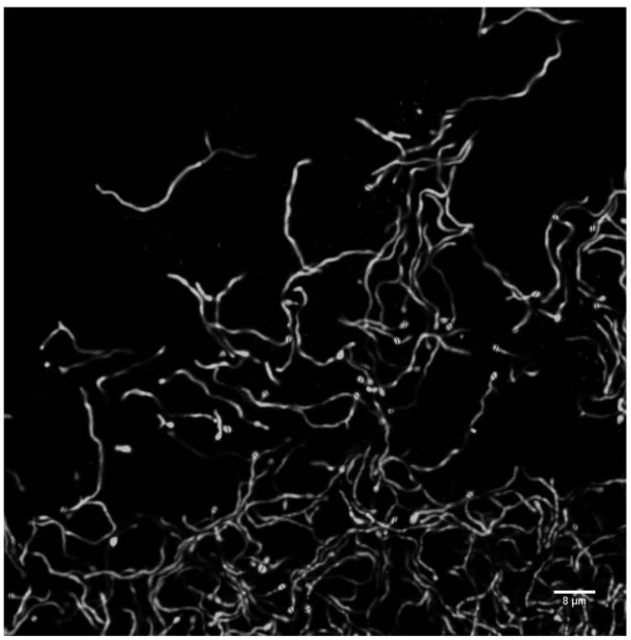

Fig. S1. MASTER IMAGES USED TO QUANTIFY SPORE DIAMETER

Streptomyces coelicolor::Tn5062[pBR3*] 15-hours. Spore diameters measured are labelled by lines.

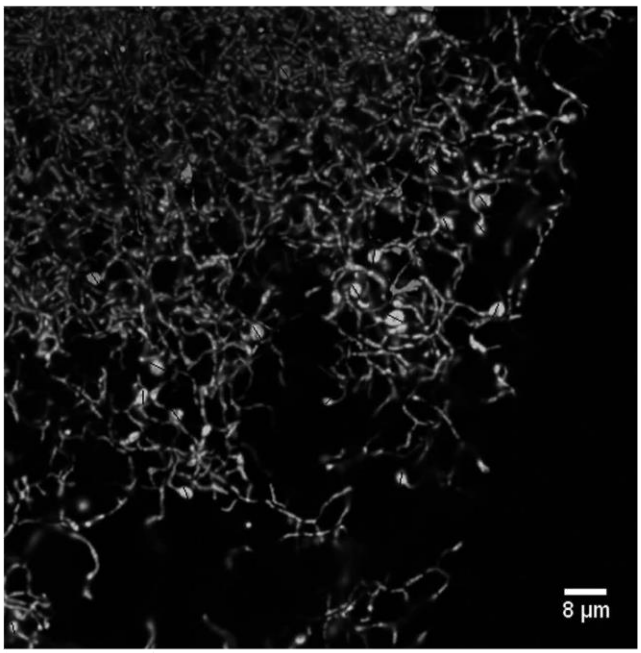

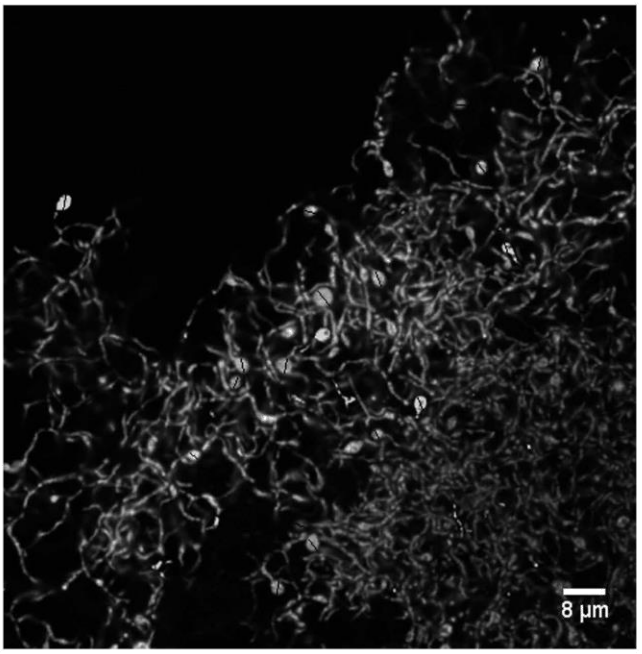

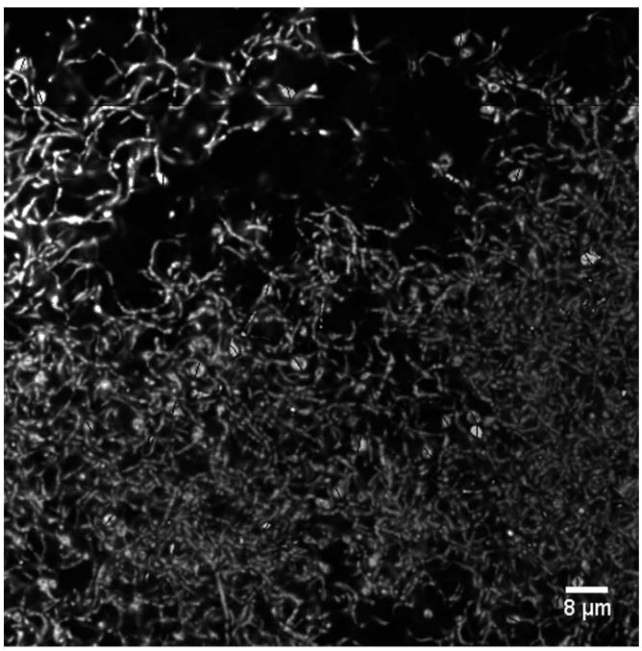

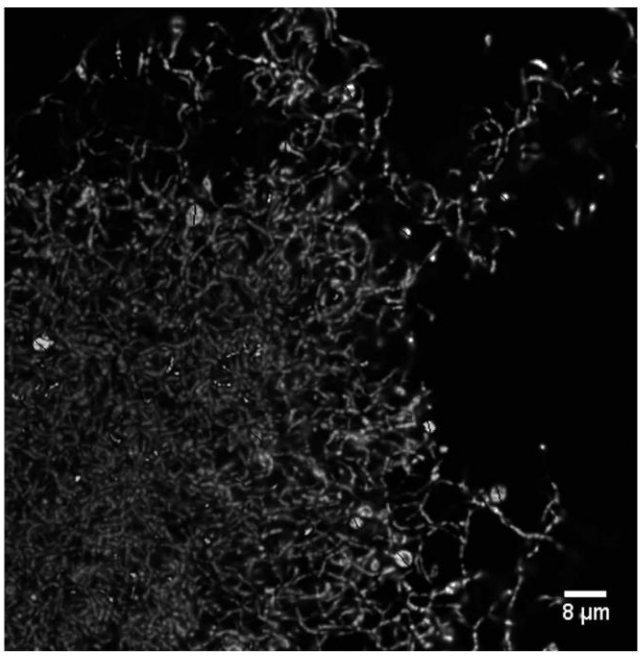

Fig. S1. MASTER IMAGES USED TO QUANTIFY SPORE DIAMETER

Streptomyces coelicolor::Tn5062[pBR3*] 15-hours. Spore diameters measured are labelled by lines.

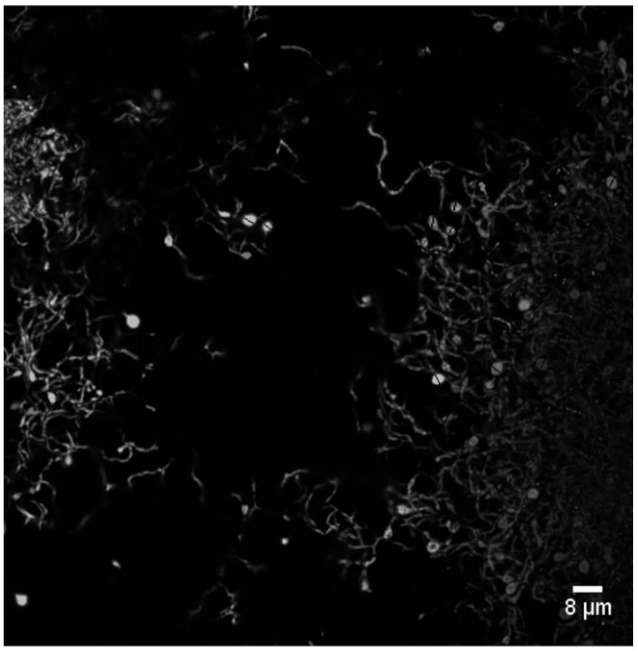

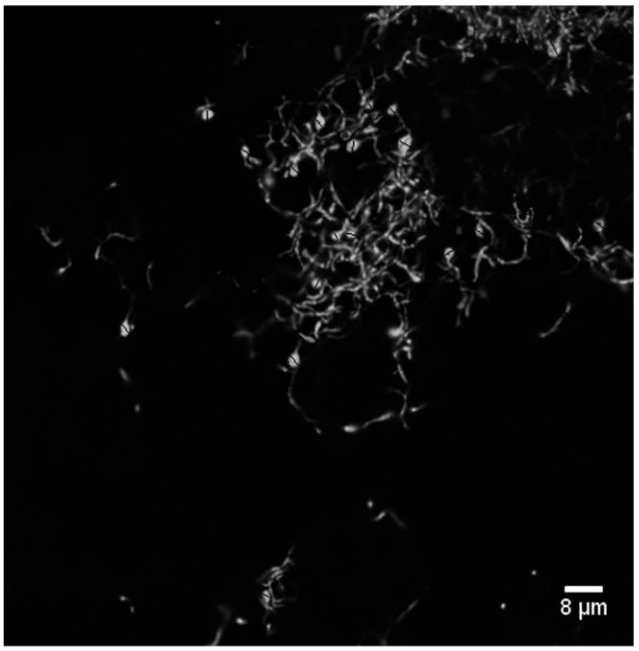

Fig. S2. MASTER IMAGES USED TO QUANTIFY SPORE DIAMETER

Streptomyces coelicolor [pMS82]. 15-hours. Spore diameters measured are labelled by lines.

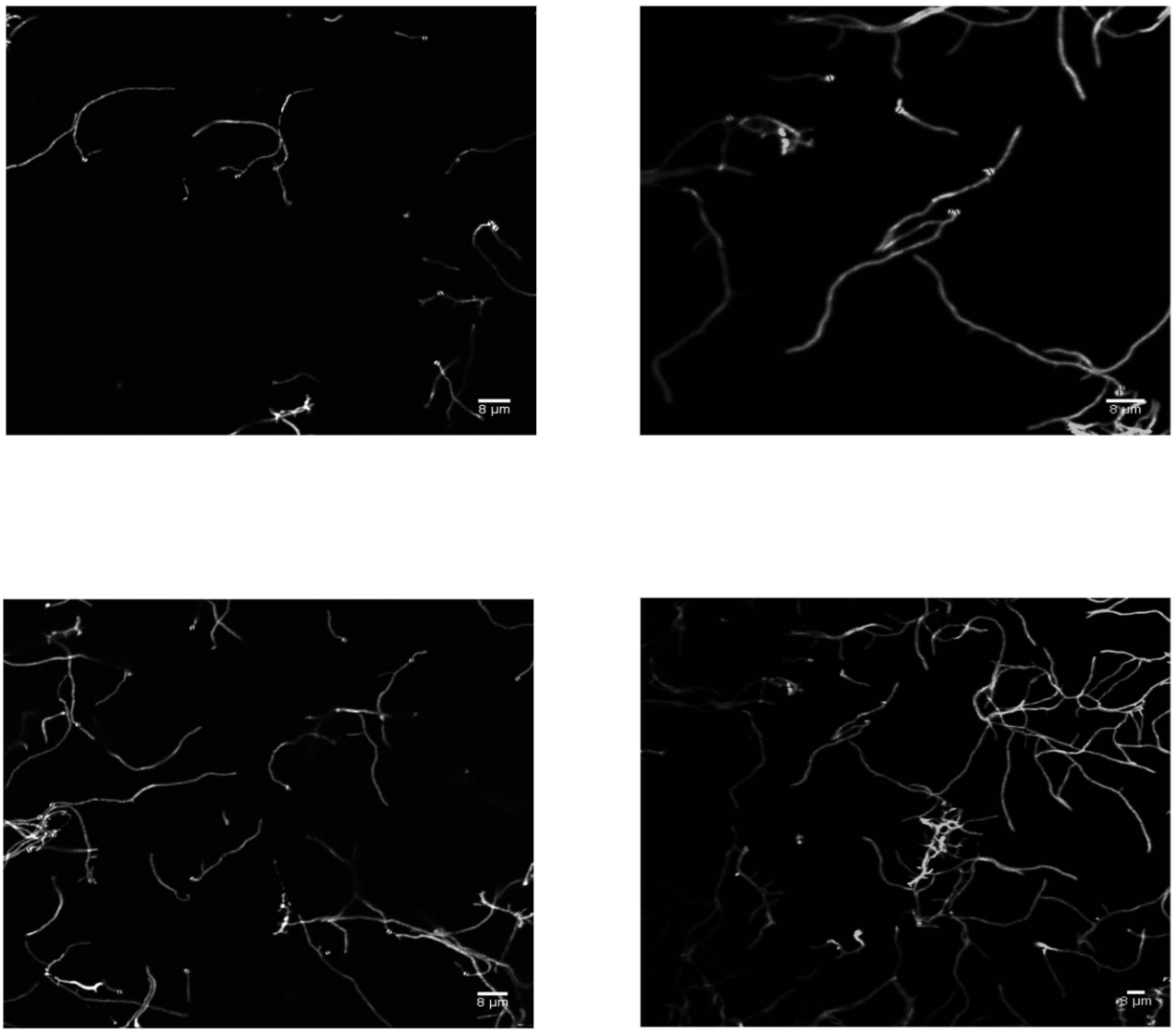

Fig. S2. MASTER IMAGES USED TO QUANTIFY SPORE DIAMETER

Streptomyces coelicolor [pMS82]. 15-hours. Spore diameters measured are labelled by lines.

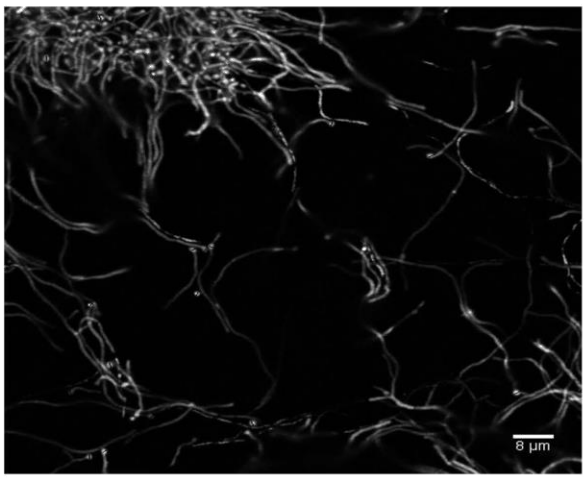

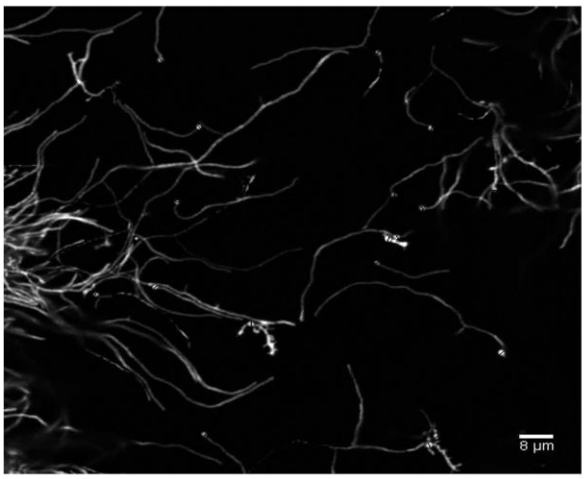

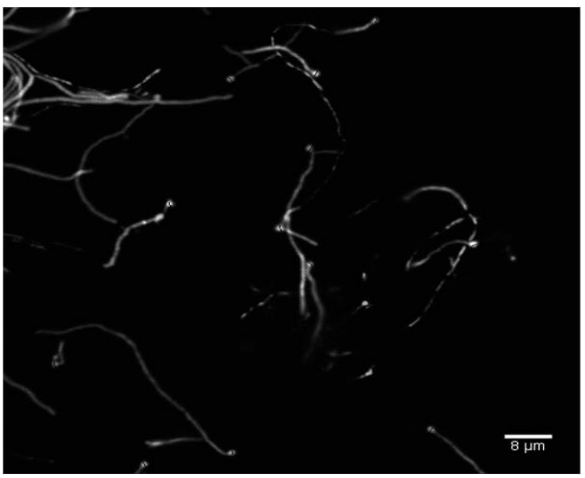

Fig. S2. MASTER IMAGES USED TO QUANTIFY SPORE DIAMETER

SCO4439::Tn5062 [pBRB3]. 15-hours. Spore diameters measured are labelled by lines.

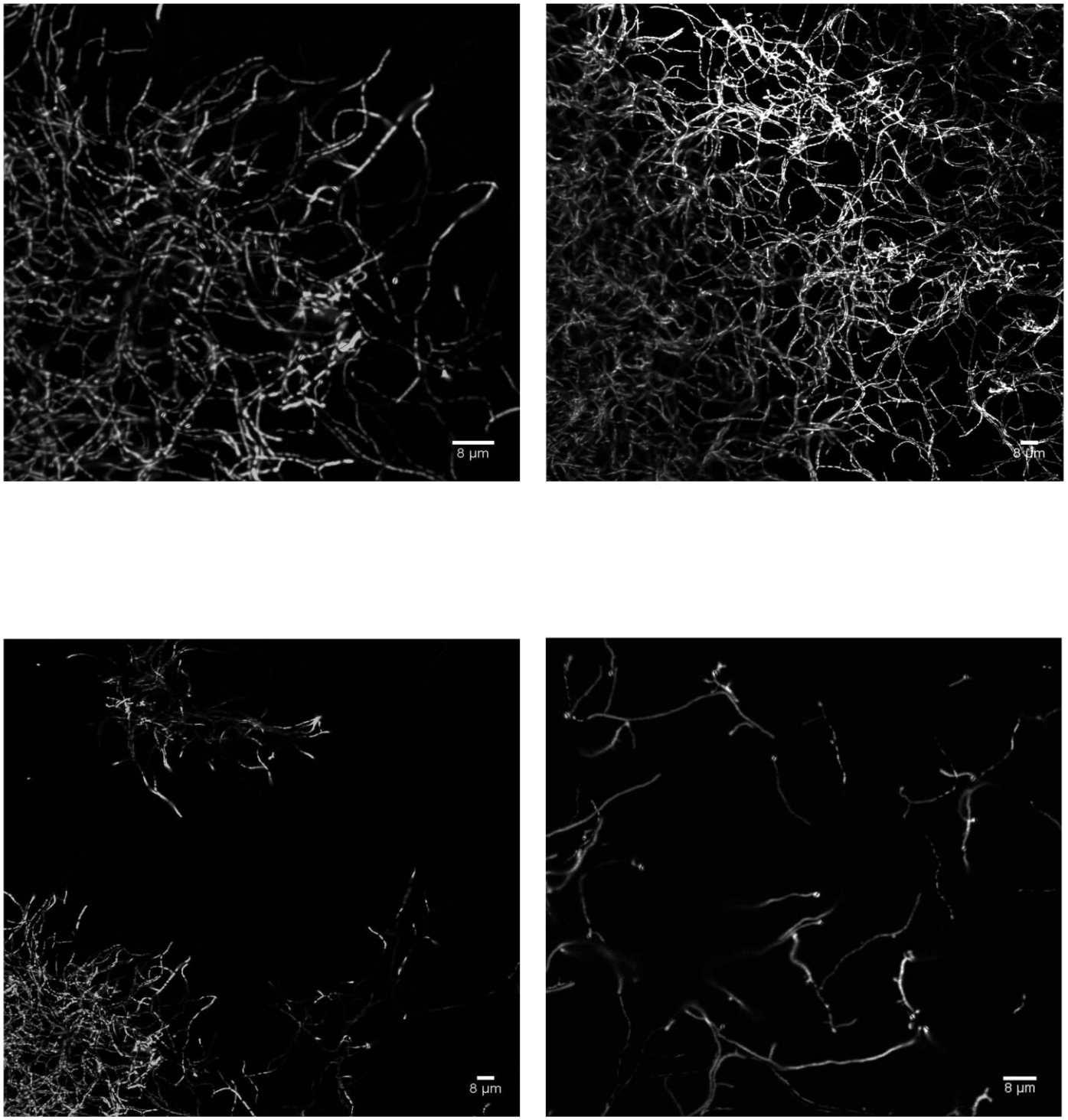

Fig. S2. MASTER IMAGES USED TO QUANTIFY SPORE DIAMETER

SCO4439::Tn5062 [pBRB3]. 15-hours. Spore diameters measured are labelled by lines.

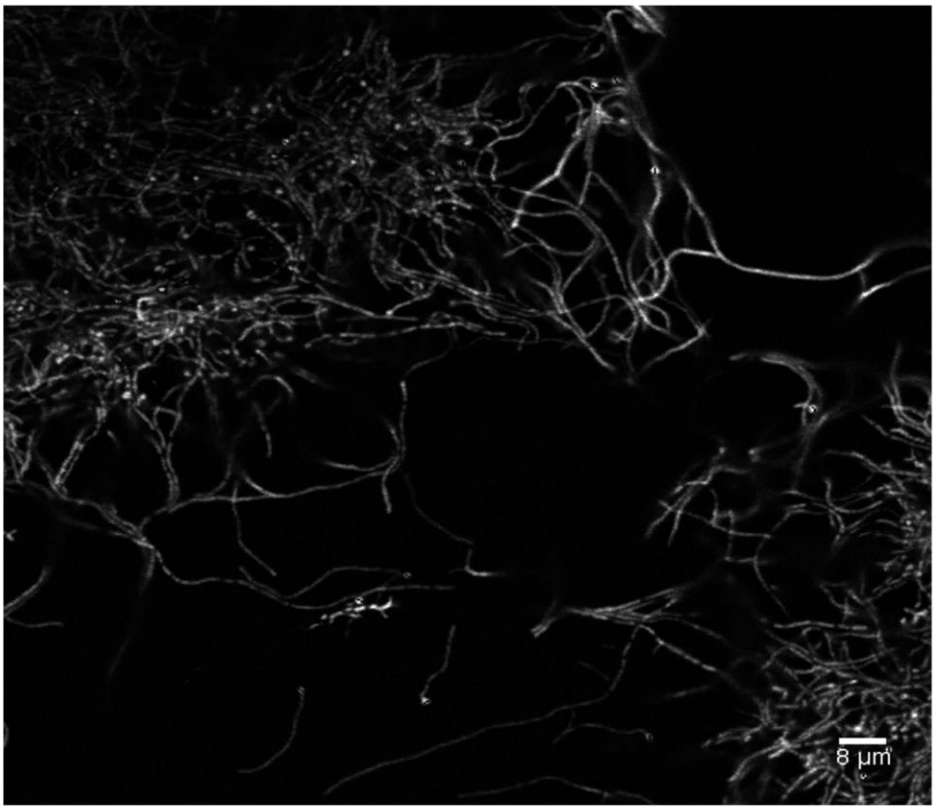

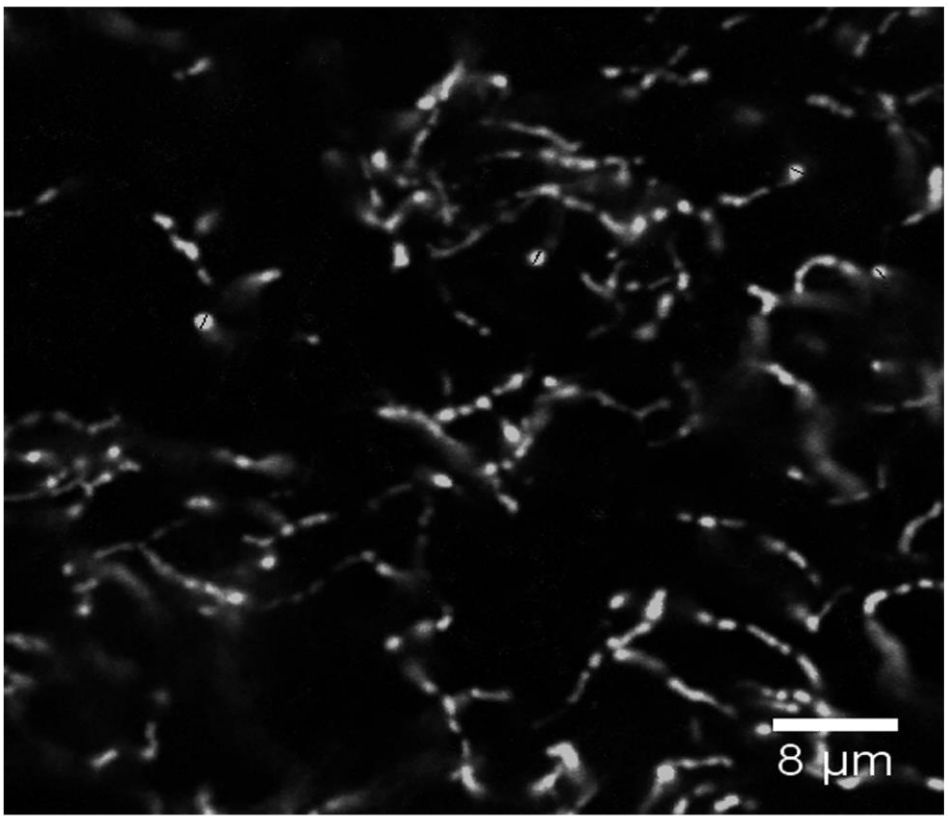

ANEXO 3
Material Suplementario del Manuscrito 3

En este anexo se incluye el material suplementario del **manuscrito 3**:

Supplementary Fig. 1. Imágenes que muestran la compartimentalización de las hifas de *S. coelicolor.*

Supplementary Fig. 2. Imágenes que muestran la permeabilidad de las hifas de MI (10 horas) a los colorantes YOPRO-1 y PI.

Supplementary Fig. 3. Imágenes que muestran la colocalización de los anillos Z, barreras de permeabilidad a PI, tabiques de membrana y tabiques de pared.

Supplementary Fig. 4. Imágenes usadas para cuantificar la compartimentalización de las hifas en ΔftsZHU133 (48h).

Supplementary Fig. 5. Imágenes que muestran la tinción de pared celular "*D-amino acid pulse-labeling"* en *S. coelicolor* y en ΔftsZHU133 (15 horas en medio GYM líquido).

Supplementary Fig. 6. Imágenes usadas para la cuantificación de protoplastos.

Supplementary Table 1. Datos de proteómica cuantitativa de la proteína FtsZ.

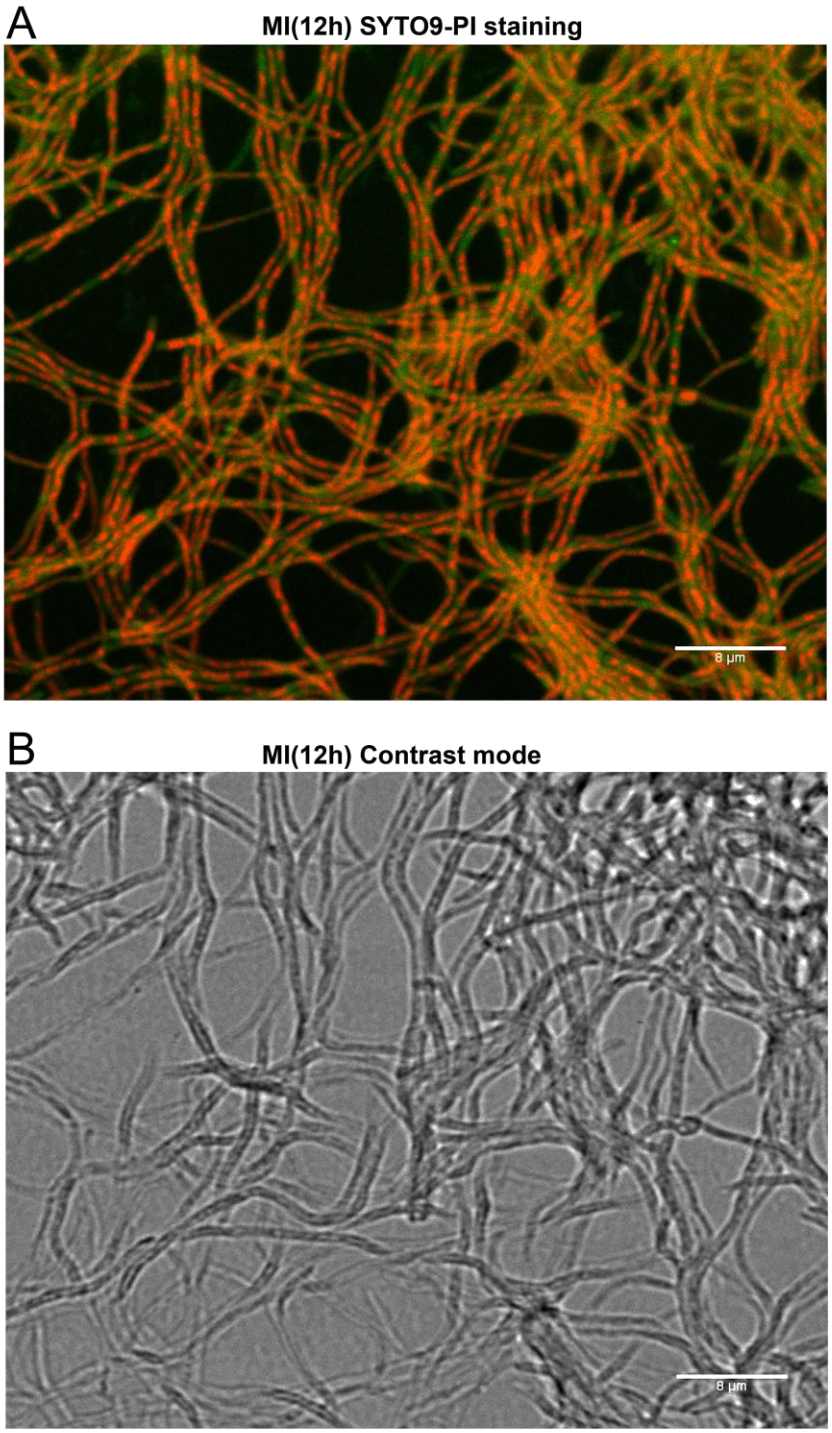

Supplementary Fig. 1. Images showing *S. coelicolor* hyphae compartmentalization. (A-D; G,H) MI; (E) transition from MI to MII;(F) sporulating hyphae. Segments and Z-rings used to quantify compartment lengths and Z-ring spacing are marked. Scale bars correspond to 8 µm.

(A) MI hyphae stained with PI (red) and SYTO9 (green).

(B) Contrast mode of the image shown in (A).

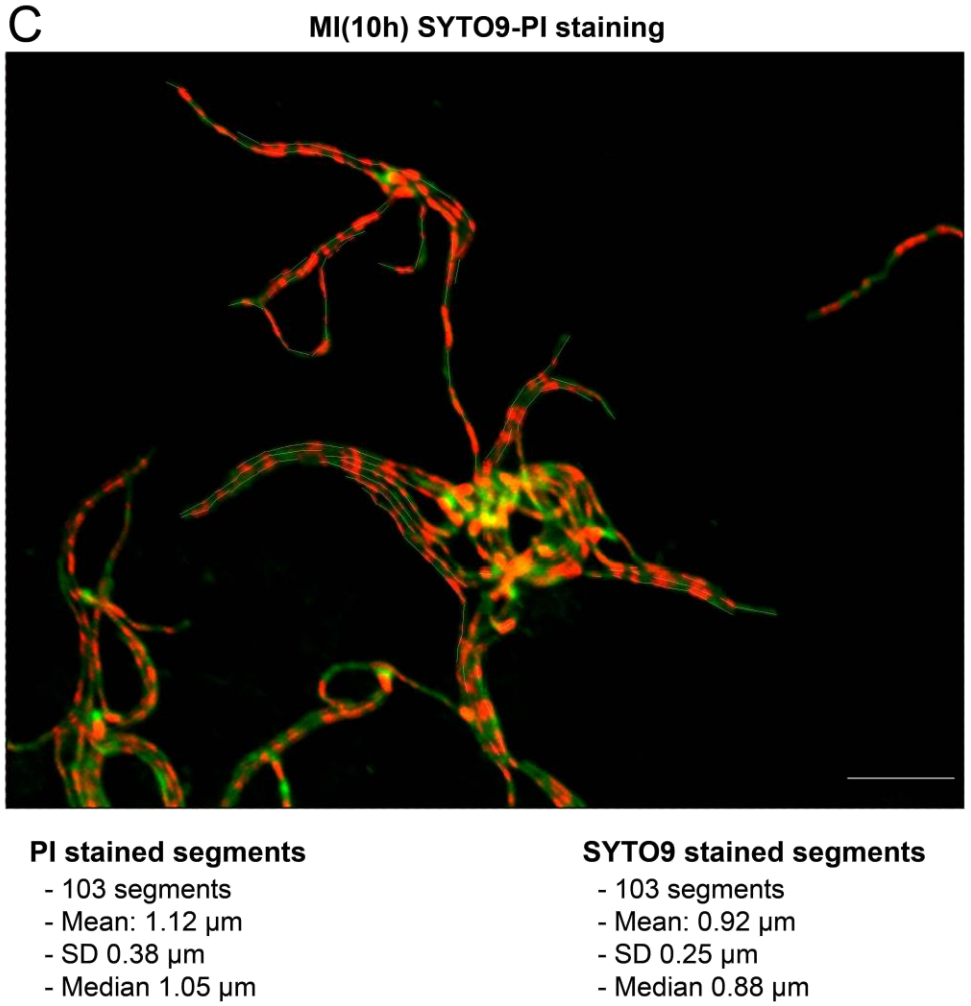

Supplementary Fig. 1. Images showing *S. coelicolor* hyphae compartmentalization. (A-D; G,H) MI; (E) transition from MI to MII; (F) sporulating hyphae. Segments and Z-rings used to quantify compartment lengths and Z-ring spacing are marked. Scale bars correspond to 8 µm.

(C) Master image used to quantify PI- and SYTO9-stained segments in the MI hyphae.

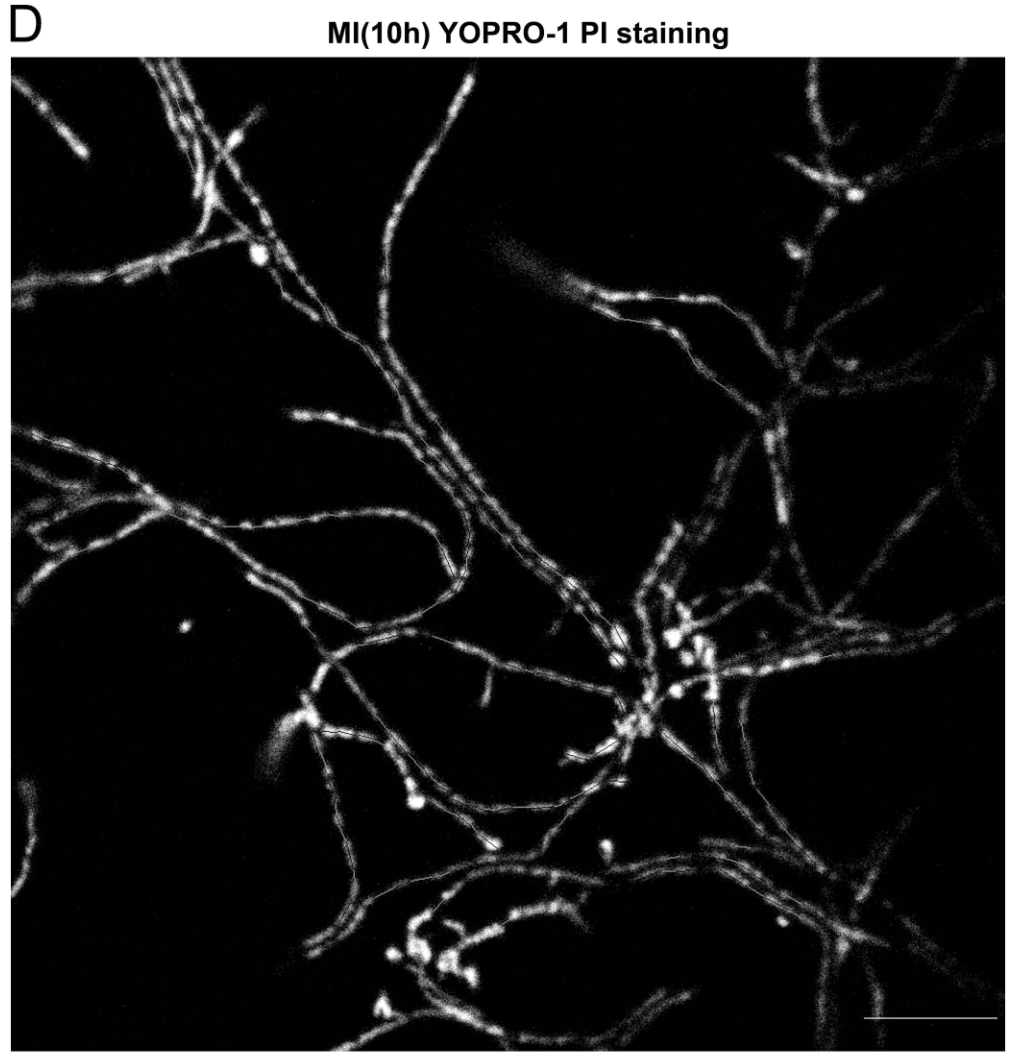

Supplementary Fig. 1. Images showing *S. coelicolor* hyphae compartmentalization. (A-D; G,H) MI; (E) transition from MI to MII; (F) sporulating hyphae. Segments and Z-rings used to quantify compartment lengths and Z-ring spacing are marked. Scale bars correspond to 8 µm.

(D) Master image used to quantify YOPRO-1- and PI-stained and unstained segments in the MI hyphae. The same segments were stained with YOPRO-1 and PI.

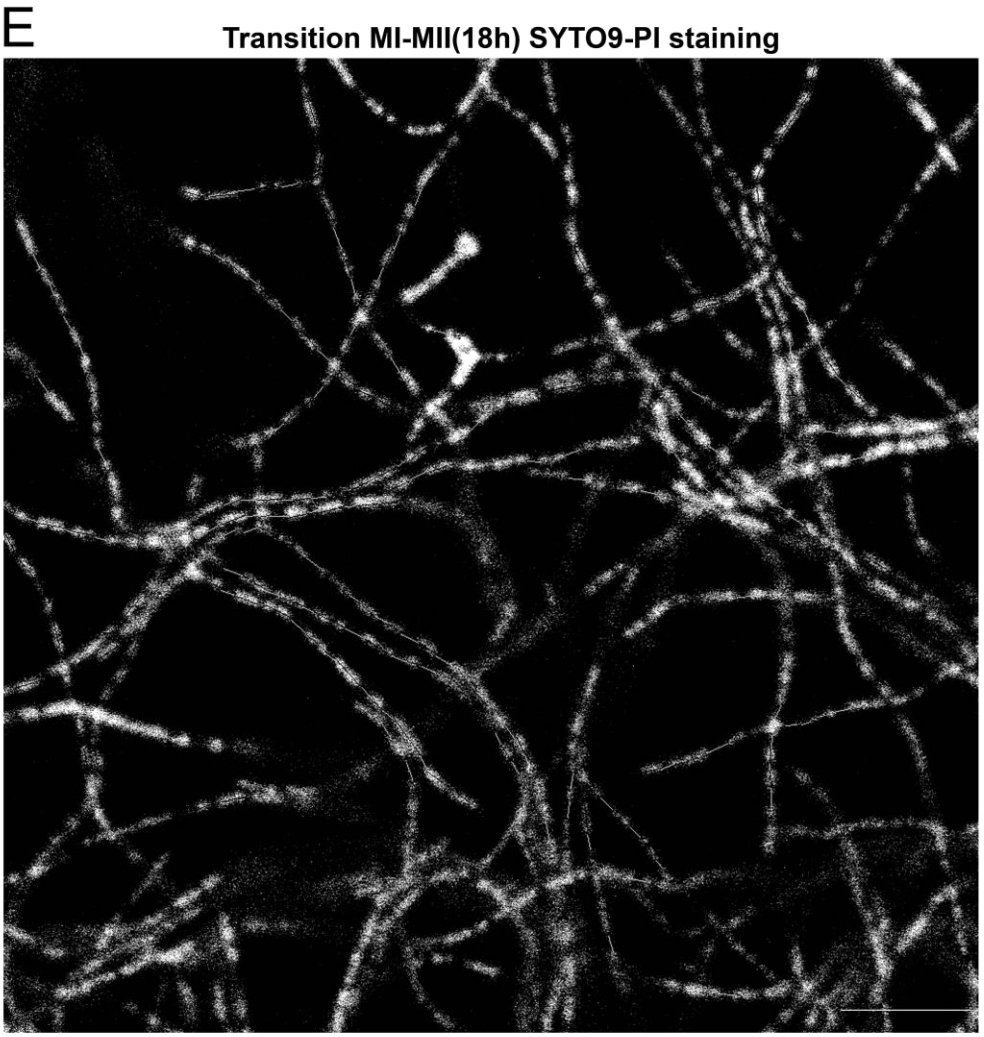

Supplementary Fig. 1. Images showing *S. coelicolor* hyphae compartmentalization. (A-D; G,H) MI; (E) transition from MI to MII;(F) sporulating hyphae. Segments and Z-rings used to quantify compartment lengths and Z-ring spacing are marked. Scale bars correspond to 8 µm.

(E) Master image used to quantify SYTO9-stained and unstained cellular segments in the transition from the MI to MII stage. Cells were stained with SYTO9 and PI, but at this stage, no cells were labelled by PI (see the manuscript for details).

F

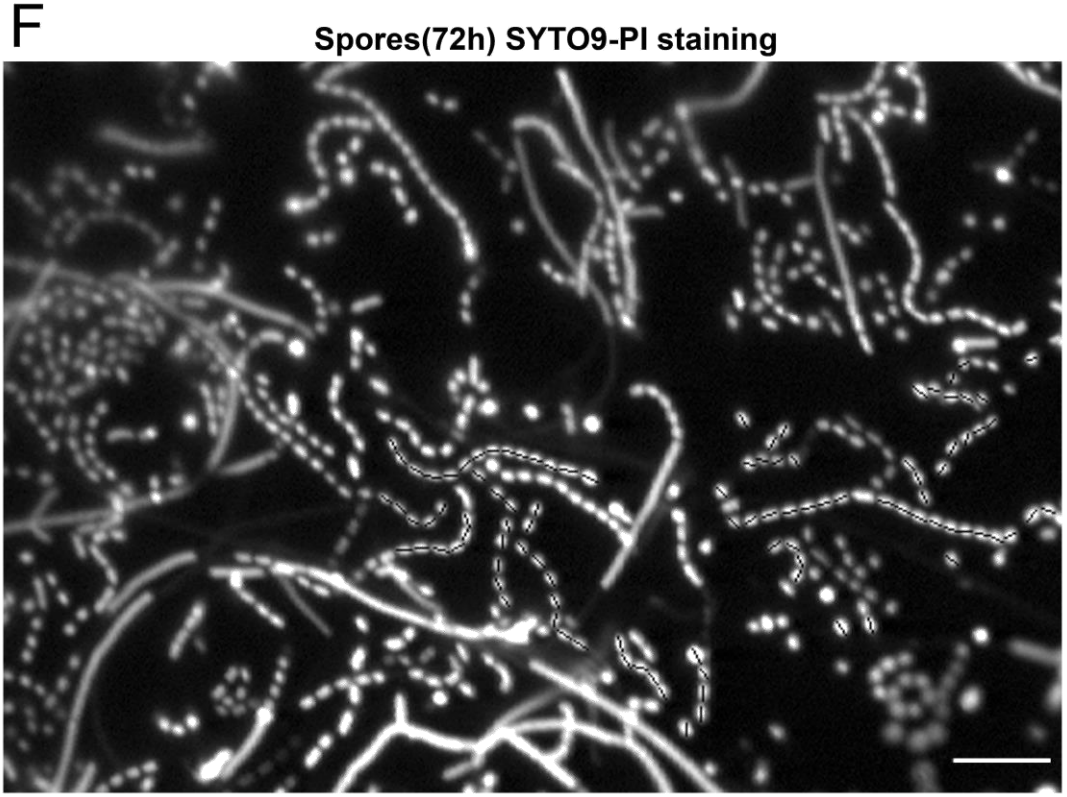

Supplementary Fig. 1. Images showing *S. coelicolor* hyphae compartmentalization. (A-D; G,H) MI; (E) transition from MI to MII;(F) sporulating hyphae. Segments and Z-rings used to quantify compartment lengths and Z-ring spacing are marked. Scale bars correspond to 8 µm.

(F) Master image used to quantify spore diameter. Hyphae were stained with PI and SYTO9.

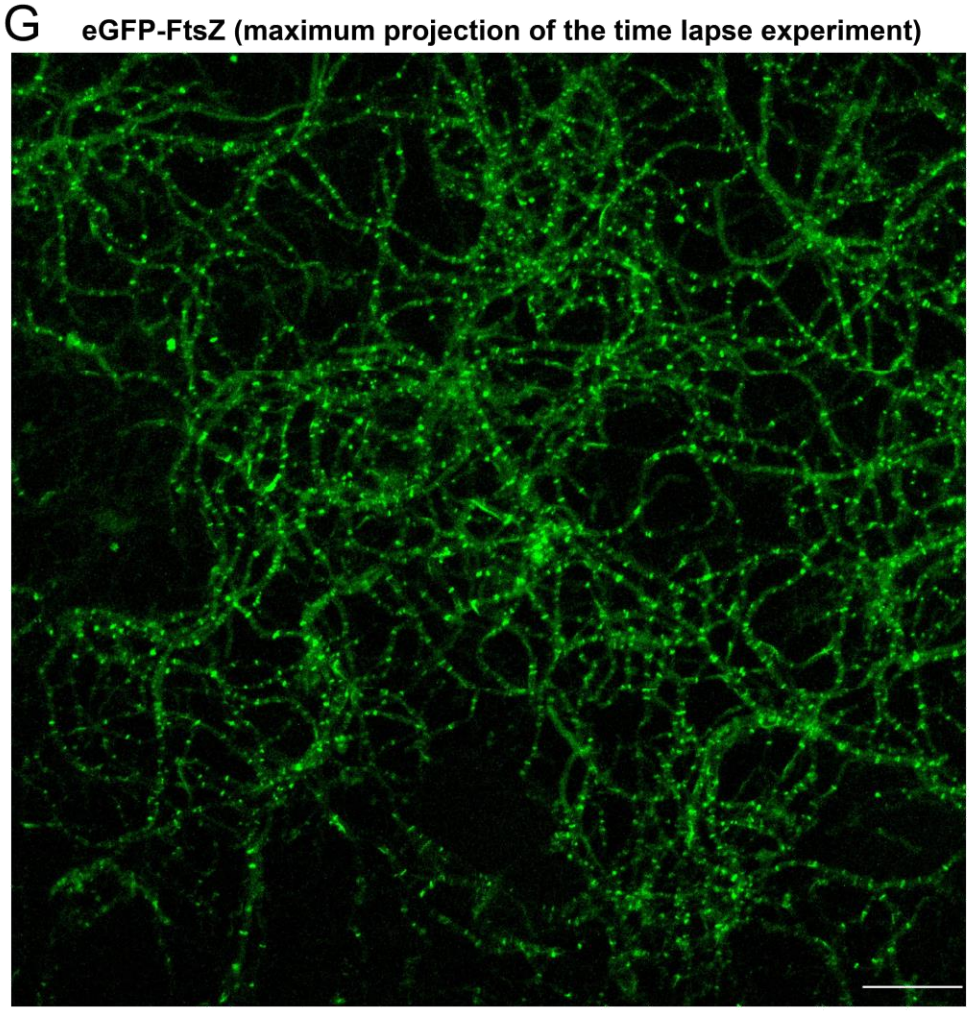

Supplementary Fig. 1. Images showing *S. coelicolor* hyphae compartmentalization. (A-D; G,H) MI; (E) transition from MI to MII;(F) sporulating hyphae. Segments and Z-rings used to quantify compartment lengths and Z-ring spacing are marked. Scale bars correspond to 8 μm.

(G) Master image (maximum projection of the time lapse experiment) used to quantify Z-ring spacing in *S. coelicolor* FM145 expressing FtsZ-eGFP.

H eGFP-FtsZ (maximum projection) processed for quantification

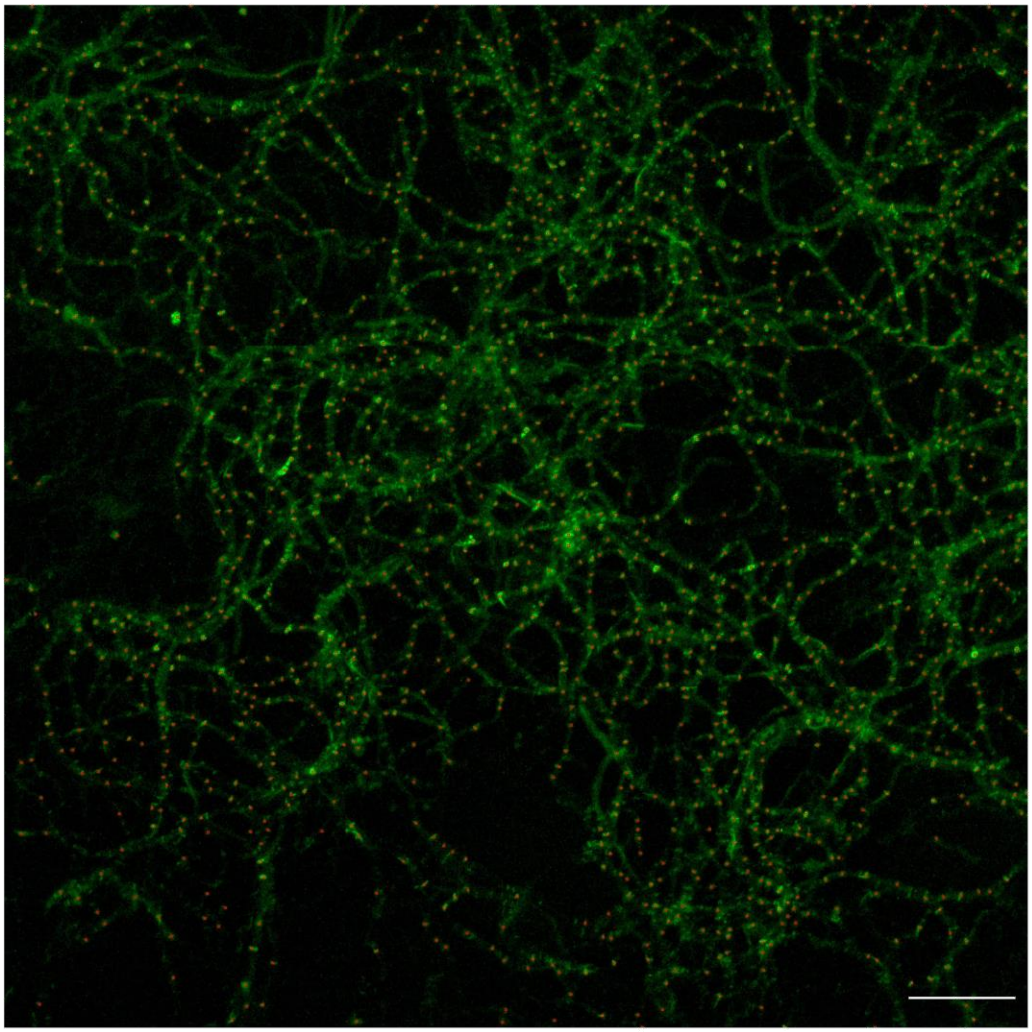

eGFP Z-ring spacing

- 1514 Z-rings
- Mean: 1.12 µm
- SD 0.48 µm
- Median 1.03 µm

Supplementary Fig. 1. Images showing *S. coelicolor* hyphae compartmentalization. (A-D; G,H) MI; (E) transition from MI to MII; (F) sporulating hyphae. Segments and Z-rings used to quantify compartment lengths and Z-ring spacing are marked. Scale bars correspond to 8 µm.

(H) Same image as (G) processed for quantification.

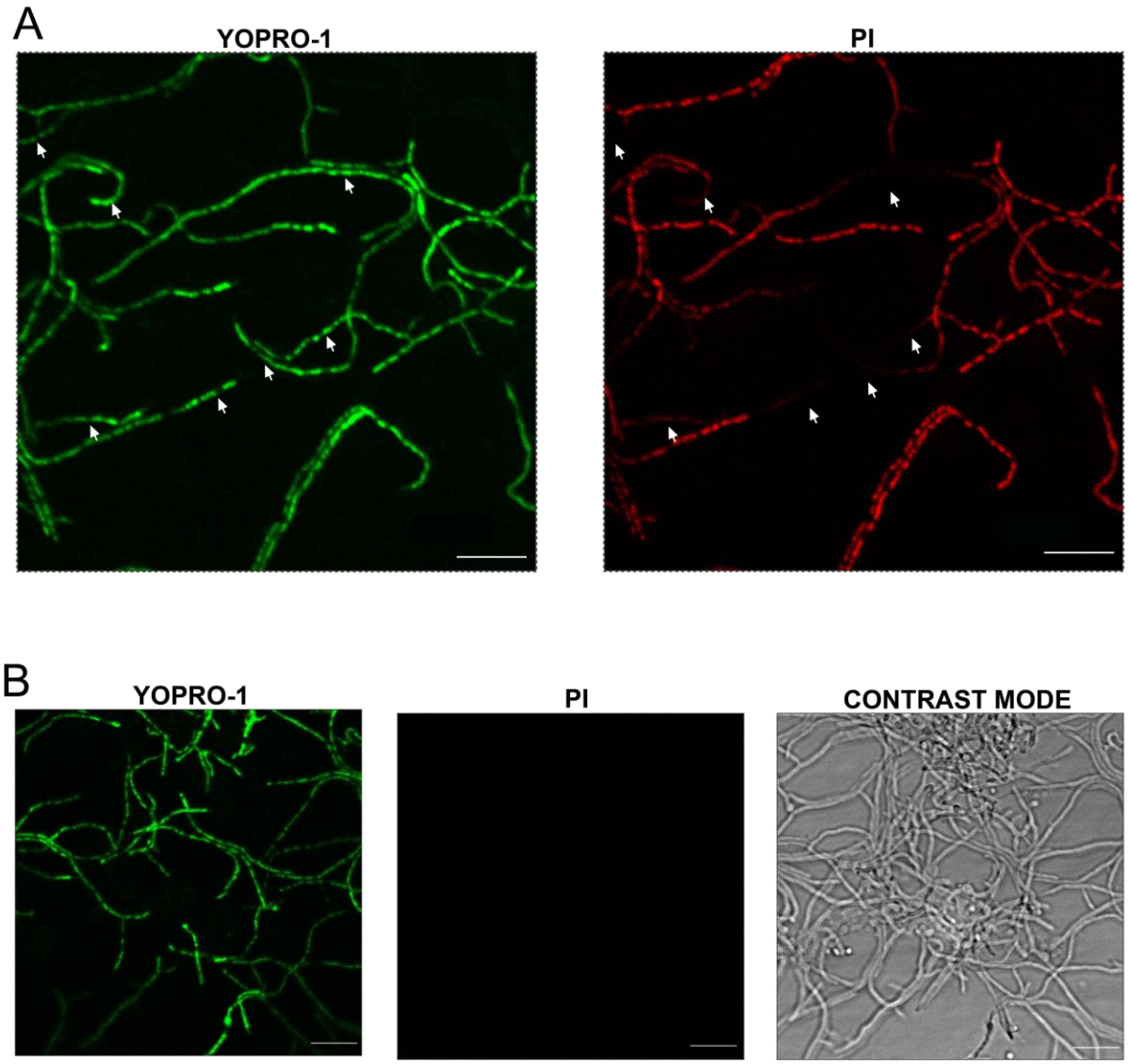

Supplementary Fig. 2. Permeability of MI hyphae (10-hours) to YOPRO-1 and PI. Scale bars correspond to 8 μm.
(A) Slowly processed samples (minutes). All segments stained with PI (red) are also stained with YOPRO-1 (green), but some segments stained with YOPRO-1 are not stained with PI (labelled with arrows).

(B) Rapidly processed samples (seconds). Dying cells are permeable to YOPRO-1 but not to PI.

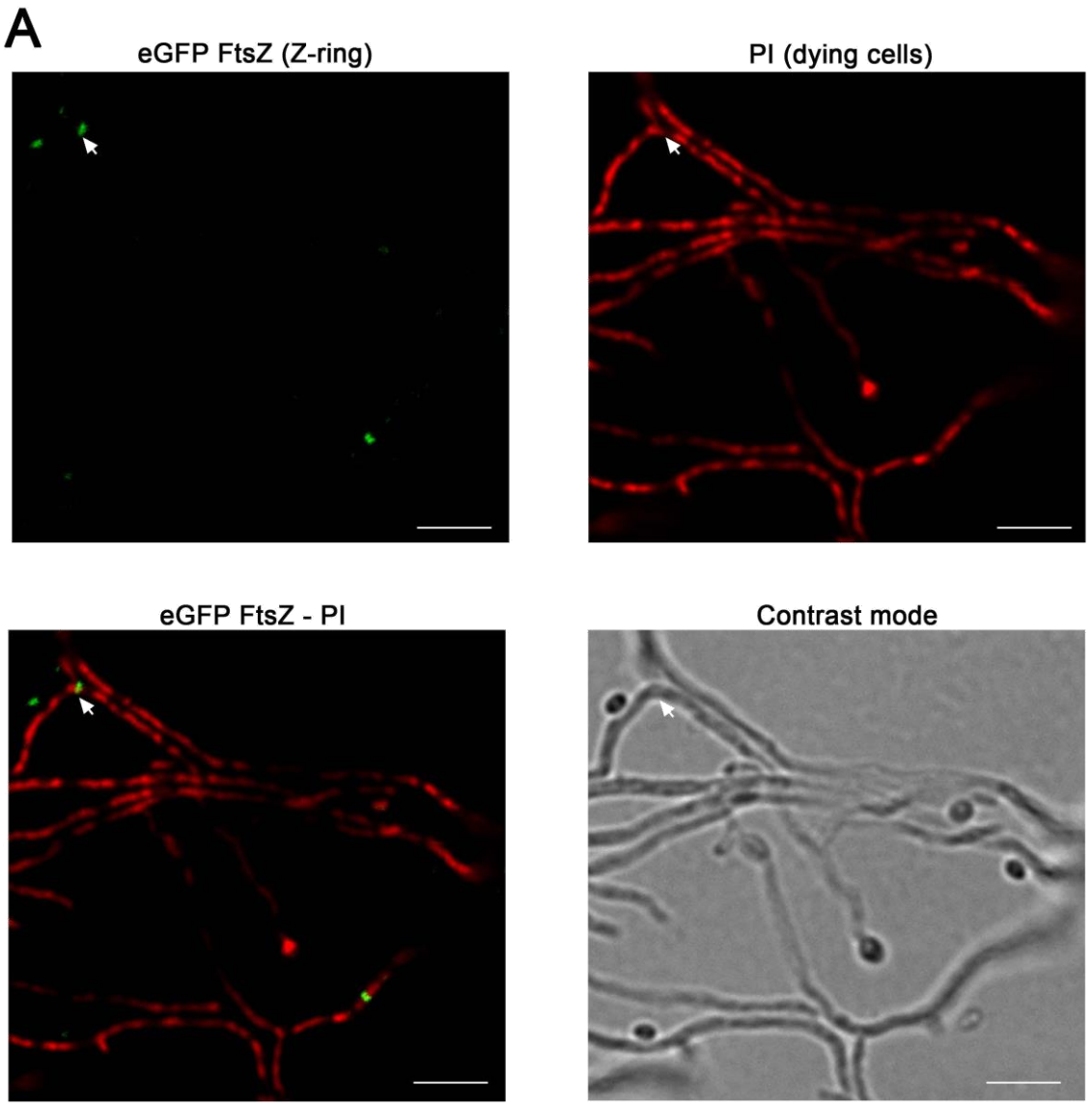

Supplementary Fig. 3. Images showing the colocalization of Z-rings, PI permeability barriers, cross-membranes and cross-walls. Scale bars correspond to 4 μm.
(A-D) eGFP-FtsZ (Z-rings, green) and PI (dying cells, red) staining. Arrows indicate Z-rings colocalizing with PI permeability borders. Ten-hour GYM solid cultures.

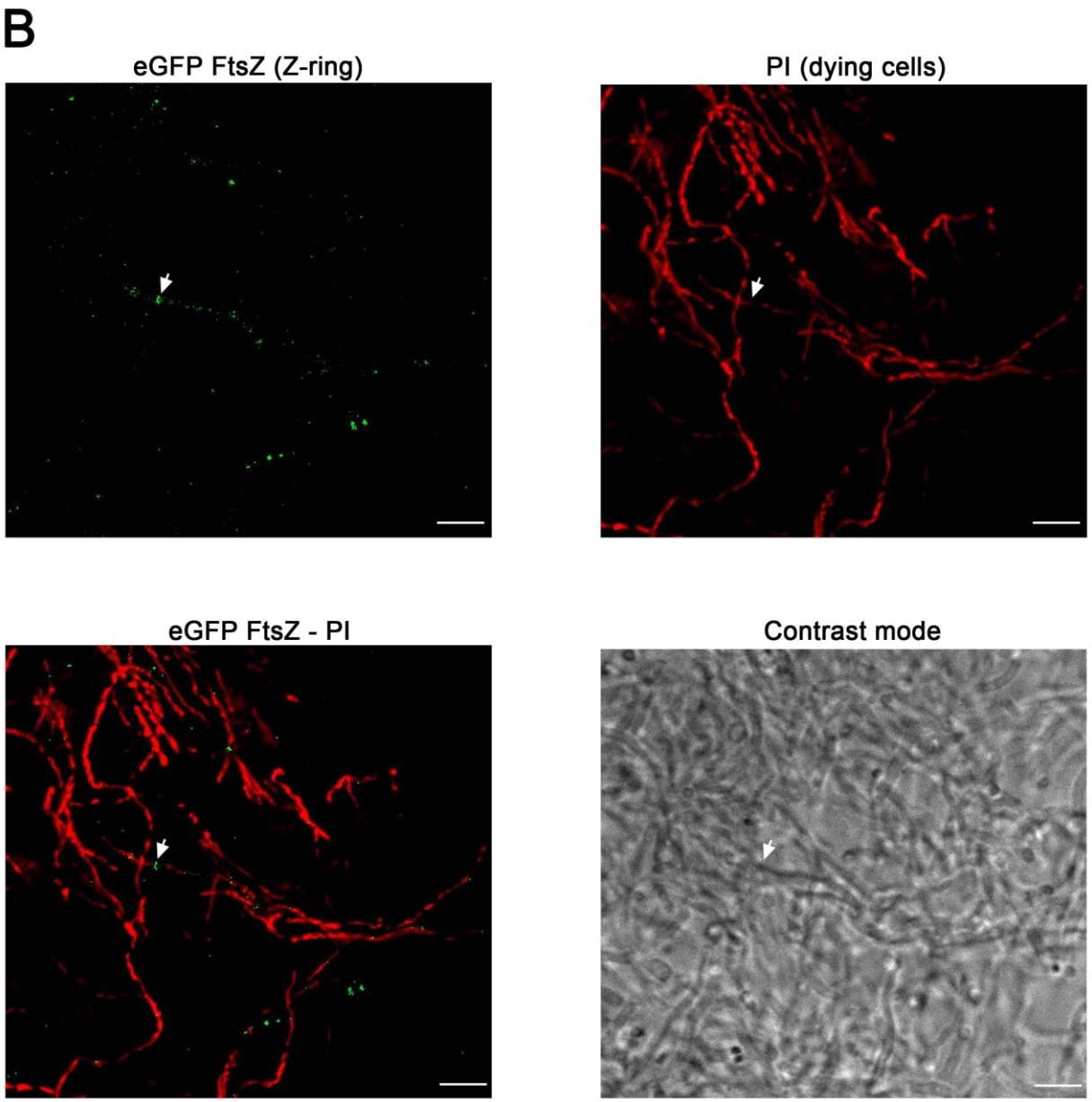

Supplementary Fig. 3. Images showing the colocalization of Z-rings, PI permeability barriers, cross-membranes and cross-walls. Scale bars correspond to 4 μm.
(A-D) eGFP-FtsZ (Z-rings, green) and PI (dying cells, red) staining. Arrows indicate Z-rings colocalizing with PI permeability borders. Ten-hour GYM solid cultures.

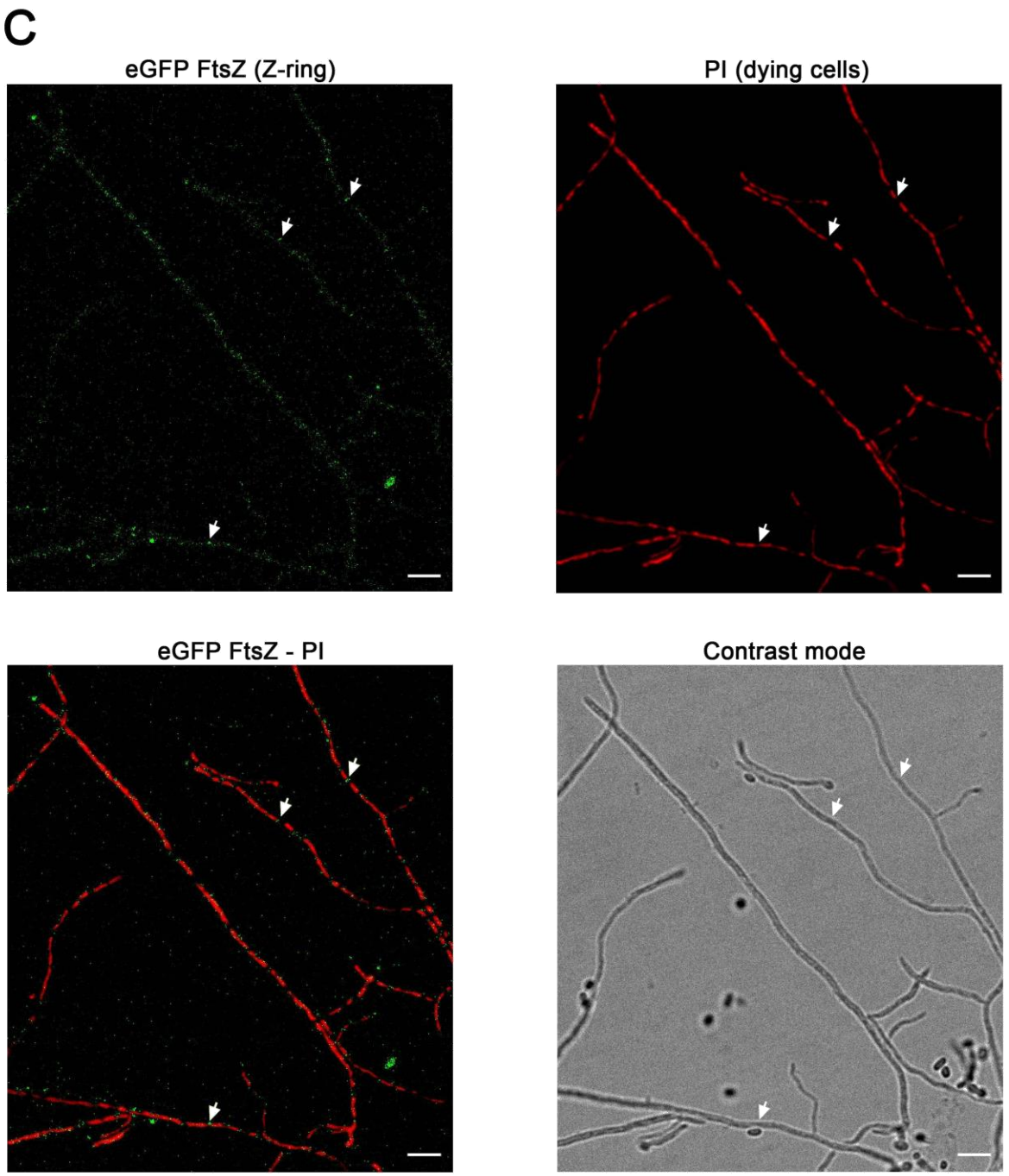

Supplementary Fig. 3. Images showing the colocalization of Z-rings, PI permeability barriers, cross-membranes and cross-walls. Scale bars correspond to 4 μm.
(A-D) eGFP-FtsZ (Z-rings, green) and PI (dying cells, red) staining. Arrows indicate Z-rings colocalizing with PI permeability borders. Ten-hour GYM solid cultures.

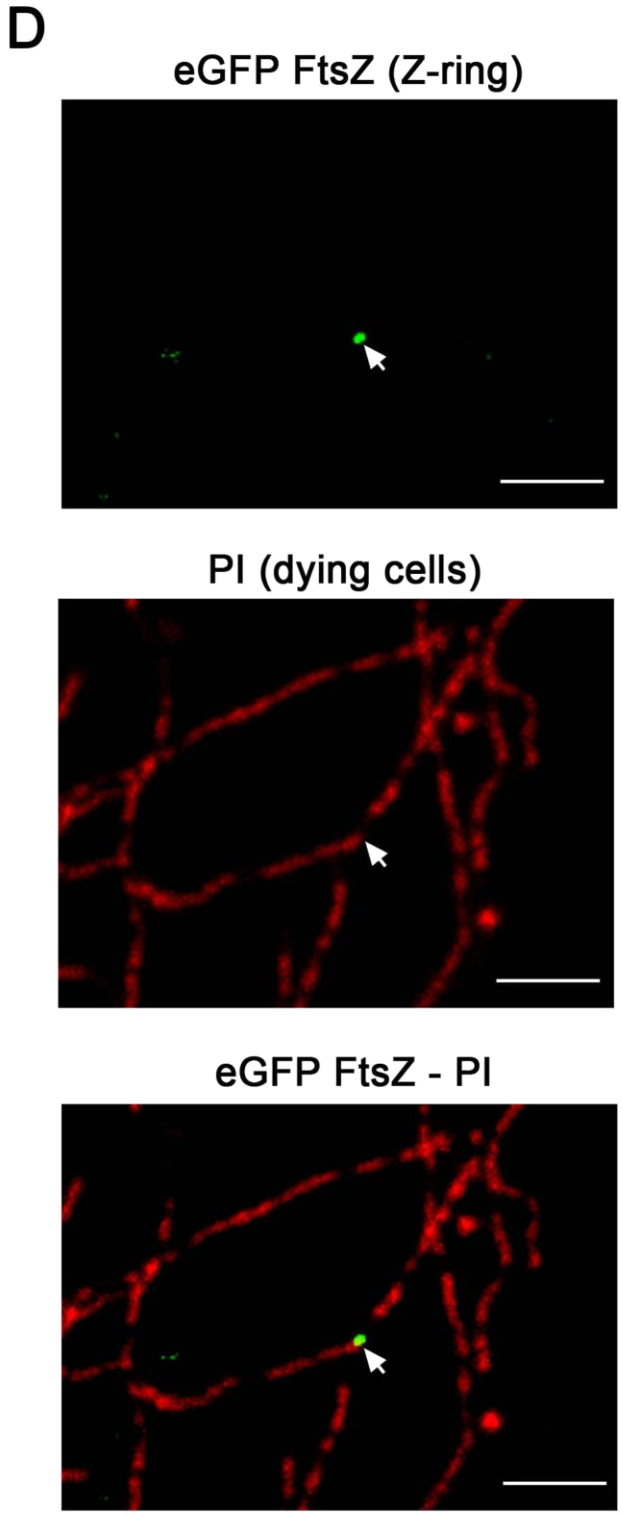

Supplementary Fig. 3. Images showing the colocalization of Z-rings, PI permeability barriers, cross-membranes and cross-walls. Scale bars correspond to 4 μm.
(A-D) eGFP-FtsZ (Z-rings, green) and PI (dying cells, red) staining. Arrows indicate Z-rings colocalizing with PI permeability borders. Ten-hour GYM solid cultures.

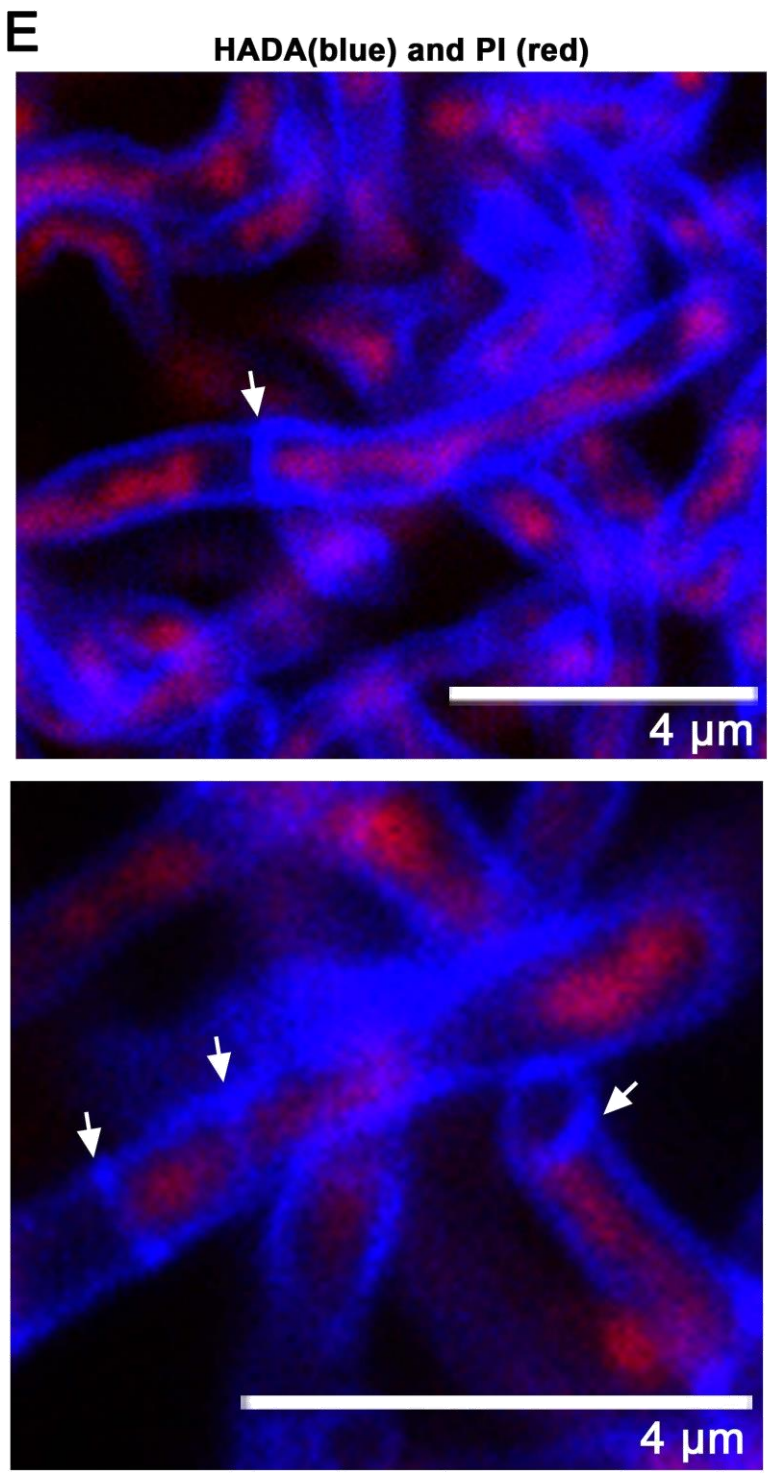

Supplementary Fig. 3. Images showing the colocalization of Z-rings, PI permeability barriers, cross-membranes and cross-walls. Scale bars correspond to 4 µm.

(E) HADA (cell wall, blue) and PI (dying cells, red) staining. Arrows indicate the colocalization between cell walls and PI permeability barriers. Fifteen-hour liquid GYM cultures.

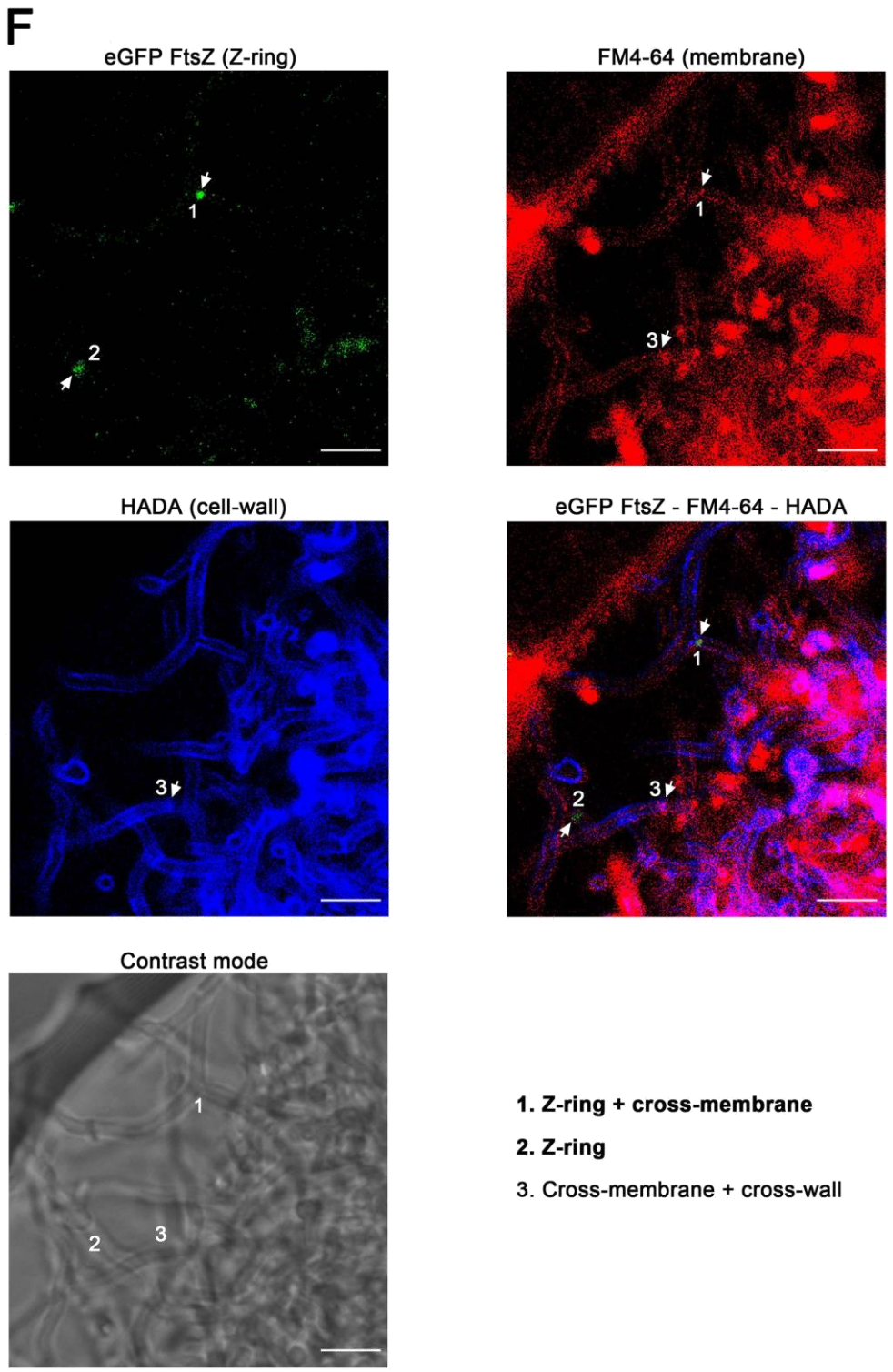

Supplementary Fig. 3. Images showing the colocalization of Z-rings, PI permeability barriers, cross-membranes and cross-walls. Scale bars correspond to 4 μm.
(F-I) eGFP-FtsZ (Z-rings, green), HADA (cell wall, blue) and FM4-64 (membrane, red) staining. Z-rings, cross-membranes and/or cross-walls colocalize in some cases (arrows).

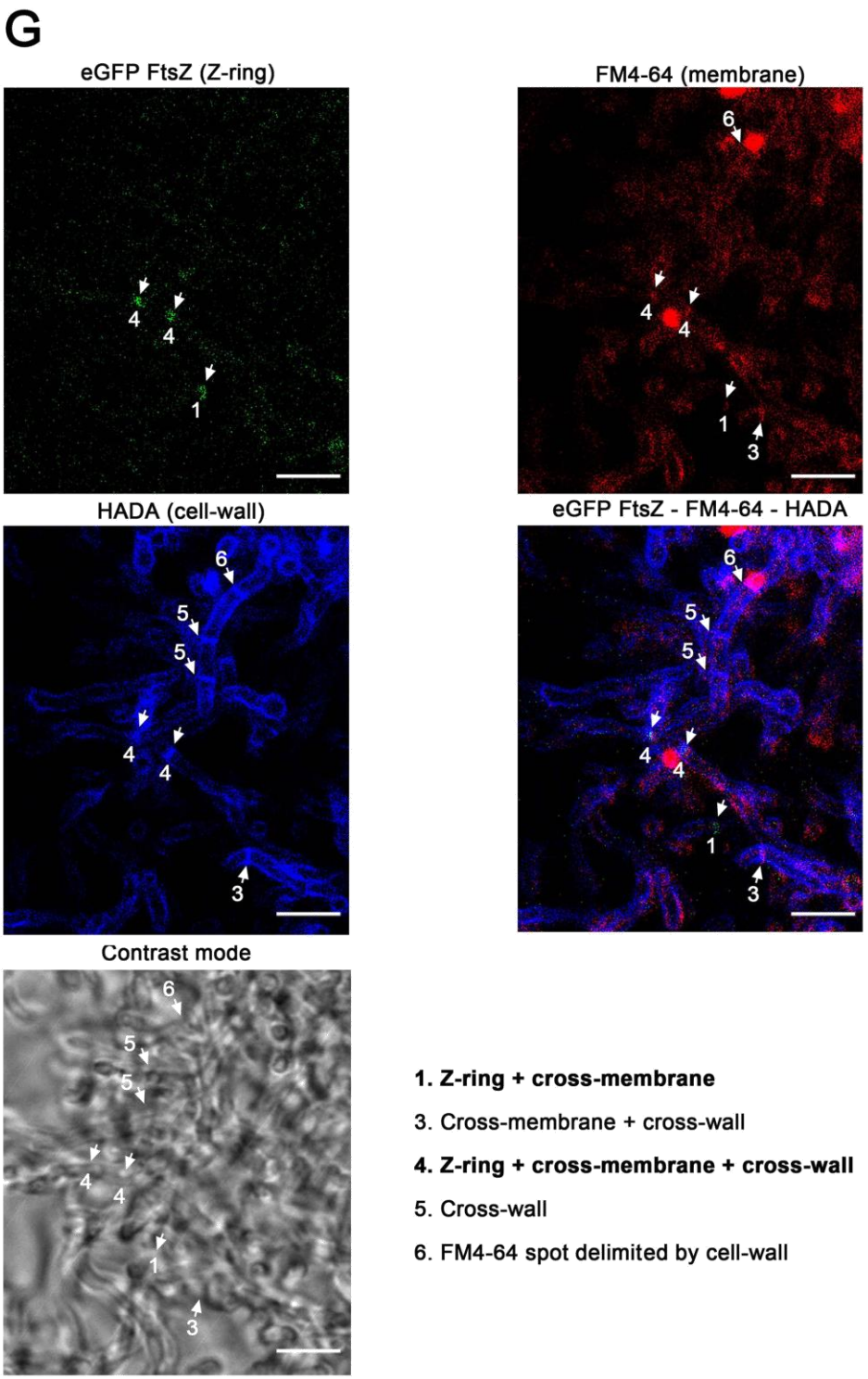

Supplementary Fig. 3. Images showing the colocalization of Z-rings, PI permeability barriers, cross-membranes and cross-walls. Scale bars correspond to 4 μm.
(F-I) eGFP-FtsZ (Z-rings, green), HADA (cell wall, blue) and FM4-64 (membrane, red) staining. Z-rings, cross-membranes and/or cross-walls colocalize in some cases (arrows).

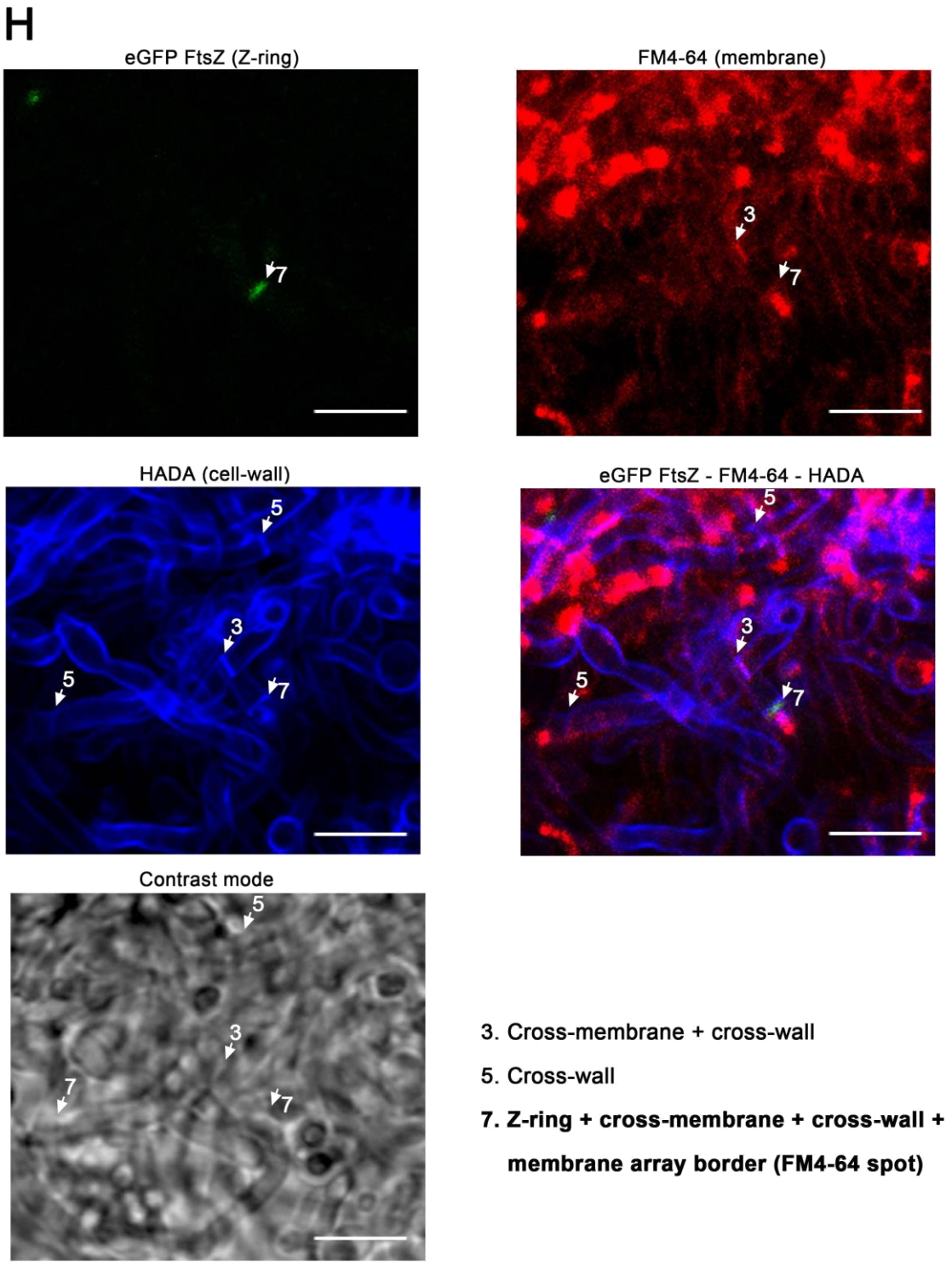

Supplementary Fig. 3. Images showing the colocalization of Z-rings, PI permeability barriers, cross-membranes and cross-walls. Scale bars correspond to 4 µm.
(F-I) eGFP-FtsZ (Z-rings, green), HADA (cell wall, blue) and FM4-64 (membrane, red) staining. Z-rings, cross-membranes and/or cross-walls colocalize in some cases (arrows).

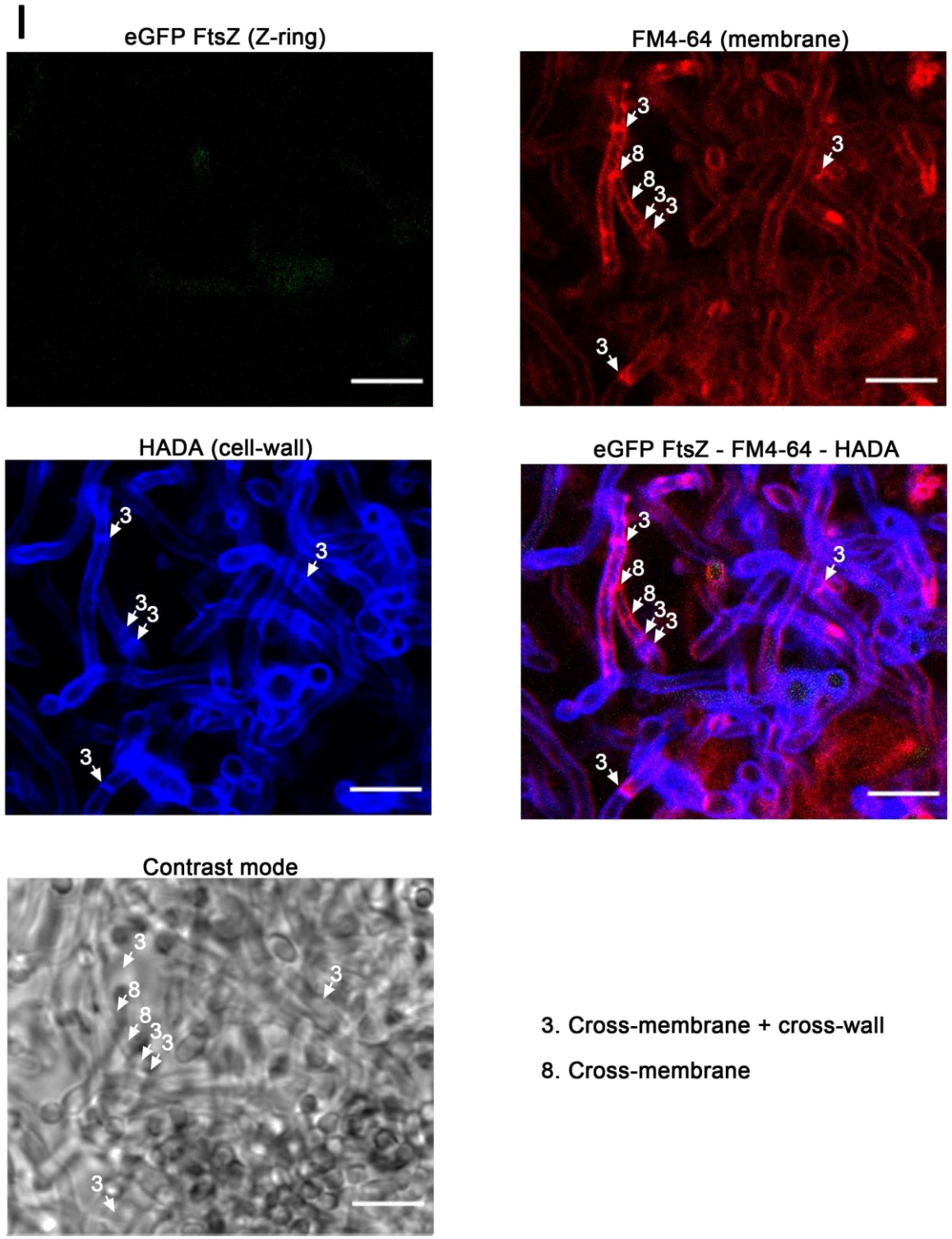

Supplementary Fig. 3. Images showing the colocalization of Z-rings, PI permeability barriers, cross-membranes and cross-walls. Scale bars correspond to 4 µm.
(F-I) eGFP-FtsZ (Z-rings, green), HADA (cell wall, blue) and FM4-64 (membrane, red) staining. Z-rings, cross-membranes and/or cross-walls colocalize in some cases (arrows).

A

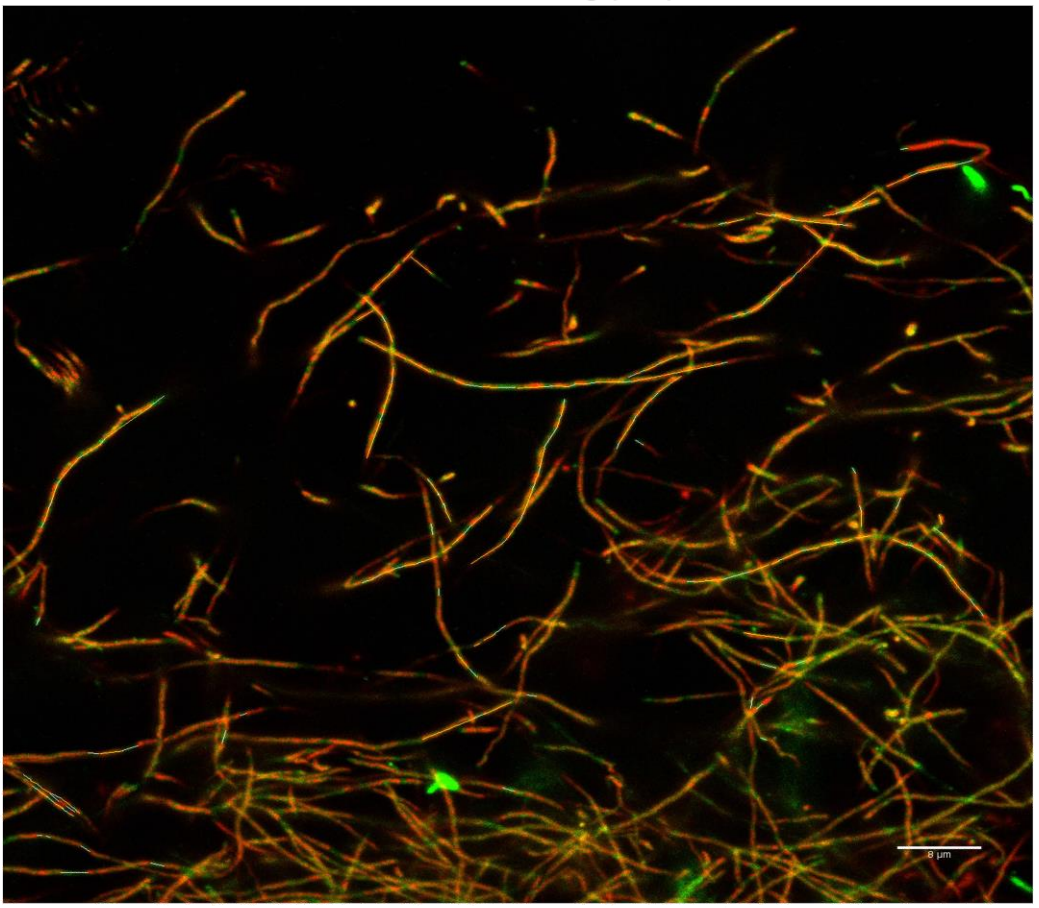

PI stained segments
- 100 segments
- Mean: 1.83 µm
- SD 1.27 µm
- Median 1.42 µm

SYTO9 stained segments
- 100 segments
- Mean: 0.85 µm
- SD 0.41 µm
- Median 0.74 µm

Supplementary Fig. 4. Master images used to quantify hyphal compartments in *ΔftsZ* HU133 (48 hours). Segments used for quantification of the compartment lengths are marked. Scale bars correspond to 8 µm.

(A) Master image used to quantify PI- (red) and SYTO9 (green)-stained segments.

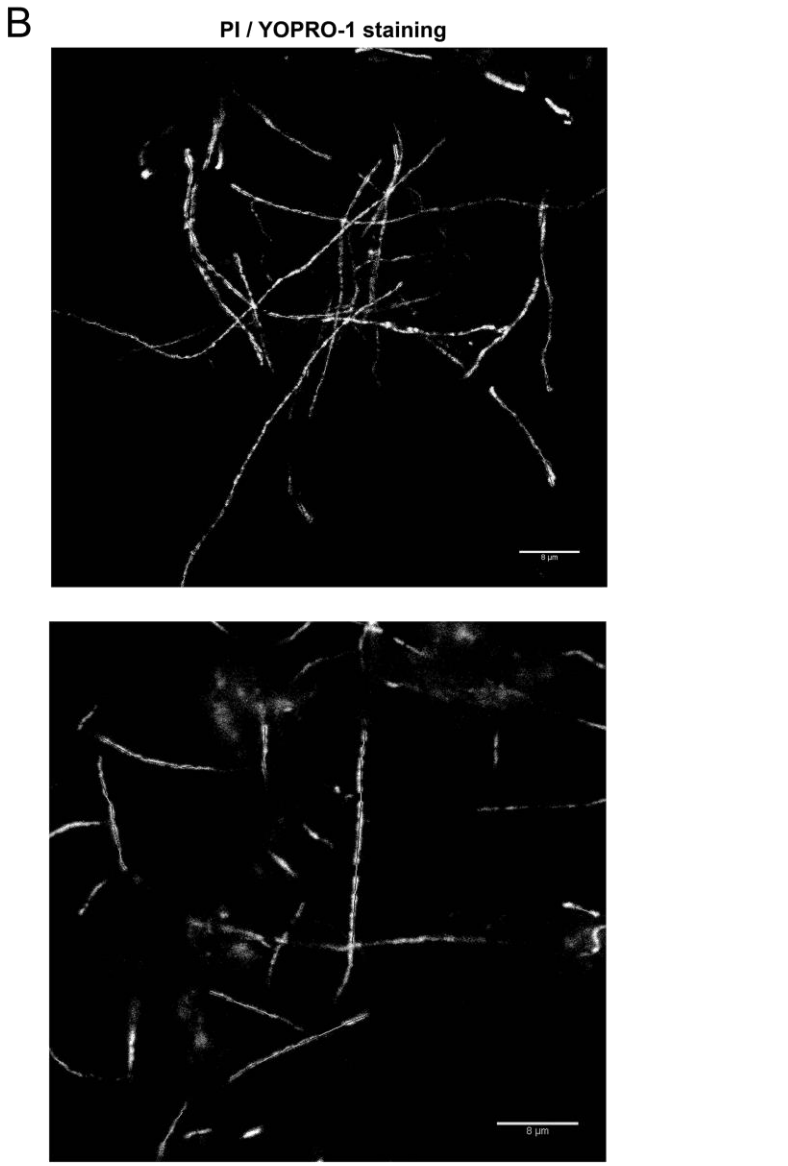

Supplementary Fig. 4. Master images used to quantify hyphal compartments in *ΔftsZ* HU133 (48 hours). Segments used for quantification of the compartment lengths are marked. Scale bars correspond to 8 µm.

(B) Master image used to quantify YOPRO-1- and PI-stained and unstained segments. The same segments were stained with YOPRO-1 and PI.

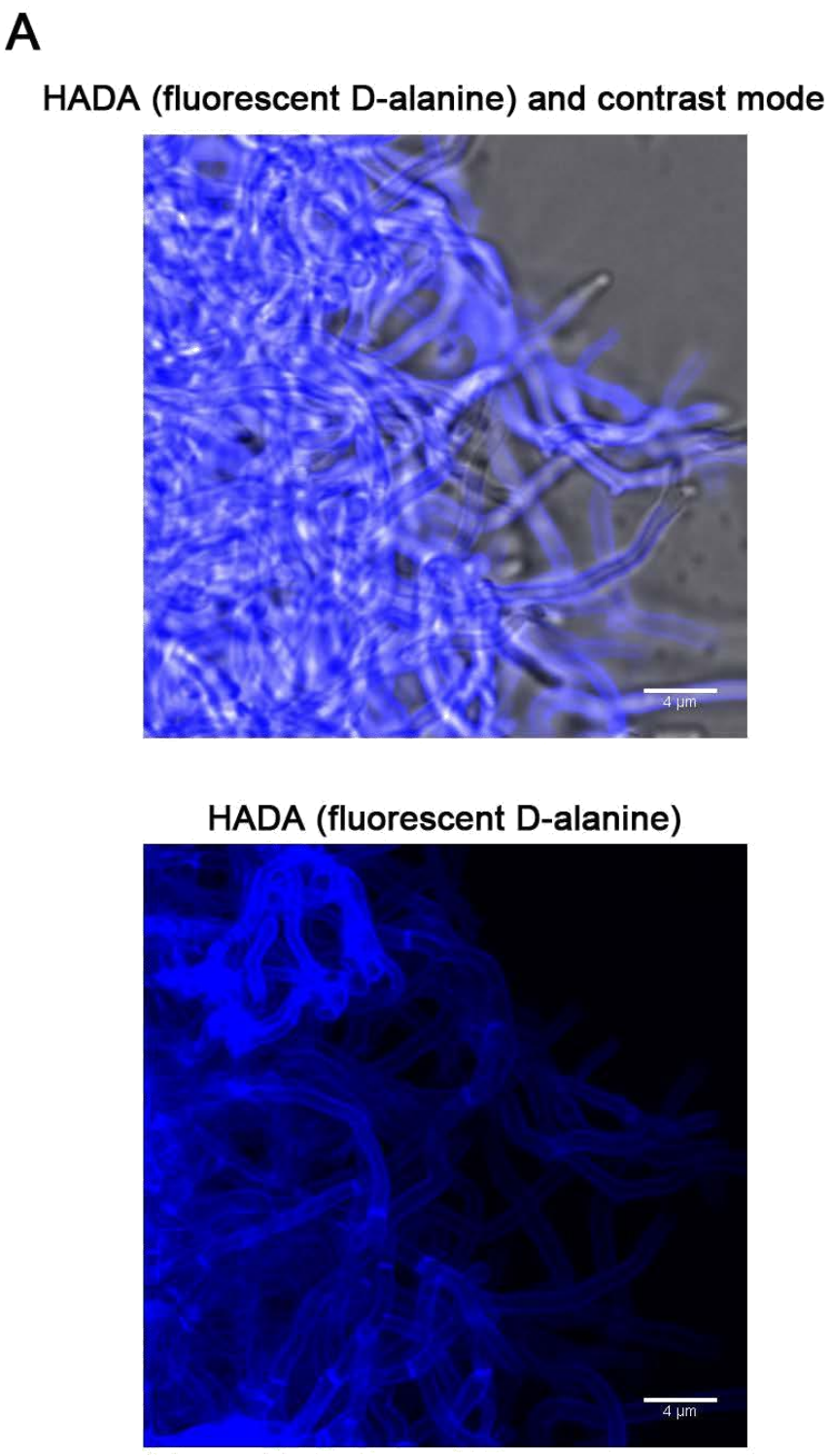

Supplementary Fig. 5. D-amino acid pulse-labeling staining (cell wall) of *S. coelicolor* and *ΔftsZ* HU133 (15 hours in liquid GYM medium). Scale bars correspond to 4 µm. (A) *S. coelicolor*

B

HADA (fluorescent D-alanine) and contrast mode

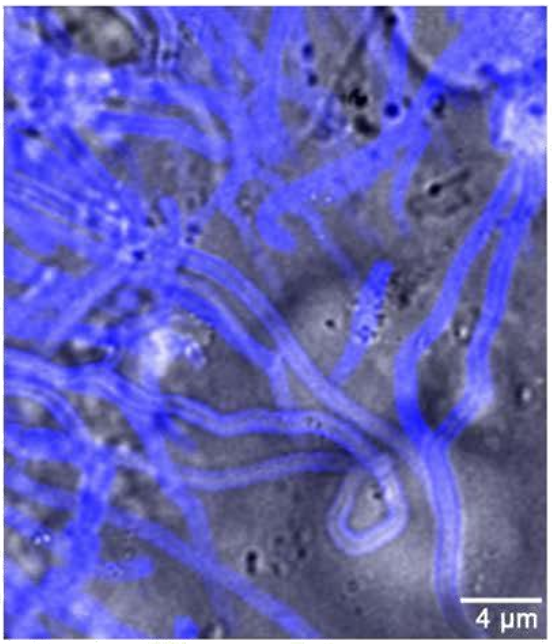

HADA (fluorescent D-alanine)

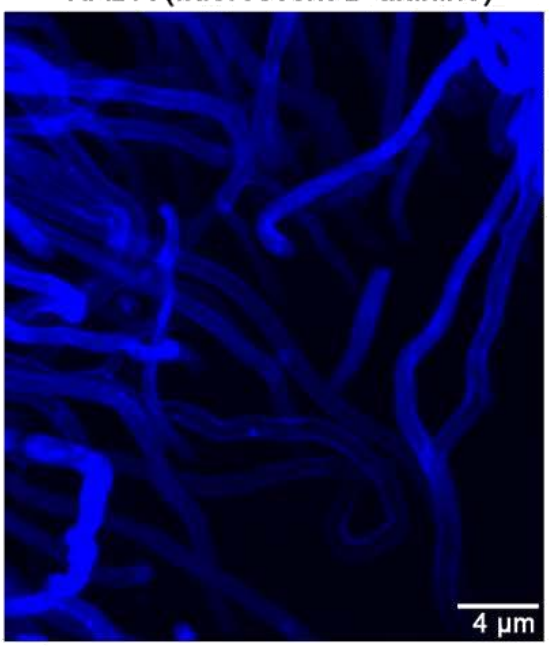

Supplementary Fig. 5. D-amino acid pulse-labeling staining (cell wall) of *S. coelicolor* and *ΔftsZ* HU133 (15 hours in liquid GYM medium). Scale bars correspond to 4 µm. (B) *ΔftsZ* HU133

A

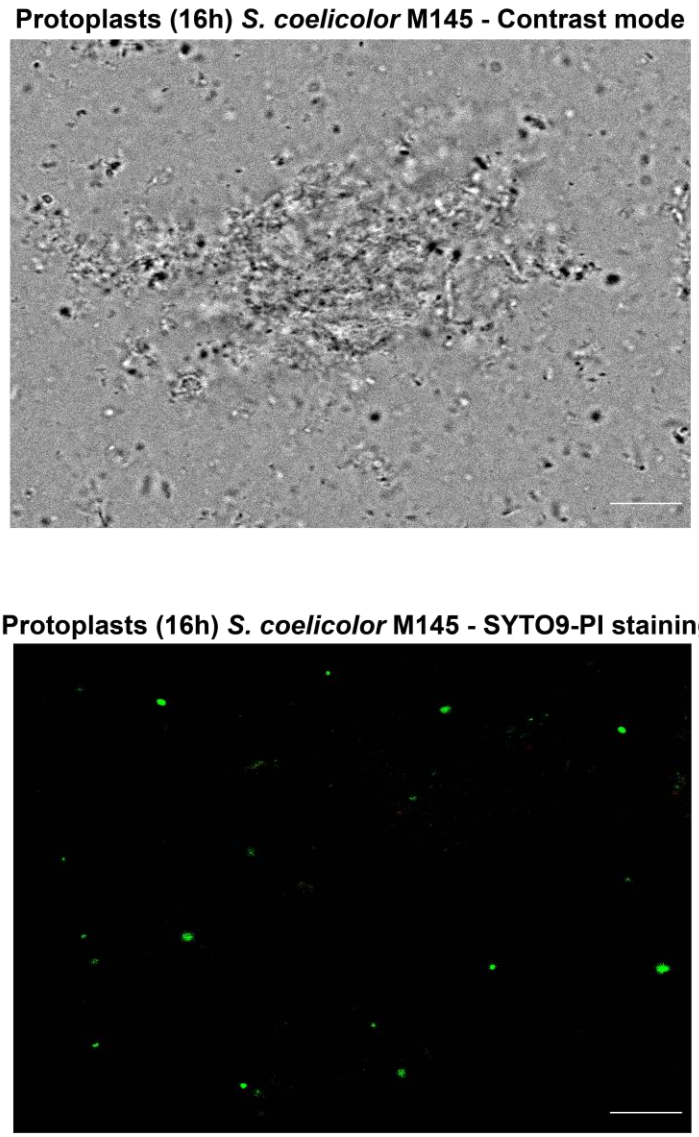

Supplementary Fig. 6. Protoplast formation and quantification. Scale bars correspond to 8 μm.

(A) Protoplasts stained with PI and SYTO9. Cell debris observed in phase contrast mode is devoid of stained cells, indicating a high efficiency of protoplast formation.

B

***S. coelicolor* M145 (16h) SYTO9-PI staining**

Protoplasts SYTO9-PI staining

- 100 protoplasts
- Mean: 2.2 µm
- SD 1.13 µm
- Median 1.9 µm

Supplementary Fig. 6. Protoplast formation and quantification. Scale bars correspond to 8 µm.

(B) Master images used to quantify protoplast diameter in *S. coelicolor* M145. Protoplasts were stained with PI and SYTO9. Protoplasts used for quantification are marked.

C

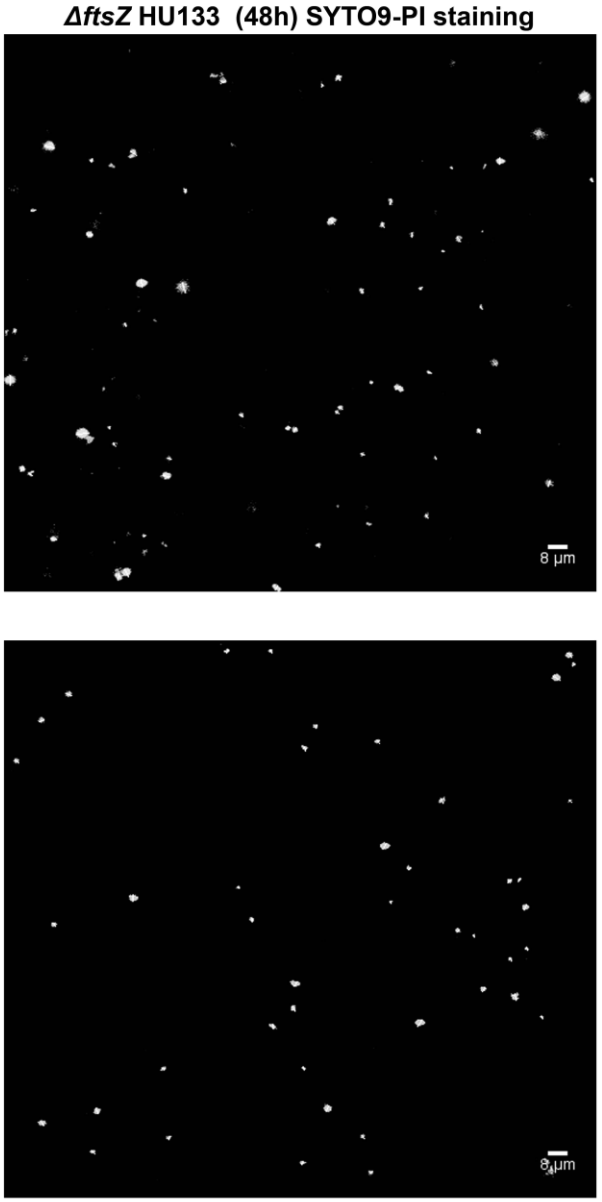

Supplementary Fig. 6. Protoplast formation and quantification. Scale bars correspond to 8 µm.

(C) Master images used to quantify protoplast diameter in *ΔftsZ* HU133. Protoplasts were stained with PI and SYTO9. Protoplasts used for quantification are marked.

Supplementary Table 1: TMT proteoimics.

(A) Peptides used for FtsZ protein abundance quantification. (B) FtsZ protein abundance. (C) FtsZ relative abundance (relative to 16-hours). R1-R4 Bilogical replicates 1-4.

(A) FtsZ peptides

FtsZ Peptides	TMT MI 16-hours				TMT MII 30-hours			TMT MII 65-hours		
	R1	R2	R3	R4	R1	R2	R3	R1	R2	R3
AAPQNYLAVIK	0.14	0.15	0.15	0.13	0.12	0.12	0.12	0.03	0.03	0.03
ANQAEDGIAELR	0.13	0.10	0.10	0.10	0.08	0.08	0.07	0.10	0.10	0.11
AVAAAEMAISSPLLEASIDGAR	0.11	0.10	0.11	0.11	0.10	0.09	0.09	0.10	0.09	0.09
DNVLGSSSAK	0.10	0.11	0.11	0.09	0.09	0.10	0.08	0.09	0.11	0.11
EEPEPAPVPEPVADLPVSPPPVPPSR	0.12	0.12	0.12	0.10	0.11	0.11	0.10	0.07	0.07	0.07
EEVDTLIVIPNDR	0.14	0.11	0.11	0.11	0.11	0.11	0.10	0.08	0.07	0.07
GADMVFVTAGEGGGTGTGGAPVVANIAR	0.11	0.12	0.11	0.10	0.12	0.11	0.12	0.08	0.07	0.06
GLGAGANPAVGR	0.11	0.11	0.11	0.10	0.10	0.10	0.09	0.08	0.09	0.09
RDNVLGSSSAK	0.10	0.12	0.10	0.10	0.10	0.10	0.09	0.09	0.10	0.10
SVMSEAGSALMGIGSAR	0.10	0.11	0.11	0.10	0.11	0.10	0.10	0.09	0.09	0.09
TYSDSAAEELDVPDFLK	0.14	0.14	0.13	0.12	0.12	0.12	0.12	0.04	0.05	0.04
VIGVGGGGVNAINR	0.13	0.12	0.12	0.11	0.11	0.10	0.10	0.07	0.06	0.07
VTVIAAGFDGGQPPSK	0.13	0.13	0.12	0.11	0.12	0.11	0.11	0.06	0.06	0.06

(B) FtsZ protein (53% sequence coverage)

Protein	TMT MI 16-hours				TMT MII 30-hours			TMT MII 65-hours			TMT abundance			q-values		
	R1	R2	R3	R4	R1	R2	R3	R1	R2	R3	MI 16h	MII 30	MII 65	MI16h vs MII65h	MI16h vs MII30h	MII30h vs MII65h
FtsZ	0.13	0.13	0.13	0.12	0.12	0.12	0.12	0.06	0.06	0.06	0.13	0.12	0.06	0.03	0.00	0.00

(C) FtsZ relative abundance (relative to 16-hours)

Sample	Time	TMT abundance			TMT ratios (relative to 16-hours)			FtsZ abundance	
		R1	R2	R3	R1	R2	R3	TMT average	TMT SD
MI 16-hours	16.00	0.13	0.13	0.13	1.00	1.00	1.00	1.00	0.00
MII 30-hours	30.00	0.12	0.12	0.12	0.90	0.90	0.90	0.90	0.00
MII 65-hours	65.00	0.06	0.06	0.06	0.49	0.44	0.43	0.45	0.03

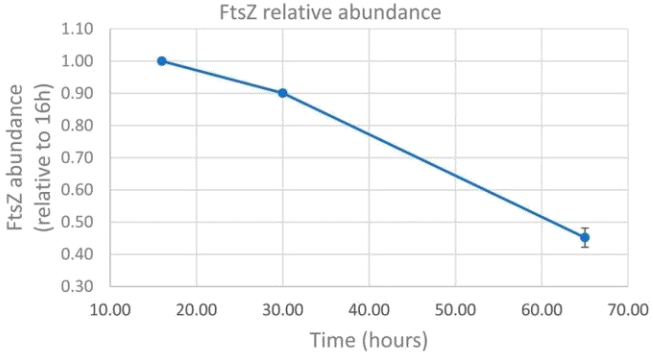

ANEXO 4
Material Suplementario del Manuscrito 4

En este anexo se incluye el material suplementario del **manuscrito 4**:

Figure S1. Diferenciación de *S. coelicolor* en biorreactores de 2L inoculados con 10^7 esporas/ml (inóculo denso) sin antiespumante.

Figure S2. Diferenciación de *S. coelicolor* en biorreactores de 2L inoculados con 10^5 esporas/ml (inóculo diluido) sin antiespumante.

Figure S3. Parámetros recogidos a lo largo del tiempo en las fermentaciones de *S. coelicolor* partiendo de inóculo denso y diluído en biorreactor de 2L (con y sin antiespumante) y matraces.

Figure S4. Geles de actividad de nucleasas no específicas de secuencia a lo largo del tiempo en las fermentaciones de *S. coelicolor* en biorreactores de 2L creciendo con y sin antiespumante.

Figure S5. Diferenciación de *S. coelicolor* en biorreactores de 2L inoculados con 10^7 esporas/ml (inóculo denso) con antiespumante.

Figure S6. Diferenciación de *S. coelicolor* en biorreactores de 2L inoculados con 10^5 esporas/ml (inóculo diluido) con antiespumante.

Figure S7. Imágenes de microscopía confocal (tinción con SYTO9-IP) de *S. coelicolor* crecido en biorreactor de 2L el momento del cambio de medio y a lo largo del tiempo tras dicho cambio.

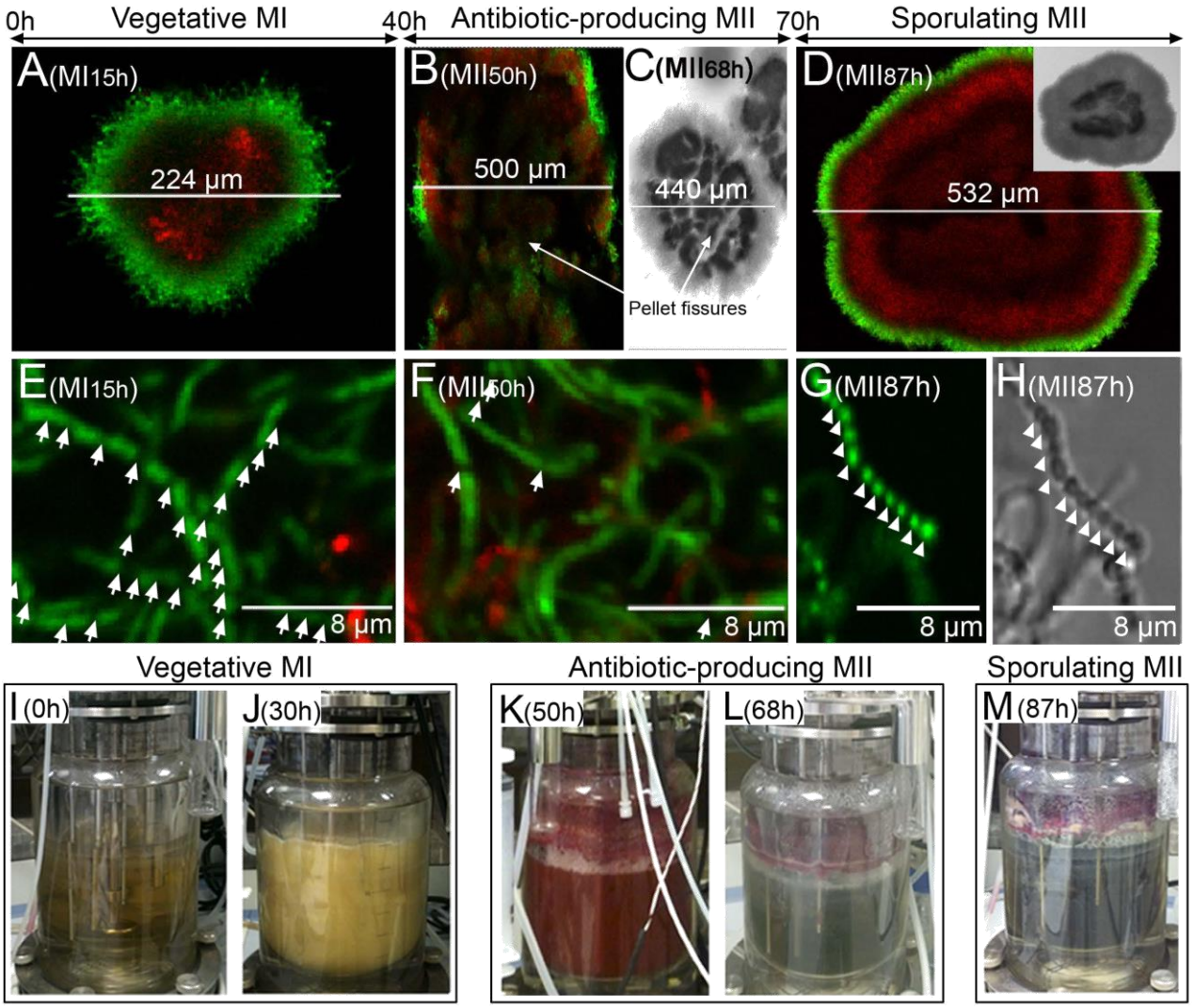

Figure S1. Differentiation of *Streptomyces coelicolor* M145 in 2-L bioreactors inoculated with 10^7 spores/ml ("dense cultures") in R5A cultures without antifoam. Upper panels, confocal laser-scanning fluorescence microscopy analysis (SYTO9/PI staining). Arrows in "E" and "F" indicate gaps (more frequent in MI than MII); arrowheads in "G" and "H" indicate spore-like structures. MI, first compartmentalized mycelium. MII second multinucleated mycelium. Magnifications (scale bars) are included inside pictures. Pictures "C", "H", and the image inside "D" correspond to interference contrast mode images. Lower panels, macroscopic view of the bioreactors; undecylprodigiosin (red) and actinorhodin (blue) productions are visible.

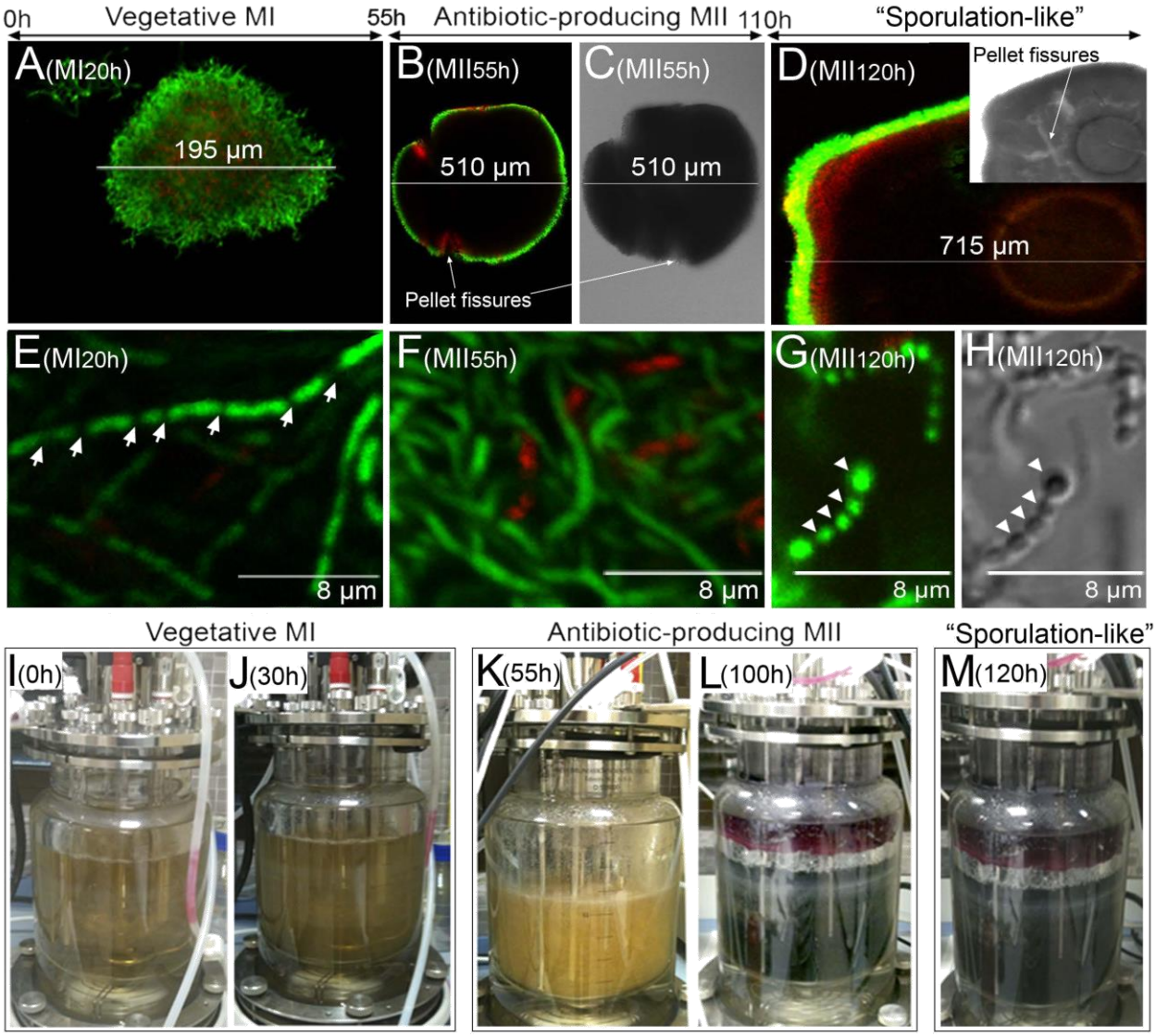

Figure S2. Differentiation of *Streptomyces coelicolor* M145 in 2l-bioreactors inoculated with 10^5 spores/ml ("diluted cultures") in R5A cultures without antifoam. Figure distribution and labelling as in Supplementary Fig. S1. See text for details.

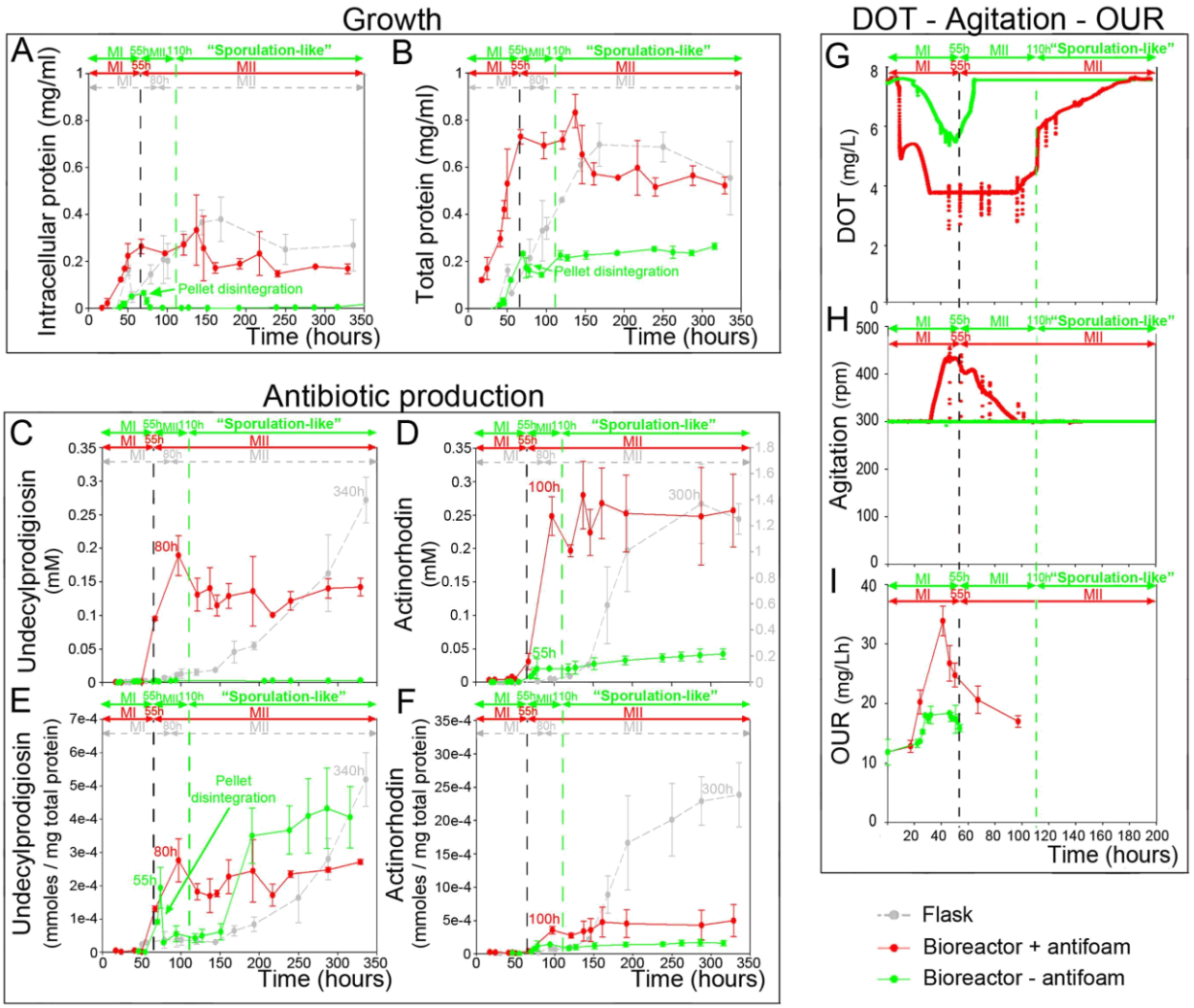

Figure S3. Time-course of fermentation parameters in fermentations of *Streptomyces coelicolor* M145 growing in 2l-bioreactors inoculated with 10^5 spores/ml ("diluted cultures") in R5A cultures without antifoam (green lines), with antifoam (red lines), and in laboratory flasks without antifoam (gray lines). (A), (B), Growth curves (intracellular protein and total protein). (C), (D), (E), (F), Antibiotic production (undecylprodigiosin and actinorhodin). Actinorhodin levels in the laboratory flasks in (D) has its own scale on the right. Time points at which maximum antibiotic productions were reached are indicated. (G), (H), (I), DOT, agitation, and OUR. Values are the average ± SD from two biological replicates.

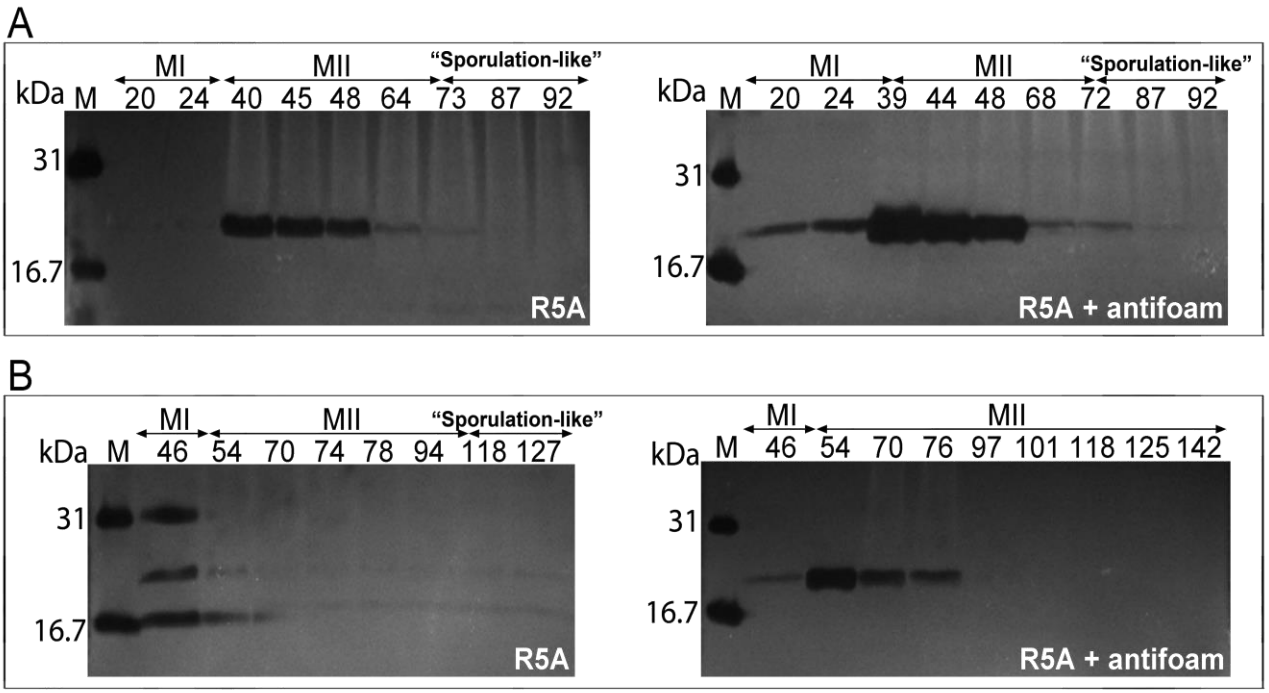

Figure S4. Time-course of non-sequence specific nucleases in fermentations of *Streptomyces coelicolor* M145 growing in 2l-bioreactors in R5A medium with and without antifoam. (A) "Dense cultures". (B) "Diluted cultures". Samples of extracellular protein were obtained at the time points indicated. Nuclease activities were normalized using the same amount of protein per well (8.5 µg). Lane M: micrococcal nuclease and DNase I, used as controls. Notice the existence of more than one nuclease (Manteca et al., 2006, Res. Microbiol. 157:143-152).

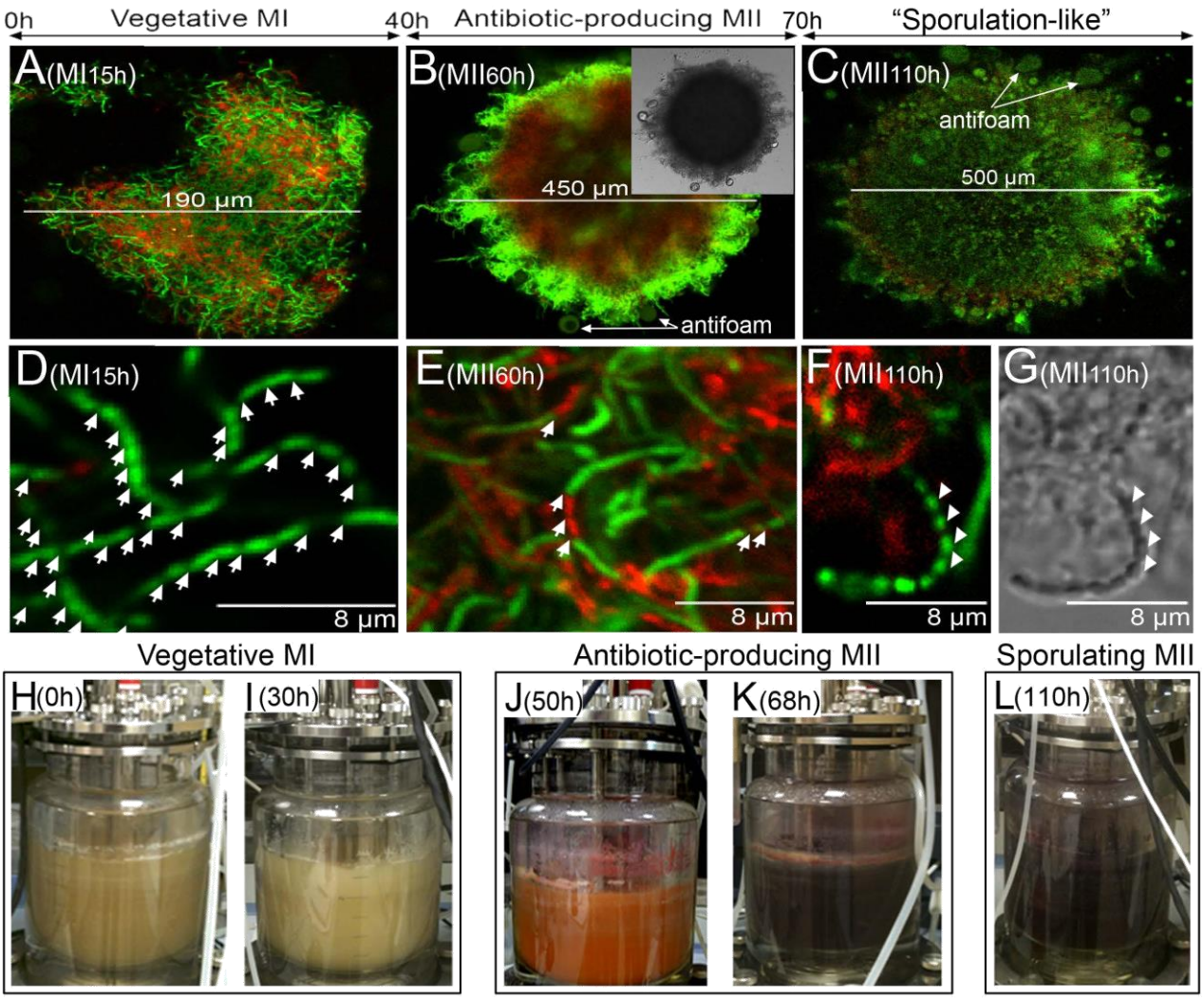

Figure S5. Differentiation of *Streptomyces coelicolor* M145 in 2-L bioreactors inoculated with 10^7 spores/ml ("dense cultures") in R5A cultures amended with antifoam. Figure distribution and labelling as in Supplementary Fig. S1. See text for details.

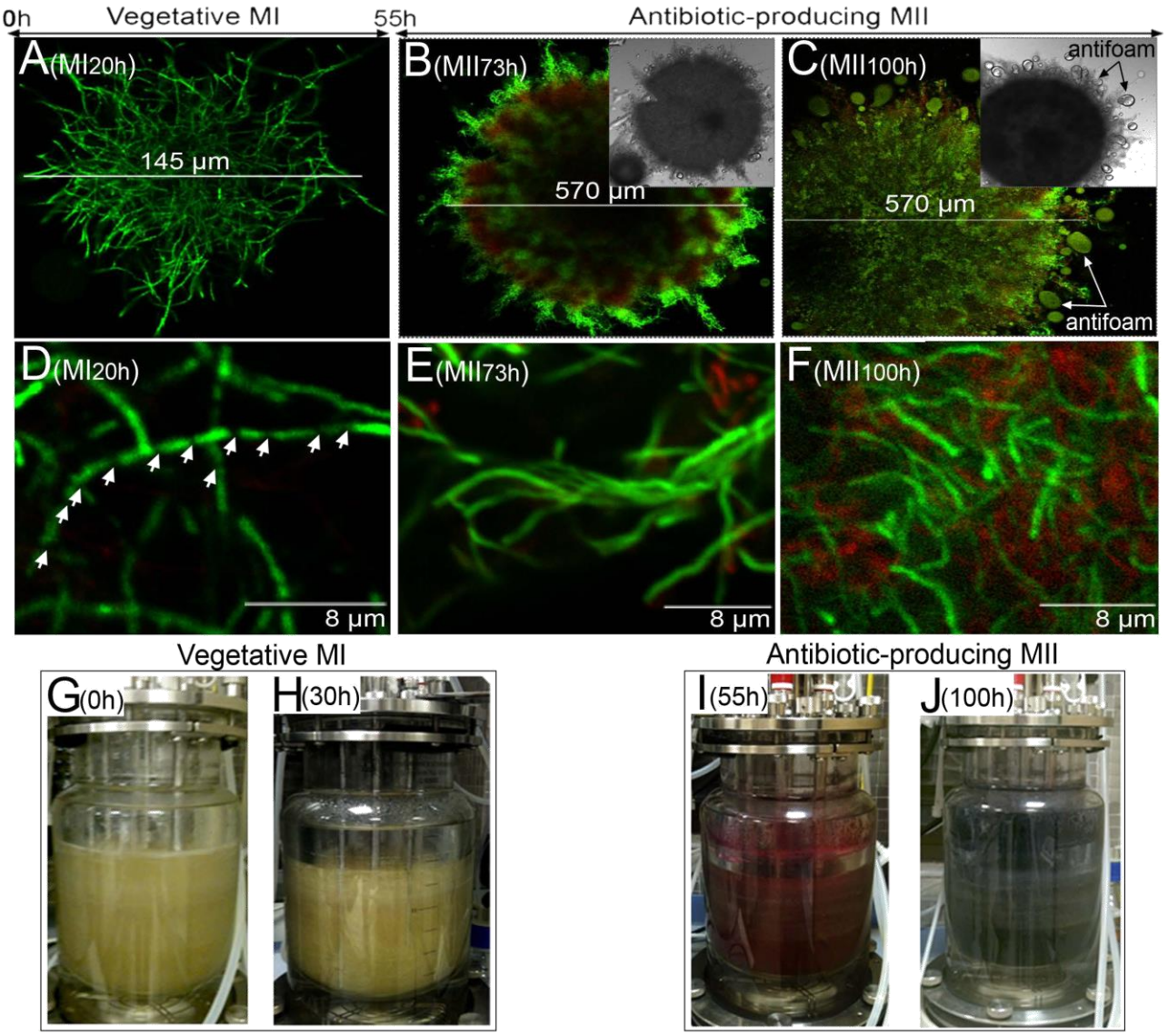

Figure S6. Differentiation of *Streptomyces coelicolor* M145 in 2l-bioreactors inoculated with 10^5 spores/ml ("diluted cultures") in R5A cultures amended with antifoam. Figure distribution and labelling as in Supplementary Fig. S1. See text for details.

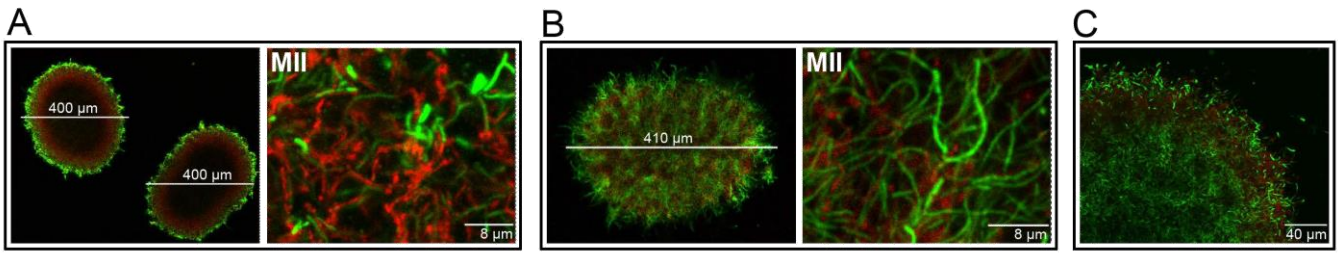

Figure S7. Confocal laser-scanning fluorescence microscopy analysis (SYTO9/PI staining) of *Streptomyces coelicolor* repeated batch fermentations. (A) 0 hours after medium replacement. (B) 19 hours after medium replacement. (C) 120 hours after medium replacement. See text for details.

ANEXO 5
Informe sobre la calidad de los artículos

INFORME SOBRE LA CALIDAD DE LOS ARTÍCULOS

La información sobre las revistas ha sido recogida de la Web Of Science (wos.fecyt.es/). Se han recogido los siguientes parámetros: el factor de impacto (FI) de cada revista, el cual corresponde al año de publicación del artículo o en el caso de los más recientes a los últimos datos publicados por Journal Citation Reports (año 2015); la categoría de JCR a la que está asociada la revista; el cuartil (Q) dentro de la misma, calculado en función de su factor de impacto. El número de veces que ha sido citado cada artículo (Citas) se ha obtenido de la página web Google Scholar (scholar.google.es/) en el momento de la escritura de la Tesis.

Manuscrito	**Revista**	**Categoría**	**Q**	**FI**	**Citas**
Manuscrito 1	MOLECULAR & CELLULAR PROTEOMICS	BIOCHEMICAL RESEARCH METHODS	Q1	5.912	Enviado
Manuscrito 2	SCIENTIFIC REPORTS	MULTIDISCIPLINARY SCIENCES	Q1	5.228	0
Manuscrito 3	NATURE COMMUNICATIONS	MULTIDISCIPLINARY SCIENCES	Q1	11.329	3
Manuscrito 4	BIORESOURCE TECHNOLOGY	BIOTECHNOLOGY & APPLIED MICROBIOLOGY	Q1	4.494	15